# IN SITU AND METEORIC $^{10}$BE CONCENTRATIONS OF FLUVIAL SEDIMENT COLLECTED FROM THE POTOMAC RIVER BASIN

A Thesis Presented

by

Charles David Trodick Jr.

to

The Faculty of the Graduate College

of

The University of Vermont

In Partial Fulfillment of the Requirements
for the Degree of Master of Science
Specializing in Geology

October, 2011

**Accepted by the Faculty of the Graduate College, The University of Vermont, in partial fulfillment of the requirements for the degree of Master of Science, specializing in Geology.**

**Thesis Examination Committee:**

_____**Advisor**
Paul R. Bierman, Ph.D.

_____
Laura Webb, Ph.D.

_____**Chairperson**
Donna M. Rizzo, Ph.D.

_____**Dean, Graduate College**
Domenico Grasso, Ph.D.

Date: July 1, 2011

## Abstract

This thesis reports and interprets in situ and meteoric $^{10}$Be concentrations of sediment collected from the Potomac River Basin, a major source of sediment for the Chesapeake Bay. It includes data for 62 fluvial sediment samples with measurements of both in situ produced and meteoric $^{10}$Be along with an additional eight samples for which only meteoric $^{10}$Be was measured. I sampled three sites on the main-stem Potomac River, and one site on the Shenandoah River (basin areas of 29796, 24851, 2254, and 4136 km$^2$). Ten Potomac River samples, including the four above, came from USGS gaging station sites at which suspended sediment was or is monitored (basin area 23 to 29796 km$^2$). Sixty samples, including the eight with only meteoric $^{10}$Be analyses, came from tributaries of the Potomac River (5 km$^2$ to 64 km$^2$).

Basin-scale erosion rates, based on interpretation of in situ $^{10}$Be concentrations, range from 3 to 39 m My$^{-1}$ with a mean and median erosion rate of 12 m My$^{-1}$. Basins in the Coastal Plain ($n$=8) have the lowest erosion rates, 4 to 39 m My$^{-1}$ with a mean of 10 m My$^{-1}$ and a median of 6 m My$^{-1}$. Basins in the Appalachian Plateau and Blue Ridge ($n$=6, $n$=8; mean erosion rates of 13 and 12 m My$^{-1}$) range from 9 to 18 m My$^{-1}$ and have a median of 13 m My$^{-1}$. Twenty samples from the Piedmont have erosion rates that range from 3 to 21 m My$^{-1}$ and a mean and median of 12 m My$^{-1}$. Seventeen samples from the Valley and Ridge have a range from 3 to 29 m My$^{-1}$, a mean of 11 m My$^{-1}$ and median of 9 m My$^{-1}$. Past studies using in situ $^{10}$Be erosion rates have found similar erosion rates measured in and near the Appalachian Mountains (3–70 m My$^{-1}$).

Erosion rates show no correlation with slope ($R^2$=0.06, $p$>0.05) and only a weak correlation with elevation ($R^2$=0.09, $p$=0.01). The range of erosion rates change little with basin area ($R^2$=0.02, $p$=0.23). Using ANOVA testing, erosion rates in the Piedmont, Blue Ridge, Valley and Ridge and Appalachian Plateau physiographic provinces are not statistically separable ($p$=0.25), but the Coastal Plain has much lower rates than the other provinces with a median half that of almost all of the other provinces ($p$<0.01) when an outlier is removed from the Coastal Plain.

A comparison of meteoric and in situ $^{10}$Be in 62 basins shows less meteoric $^{10}$Be in the sediments than expected given the in situ $^{10}$Be concentrations. The lower meteoric $^{10}$Be concentrations most likely reflect lack of knowledge of where meteoric $^{10}$Be resides in many of my basins.

United States Geologic Survey sediment yield data ($n$=10) suggest that rates of sediment export are similar to rates of sediment generation in the Potomac Basin. Brown et al. (1988) calculated erosion indexes that compare the amount of meteoric $^{10}$Be entering the basin and the amount of meteoric $^{10}$Be leaving the basin. Brown et al.'s (1988) erosion indexes from the Chesapeake Bay Watershed show two thirds, 29 of 45, of their basins had more meteoric $^{10}$Be entering the basin than leaving. Their average erosion index was 0.87. Of the ten gauged basins I analyzed, eight had more meteoric $^{10}$Be entering the basin than leaving. My average erosion index was 0.65. Meteoric $^{10}$Be concentrations used for the erosion index calculations were updated with modern standards and delivery rates.

**Acknowledgements**

I want to thank Dr. Paul Bierman for many things. He took me in when I had no other options and gave me an amazing project to work on. I want to thank Eric Portenga, Luke Reusser, Dr. Milan Pavich, and Dr. Paul Bierman for all of the help in the field. I also want to thank them, along with Lee Corbett for training and working with me in the lab as much as they did. They also frequently worked with me to help me think about my research and what it means. I want to thank Dr. Donna Rizzo for helping me with my statistics and generally helping me with my research. I want thank Dr. Alan Gellis at the USGS for sending me his sediment yield data. I want to thank Dr. Laura Webb for helping me with my Proposal, Progress Report, and Thesis. I want to thank Dr. Andrea Lini for the various bits of help he has given while at the University of Vermont. I also want to thank everyone at Lawrence Livermore National Laboratory.

Outside of my research I need to thank Hannah Roberts for all of the support she has given me since I have been at the University of Vermont. I want to thank my parents, Pam and Chuck Trodick, for their unending support and love. Finally I need to thank the many graduate students that I have spent time with.

Research Supported by National Science Foundation grant EAR-310208 and U. S. Geological Survey grant 08ERSA0582. This work performed in part under the auspices of the Department of Energy by Lawrence Livermore National Laboratory under Contract DE-AC52-07NA27344.

## Table of Contents

## List of Tables

## List of Figures

## Chapter 1 - Introduction

*"The Potomac River has long been viewed as the Nation's River because of its pivotal role in the development of the United States and as the seat of my national government* (EPA, US, 2001)*."*

Today, the Potomac Watershed (37995 $km^2$) contributes a significant amount, over 1.93 x $10^{12}$ g $y^{-1}$, of sediment to the Chesapeake Bay, a valuable natural resource (Stanton, 1993). The United States spends a large amount of money, time and energy protecting the Chesapeake Bay (EPA, US, 2001). Responsible management requires good estimates, not only of current rates of sediment delivery to the bay, but also background (pre-disturbance) rates of sediment generation from major river basins feeding the Chesapeake Bay. Because background rates of sediment generation are not well understood, it is difficult to determine how much sediment was transported to the Chesapeake Bay before humans started affecting the system.

Two main rivers, the Potomac River and the Susquehanna River, feed the Chesapeake Bay (Figure 1.1). The Susquehanna River and the Potomac River have current sediment yield data (Gellis, et al., 2004). Today, the Potomac River contributes 44% of the riverine sediment entering the Chesapeake Bay and the Susquehanna River contributes 27% (Gellis, et al., 2004). The Susquehanna River also has background rates of sediment generation (Reuter, et al., 2006).

This thesis explores in situ and meteoric beryllium-10 ($^{10}$Be) concentrations measured in fluvial sediment samples collected from the Potomac River Basin. The data present in this thesis is a direct comparison between the two different cosmogenic isotopic systems. It presents and interprets the isotopic data from 62 fluvial sediment samples with measurements of both in situ produced and meteoric $^{10}$Be along with an additional eight samples in which only meteoric $^{10}$Be was measured (Figure 1.2). I took 10 samples from U.S. Geological Survey gaging stations within the 37995 km$^2$ basin. These samples allow for a comparison between sediment yields and sediment generation rates.

Beryllium-10 is found both within and on mineral grains. The $^{10}$Be found in grains, in situ $^{10}$Be, is produced when high-energy, fast cosmic ray neutrons interact with the nuclei of oxygen and nitrogen (Bierman, 1994; Lal, 1998). The concentration of in situ $^{10}$Be changes based on how long the sediment is exposed to cosmogenic radiation; this is true both in bedrock and as material on slopes.

Meteoric $^{10}$Be forms in the atmosphere where cosmic rays interact with oxygen and nitrogen atoms. Meteoric $^{10}$Be rains out of the atmosphere and absorbs onto soil grains, including clay and organic particles (Pavich, et al., 1984). In some geologic settings, meteoric $^{10}$Be concentration appears to reflect how long the sediment resides on hill slopes before entering the river channel (Jungers, et al., 2009). In general, the longer sediment sits at or near Earth's surface, the higher the concentration of in situ and meteoric $^{10}$Be and the slower the erosion rate.

Suspended sediment concentrations measured at gaging stations, when convolved with flow data, provide estimates of modern rates of sediment yield (Judson, 1968; Judson & Ritter, 1964; Gellis, et al., 2004). Suspended sediment concentrations are measured by taking periodic samples from a river or stream over a certain duration of time. Then, the ratio of sediment to water in each sample is determined and this is multiplied by the amount of water flowing down the stream.

Brown et al. (1988) examined erosion in the Chesapeake Bay Watershed by first calculating how much meteoric $^{10}$Be was deposited in a gaged basin using the global average delivery rate of meteoric $^{10}$Be. Then, they measured the meteoric $^{10}$Be concentration in riverine sediment leaving the gaged basin and compiled contemporary sediment yields to determine the flux (atoms/year) of meteoric $^{10}$Be leaving the gaged basin. With this information, they calculated an erosion index, which can suggest whether or not a basin is in short-term steady state in regards to meteoric $^{10}$Be. Applying this approach to a single sample, which was taken from a location that I resampled, in the Potomac River Basin, Brown et al. (1988) found that slightly more meteoric $^{10}$Be entered the basin than left the basin.

### *Motivations and Objectives*

This thesis presents in situ and meteoric $^{10}$Be data from 62 fluvial sediment samples along with an additional eight samples in which only meteoric $^{10}$Be was measured (Figure 1.2). I collected the fluvial sediment for this study from basins in each of the five physiographic provinces in the Potomac Watershed. I converted the in situ and

meteoric $^{10}$Be data to erosion rates which characterize how the landscape has changed in the mid-Atlantic region over $10^3 – 10^5$ year timescale.

With my samples, I am trying to develop a better understanding of how landscapes erode and what affects the amount of meteoric $^{10}$Be leaving the system. I want to understand better the relationship between in situ and meteoric $^{10}$Be in an attempt to determine whether one can use meteoric $^{10}$Be concentrations to determine erosion rates. I compared my in situ and meteoric $^{10}$Be erosion rates with modern sediment yield data. I also compared my meteoric $^{10}$Be data with previous meteoric $^{10}$Be data collected in the region by Brown et al. (1988) to see if there have been changes over time in meteoric $^{10}$Be export rates.

The three main objectives of my research are:

- to explore how in situ $^{10}$Be erosion rates and meteoric $^{10}$Be concentrations are affected by different environmental factors.
- to compare in situ and meteoric $^{10}$Be erosion rates and sediment yields from the same basins.
- to compare my meteoric $^{10}$Be data with previous meteoric $^{10}$Be data collected in the region by Brown et al. (1988).

### *Thesis Structure*

Chapter 2 contains a short literature review on the physical setting in which my research took place and past research relating to the use of cosmogenic isotopes to study

erosion rates by the analysis of fluvial sediments, including work done near the Potomac River Basin. There also is a discussion of the controls on sediment yield and sediment generation. Chapter 3 describes the study methods including sampling strategy, field techniques, laboratory work, and analytical procedures. Chapter 4 presents all of my data. Chapter 5 contains my discussion. Chapter 6 contains conclusions of the research and recommendations for future work. Appendix A contains tables of all the data used and generated for this project. Appendix B contains sample sheets for each of my samples and topographic maps showing the location of each sample site, along with a few pictures. A disk is included with all data tables in excel format.

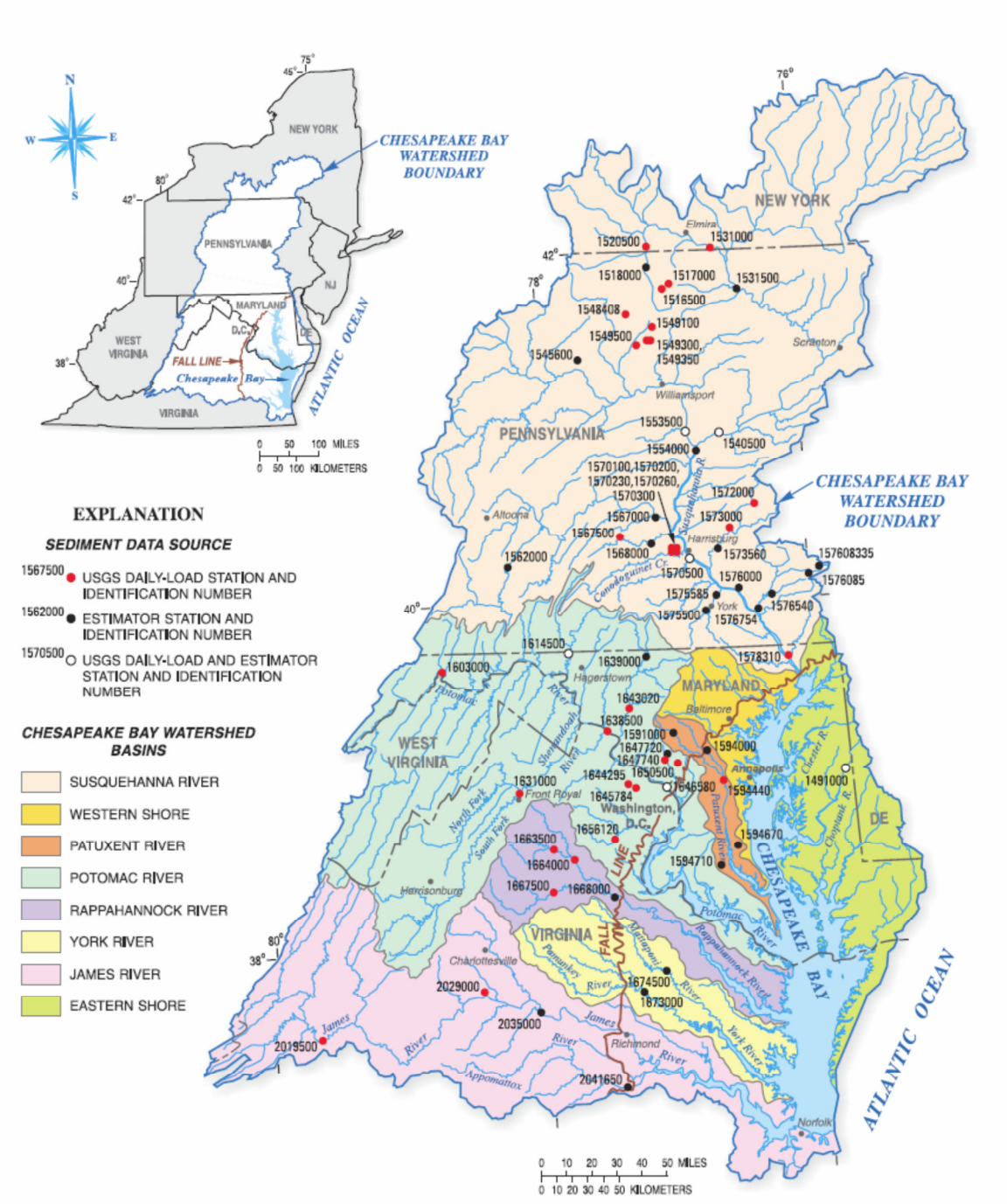


**Figure 1.1 - Map of the Chesapeake Bay Watershed.**
This map show all of the major watersheds that drain into the Chesapeake Bay including, the Susquehanna River (tan), the James River (pink), and the Potomac River (green). Each of the numbered dots is a gaging station. I sampled at all but 3 of the gaging stations in the Potomac Watershed. Figure from Gellis et al. **(2004)**.

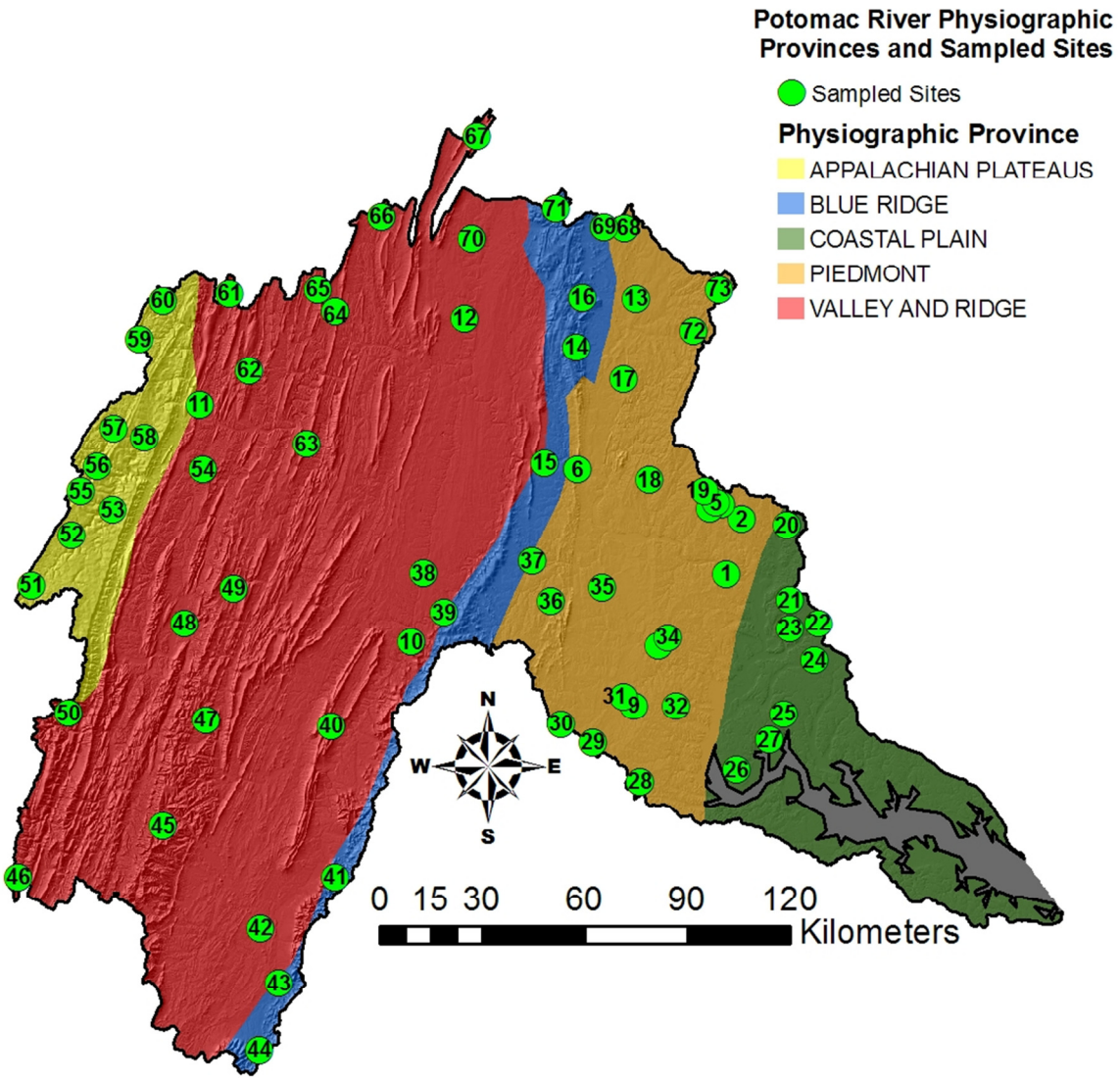


**Figure 1.2 - Map of the Potomac River Basin.**
The green dots are the sampled sites. Each colored region on the map is a different physiographic province (from USGS). The green area is the Coastal Plain, the orange region is the Piedmont, and the blue portion is the Blue Ridge, the red area in the Valley and Ridge, and the yellow section is the Appalachian Plateau. The background is a shaded digital elevation model (USGS digital data, http://seamless.usgs.gov/).

## Chapter 2 – Background and Literature Review

### *Potomac River Basin Physiography*

The Potomac River Basin occupies 38019 $km^2$ in four states and the District of Colombia (Virginia, 14846 $km^2$; Maryland, 9889 $km^2$; West Virginia, 9039 $km^2$; Pennsylvania, 4,066 $km^2$; District of Columbia, 179 $km^2$) (ICPRB, 2011). Based on the 2005 census, around 5.8 million people live in the Potomac River Basin, ¾ of which live in the Washington DC area (ICPRB, 2011). Agriculture, forestry, coal mining, paper, chemicals, and electronics are the important industries of the Potomac Watershed (Gerhart, 1991).

The Potomac River starts to be affected by tides after the river crosses the Fall Line a few kilometers upstream from Washington, D. C. (Gerhart, 1991). About 15% of the water and 44% of the riverine sediment flowing into the Chesapeake Bay comes from the Potomac River (Gerhart, 1991; Gellis, et al., 2004). Only 3% of the watershed is regulated by dams and none of the reservoirs are over 7.5 $km^2$ (Gerhart, 1991).

### *Physiographic Provinces*

The Potomac River basin includes five physiographic provinces, the Appalachian Plateau, Valley and Ridge, Blue Ridge, Piedmont, and Coastal Plain (Figure 1.2). The Appalachian Plateau Province contains 6% of the Potomac River Basin. The province is made up of a thick, uplifted section of sedimentary rock composed of sandstone, shale, and limestone (Fenneman, 1938). The Valley and Ridge Province contains 57% of the

Potomac River Basin. The province is characterized by a series of parallel ridges with small valleys (EPA, US, 2001). The ridges are made up of well-cemented sandstone and conglomerates while the valleys are limestone, dolomite, and shale (Trapp & Horn, 1997). The Blue Ridge Province contains 7% of the Potomac River Basin. The highlands of the Blue Ridge are made up of low-grade metamorphic rocks while the valleys contain sedimentary rocks (Milici, 1995).

The Piedmont Province contains 20% of the Potomac River Basin. The Piedmont is made up of tightly folded and faulted metasedimentary and plutonic rocks. The Piedmont also contains sedimentary basins filled with shale, sandstone, and conglomerate, along with the occasional basaltic lava flows and minor coal beds (Trapp & Horn, 1997). The Coastal Plain Province borders the Atlantic Ocean (Trapp & Horn, 1997) and contains 10% of the Potomac River Basin. The Coastal Plain mostly is made up of semiconsolidated to unconsolidated sediments, typically, silt, clay, and sand, with small amounts of gravel and lignite. There are also some areas containing limestone and sandstone (Trapp & Horn, 1997).

### *Modern Climate of the Potomac River Basin*

Based off of the Köppen climate classification system the Potomac River Basin has a humid subtropical climate (Kottek, et al., 2006) which is commonly referred to as a temperate climate. The basin experiences all four season including hot humid summers, cool winters and warm springs and falls. The basin averages 100 cm $y^{-1}$ of precipitation and has a range from 89 to 132 cm $y^{-1}$. The central portions of the basin experience the

lowest average annual precipitation, around 89 cm, while the western mountains and the Coastal Plain average around 112 cm (Gerhart, 1991) (Figure 2.1). About a third of the precipitation falls as snow (water equivalent of 37 cm $y^{-1}$) (NCDC, 2004).

### *Geologic and Human History*

Rivers have been flowing in the region of the Potomac River for at least the past 30 million years (Stanton, 1993). Around 6 to 7 Ma sea level in the modern D. C. area dropped to near current levels. This drop in sea level exposed the Coastal Plain and allowed the rivers in the region to deposit the sediments found there (Reed, et al., 1980). About 2 Ma, slow uplift steepened the local land surface and allowed the Potomac River to capture many of the small rivers in the region (Reed, et al., 1980). Around this time continental glaciation began which lowered sea level causing the Potomac River to cut deep valleys in the Piedmont (Reed, et al., 1980).

Around 12000 BP Nomadic Native Americans started inhabiting the Potomac River Basin (Stanton, 1993). About 1800 BP, Native Americans began practicing the first agriculture in the Potomac Watershed (Stanton, 1993). In 1634, the first European colony of the region, Maryland, was founded on the banks of the Potomac River (Stanton, 1993). After the founding of the colony, settlers removed most of the forest from the Coastal Plain for tobacco agriculture. In the late 1690s, the agriculture started to spread to the Piedmont (Costa, 1975). In 1791, the United States founded Washington, D. C. (Stanton, 1993). After the American Revolution, agriculture almost permanently left the Coastal Plain and spread to the Piedmont and lowlands of the Valley and Ridge, where the

majority of agriculture still is today (Brown, 1943). The movement of farming allowed the forests of the Coastal Plain to almost completely grow back (Brown, 1943). The Potomac experienced some mill damming from the 1600s up through the 1800s, mainly in the northern section of the basin, in and near Pennsylvania (Merritts & Walter, 2003; Merritts, et al., 2006; Walter & Merritts, 2008). Forest, 52% of the basin, and agriculture, 36% of the basin, dominate the land use in the Potomac River Basin, today. The rest of the watershed contains developed land, 11%, barren land, 0.5%, and water, 0.5% (Figure 2.2).

### *Cosmogenic Nuclides, In Situ and Meteoric $^{10}$Be*

This project focused solely on $^{10}$Be, using it to estimate rates of sediment generation, because $^{10}$Be has a relatively long half-life and allows for easy measurement (Lal & Arnold, 1985). Beryllium-10 is found both in and on mineral grains. In situ $^{10}$Be, that within the grains, is produced when high-energy, fast cosmic ray neutrons interact with the nuclei of oxygen and nitrogen (Bierman, 1994; Lal, 1998). Meteoric $^{10}$Be forms in the atmosphere where cosmic rays interact with oxygen and nitrogen atoms. Meteoric $^{10}$Be rains out and sorbs to soil grains, including clay and organic particles (Pavich, et al., 1984). Once absorbed to the soil grains, meteoric $^{10}$Be does not leave the grain during transport (Pavich, et al., 1984; Jungers, et al., 2009). The concentration of in situ $^{10}$Be changes based on how long the sediment experiences exposure to cosmogenic radiation, both in rocks and as material on slopes. Meteoric $^{10}$Be concentration appears to reflect how long the sediment resides on hill slopes before entering the river channel (Jungers, et

al., 2009). The longer sediment sits at or near Earth's surface, the higher the concentration of in situ and meteoric $^{10}$Be and the slower the erosion rate. Sediment with lower concentrations of in situ and meteoric $^{10}$Be experiences a shorter period of exposure and indicates a faster erosion rate.

### *In Situ $^{10}$Be*

Analysis of in situ $^{10}$Be concentration in fine quartz sand carried by rivers has become an important technique for understanding long-term erosion rates (Brown, et al., 1995; Bierman & Steig, 1996; Granger, et al., 1996; Bierman & Nichols, 2004; von Blanckenburg, 2005). In situ $^{10}$Be in river sediment allows geologists to estimate erosion rates over $10^3$ to $10^6$ year time scales (Brown, et al., 1995; Bierman & Steig, 1996; Granger, et al., 1996). $^{10}$Be is easily measured in quartz (Lal & Arnold, 1985), which has great resistance to weathering and little reactivity to many acids (Kohl & Nishiizumi, 1992). The production curve of in situ $^{10}$Be is exponential with depth. Biota can churn the soil and mix the quartz grains so there is no depth dependence to the depth at which stirring reaches (Jungers et al., 2009).

Calculation of erosion rates from measured in situ $^{10}$Be concentrations requires several assumptions. Erosion rates must stay steady over time but not necessarily space (Bierman, 1994). In situ $^{10}$Be must remain in the quartz in which it forms (Kohl & Nishiizumi, 1992). The in situ $^{10}$Be concentration of the sample must be representative of the average concentration in the basin (Bierman & Steig, 1996). The average latitude and elevation of the basin from which the sample came must be known (Nishiizumi, et al.,

1989) to calibrate production rates (Lal, 1988; Dunai, 2000; Desilets & Zreda, 2000; Lifton, et al., 2008). In situ $^{10}$Be erosion rates only represent areas with bedrock that contains quartz (Brown, et al., 1995). Minimal amounts of quartz should dissolve during the weathering process and sediment should not be repeatedly uncovered and buried (Brown, et al., 1995).

### *Meteoric $^{10}$Be*

Recently geomorphologists have started using meteoric $^{10}$Be for calculating basin scale erosion rates (Bierman, et al., 2008; Reusser, et al., 2008; Willenbring & von Blanckenburg, 2010) but many assumptions have to be valid for this approach to work. Meteoric $^{10}$Be must adhere and remain on the surface of the sediment (Jungers, et al., 2009). The basin needs to be in steady state (Willenbring & von Blanckenburg, 2010). The main uncertainty with applying meteoric $^{10}$Be in the past was determining the delivery rate from the atmosphere to the surface. This had been estimated many ways (Monaghan, et al., 1986). The nominal value of 1.3 x $10^6$ atoms $g^{-1}$ $y^{-1}$ was generally accepted for humid regions (Pavich, et al., 1984). Recently, Graley et al. (2010) compiled numerous measurements and, using the precipitation and latitude relationship with delivery, determined deposition rates of meteoric $^{10}$Be. Because meteoric $^{10}$Be moves in the soil profile, pedogenic rather than nuclear processes control meteoric $^{10}$Be concentration at the surface and its depth distribution and concentration changes over time and space (Graly, et al., 2010).

Meteoric $^{10}$Be has larger concentrations in the B horizon of well-developed soils than the A horizon (Jungers, et al., 2009; Graly, et al., 2010) or there can be larger concentrations of meteoric $^{10}$Be at the top of the soil with a steady decline deeper into the soil (Graly, et al. 2010). These two profiles can affect the timescale reflected by the meteoric $^{10}$Be from a sample. The profile with a large amount of meteoric $^{10}$Be in the B horizon then the timescale is the same as in in situ applications (von Blanckenburg, 2005). If the largest concentrations are found at the surface the timescales reflected are potentially much shorter (Willenbring & von Blanckenburg, 2010).

Meteoric $^{10}$Be may not remain adhered to grains. Graley et al. (2010) showed that soils with a pH below 3.9 inhibit meteoric $^{10}$Be accumulation but Pavich, Brown and Harden, et al. (1986) show that a significant amount still accumulates. Valette-Silver et al. (1986) in lab tests showed Be starts to become mobile at a pH of 5.2 and fully mobile around a pH of 4. However, Takahashi (1999) showed that Be does not become mobile until the pH equals 2. The ability of the soil to incorporate cations, including Be, can be quantified empirically as the cation exchange capacity (CEC) which is directly related to pH (Birkeland, 1999). A significant portion of meteoric $^{10}$Be found in the soil attaches to organic matter, clays, or oxyhydroxides via the CEC (Barg, et al., 1997). The reason pH is so important is that the lower the pH the lower the CEC and therefore the less meteoric $^{10}$Be the soil can sorb.

Another potential factor that could affect the amount of meteoric $^{10}$Be found in a sample is grain size. It stands to reason the two samples of equal size but different grain

sizes would have different concentrations of meteoric $^{10}$Be because the sample with smaller grain sizes has a larger surface area for the meteoric $^{10}$Be to sorb on.

### *Controls on Sediment Generation and Yield*

Suspended sediment concentrations, measured at gaging stations, when convolved with flow data, provide estimates of modern rates of sediment yield (Judson, 1968; Judson & Ritter, 1964; Gellis, et al., 2004). Three main factors control sediment yield: land cover, climate, and rock erodability (Holeman, 1968). Many contemporary land-use practices, including agriculture, construction, mining, and the clear-cutting of forests, increase short-term sediment yields (Costa, 1975; Hewawasam, et al., 2002; Jennings, et al., 2003; Noren, et al., 2002; Wolman & Schick, 1967). Damming rivers and streams temporarily lowers sediment yields downstream from the dams (Merritts & Walter, 2003). Much of the sediment eroded from hill slopes resides on colluvial footslopes, in alluvial fans, and in river terraces for centuries or more, slowing transport out of the basin (Schumm, 1977; Trimble, 1977; Walling, 1983). Conversely, some sediment rapidly moves through the system because of agriculture, construction, or mining (Wilkinson & McElroy, 2007).

Sediment yield describes how much sediment is exported from a basin (Evans, et al., 2000). Sediment generation rates describe how rapidly the creation of sediment occurs in the basin. Equating sediment yield and sediment generation implies steady-state behavior and assumes no change in the volume of sediment stored within a basin, an assumption repeatedly questioned for short time scales (Meade, 1969; Trimble, 1977;

Trimble, 1999; Walling, 1983). The timescales of sediment generation measurement and modern sediment yield present a problem. Sediment generation rates represent timescales of $10^3$ to $10^6$ years (Brown, et al., 1995; Bierman & Steig, 1996; Granger, et al., 1996), while sediment yields are typically on the scale of 10 to 100 years depending on how long the river has been monitored (Kirchner, et al., 2001). Tomkins et al. (2007) discovered this first hand when they calculated modern denudation rates that are about 25% as large as the long-term denudation rates in Southeastern Australia. They determine there must be "high-magnitude, low frequency extreme events" that has not been recorded in the modern record therefore causing the modern sediment export rates to be much lower than the long-term denudation rates. Gardner et al. (1987) showed analytically that there can be up to an order of magnitude difference between modern denudation rates and long-term denudation rates caused by the difference in timescale.

When there are high sediment generation rates and low sediment yields, a large amount of sediment is produced and stored in the basin. When sediment yield is high and sediment generation rates low, sediment leaves the basin faster than it is generated. Brown et al. (1988) examined whether basins, in the Chesapeake Bay Watershed, were generating more sediment or losing more sediment than was being exported than was by calculating an erosion index. First, the deposition rate of meteoric $^{10}$Be in a basin must be determined. Second, the amount of meteoric $^{10}$Be leaving the basin must be determined by convolving measured meteoric $^{10}$Be concentration in river sediments with contemporary sediment yields. Brown et al. (1988) used the equation below to calculate

the erosion index. *A* is the basin area in $cm^2$; *SL* is the average annual sediment load in g $yr^{-1}$, *M* is the concentration

$$EI = \frac{SL*M}{A*Q} \qquad \textbf{Equation 2-1}$$

of meteoric $^{10}Be$ in the sample in atoms $g^{-1}$ and *Q* is the deposition rate of meteoric $^{10}Be$ in atoms $cm^{-2}$ $y^{-1}$. The erosion index (*EI*) is unitless. Theoretically, if more meteoric $^{10}Be$ enters the basin than leaves, sediment yield would be lower than sediment generation and the erosion index would be less than 1. If less meteoric $^{10}Be$ enters the basin than leaves, sediment yield would be higher than the sediment generation and the erosion index would be greater than 1.

In reality, erosion indexes are complicated. They measure whether more meteoric $^{10}Be$ is entering the basin or leaving the basin. In a perfect system this would be a good proxy for sediment generation and sediment yield. For the erosion index to work correctly when meteoric $^{10}Be$ is deposited in a basin it must stay near the top layer of soil and in many systems it is found mostly in the B horizon of the soil (Jungers, et al., 2009; Graly, et al., 2010). Also, the sediment moving in the streams must be coming from the top of the soil column, which cannot be guaranteed in many systems. Because of these uncertainties, erosion indexes are uncertain.

In the southern and central Appalachian highlands, sediment yield and sediment generation rates appear well matched (Matmon, et al., 2003; Reuter, et al., 2006). Other regions show large differences between sediment yield and sediment generation,

including previously glaciated regions of Europe (Scaller, et al., 2001), parts of Idaho (Kirchner, et al., 2001), agriculturally affected tropical highlands (Hewawasam, et al., 2002), the heavily farmed mid-Atlantic Piedmont (Reuter, et al., 2006) and the passive margin of Western Australia, which experiences wildfires and flooding (Tomkins, et al., 2007). These findings suggest both human modification of landscapes (Hewawasam, et al., 2002; Reuter, et al., 2006), and natural variability in sediment delivery (Kirchner, et al., 2001) share responsibility for these differences.

### *Geomorphic Models of Appalachian Landscape Evolution*

Many geomorphologists have created models to describe the evolution of the Appalachian Mountains. William Morris Davis and John Hack have developed the most commonly referenced models. Davis' *Geographic Cycle* (1899) evolved from his observations in the Susquehanna River Basin and the Appalachian Mountains. Davis' (1899) model is based on the peneplain concept and suggests that in an undisturbed landscape, the land will erode over time, until the land is completely flat. Hack's model (1960) of *dynamic equilibrium* suggests the morphology of the landscape reflects erosional resistance of the underlying rock over the long-term. Hack's model theorizes that differences in the erosional resistance of rocks are compensated for by slope; the stronger the lithology, the steeper the slope and the weaker the lithology, the shallower the slope.

## *Past Erosion Rate Studies*

Many previous projects have determined in situ $^{10}$Be estimates of erosion rates in the Appalachian Mountains (Matmon, et al., 2003; Reuter, et al., 2006; Duxbury, 2009; Sullivan, 2007). All of the results presented in this section reflect values published in Portenga and Bierman (2011). Portenga and Bierman (2011) recalculated all of the erosion rates using standard methods.

### *Reston, Virginia, 1996*

Lal et al. (1996) measured in situ produced cosmogenic $^{14}$C and $^{10}$Be in quartz chips taken from a quartz vein in a soil profile near Reston, Virginia. They calculated erosion rates around 30 m My$^{-1}$ using $^{14}$C and 3 m My$^{-1}$ using $^{10}$Be. The large difference in erosion can be explained by non-steady erosion. The quartz vein eroded at the slower of the two rates and was then covered in soil. Then, erosion started to occur at the pre-burial rate again. In terms of the general erosion of the Piedmont, these erosion rates suggest that the Piedmont may have experienced short-term cycles of rapid deposition followed by erosion that removed the recently deposited soil.

### *Mammoth Cave National Park, 2001*

Granger et al. (2001) used in situ $^{26}$Al and $^{10}$Be to examine incision of the Green River in Kentucky from the Pliocene to the Pleistocene. The cosmogenic $^{26}$Al and $^{10}$Be were measured in fluvial sediments collected from different levels of Mammoth Cave, Kentucky. The sediments record the former water table positions resulting from incision

and aggradation of the Green River. Drainage reorganizations and major climate changes correlate well with the incision history of the Green River. Measurements of the cosmogenic isotopes indicate that the sandstone uplands have been eroding at a rate of 2–7 m $My^{-1}$ over the last 3.5 million years. There were increased river incision rates during the Pleistocene of around 30 m $My^{-1}$.

***The Great Smoky Mountains National Park, 2003***

Matmon et al. (2003) determined erosion rates using in situ $^{26}Al$ and $^{10}Be$ in the Great Smoky Mountains National Park. The Great Smoky Mountains, in the humid southern Appalachians, are located between Tennessee and North Carolina. They are the highest mountains in the region. The mountains are composed of medium grade, metamorphosed quartz-rich sedimentary rocks and gneiss that form steep, soil-covered and vegetated slopes. The mean annual rainfall is 140–230 cm. They measured cosmogenic nuclide concentrations in bedrock, alluvial sediments and colluvium. They found erosion rates from 17 to 57 m $My^{-1}$.

***Susquehanna and Potomac Rivers, 2004***

Reusser, Bierman and Pavich et al. (2004) did cosmogenic isotope analysis to investigate rates of fluvial bedrock incision in the Appalachians. Using the Susquehanna and Potomac Rivers, which drain the Atlantic passive margin, they measured the rate and timing of bedrock incision that started 35 ka, at the onset of the last glacial maximum. They discovered that the Susquehanna and the Potomac River Valleys were lowering into

the Piedmont Province. These findings reflect late Cenozoic sea-level fall, slow flexural uplift due to offshore sediment loading, and isostatic response to denudation. They sampled from Holtwood Gorge on the Susquehanna and Great Falls/Mather Gorge on the Potomac. They looked for fluvially eroded bedrock surfaces that were exposed as the rivers incised to lower levels. The samples allowed them to examine the effects of rapidly changing climate on river incision rates. They discovered in situ $^{10}$Be concentrations could be used for direct models of terrace abandonment ages (Reusser, et al., 2004).

The results of Reusser, Bierman and Pavich, et al. (2004) indicate that after 35,000 years ago, incision on both rivers increased markedly (600–800 m My$^{-1}$). The abandonment and exposure of bedrock terraces on the Susquehanna and Potomac Rivers support these findings. The results suggest that the Susquehanna and Potomac Rivers are capable of periodic rapid incision rates 1 to 2 orders of magnitude higher than the long-term incision rates. Reusser, Bierman and Pavich, et al. (2004) believe that this rapid incision occurred during a period of cold, stormy and unstable climate, and that incision rates slowed with the transition to the warmer and more stable Holocene climate.

***Susquehanna River Basin, 2006***

Reuter et al. (2006) worked in the Susquehanna River Basin. They collected fluvial sediments in three physiographic provinces comprising 3 distinct lithologies including sandstone in the Appalachian Plateau, sandstone and shale in the Valley and Ridge, and schist in the Piedmont. Reuter et al. (2006) found erosion rates correlated with slope, but not lithology. The small basins sampled had in situ $^{10}$Be erosion rates of 4–70

m $My^{-1}$ and indicated that steep slopes are eroding faster than shallow slopes. They found erosion rates increase toward the Susquehanna headwaters (Piedmont (6–16 m $My^{-1}$), Valley and Ridge (4–37 m $My^{-1}$), Appalachian Plateaus (7–70 m $My^{-1}$). These findings suggest that the system is exhibiting a transient response to drainage network perturbation and is not in steady state (Reuter, et al., 2006).

***New River, 2005***

Ward et al. (2005) determined the incision history of the New River, in Virginia, using cosmogenic in situ $^{10}Be$ exposure dating. In route to the Gulf of Mexico, the New River flows through crystalline metasedimentary and metaigneous rocks of the Blue Ridge, carbonates of the Valley and Ridge, and clastic and carbonate rocks of the Cumberland Plateau in the Appalachian Mountains. The New River is wider and shallower when flowing through more resistant units, and incises deeply when flowing through less resistant units. They collected terrace soils and bedrock samples at four sites along the New River.

By using cosmogenic radionuclide dating of the terrace soil and bedrock samples, Ward et al. (2005) were able to infer the incision and aggradation history of the New River over the last few million years. The dates help in understanding which variables affect river incision such as; bedrock lithologies, climate and drainage network organization. Around 955 ka, the New River was incising at an average rate of 43 m $My^{-1}$, through alluvial fill and bedrock. There was also punctuated periods of faster downcutting when rates reached around 100 m $My^{-1}$. In between erosion events,

extensive terraces were formed that indicate times of large scale aggradation. Ward, et al. (2005) believe these data point to short periods of disequilibrium where incision rates exceeded the rates of erosion of the surrounding landforms.

***Blue Ridge Escarpment, 2007***

Sullivan (2007) studied the geomorphologic evolution of the Blue Ridge Escarpment, in North Carolina and Virginia, using cosmogenic isotope analysis. They used in situ $^{10}$Be to describe how the Blue Ridge Escarpment has evolved over time. They collected fluvial samples and a bedrock sample of schist, along four transects perpendicular to the Blue Ridge Escarpment. These samples allowed them to investigate what variables may affect the evolution of this landform including; basin slope, relative position of the Brevard Fault Zone, and landscape position. They found basin-averaged erosion rates of 5–49 m My$^{-1}$. The data suggest that the erosion, which shaped the Blue Ridge Escarpment, occurred after rifting in the Mesozoic, around 200 Ma. They discovered a correlation between slope and erosion rate. The data indicates that the escarpment is retreating only very slowly and that the area is lowering at very slow rates.

**Shenandoah River Basin, 2009**

Duxbury (2009) collected 57 samples from the Shenandoah River Basin, a tributary of the Potomac River, including five bedrock samples and 52 fluvial samples. She measured in situ $^{10}$Be concentrations in each sample to determine in situ $^{10}$Be erosion rates. They calculated erosion rates between 3-48 m My$^{-1}$ for the fluvial samples and 2-11

m $My^{-1}$ for the bedrock samples. Duxbury found no correlation between in situ $^{10}Be$ erosion rates and slope and they saw little difference between in situ $^{10}Be$ erosion rates in regions of different rock type. This information supports Hack's (1960) theory of *Dynamic Equilibrium*.

***Dolly Sods, West Virginia, 2007***

Hancock and Kirwan (2007) determined erosion rates using in situ $^{10}Be$ from exposed bedrock on high elevation surfaces in Dolly Sods, West Virginia, and the Appalachian plateau. Dolly Sods, a broad, gently rolling upland, is situated around 300 km southwest of the late Wisconsinin glacial maximum. The bedrock is mainly quartz conglomerates and sandstones. They collected bedrock samples from bedrock blocks, tors, and outcrops. Also, quartz clasts were taken from the conglomerate to determine the erosional history.

The average in situ erosion rate from the bedrock outcrops was 7 m $My^{-1}$. The average in situ $^{10}Be$ erosion rate from the conglomerates was 6 m $My^{-1}$. These data indicate that the erosion at Dolly Sods is slow, despite the fact that it experienced a periglacial climate during parts of the last 2.4 my. These bedrock in situ $^{10}Be$ erosion rates are, on average, much lower than fluvial in situ $^{10}Be$ erosion rates measured in samples from the Appalachians. Hancock and Kirwan (2007) believe that the bedrock erosion rates are low because the region is in disequilibrium. They show that the topographic relief is increasing at a rate of around 10-790 m $My^{-1}$ as evidence of the disequilibrium. The observation of increasing relief is inconsistent with Hack's (1960)

theory which causes them to believe that the Dolly Sods landscape in the process of transitioning to a state of equilibrium. The region must be adjusting to climatically-driven increases in the rates of fluvial incision, which causes the large changes in relief.

### *Potomac and Susquehanna Bedrock, 2010*

Portenga, Bierman and Trodick et al. (2010) collected 72 samples from spur-ridge and ridge-top bedrock outcrops within the Potomac and Susquehanna River Basins and calculated in situ $^{10}$Be erosion rates for each of these samples. 46 samples came from the Potomac River Basin and 26 came from the Susquehanna River Basin. The Potomac erosion rates range from 1 to 66 m $My^{-1}$ and the Susquehanna ranges from 2 to 28 m $My^{-1}$. They discovered similar rates of erosion between the bedrock outcrops from their study and the drainage basins erosion rates from my study. This leads to the conclusion that the Central Appalachians have reached a general state of equilibrium which disagrees with some previous studies (Reuter, et al., 2006; Hancock & Kirwan, 2007).

### *Thermochronology*

Several projects have used thermochronology to determine long-term erosion rates in the Appalachian Mountains. In most thermochronology studies, fission track dating is the technique used. Fission track dating involves analyzing the damage trails left by fission fragments in certain uranium bearing minerals. Typically the dating is done by counting the number of fission events produced during the decay of $^{238}$U in accessory minerals, usually zircon. This allows researchers to determine when the rock cooled

below its closure temperature (Roden, 1991; Pazzaglia & Brandon, 1996; Spotila, et al., 2004; Naeser, et al., 2004). Knowing when the rock reached its closure temperature allows researchers to determine many things about the rock including the age of the rock and the erosion rate of the rock if the geothermal gradient is assumed.

Naeser, et al. (2004) inferred erosion rates of 20 m $My^{-1}$ in the Blue Ridge Province. Pazzaglia and Brandon (1996) found an average erosion rate of 29 m $My^{-1}$ for the entire Appalachians Mountains. Spotila et al. (2004) found erosion rates between 9 m $My^{-1}$–29 m $My^{-1}$ along the Blue Ridge escarpment. Roden (1991) found erosion rates of 16 m $My^{-1}$–36 m $My^{-1}$ in the Southern Appalachian Basin of Maryland, Virginia and West Virginia.

***Implications of Past Studies for Potomac Erosion Rates***

These previous studies make it possible to craft hypotheses about erosion rates in the Potomac Basin. First, the measured erosion rates in the region range from 1 to 70 m $My^{-1}$. Most of my erosion rates should fall in that range. Potomac Basin erosion rates should be most similar to Duxbury's (2009) fluvial samples because they came from the Shenandoah River, a tributary of the Potomac River. Duxbury's (2009) average in situ $^{10}Be$ erosion rate of 11 m $My^{-1}$ should be very similar to my average erosion rate especially in the Blue Ridge Province. Also, I should see clear similarities with Portenga, Bierman and Trodick et al.'s (2010) bedrock samples from the Potomac Watershed. My erosion rates should be similar to their average bedrock erosion rate of 15 m $My^{-1}$ in the Potomac River Basin.

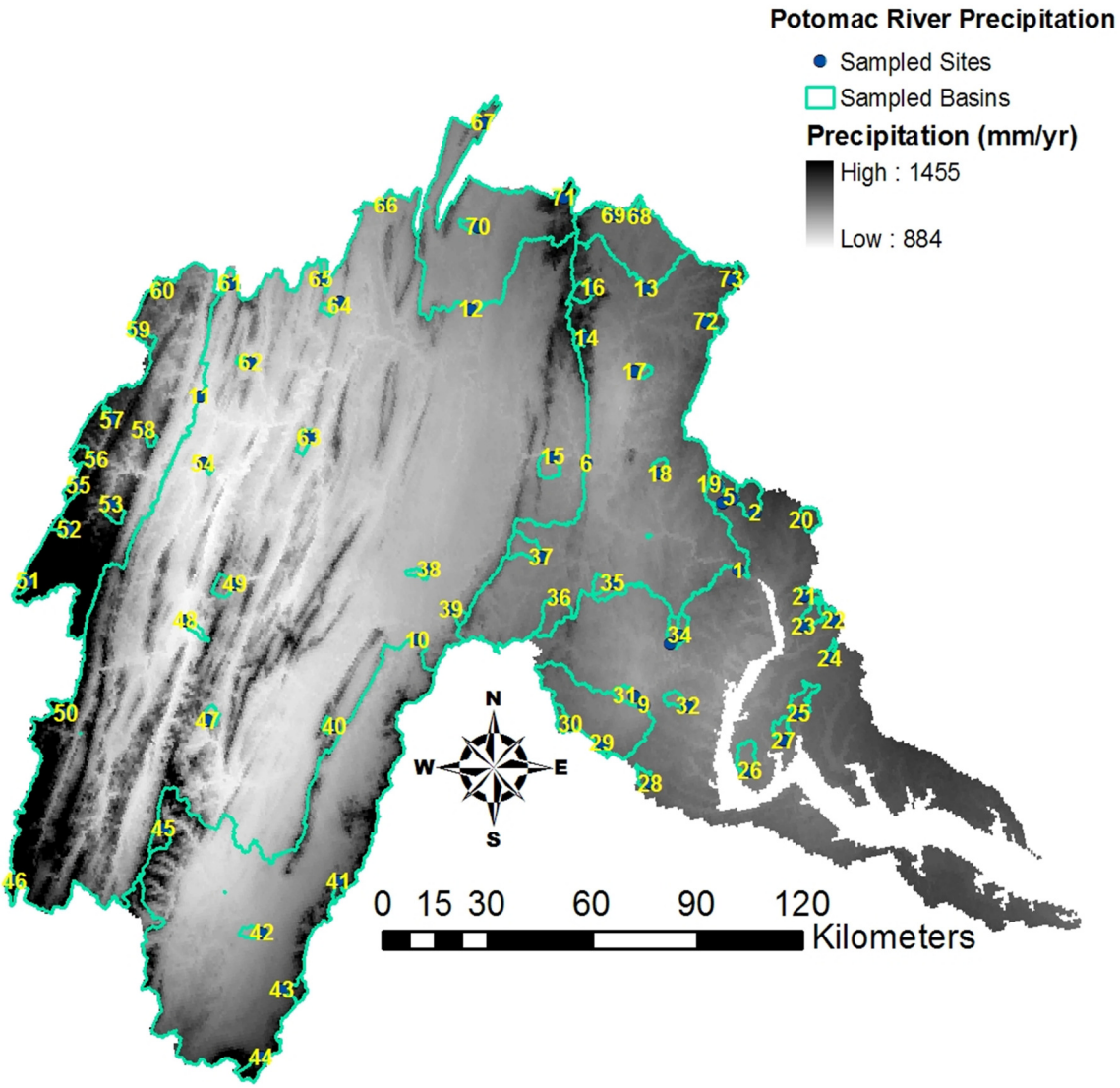


**Figure 2.1 – Precipitation in the Potomac Watershed.**
A map of the Potomac Watershed showing average annual precipitation in millimeters per year; the dark regions have higher rainfall and lighter regions have lower rainfall (from http://worldclim.org/). The turquoise polygons are the sampled basins and the dark blue dots are the sample sites and the yellow labels are the sample number.

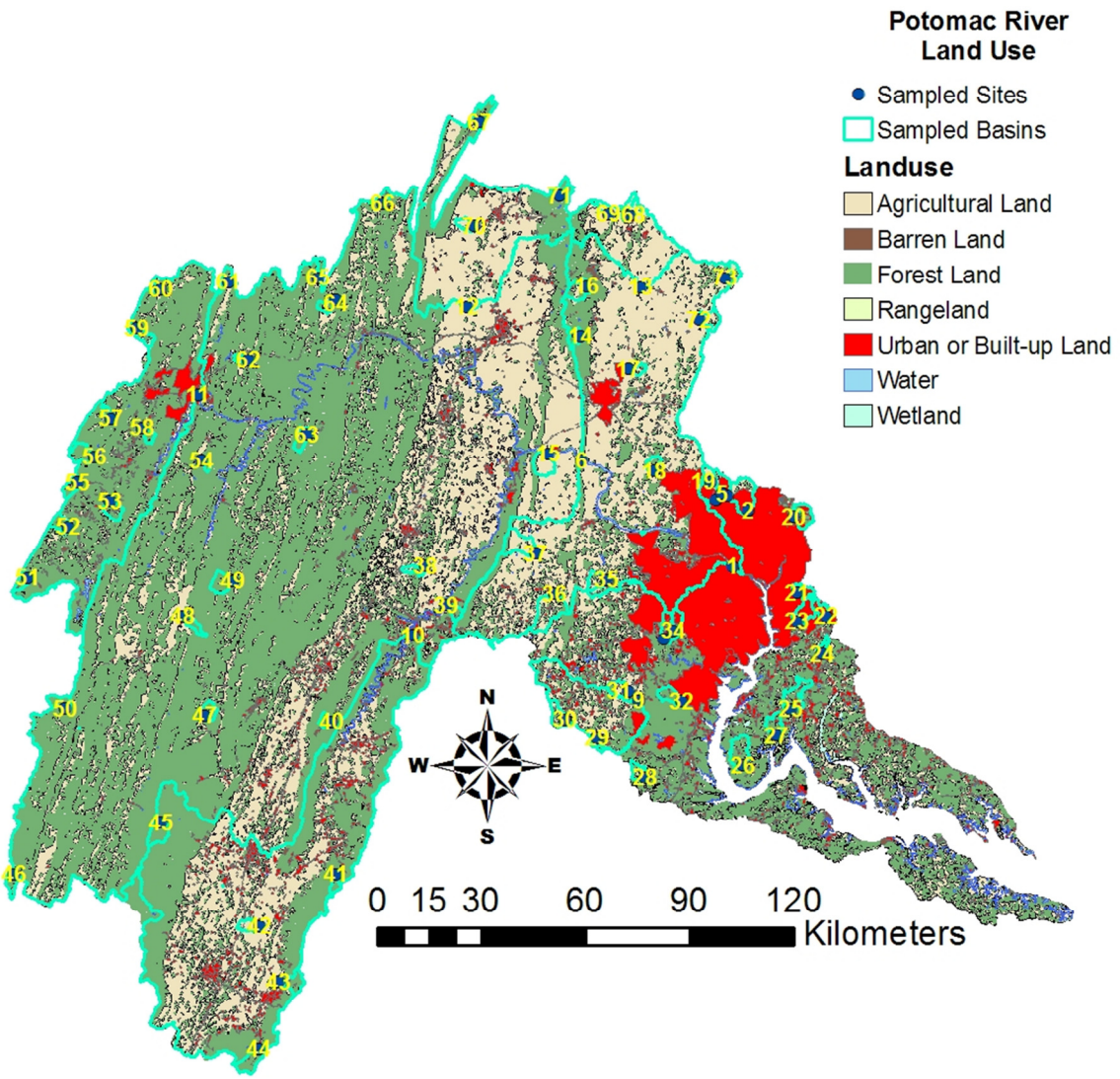


**Figure 2.2 – Land Use in the Potomac Basin.**
A map of the Potomac Watershed showing the different land uses of the region. Red is developed land, light yellow is agriculture land, and green is forest (NOAA, 2010). The turquoise polygons are the sampled basins and the dark blue dots are the sample sites and the yellow labels are the sample number.

# Chapter 3 - Methods

## *Sampling Strategy*

I collected sediment samples from 71 stream and river basins in the Potomac Drainage Basin. I sampled 10 basins at locations with U.S. Geological Survey gaging stations or former gaging stations, which have long-term sediment yield records (Gellis, et al., 2004). In ArcGIS, I split the Potomac Basin into separate physiographic provinces and used a slope DEM to find small river basins. Then, using topographic maps, I found each sampling site and traced its basin. After tracing the basin, I examined it on the topographic map to see if there were potential disturbances within the basin that could affect my sampling, including quarrying and gravel pits. If there were significant disturbances in a basin, I did not sample it. I selected 61 small (5–100 $km^2$) basins of the Potomac River and its tributaries in this manner (Figure 3.1). Basins have different land uses (Figure 2.2), elevation (Figure 3.1) and different mean slopes (Figure 3.2).

At each sampling site, I collected fine sand in the middle of the stream or on point bars and sieved the sand on site to between 250 and 850 µm before collecting 0.5 kg to 2 kg of sample, depending on the amount of quartz in the sample. At each sampling site, I took several pictures, determined the latitude and longitude of the site using GPS and marked the sample site in a Delorme Atlas.

### *Lab Methods*

After collection, samples were returned to the University of Vermont for processing. First, I dried and sieved each sample. Then, I took an aliquot from each sample for meteoric $^{10}$Be analysis and magnetically separated the rest of the sample for in situ $^{10}$Be processing. The in situ $^{10}$Be samples went through repeated ultrasonic etching in hot 6N HCl, followed by dilute HF/$HNO_3$, that dissolves most minerals except quartz (Kohl & Nishiizumi, 1992). The in situ $^{10}$Be samples had all organic material, including coal, removed in a high temperature burn of 500° C for 5 hours. Density separation removed any remaining heavy minerals in the in situ $^{10}$Be samples, before a 7-day, weak acid (HF and $HNO_3$) etch.

Before the final round of processing, the samples went through a quartz purity test. I took a 0.250 gram aliquot of each sample and dissolved it in a concentrated HF/$H_2SO_4$ solution. Then each sample had the HF evaporated off leaving just the dissolved sample in $H_2SO_4$. This solution was diluted with Milliq-Q water (DI water that has been further cleaned) and analyzed on a JY Horiba ICP-OES. The best samples have less than 100 ppm Al, Fe and Ti along with around 10 ppm Na, Ca and K. If samples had more than the desired amounts of any of these elements, they went through another density separation if dark heavy minerals were visible, a 7-day weak acid (HF and $HNO_3$) etch, and return for another quartz purity test.

For in situ $^{10}$Be measurements, I dissolved purified quartz in concentrated HF in the presence of $^{9}$Be SPEX brand carrier. I dried each sample with $HClO_4$ and HCl before

removing Fe by anion chromatography and separating Be with cation chromatography. BeOH was precipitated, dried and burned followed by a mixing with Nb in 1:1 molar ratio before packing into targets for isotopic analysis.

I used a flux-fusion method modified from Stone (1998) to extract meteoric $^{10}Be$, which adheres to the surface of sediment and soil grains, from each of my meteoric $^{10}Be$ samples. First, I powdered the sample and then spiked with $^{9}Be$. Then, I added $KHF_2$ and $Na_2SO_4$ to the sample and fused each sample in a platinum crucible over a natural gas/$O_2$ flame. I removed potassium using $HClO_4$ and cation chromatography removed B. I precipitated $Be(OH)_2$ with $NH_4OH$ and burned each sample to form BeO. I measured beryllium isotopic ratios with an Accelerator Mass Spectrometer (AMS) at the Lawrence Livermore National Laboratory and normalized to standard 07KNSTD3110 with a reported $^{10}Be/^{9}Be$ ratio of $2.85 \times 10^{-12}$ (Nishiizumi, et al., 2007).

Every in situ and meteoric $^{10}Be$ batch that I processed contained one full process blank that was treated the same way as the samples only no sample was added to it. These blanks were run on the AMS along with the other samples. The blank ratios were then subtracted from the ratios of the samples that they were processed with. This corrects for any background $^{10}Be$ in AMS or added in processing. The uncertainty reported with each sample reflects the greater of the internal error (controlled by counting statistics) and the external error (controlled by reproducibility over multiple analyses). A small uncertainty is introduced by the correction made for blanks and boron isobaric interference. For these

samples, both of those corrections are very small and thus introduce minimal uncertainty. None of my sample errors were much over 2%.

### *Data Calculations*

I determined an effective elevation, longitude and latitude for each basin using ArcGIS and Matlab R2010a. Luke Reusser created a model in ArcGIS that exports elevation, longitude, and latitude as ASCII grid files for each cell in any size watershed and elevation datasets of any resolution. I fed the ASCII grid files directly into a Matlab script that determined the effective elevation and latitude needed by the CRONUS calculator, which calculates the erosion rate for each sample (Balco, et al., 2008). The Matlab script reduces the ASCII grid files of elevation and latitude to a single point representing the entire basin. The elevation and latitude grids are used to calculate the ELD scaling factor for each cell. The average scaling factor for all cells, or the effective ELD, is used in conjunction with the actual effective latitude for the basin to back-calculate the corresponding effective elevation (Portenga & Bierman, 2011).

I fed this information along with the final data from LLNL into the CRONUS calculator to determine basin scale erosion rates using the in situ $^{10}$Be data (Balco, et al., 2008). Measured in situ $^{10}$Be concentrations were corrected for basin elevation and latitude based on the scaling scheme of Lal (1991) and Stone (2000). Basin-scale erosion rates were modeled using the interpretive model of Bierman and Steig (1996) with a normalized sea level, high latitude in situ $^{10}$Be production rate of 4.9 atoms g quartz$^{-1}$ yr$^{-1}$, an attenuation depth of 160 g cm$^{-2}$, and assuming a rock density of 2.7 g cm$^{-3}$.

I calculated the deposition rate of meteoric $^{10}$Be in each basin using Equation 2 from Graly et al. (2010), seen below as Equation 3-1. *P* is the annual precipitation in cm of the sample site and *L* is the latitude, in decimal degrees. The calculated deposition rate is in atoms $cm^{-2}$ $y^{-1}$.

$$Q = P * \left(\frac{1.44}{1+e^{(30.7-L)/4.36)}+0.63}\right) \qquad \textbf{Equation 3-1}$$

Next, I needed to normalize my meteoric $^{10}$Be concentrations, because meteoric $^{10}$Be deposition rates vary from basin to basin. Deposition rates vary by latitude and precipitation. Given two basins sitting at different latitudes and experiencing different amounts of precipitation but with all other variables equal, each basin will have different deposition rates. Therefore over a fixed period of time these basins will have different concentrations of meteoric $^{10}$Be in the soil. To normalize my meteoric $^{10}$Be concentrations, I divided each deposition rate by the lowest calculated deposition rate to get ratio between the basin production rate and the lowest observed production rate. Next, I divided each measured meteoric $^{10}$Be concentration by the ratio for each basin. This gives me a normalized meteoric $^{10}$Be concentration, accounting for differing deposition rates between basins. I divided each deposition rate by the lowest calculated deposition rate so concentration in basins with the lowest deposition rates would not change a large amount. I use this concentration for all future analyses of meteoric $^{10}$Be concentrations.

Also, I needed to normalize my in situ $^{10}$Be concentrations, because like meteoric $^{10}$Be deposition rates, in situ $^{10}$Be production rates vary from basin to basin. Production rates vary by latitude and elevation. Given two basins sitting at different latitudes and

elevation each basin will have different production rates. Therefore, these basins will have different concentrations of in situ $^{10}$B even if they are eroding at the same rate. The production rates were determined in the CRONUS calculator (Balco, et al., 2008) and I used the total production rates. To normalize my in situ $^{10}$Be concentrations I divided each basin-specific production rate by 4.9 atoms g quartz$^{-1}$ yr$^{-1}$, the sea level, high latitude in situ $^{10}$Be production rate, to get a ratio between the observed production rate and the expected production rate. Next, I divided each measured in situ $^{10}$Be concentration by the ratio for each basin. This gives me a normalized in situ $^{10}$Be concentration, accounting for differing production rates between basins. I use this concentration for all future analyses of in situ $^{10}$Be concentrations.

For an easier comparison of meteoric and in situ $^{10}$Be normalized concentrations, I divided each normalized concentration by its highest respective normalized concentration. These final standardized data allow for an easy comparison between meteoric and in situ $^{10}$Be normalized concentrations because the standardized concentrations should line up on a 1 to 1 line. Then, as a way to quantify the difference between the standardized in situ and meteoric $^{10}$Be concentrations, I divided the standardized meteoric $^{10}$Be concentration by the standardized in situ $^{10}$Be concentration for each basin. This ratio allows me to determine if any known variables (ex. average slope, annual rainfall, etc.) are potentially affecting the relationship between normalized in situ $^{10}$Be concentrations and normalized meteoric $^{10}$Be concentrations.

I also calculated model erosion rates using my meteoric $^{10}$Be concentrations. I use equation 3-2 below, where M equals my un-normalized meteoric $^{10}$Be concentrations in atoms per gram and $\rho$ equals the density of the rock at 2.7 grams per cm$^2$. $Q$ is the basin specific meteoric $^{10}$Be deposition rate. This equation is the same as equation 21 reported in Willenbring and von Blanckenburg (2010) except the meteoric $^{10}$Be erosion rate (*MER*) is converted to meters per million year.

$$MER = \frac{\frac{Q}{\rho * M}}{10^8} \qquad \textbf{Equation 3-2}$$

I converted my erosion rates, both meteoric and in situ $^{10}$Be, into long-term sediment export rates (*LTSE*) using the units of grams per year to maintain consistency with modern sediment yields. I used the equation below, where *ER* is the erosion rate in meters per million year and $A_m$ is the basin area in m$^2$.

$$LTSE = ER * A_m * \rho \qquad \textbf{Equation 3-3}$$

### *Statistical Analysis*

Most of my data analysis was performed using JMP 9. First, I created box plots of my in situ and meteoric $^{10}$Be erosion rates and examined outliers (Figure 3.3 and Figure 3.4). For the in situ $^{10}$Be erosion rate outliers, I looked back at the sampling sites to see if I possibly collected sediment that either did not come from the basin or did not represent the basin as a whole. All situ $^{10}$Be erosion rate analyses were repeated, with and without the outliers. One outlier sticks out for in situ $^{10}$Be erosion rates, 39 m My$^{-1}$, in the Coastal Plain, POT20. I took the sample just downstream from a U.S. Department of Agriculture

testing site where soil may be imported or disturbed. That possibility combined with the fact that the outlier is 30 m $My^{-1}$ higher than the 2nd highest Coastal Plain in situ $^{10}Be$ erosion rate, 9 m $My^{-1}$, casts doubt on the veracity of the sample.

After doing the initial analysis of the meteoric $^{10}Be$ erosion rates, I discovered 21% were outliers and that 58% of the meteoric $^{10}Be$ erosion rates are at least twice the in situ erosion rates from the same basin. Because of these observations, I did all meteoric statistics on the normalized meteoric $^{10}Be$ concentrations not excluding any outliers.

I did $\log_{10}$ transformations of my in situ $^{10}Be$ erosion rates both with and without outliers. I also, did $\log_{10}$ transformations of my normalized meteoric $^{10}Be$ concentrations with all outliers included. Then, I tested each of the transformations and the original data to determine if they were normally distributed, using the Shapiro-Wilk W Test (Figure 3.5 - Figure 3.10). Next, I chose the most normally distributed group of data or transformations to use for future analysis. In this case, the $\log_{10}$ transformations of the in situ $^{10}Be$ erosion rates including outliers and the normalized meteoric $^{10}Be$ concentrations data had the highest W-Value, meaning they were the closest to normally distributed (Figure 3.6 and Figure 3.10). After the 2 outliers were removed from the in situ $^{10}Be$ erosion rate population the original data was closest to normally distributed (Figure 3.7).

I analyzed both the in situ $^{10}Be$ erosion rates and normalized meteoric $^{10}Be$ concentrations with respect to average slope, basin area, and effective elevation using regression analysis with a 95% confidence interval. I also analyzed both with respect to physiographic province and land use, using one-way ANOVA tests with a 95%

confidence level. I did all of these analyses in the statistical program JMP. I also did basic summary statistics in Excel and created graphs in Matlab. All maps were made in ArcGIS.

### *Updating Brown et al.* (1988)

Brown et al. (1988) collected 45 fluvial sediment samples from USGS gauging stations on rivers flowing into the Chesapeake Bay. Since they originally calculated their meteoric $^{10}$Be concentrations, many things have changed including the value of the $^{10}$Be standard, estimates of the $^{10}$Be half-life, and the estimates of the meteoric $^{10}$Be deposition rate. I updated all of Brown et al. (1988) meteoric $^{10}$Be concentrations, updating the standard from KNSTD to 07KNSTD by multiplying each of Brown et al.'s reported meteoric $^{10}$Be concentrations by 0.9042. Next, I updated their meteoric $^{10}$Be deposition rates by using equation 3.1. I used both the latitude and annual rainfall published in Brown et al. (1988) in this equation. With the new meteoric $^{10}$Be deposition rate for each basin, I normalized Brown et al.'s (1988) meteoric $^{10}$Be concentrations the same way I normalized mine. I was also able to calculate new erosion indices for each of Brown et al (1988) basins using the sediment yields reported in their paper.

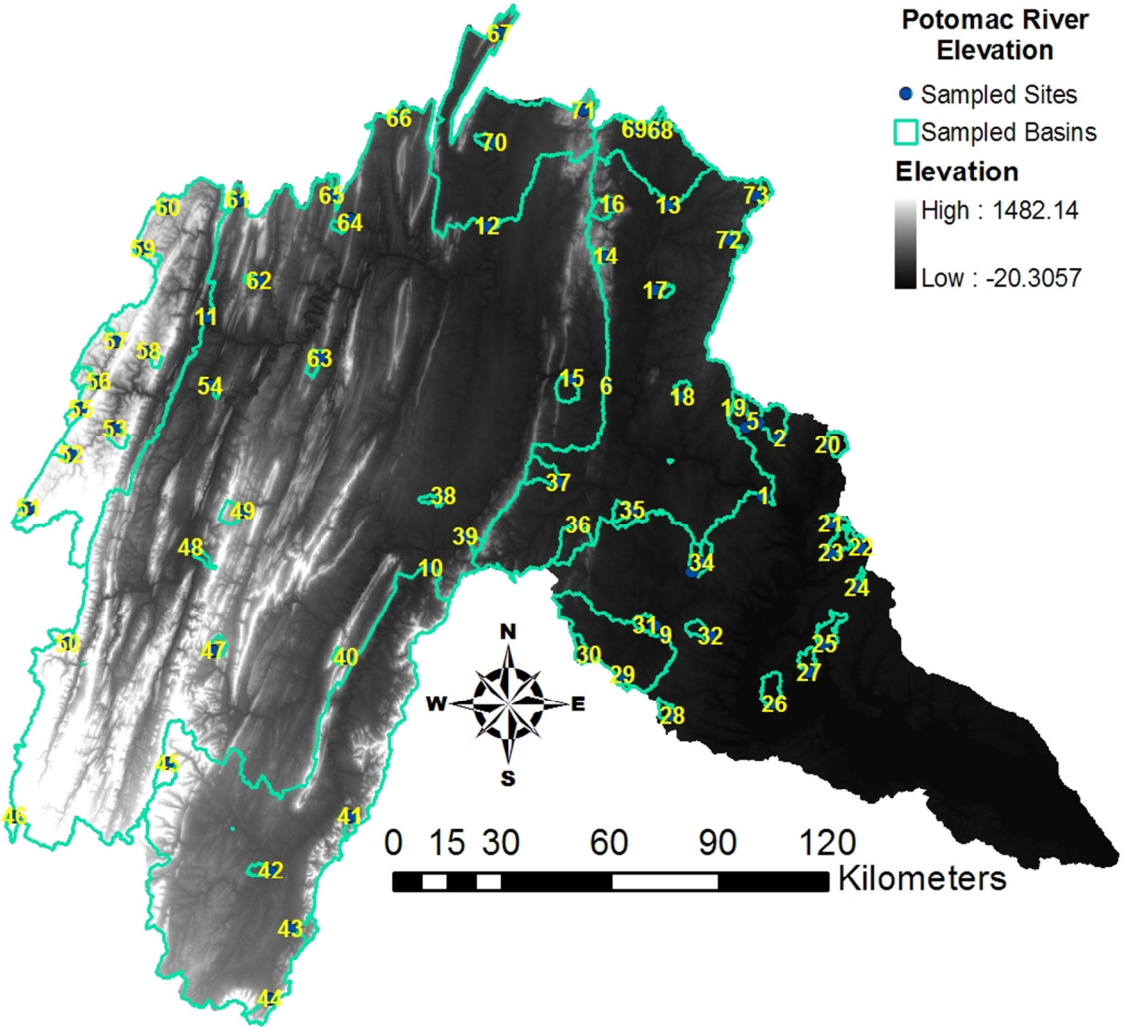


**Figure 3.1 - Elevation in the Potomac Watershed.**
A map of the Potomac Watershed showing the elevation of the land surface in meters, the dark regions have lower elevation and lighter regions have higher elevation (USGS digital data, http://seamless.usgs.gov/). The turquoise polygons are the sampled basins and the dark blue dots are the sample sites and the yellow labels are the sample number.

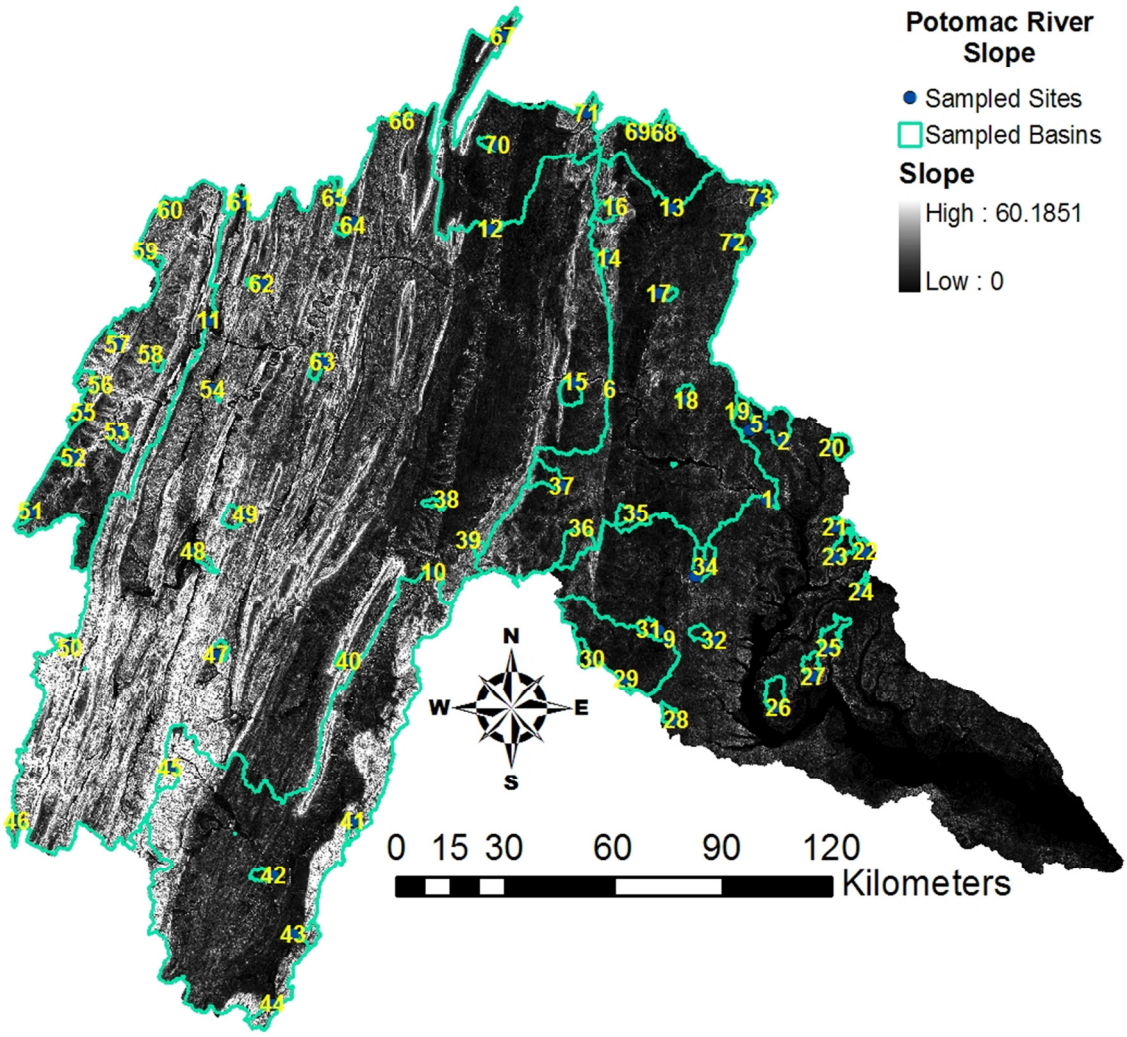


**Figure 3.2 – Slope in the Potomac Watershed.**
A map of the Potomac Watershed showing the slope of the land surface in degrees, the dark regions have lower slope and lighter regions have higher slope (USGS digital data, http://seamless.usgs.gov/). The turquoise polygons are the sampled basins and the dark blue dots are the sample sites and the yellow labels are the sample number.

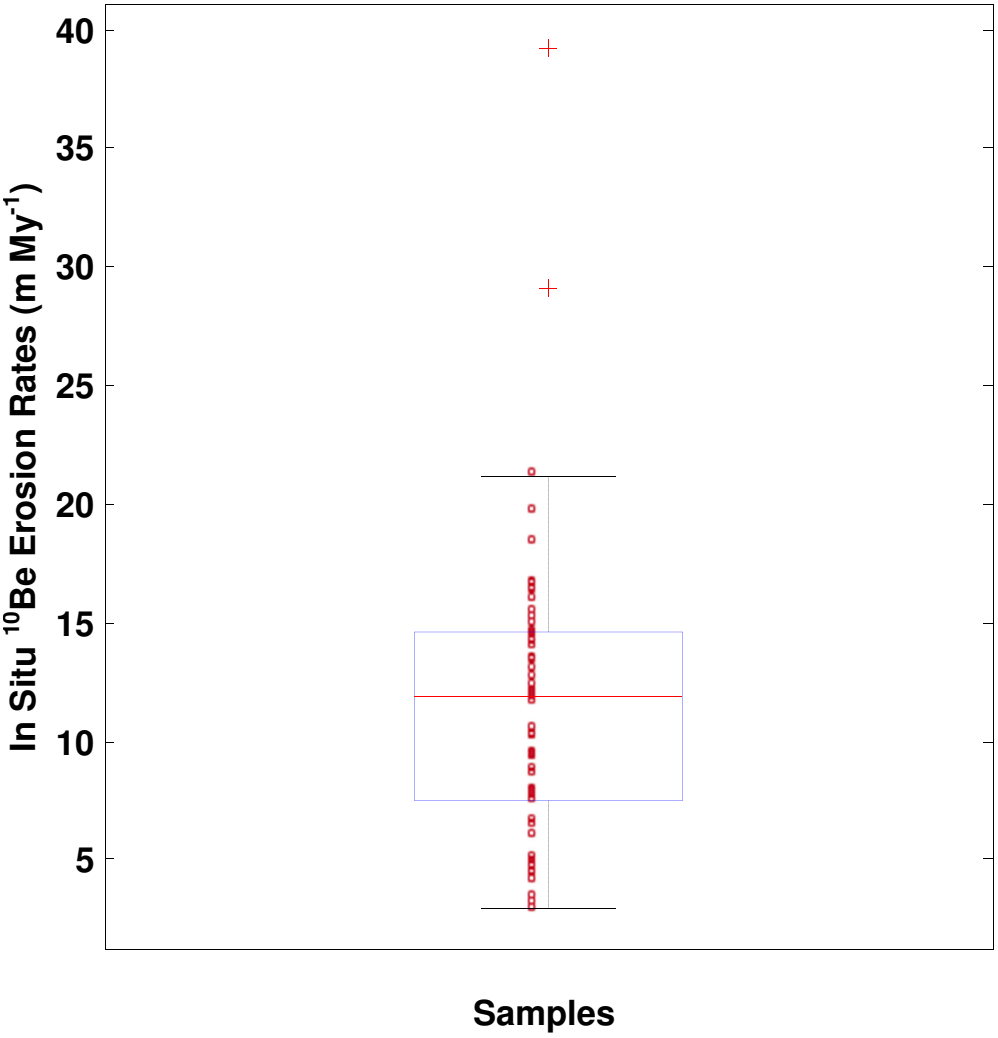


**Figure 3.3 – In Situ $^{10}$Be Erosion Rate Box Plot.**
A box plot of all of Potomac River Basin in situ $^{10}$Be erosion rates. The y-axis is the erosion rate in m My$^{-1}$. The red line in the middle of the box is the median. The bottom of the box is the 25% quartile, and the top of the box is the 75% quartile. The bottom whisker is the 25% quartile - 1.5 * the interquartile range, the top whisker is the 75% quartile + 1.5 * the interquartile range. The interquartile range is equal to the 75% quartile - 25% quartile. All points out side of the whiskers, the red crosses, are statistical outliers. All other data points are small red circles.

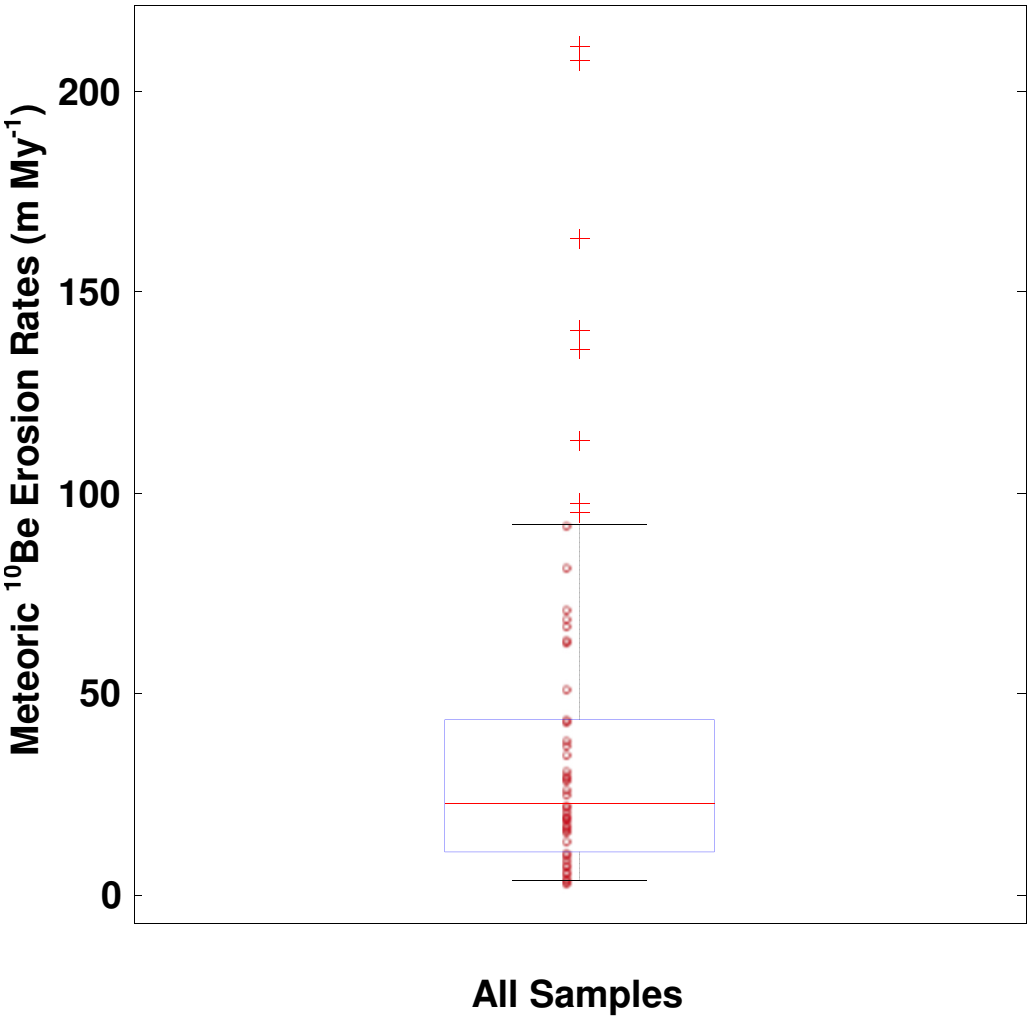


**Figure 3.4 – Meteoric $^{10}$Be Erosion Rate Box Plot.**
A box plot of all of Potomac River Basin meteoric $^{10}$Be erosion rates. The y-axis is the erosion rate in m My$^{-1}$. The red line in the middle of the box is the median. The bottom of the box is the 25% quartile, and the top of the box is the 75% quartile. The bottom whisker is the 25% quartile - 1.5 * the interquartile range, the top whisker is the 75% quartile + 1.5 * the interquartile range. The interquartile range is equal to the 75% quartile - 25% quartile. All points out side of the whiskers, the red crosses, are statistical outliers. All other data points are small red circles.

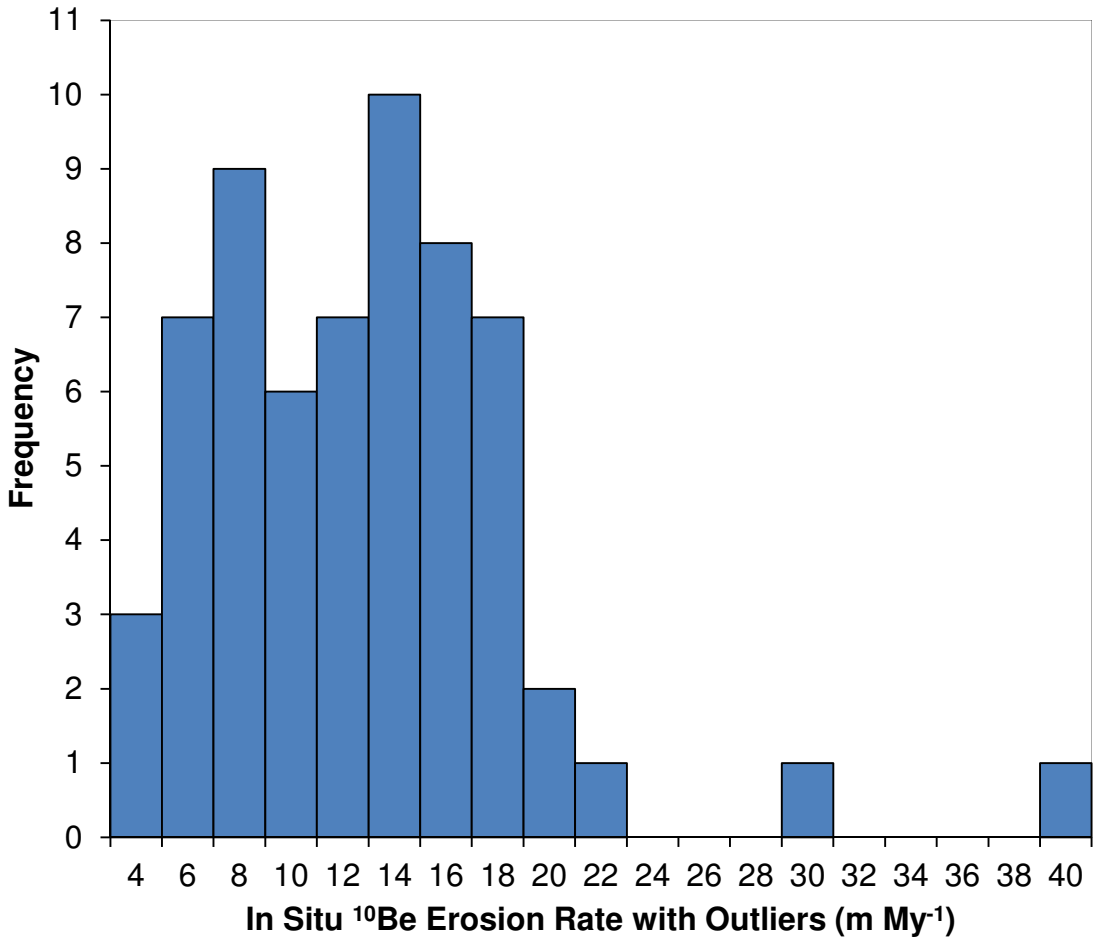


**Figure 3.5 – In Situ $^{10}$Be Erosion Rate Histogram with Outliers.**
A histogram of Potomac River Basin in situ $^{10}$Be erosion rates in m My$^{-1}$ with all outliers included. The analysis shows the data are not normally distributed (W<0.01).

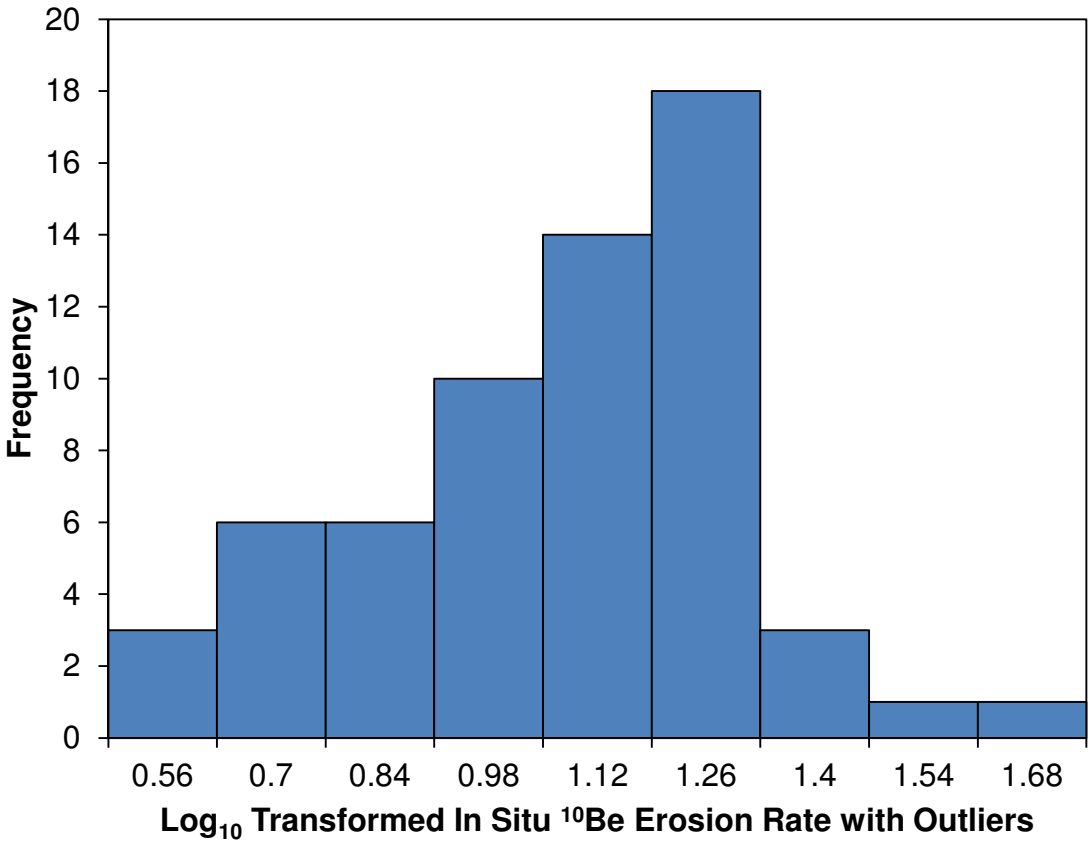


**Figure 3.6 – $Log_{10}$ Transformation of In Situ $^{10}Be$ Erosion Rates Histogram with Outliers Included.**
A histogram of Potomac River Basin $log_{10}$ transformed in situ $^{10}Be$ erosion rates with all outliers included. The analysis shows the data are somewhat normally distributed (W=0.07).

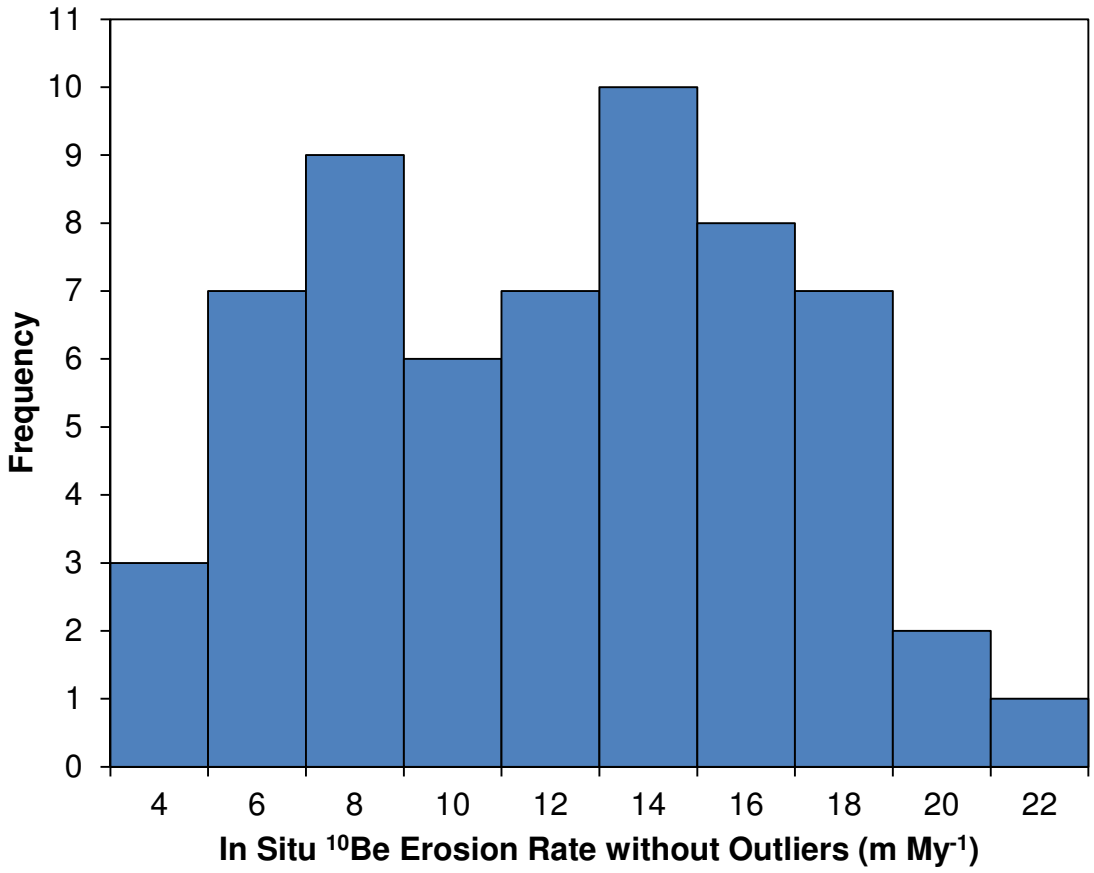


**Figure 3.7 - In Situ $^{10}$Be Erosion Rates Histogram without Outliers.**
A histogram of Potomac River Basin in situ $^{10}$Be erosion rates without 2 outliers. The analysis shows the data are normally distributed (W=0.17).

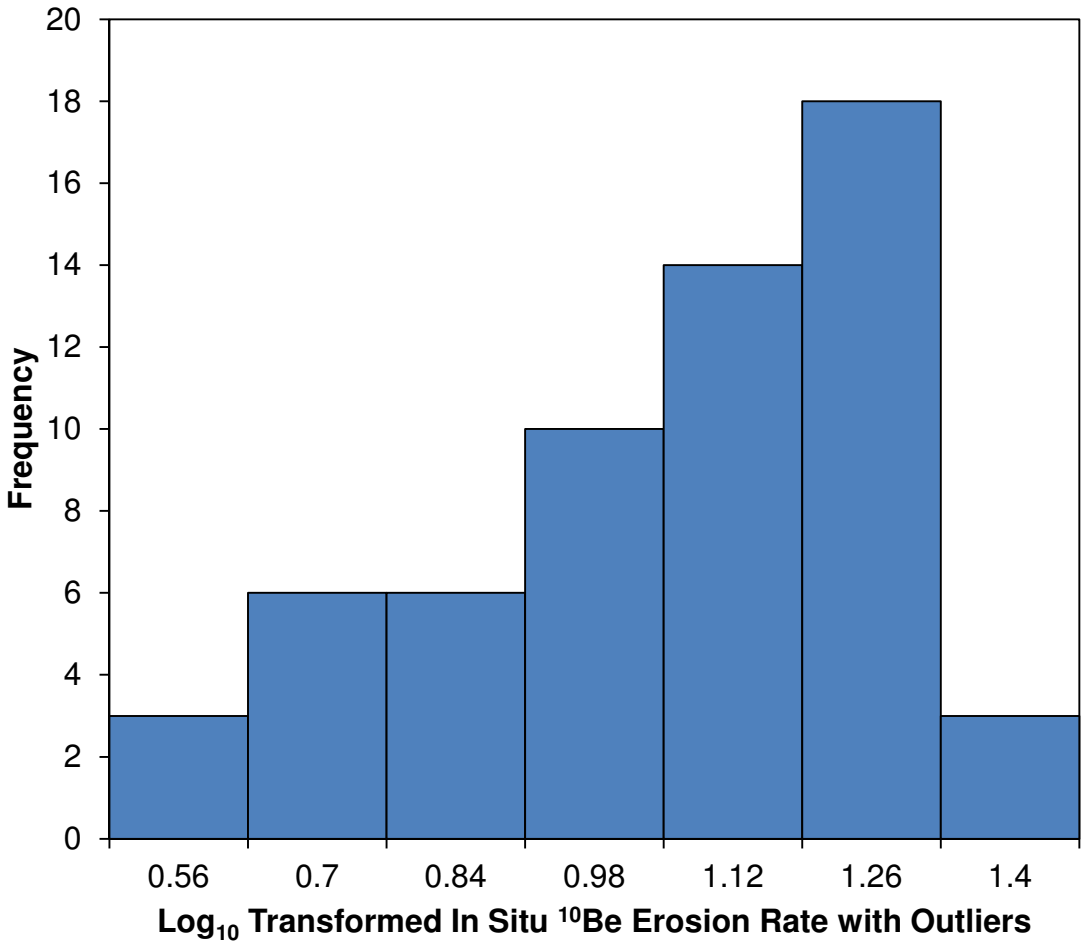


**Figure 3.8 - $Log_{10}$ Transformation of In Situ $^{10}$Be Erosion Rates Histogram without Outliers.**
A histogram of Potomac River Basin $log_{10}$ transformed in situ $^{10}$Be erosion rates without 2 outliers. The analysis shows the data are not normally distributed ($W<0.01$).

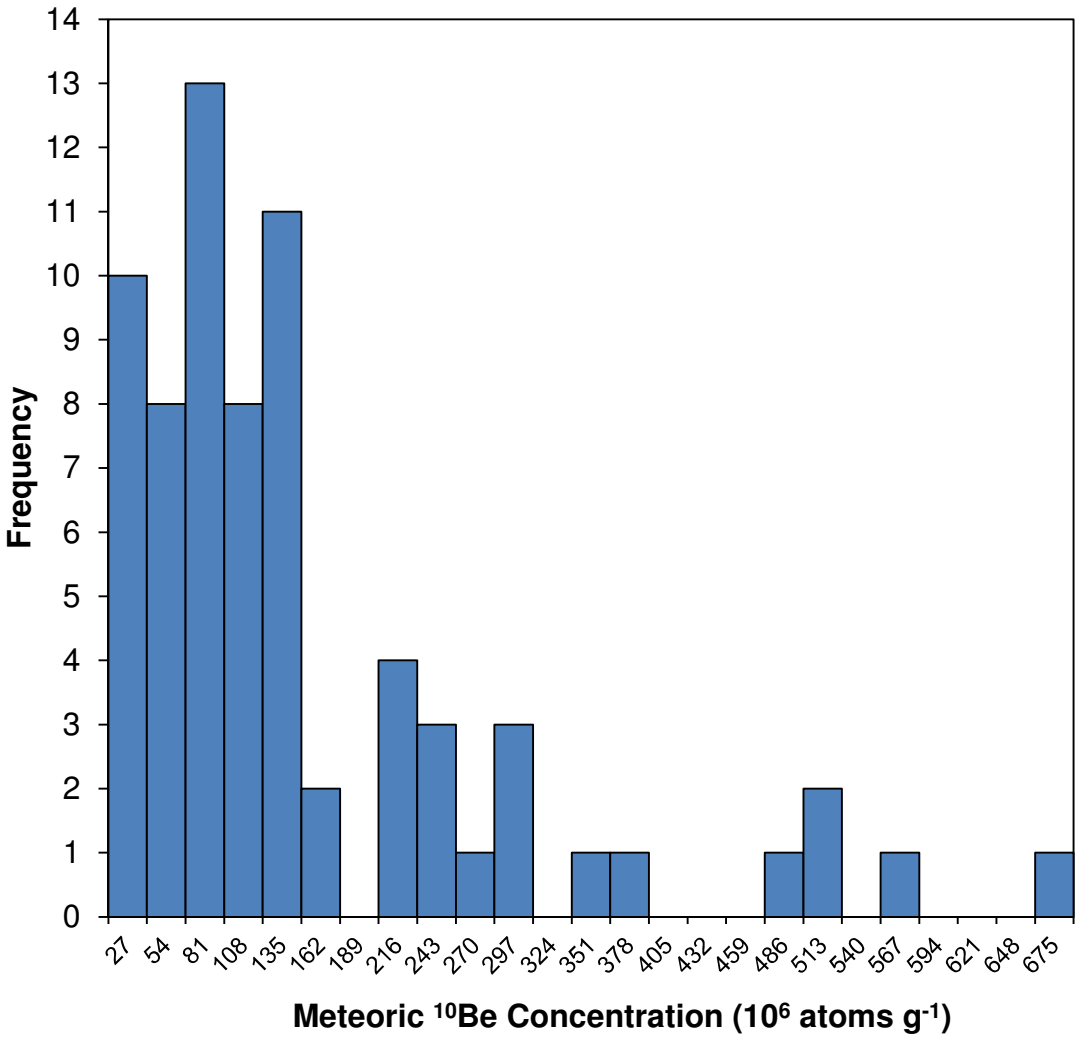


**Figure 3.9 - Meteoric $^{10}$Be Concentrations Histogram of All Samples.**
A histogram of Potomac River Basin meteoric $^{10}$Be concentrations. The analysis shows the data are not normally distributed (W<0.01).

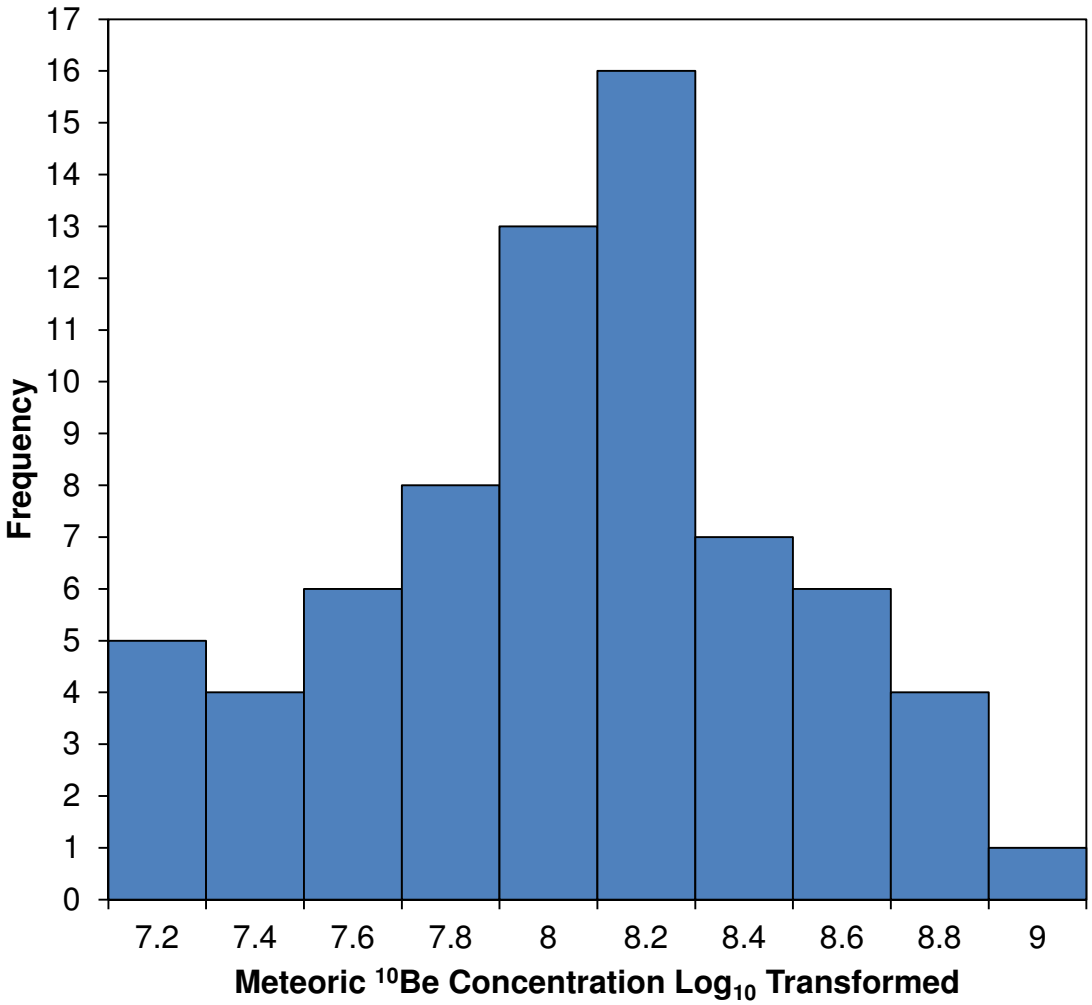


**Figure 3.10 - $Log_{10}$ Transformation of Meteoric $^{10}Be$ Concentrations Histogram of all data included.**
A histogram of Potomac River Basin $log_{10}$ transformed meteoric $^{10}Be$ concentrations. The analysis shows the data are normally distributed (W=0.49).

# Chapter 4 - Data

## *In Situ $^{10}$Be*

Potomac River samples measured for in situ $^{10}$Be ($n$=62) (Table A.1), had a range of normalized, to high latitude and sea-level, $^{10}$Be concentrations from 9.72 x $10^4$ to 9.14 x $10^5$ atoms $g^{-1}$ quartz with a mean of 3.43 x $10^5$ atoms $g^{-1}$ quartz, median of 2.79 x $10^5$ atoms $g^{-1}$ quartz (Figure 4.1 and Figure 4.2). Within each province, in situ $^{10}$Be concentration ranges were: Coastal Plain, 9.72 x $10^4$ to 8.08 x $10^5$ atoms $g^{-1}$ quartz; Appalachian Plateau, 1.69 x $10^5$ to 3.08 x $10^5$ atoms $g^{-1}$ quartz; Blue Ridge, 1.94 x $10^5$ to 3.41 x $10^5$ atoms $g^{-1}$ quartz; Piedmont, 1.66 x $10^5$ to 9.14 x $10^5$ atoms $g^{-1}$ quartz and Valley and Ridge, 1.05 x $10^5$ to 8.18 x $10^5$ atoms $g^{-1}$ quartz (Table 4.1 and Figure 4.3). The larger basins which contain many of the physiographic provinces have $^{10}$Be concentrations of 1.89 x $10^5$ and 2.01 x $10^5$ atoms $g^{-1}$ quartz.

In situ, basin-scale, $^{10}$Be erosion rates range from 3 to 39 m $My^{-1}$ with a mean and median of 12 m $My^{-1}$ and two outliers, one in the Coastal Plain 39 m $My^{-1}$ and one in the Valley and Ridge 29 m $My^{-1}$ (Figure 3.3); the data do not show a normal distribution ($w<0.01$) (Figure 3.5), but when $\log_{10}$ transformed the data become more normally distributed ($w=0.07$) (Figure 3.6). When the outliers are removed, the data are normally distributed (0.17) (Figure 3.7), but when $\log_{10}$ transformed, the data, without outliers, are no longer normally distributed ($w<0.01$) (Figure 3.8). All of the analyses were done on the $\log_{10}$ transformed the data including outliers and the original data without outliers because they were the most normally distributed. When considered by physiographic

province, the erosion rate ranges are: Coastal Plain, 4 to 39 m $My^{-1}$; Appalachian Plateau, 10 to 18 m $My^{-1}$; Blue Ridge, 9 to 16 m $My^{-1}$; Piedmont, 3 to 21 m $My^{-1}$ and Valley and Ridge, 3 to 29 m $My^{-1}$ (Table 4.1 and Figure 4.4). The larger basins, which include many physiographic provinces, have in situ $^{10}Be$ erosion rates of 16 and 17 m $My^{-1}$.

In situ $^{10}Be$ erosion rates, including outliers, show no correlation with slope ($R^2$=0.06, $p$>0.05), but a weak correlation with elevation ($R^2$=0.10, $p$=0.01) (Figure 4.5 and Figure 4.6). The range of in situ $^{10}Be$ erosion rates including outliers changes a lot with basin area but has no correlation ($R^2$=0.02, $p$=0.23) (Figure 4.7). The in situ $^{10}Be$ erosion rates including outliers grouped by physiographic provinces show no statistical inseparability using an ANOVA ($p$=0.13) (Figure 4.4). In situ $^{10}Be$ erosion rates, excluding outliers, grouped by physiographic provinces show the Coastal Plain is statistically dissimilar using ANOVA ($p$<0.01). The other four physiographic provinces show no statistical differences ($p$=0.25) (Figure 4.4). In situ $^{10}Be$ erosion rates, including outliers, show a weak correlation with weighted average and min soil pH, ($R^2$=0.06, $p$=0.049; $R^2$=0.07, $p$=0.04) (Figure 4.8, Figure 4.9) but no correlation with max soil pH ($R^2$=0.05, $p$=0.08) (Figure 4.10).

### *Meteoric $^{10}Be$*

Potomac River Basin samples measured for meteoric $^{10}Be$ ($n$=70) (Table A.1), had a range of normalized $^{10}Be$ concentrations from 1.02 x $10^7$ to 6.62 x $10^8$ atoms $g^{-1}$ sediment with a mean of 1.39 x $10^8$ atoms $g^{-1}$ sediment , median of 9.61 x $10^7$ atoms $g^{-1}$ sediment (Figure 4.11). The data are not normally distributed (w<0.01) (Figure 3.9), but

when $\log_{10}$ transformed, the data becomes more normally distributed (w=0.49) (Figure 3.10). Within each province, meteoric $^{10}$Be concentration ranges were: Valley and Ridge, 3.02 x $10^7$ to 3.42 x $10^8$ atoms $g^{-1}$ sediment; Appalachian Plateau, 3.18 x $10^7$ to 3.68 x $10^8$ atoms $g^{-1}$ sediment; Piedmont, 2.26 x $10^7$ to 2.84 x $10^8$ atoms $g^{-1}$ sediment; Blue Ridge, 1.31 x $10^7$ to 2.31 x $10^8$ atoms $g^{-1}$ sediment and Coastal Plain, 1.02 x $10^7$ to 3.11 x $10^7$ atoms $g^{-1}$ sediment (Table 4.2 and Figure 4.12). The larger basins which flow through many of the physiographic provinces have concentrations of 6.00 x $10^7$ and 6.49 x $10^7$ atoms $g^{-1}$ sediment.

Meteoric, basin-scale, $^{10}$Be erosion rates modeled using the approach of Willenbring and von Blanckenburg (2010) range from 3 to 212 m $My^{-1}$ with a mean of 40 m $My^{-1}$ and a median of 22 m $My^{-1}$ (Figure 3.4). By province, the model erosion rate ranges are: Appalachian Plateau, 6 to 67 m $My^{-1}$; Valley and Ridge, 3 to 71 m $My^{-1}$; Piedmont, 4 to 95 m $My^{-1}$; Coastal Plain, 69 to 212 m $My^{-1}$ and Blue Ridge, 9 to 164 m $My^{-1}$ (Table 4.2 and Figure 4.13). The larger basins, which include many physiographic provinces, have meteoric $^{10}$Be model erosion rates of 36 and 33 m $My^{-1}$.

Normalized meteoric $^{10}$Be concentrations show a weak correlation with slope ($R^2$=0.06, $p$=0.04) (Figure 4.14) and no correlation with elevation ($R^2$<0.01, $p$=0.82) (Figure 4.15). Normalized meteoric $^{10}$Be concentrations show a pattern similar to what others have seen with basin area and in situ $^{10}$Be erosion rates (Duxbury, 2009; Matmon, et al., 2003; Reuter, et al., 2006; Sullivan, 2007), small basins show large variability while large basins show less variability but there is no correlation of concentration with

area ($R^2$<0.01, $p$=0.63) (Figure 4.16). Meteoric $^{10}$Be concentrations in Coastal Plain sediments are statistically dissimilar than the other provinces using ANOVA ($p$<0.01). The other four physiographic provinces have statistically similar meteoric $^{10}$Be concentrations ($p$=0.06) (Figure 4.12). Meteoric $^{10}$Be concentrations show a weak correlation with max and min soil pH, ($R^2$=0.16, $p$<0.01; $R^2$=0.07, $p$=0.03) (Figure 4.17, Figure 4.18) but no correlation with weighted average soil pH ($R^2$=0.02, $p$=0.25) (Figure 4.19).

**Table 4.1 - In Situ $^{10}$Be Summary Statistics**

| | | Normalized In Situ $^{10}$Be Concentrations (atoms g$^{-1}$) | | | | In Situ $^{10}$Be Erosion Rates (m My$^{-1}$) | | | |
|---|---|---|---|---|---|---|---|---|---|
| Province | Amount | Min | Max | Mean | Median | Min | Max | Mean | Median |
| All | 62 | 9.72E+04 | 9.14E+05 | 3.43E+05 | 2.79E+05 | 3 | 39 | 12 | 12 |
| CP | 8 | 9.72E+04 | 8.08E+05 | 5.20E+05 | 5.32E+05 | 4 | 39 | 10 | 6 |
| Pied | 21 | 1.66E+05 | 9.14E+05 | 3.36E+05 | 2.68E+05 | 3 | 21 | 12 | 12 |
| BR | 8 | 1.94E+05 | 3.41E+05 | 2.64E+05 | 2.44E+05 | 9 | 16 | 12 | 13 |
| VR | 17 | 1.05E+05 | 8.18E+05 | 3.60E+05 | 3.24E+05 | 3 | 29 | 11 | 9 |
| AP | 6 | 1.69E+05 | 3.08E+05 | 2.35E+05 | 2.35E+05 | 10 | 18 | 13 | 13 |

**Table 4.2 - Meteoric $^{10}$Be Summary Statistics**

| | | Meteoric $^{10}$Be Concentrations (atoms g$^{-1}$) | | | | Meteoric $^{10}$Be Erosion Rates (m My$^{-1}$) | | | |
|---|---|---|---|---|---|---|---|---|---|
| Province | Amount | Min | Max | Mean | Median | Min | Max | Mean | Median |
| All | 70 | 1.02E+07 | 6.62E+08 | 1.39E+08 | 9.61E+07 | 3 | 212 | 40 | 22 |
| CP | 8 | 1.02E+07 | 3.11E+07 | 1.88E+07 | 1.74E+07 | 69 | 212 | 132 | 125 |
| Pied | 21 | 2.26E+07 | 4.79E+08 | 1.20E+08 | 7.47E+07 | 4 | 95 | 35 | 29 |
| BR | 8 | 1.31E+07 | 2.31E+08 | 9.89E+07 | 8.86E+07 | 9 | 164 | 40 | 24 |
| VR | 21 | 3.02E+07 | 6.62E+08 | 2.07E+08 | 1.20E+08 | 3 | 71 | 20 | 18 |
| AP | 10 | 3.18E+07 | 3.68E+08 | 1.80E+08 | 1.78E+08 | 6 | 67 | 19 | 12 |

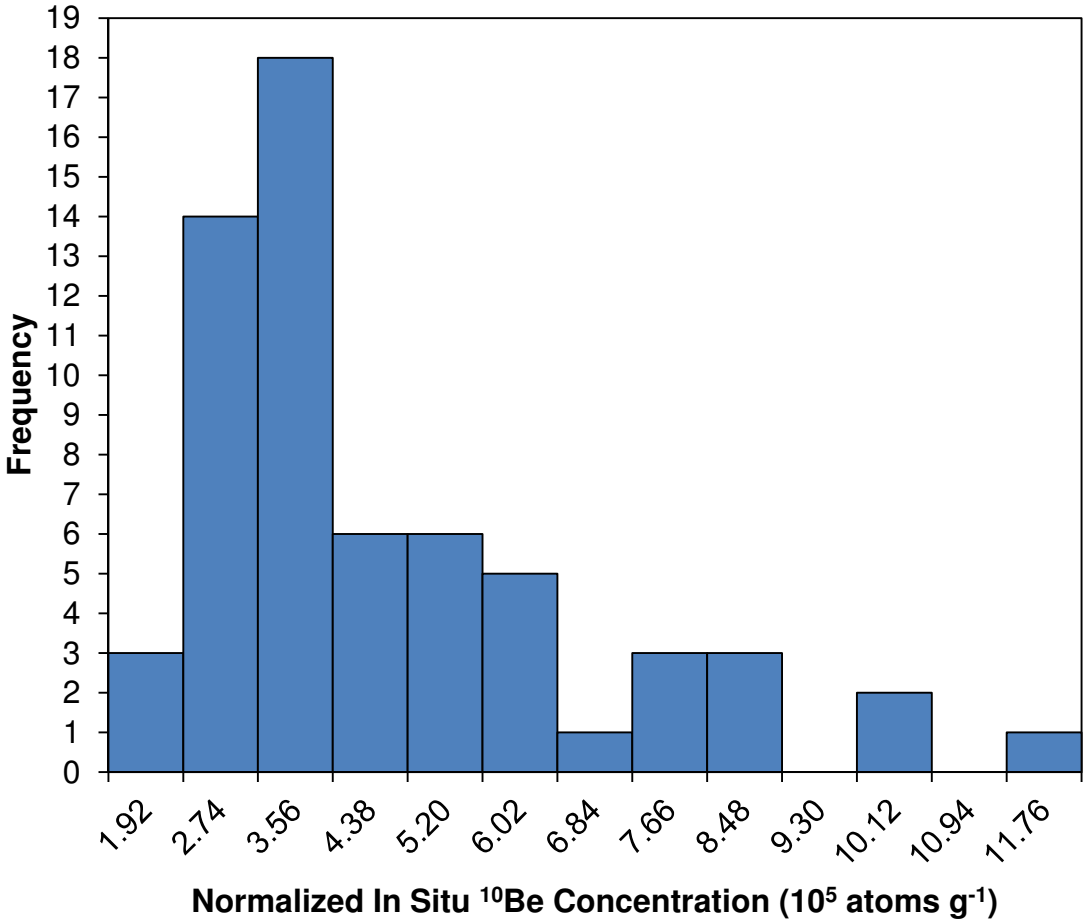


**Figure 4.1 - In Situ $^{10}$Be Concentrations Histogram.**
A histogram showing the variability of normalized in situ $^{10}$Be concentrations from the Potomac River Basin samples. The x-axis shows the ranges of normalized in situ $^{10}$Be concentrations in atoms/g. (W<0.01)

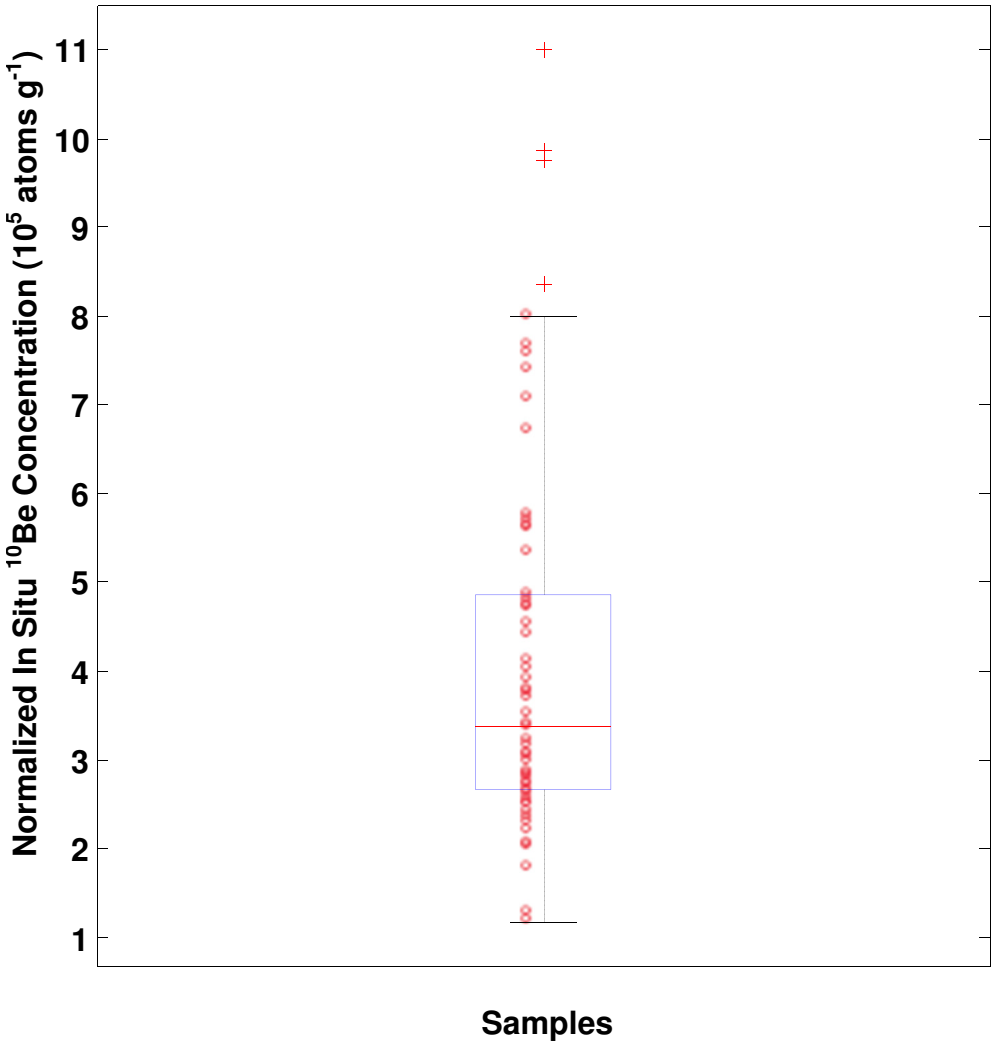


**Figure 4.2 - A Boxplot of all of Potomac River Basin Normalized In Situ $^{10}$Be Concentrations.**
The y-axis is the normalized in situ $^{10}$Be concentrations in atoms g quartz$^{-1}$. The red line in the middle of the box is the median. The bottom of the box is the 25% quartile, and the top of the box is the 75% quartile. The bottom whisker is the 25% quartile - 1.5 * the interquartile range, the top whisker is the 75% quartile + 1.5 * the interquartile range. The interquartile range is equal to the 75% quartile - 25% quartile. All points out side of the whiskers, the red crosses, are statistical outliers if the data are normally distributed. All other data points are small red circles.

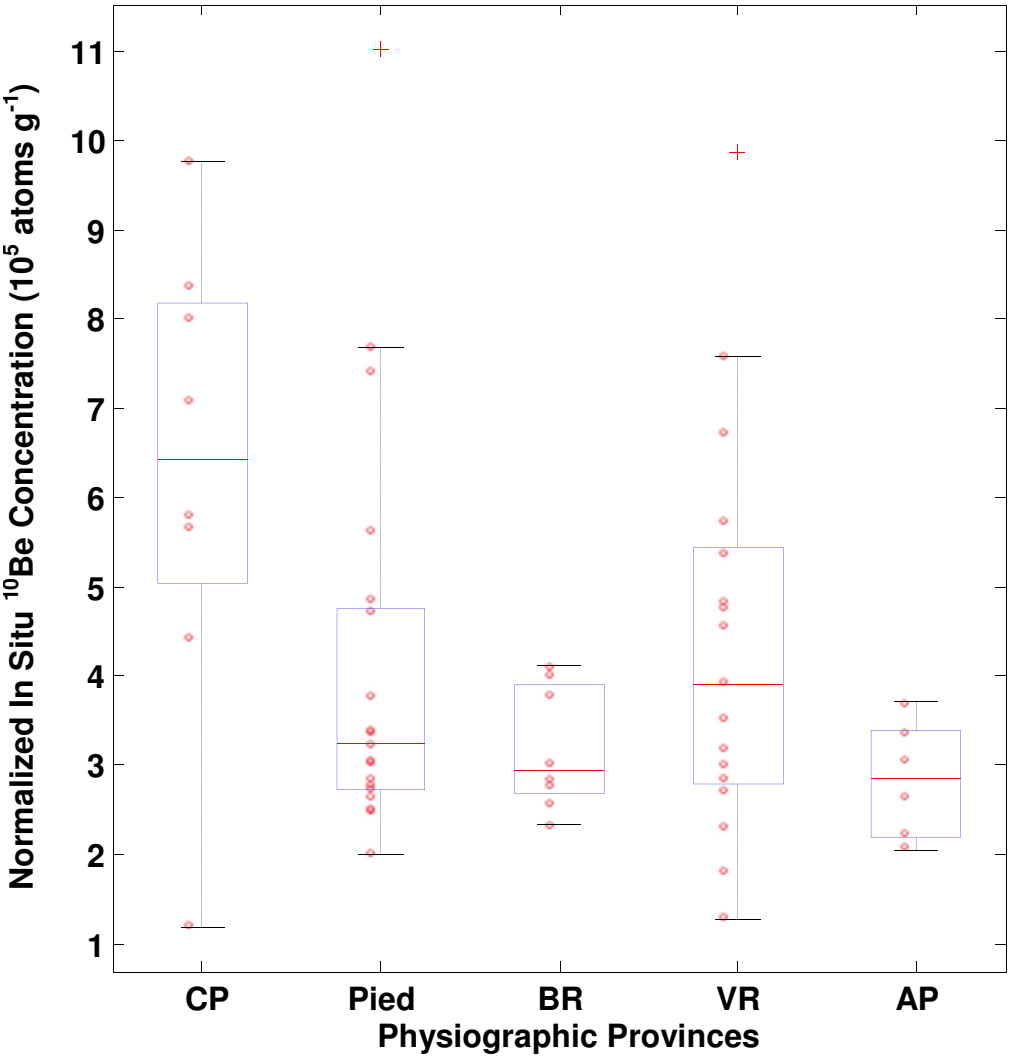


**Figure 4.3 - Normalized In Situ $^{10}$Be Concentration against Physiographic Province.** CP is the Coastal Plain, Pied is the Piedmont, BR is the Blue Ridge, VR is the Valley and Ridge, and AP is the Appalachian Plateau. The y-axis is the normalized in situ $^{10}$Be concentration in atoms g quartz$^{-1}$. The red line in the middle of the box is the median. The bottom of the box is the 25% quartile, and the top of the box is the 75% quartile. The bottom whisker is the 25% quartile - 1.5 * the interquartile range, the top whisker is the 75% quartile + 1.5 * the interquartile range. The interquartile range is equal to the 75% quartile - 25% quartile. All points out side of the whiskers, the red crosses, are statistical outliers if the data are normally distributed. All other data points are small red circles (p=0.02).

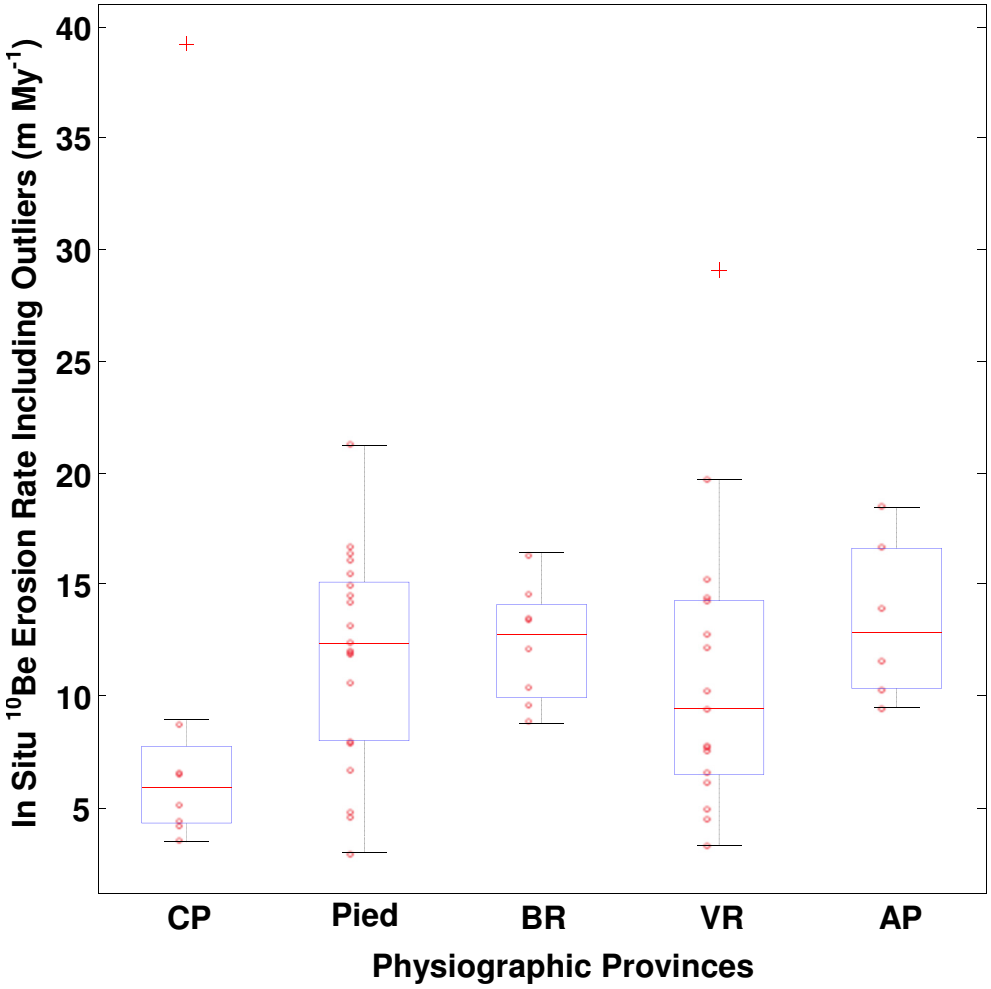


**Figure 4.4 - In Situ $^{10}$Be Erosion Rate Including Outliers against Physiographic Province.**
CP is the Coastal Plain, Pied is the Piedmont, BR is the Blue Ridge, VR is the Valley and Ridge, and AP is the Appalachian Plateau. The y-axis is the in situ $^{10}$Be erosion rate in m My$^{-1}$. The red line in the middle of the box is the median. The bottom of the box is the 25% quartile, and the top of the box is the 75% quartile. The bottom whisker is the 25% quartile - 1.5 * the interquartile range, the top whisker is the 75% quartile + 1.5 * the interquartile range. The interquartile range is equal to the 75% quartile - 25% quartile. All points out side of the whiskers, the red crosses, are statistical outliers if the data are normally distributed. All other data points are small red circles (with outliers p=0.14, without outliers p<0.01).

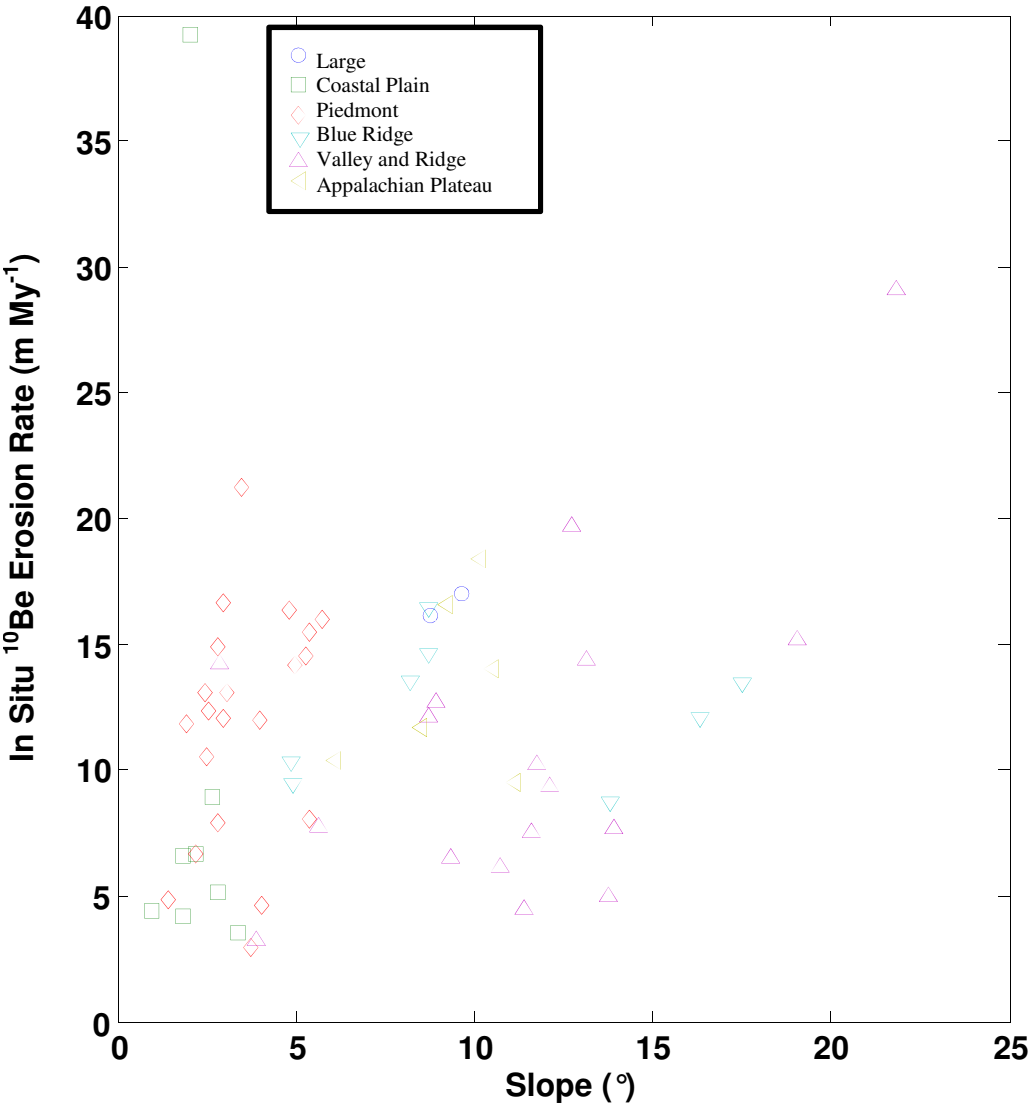


**Figure 4.5 - In Situ $^{10}$Be Erosion Rate Including Outliers against Average Slope.** The y-axis is the in situ $^{10}$Be erosion rate in m My$^{-1}$. The x-axis is the average slope in degrees. The blue circles are samples from large basins that occupy many physiographic provinces. The green squares are from the Coastal Plain, red diamond, Piedmont, turquoise upside down triangle Blue Ridge, purple triangle Valley and Ridge, yellow sideways triangle Appalachian Plateau. In situ erosion rates show no correlation with slope ($R^2$=0.06, $p$>0.05).

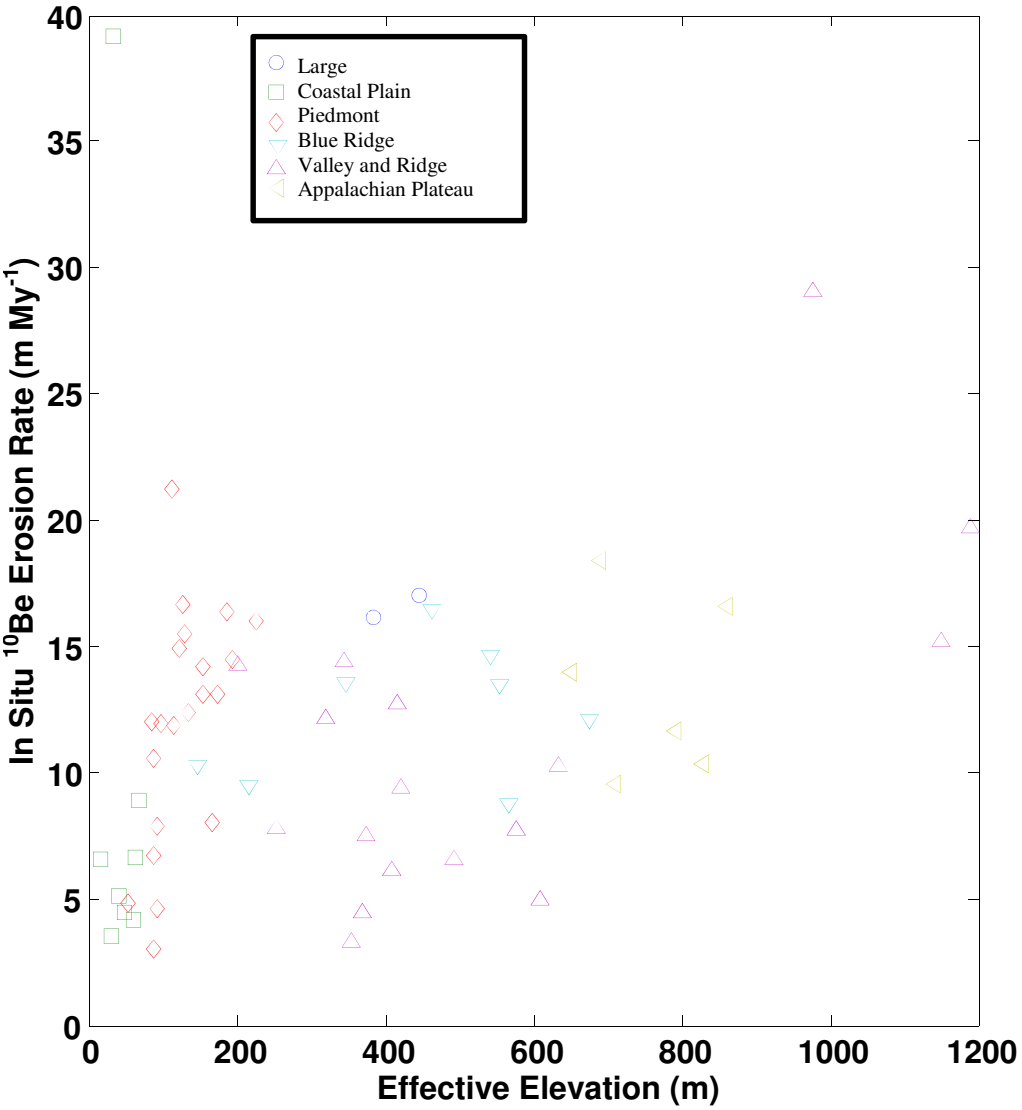


**Figure 4.6 - In Situ $^{10}$Be Erosion Rate Including Outliers against Effective Elevation.** The y-axis is the in situ $^{10}$Be erosion rate in m My$^{-1}$. The x-axis is the effective elevation in meters. The blue circles are samples from large basins that occupy many physiographic provinces. The green squares are from the Coastal Plain, red diamond, Piedmont, turquoise upside down triangle Blue Ridge, purple triangle Valley and Ridge, yellow sideways triangle Appalachian Plateau. In situ erosion rates show a weak correlation with effective elevation ($R^2$=0.09, $p$=0.01).

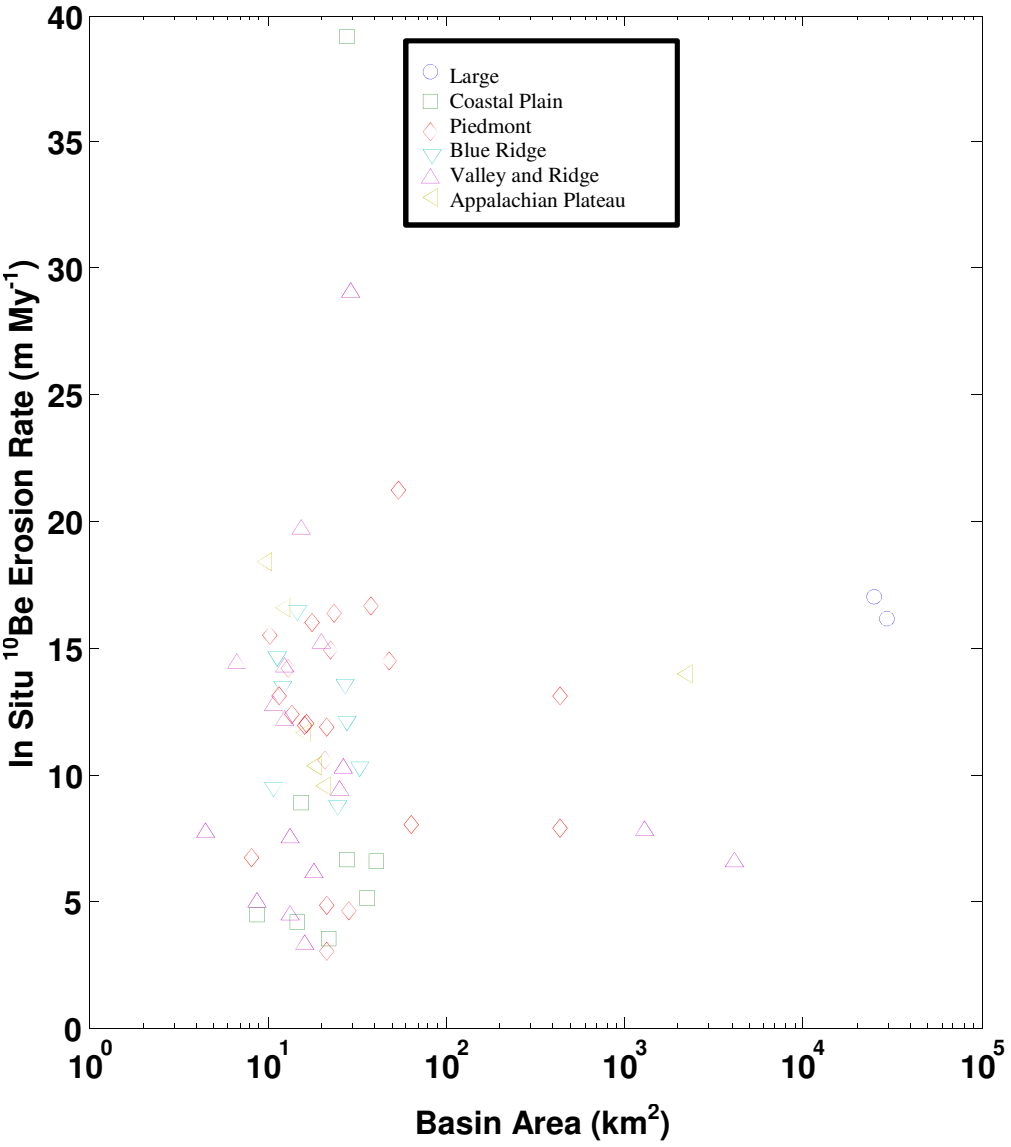


**Figure 4.7 - In Situ $^{10}$Be Erosion Rate Including Outliers against Basin Area.** The y-axis is the in situ $^{10}$Be erosion rate in m My$^{-1}$. The x-axis is the basin area in km$^2$ on a log scale. The blue circles are samples from large basins that occupy many physiographic provinces. The green squares are from the Coastal Plain, red diamond, Piedmont, turquoise upside down triangle Blue Ridge, purple triangle Valley and Ridge, yellow sideways triangle Appalachian Plateau. In situ erosion rates show no correlation with basin area ($R^2$=0.02, $p$=0.23).

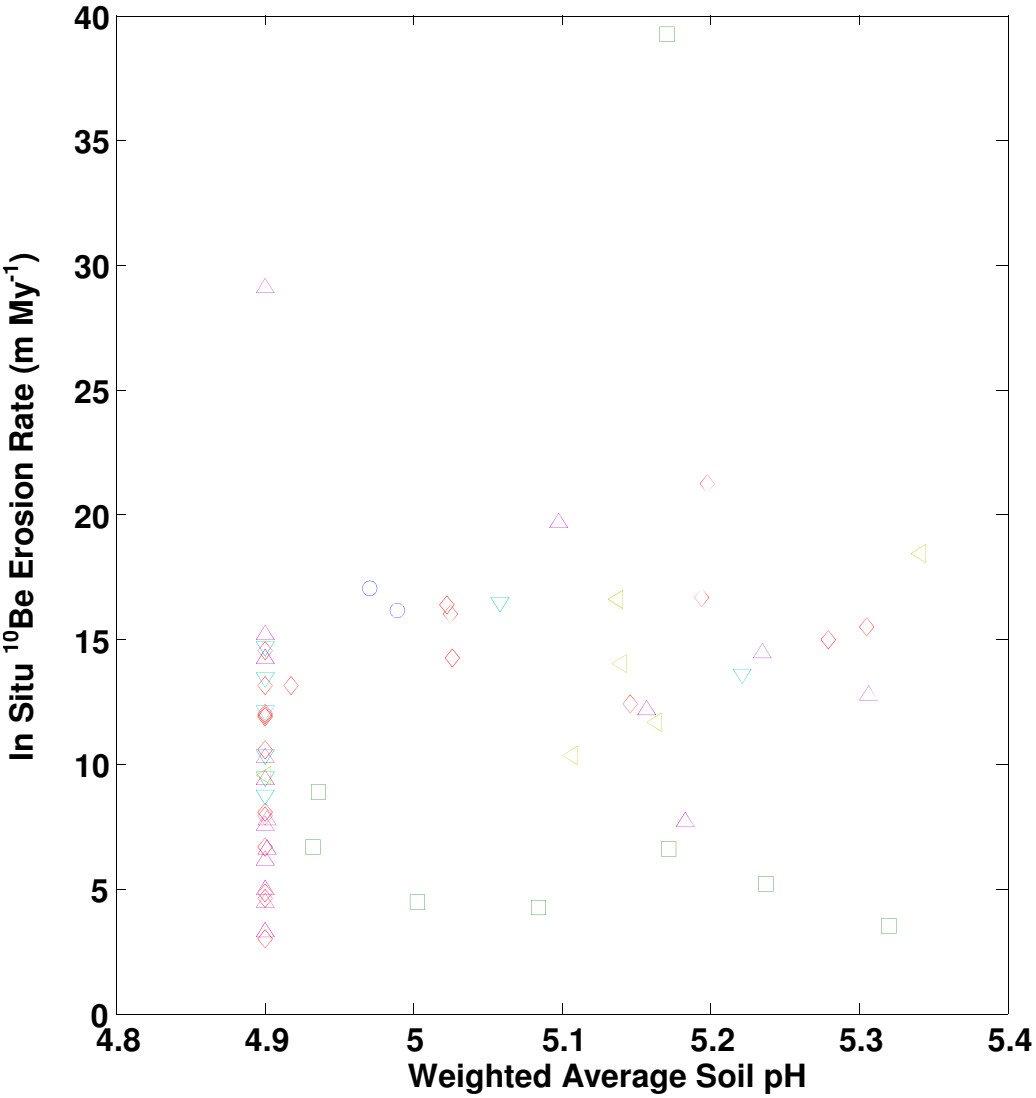


**Figure 4.8 - In Situ $^{10}$Be Erosion Rate Including Outliers against Weighted Average Soil pH.**
The y-axis is the in situ $^{10}$Be erosion rate in m My$^{-1}$. The x-axis is the weighted average soil pH. The blue circles are samples from large basins that occupy many physiographic provinces. The green squares are from the Coastal Plain, red diamond, Piedmont, turquoise upside down triangle Blue Ridge, purple triangle Valley and Ridge, yellow sideways triangle Appalachian Plateau. In situ erosion rates show a weak correlation with weighted average soil pH ($R^2$=0.06, $p$=0.049). Data taken from http://soils.usda.gov/survey/geography/ssurgo/.

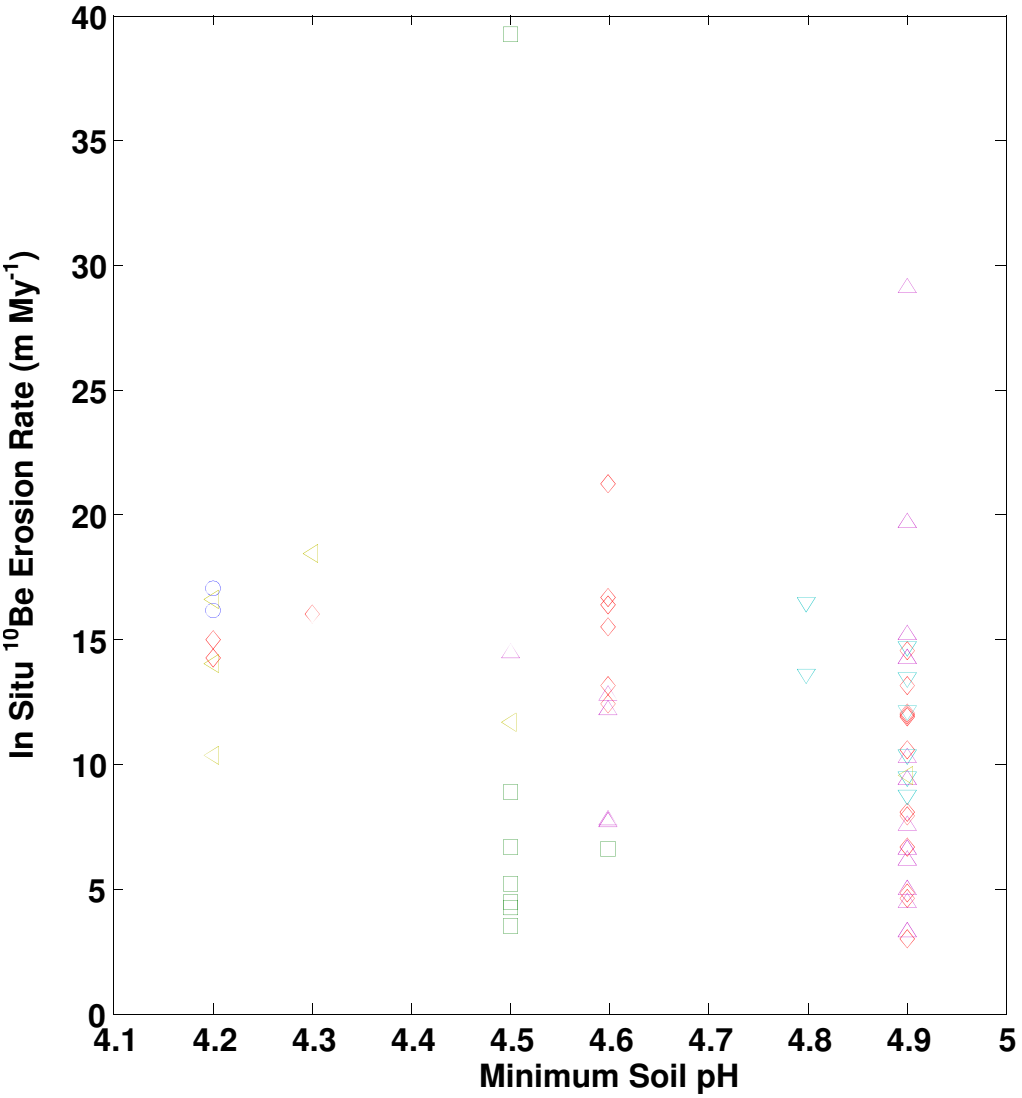


**Figure 4.9 - In Situ $^{10}$Be Erosion Rate Including Outliers against Minimum Soil pH.** The y-axis is the in situ $^{10}$Be erosion rate in m My$^{-1}$. The x-axis is the minimum soil pH. The blue circles are samples from large basins that occupy many physiographic provinces. The green squares are from the Coastal Plain, red diamond, Piedmont, turquoise upside down triangle Blue Ridge, purple triangle Valley and Ridge, yellow sideways triangle Appalachian Plateau. In situ erosion rates show a weak correlation with minimum soil pH ($R^2$=0.05, $p$=0.08). Data taken from http://soils.usda.gov/survey/geography/ssurgo/.

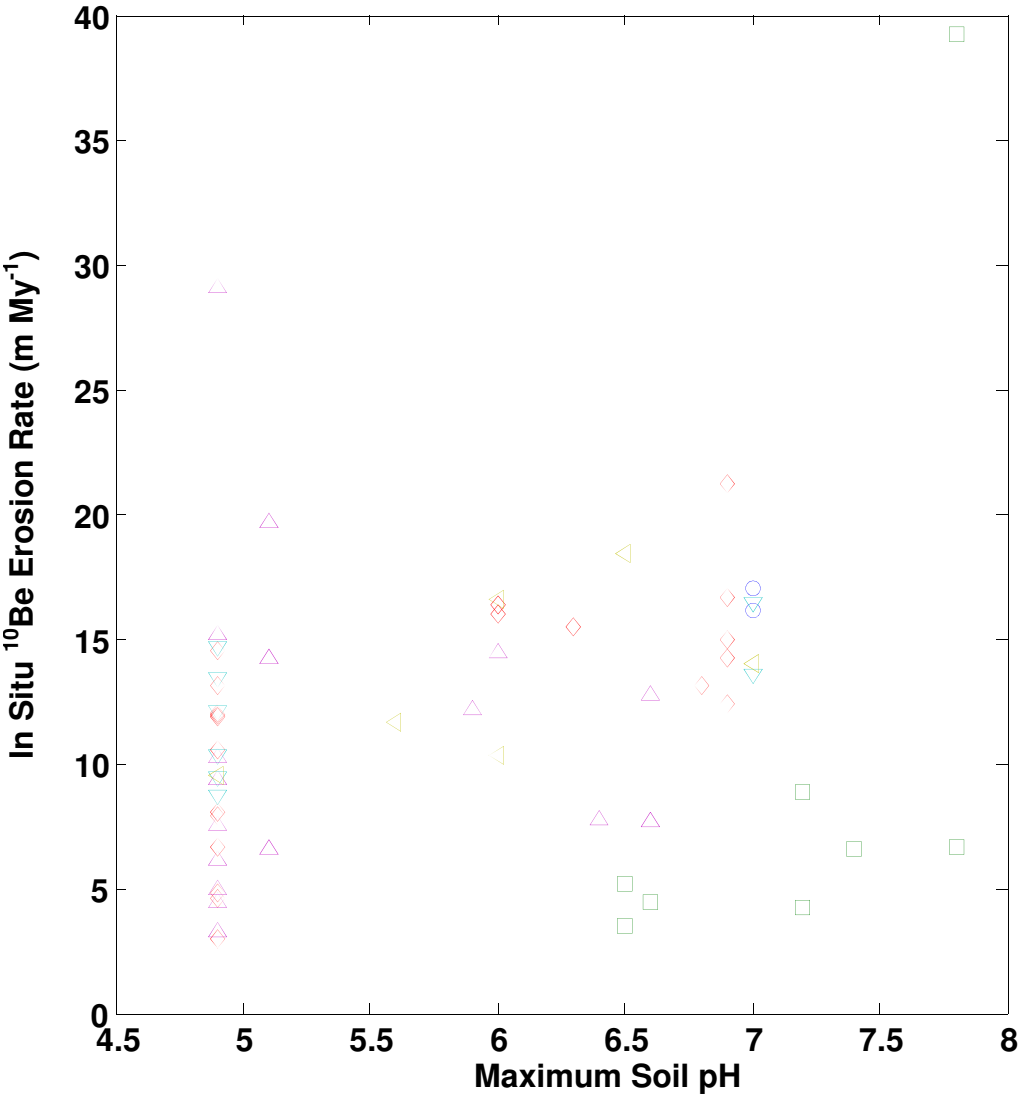


**Figure 4.10 - In Situ $^{10}$Be Erosion Rate Including Outliers against Maximum Soil pH.**
The y-axis is the in situ $^{10}$Be erosion rate in m My$^{-1}$. The x-axis is the maximum soil pH. The blue circles are samples from large basins that occupy many physiographic provinces. The green squares are from the Coastal Plain, red diamond, Piedmont, turquoise upside down triangle Blue Ridge, purple triangle Valley and Ridge, yellow sideways triangle Appalachian Plateau. In situ erosion rates show a weak correlation with maximum soil pH ($R^2$=0.05, $p$=0.08). Data taken from http://soils.usda.gov/survey/geography/ssurgo/.

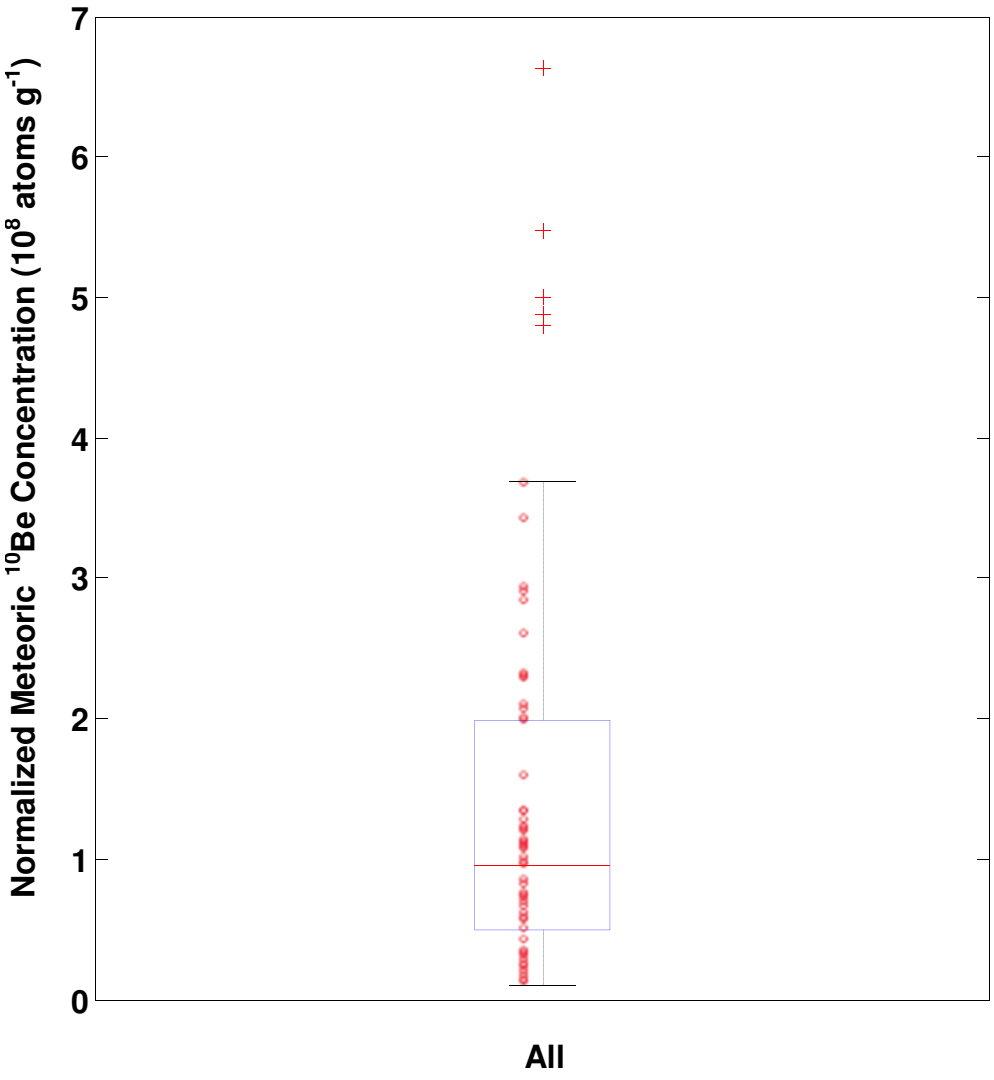


**Figure 4.11 - Box Plot of Potomac River Basin Normalized Meteoric $^{10}$Be Concentrations.**

A box plot of all of Potomac River Basin meteoric $^{10}$Be concentrations. The y-axis is the normalized meteoric $^{10}$Be concentration in atoms g sediment$^{-1}$. The red line in the middle of the box is the median. The bottom of the box is the 25% quartile, and the top of the box is the 75% quartile. The bottom whisker is the 25% quartile - 1.5 * the interquartile range, the top whisker is the 75% quartile + 1.5 * the interquartile range. The interquartile range is equal to the 75% quartile - 25% quartile. All points out side of the whiskers, the red crosses, are statistical outliers if the data are normally distributed. All other data points are small red circles.

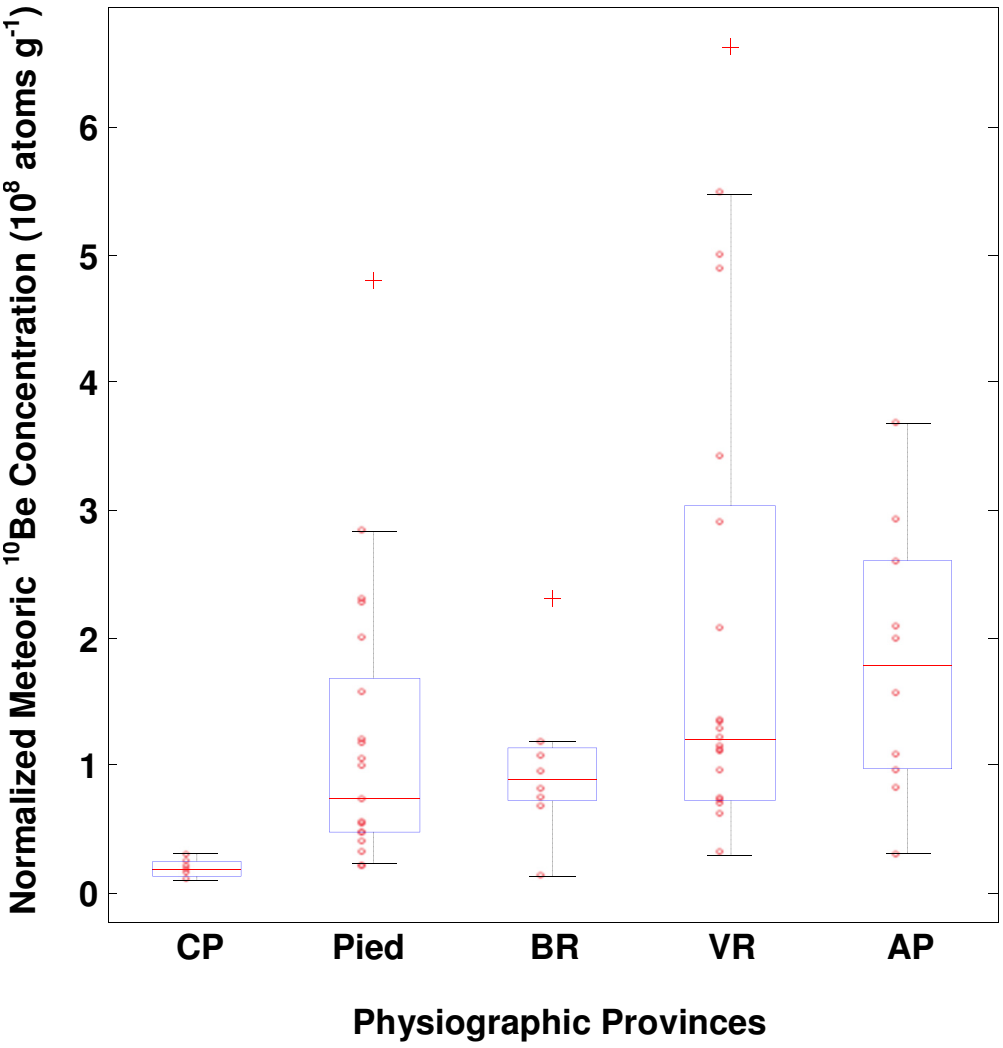


**Figure 4.12 - Normalized Meteoric $^{10}$Be Concentration against Physiographic Provinces.**
CP is the Coastal Plain, Pied is the Piedmont, BR is the Blue Ridge, VR is the Valley and Ridge, and AP is the Appalachian Plateau. The y-axis is the normalized meteoric $^{10}$Be concentration in atoms g sediment$^{-1}$. The red line in the middle of the box is the median. The bottom of the box is the 25% quartile, and the top of the box is the 75% quartile. The bottom whisker is the 25% quartile - 1.5 * the interquartile range, the top whisker is the 75% quartile + 1.5 * the interquartile range. The interquartile range is equal to the 75% quartile - 25% quartile. All points out side of the whiskers, the red crosses, are statistical outliers if the data are normally distributed. All other data points are small red circles (p=0.01).

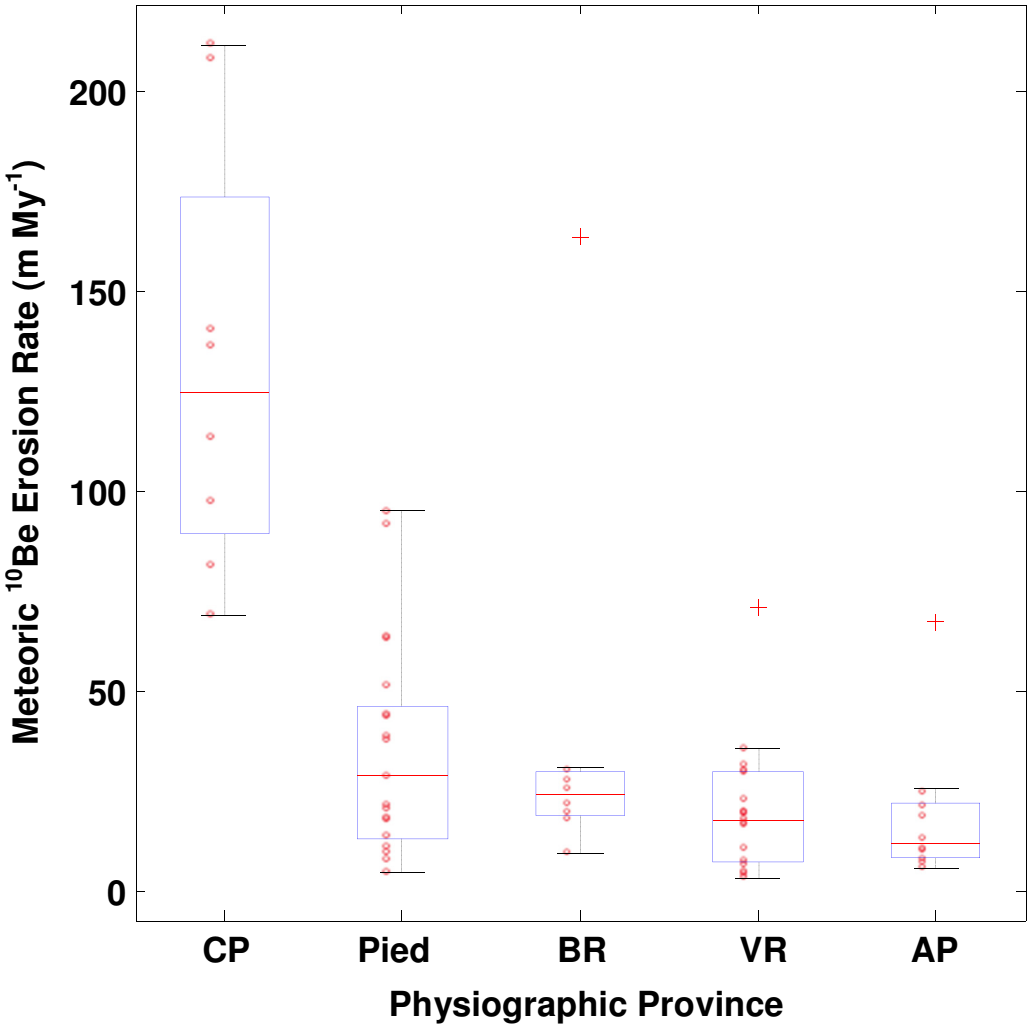


**Figure 4.13 - Meteoric $^{10}$Be Erosion Rate against Physiographic Provinces.**
CP is the Coastal Plain, Pied is the Piedmont, BR is the Blue Ridge, VR is the Valley and Ridge, and AP is the Appalachian Plateau. The y-axis is the meteoric $^{10}$Be erosion rate in m My$^{-1}$. The red line in the middle of the box is the median. The bottom of the box is the 25% quartile, and the top of the box is the 75% quartile. The bottom whisker is the 25% quartile - 1.5 * the interquartile range, the top whisker is the 75% quartile + 1.5 * the interquartile range. The interquartile range is equal to the 75% quartile - 25% quartile. All points out side of the whiskers, the red crosses, are statistical outliers if the data are normally distributed. All other data points are small red circles. The Piedmont, Blue Ridge, Valley and Ridge and Appalachian Plateau show statistical similarities ($p$=0.12). The Coastal Plain has much higher rates than the other provinces with a median five times higher than all of the other provinces ($p$<0.01).

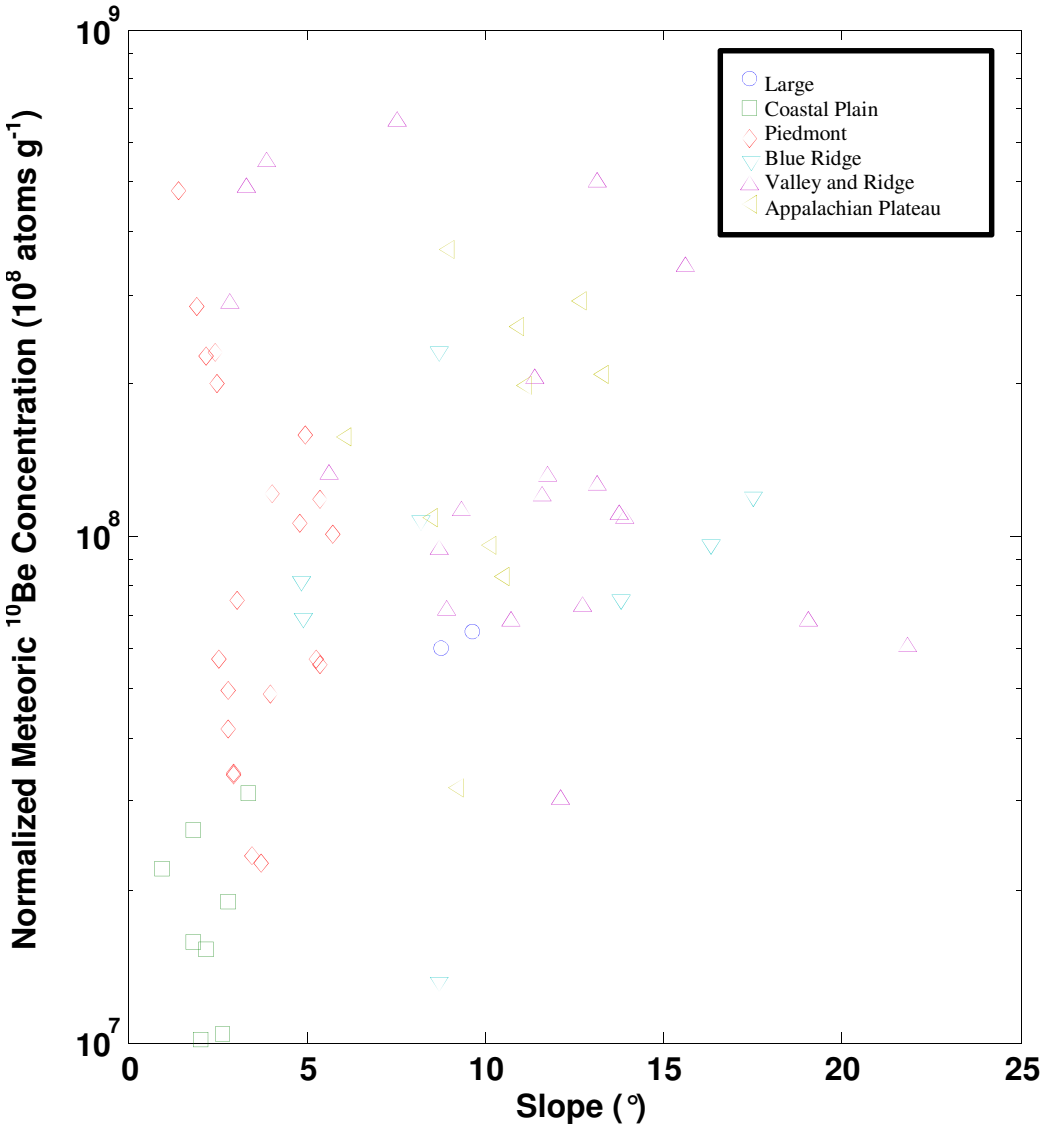


**Figure 4.14 - Normalized Meteoric $^{10}$Be Concentration against Average Slope.** The y-axis is the normalized meteoric $^{10}$Be concentration in atoms g sediment$^{-1}$ in log scale. The x-axis is the average slope in degrees. The blue circles are samples from large basins that occupy many physiographic provinces. The green squares are from the Coastal Plain, red diamond, Piedmont, turquoise upside down triangle Blue Ridge, purple triangle Valley and Ridge, yellow sideways triangle Appalachian Plateau. Normalized meteoric $^{10}$Be concentrations shows a weak correlation with slope ($r^2$=0.06, $p$=0.04).

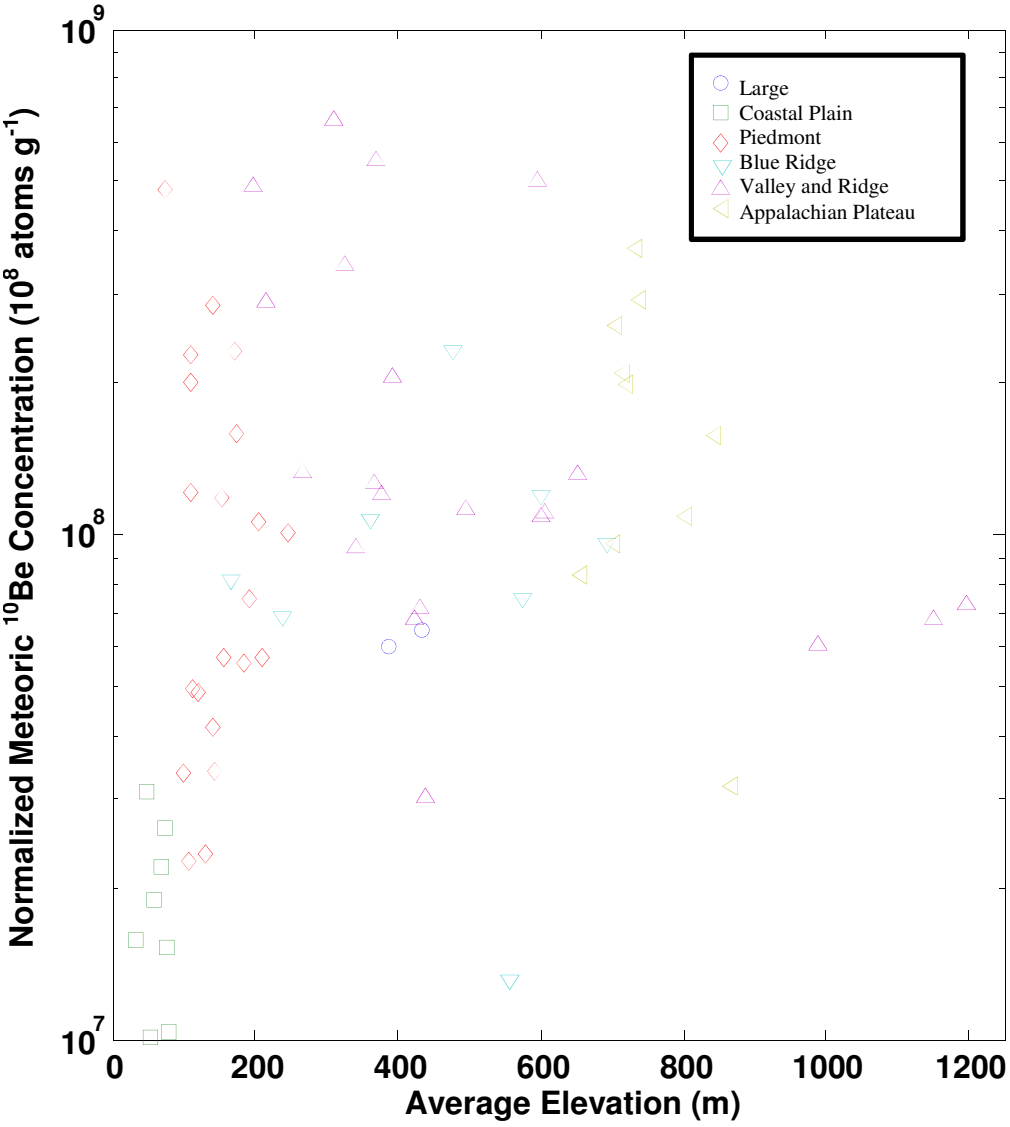


**Figure 4.15 – Normalized Meteoric $^{10}$Be Concentration against Effective Elevation.** The y-axis is the normalized meteoric $^{10}$Be concentration in atoms g sediment$^{-1}$ on a log scale. The x-axis is the average elevation in meters. The blue circles are samples from large basins that occupy many physiographic provinces. The green squares are from the Coastal Plain, red diamond, Piedmont, turquoise upside down triangle Blue Ridge, purple triangle Valley and Ridge, yellow sideways triangle Appalachian Plateau. Normalized meteoric $^{10}$Be concentrations show a weak correlation with effective elevation ($R^2$=0.06, $p$=0.04).

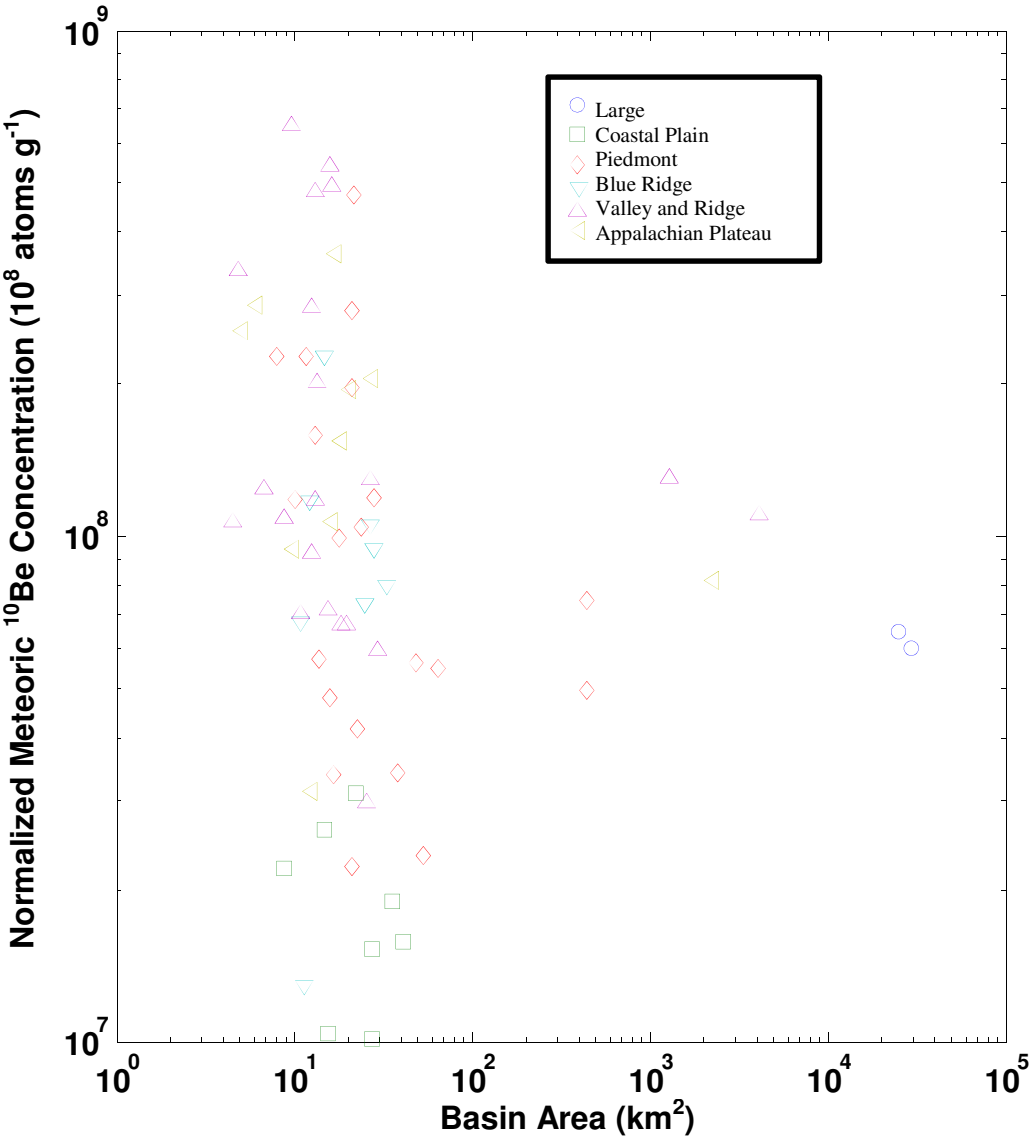


**Figure 4.16 - Normalized Meteoric $^{10}$Be Concentration against Basin Area.** The y-axis is the normalized meteoric $^{10}$Be concentration in atoms g sediment$^{-1}$ on a log scale. The x-axis is the basin area in km$^2$ on a log scale. The blue circles are samples from large basins that occupy many physiographic provinces. The green squares are from the Coastal Plain, red diamond, Piedmont, turquoise upside down triangle Blue Ridge, purple triangle Valley and Ridge, yellow sideways triangle Appalachian Plateau. Normalized meteoric $^{10}$Be concentrations show no correlation with basin area ($R^2$<0.01, $p$=0.63).

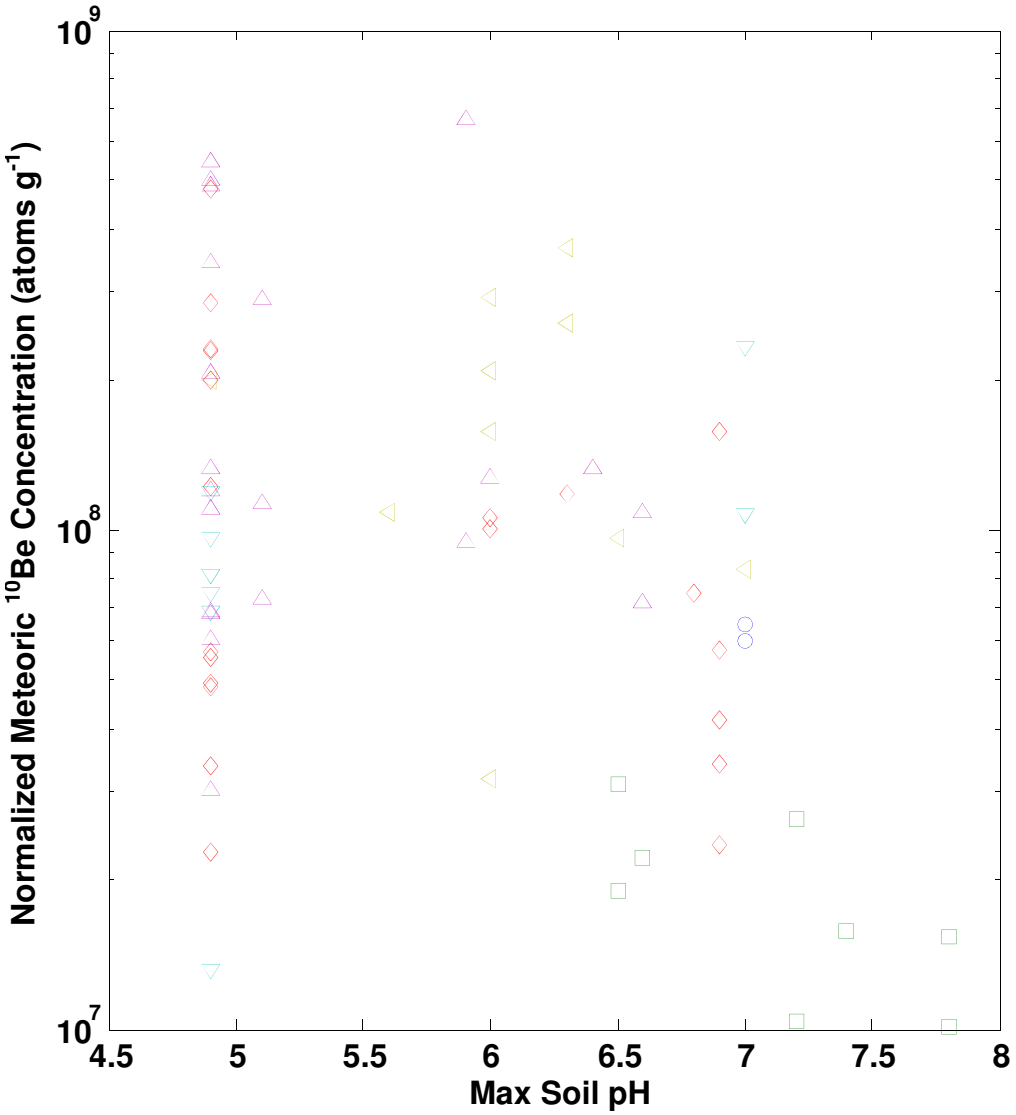


**Figure 4.17 - Normalized Meteoric $^{10}$Be Concentrations against Maximum Soil pH.** The y-axis is the normalized meteoric $^{10}$Be concentration in atoms g sediment$^{-1}$ on a log scale. The x-axis is the maximum soil pH. The blue circles are samples from large basins that occupy many physiographic provinces. The green squares are from the Coastal Plain, red diamond, Piedmont, turquoise upside down triangle Blue Ridge, purple triangle Valley and Ridge, yellow sideways triangle Appalachian Plateau. Normalized meteoric $^{10}$Be concentrations show a weak correlation with maximum soil pH ($R^2$=0.16, $p$<0.01). Data taken from http://soils.usda.gov/survey/geography/ssurgo/.

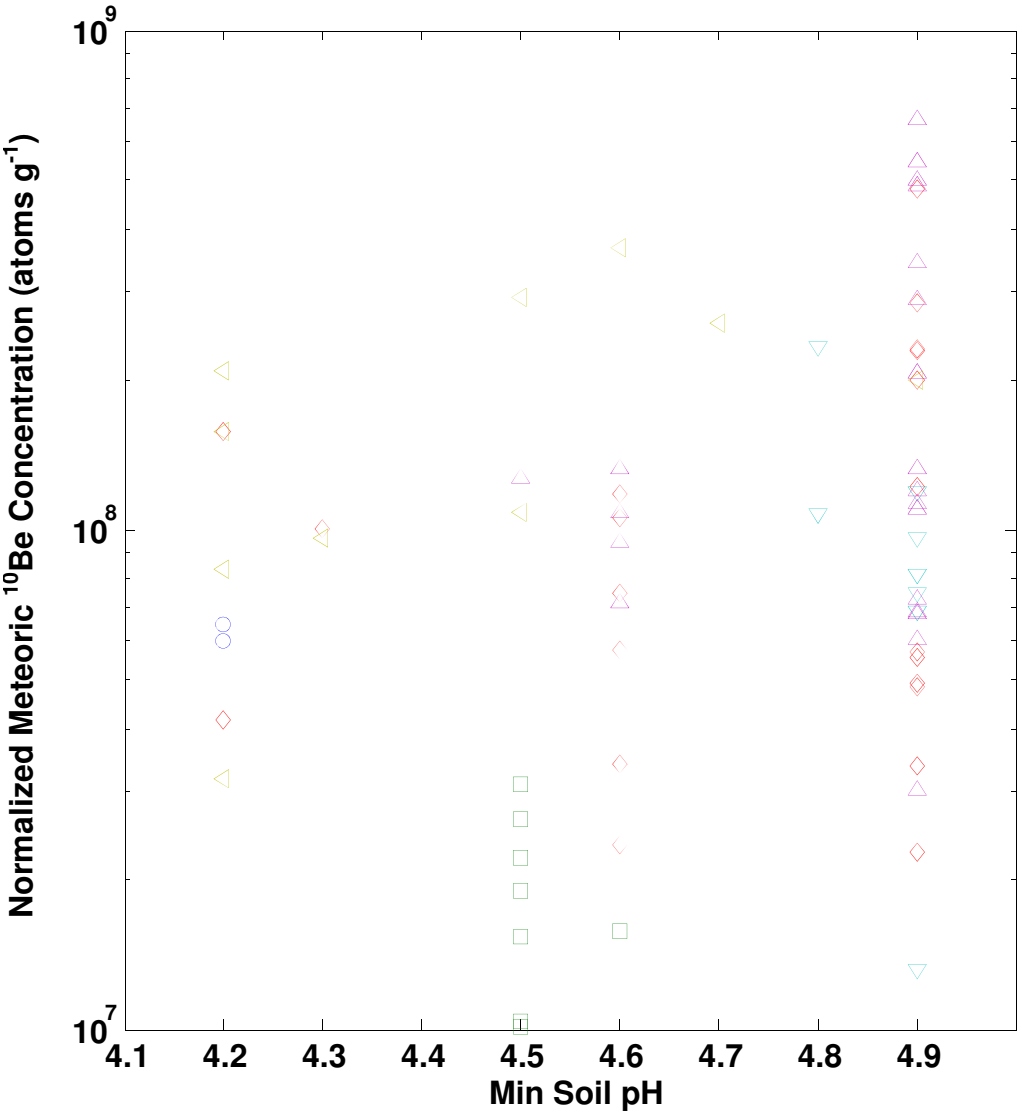


**Figure 4.18 - Normalized Meteoric $^{10}$Be Concentrations against Minimum Soil pH.** The y-axis is the normalized meteoric $^{10}$Be concentration in atoms g sediment$^{-1}$ on a log scale. The x-axis is the minimum soil pH. The blue circles are samples from large basins that occupy many physiographic provinces. The green squares are from the Coastal Plain, red diamond, Piedmont, turquoise upside down triangle Blue Ridge, purple triangle Valley and Ridge, yellow sideways triangle Appalachian Plateau. Normalized meteoric $^{10}$Be concentrations show a weak correlation with minimum soil pH ($R^2$=0.07, $p$=0.03). Data taken from http://soils.usda.gov/survey/geography/ssurgo/.

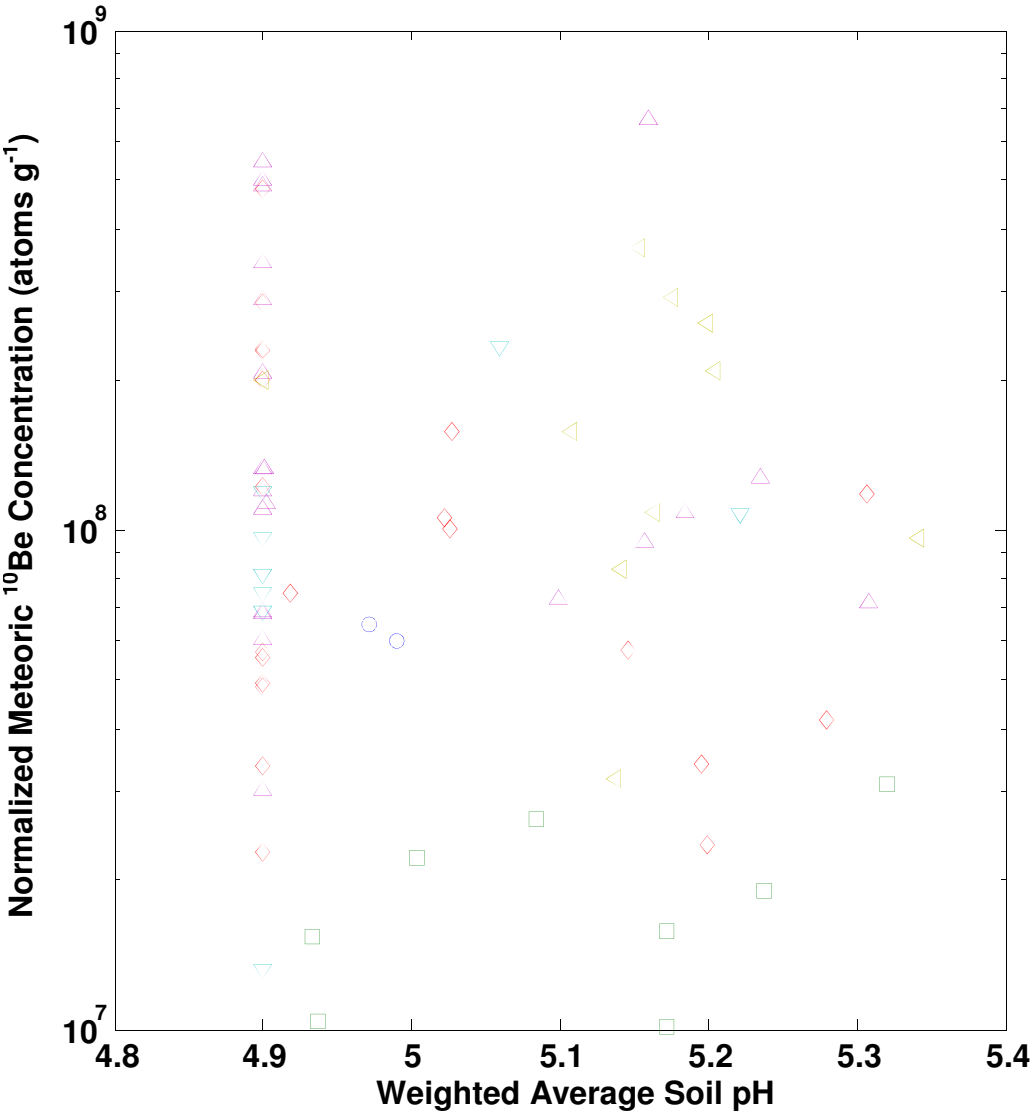


**Figure 4.19 - Normalized Meteoric $^{10}$Be Concentrations against Weighted Average Soil pH.**
The y-axis is the normalized meteoric $^{10}$Be concentration in atoms g sediment$^{-1}$ on a log scale. The x-axis is the weighted average soil pH. The blue circles are samples from large basins that occupy many physiographic provinces. The green squares are from the Coastal Plain, red diamond, Piedmont, turquoise upside down triangle Blue Ridge, purple triangle Valley and Ridge, yellow sideways triangle Appalachian Plateau. Normalized meteoric $^{10}$Be concentrations show no correlation with weighted average soil pH ($R^2$=0.02, $p$=0.25). Data taken from http://soils.usda.gov/survey/geography/ssurgo/.

# Chapter 5 – Discussion

With all of my data and the previous information collected about the region, I was able to do large amount of analysis on the Potomac Watershed. First, I assume that in situ $^{10}$Be erosion rates represent the actual erosion rates from the basin integrated over the last $10^4$ to $10^5$ years. With this assumption, I am able to analyze what, if any, landscape-scale variables affect the in situ $^{10}$Be erosion rates. Erosion rates modeled from meteoric $^{10}$Be in fluvial sediments appear unrepresentative for most basins, based on a lack of correlation with the in situ $^{10}$Be erosion rates. Thus, I examine the variables affecting meteoric $^{10}$Be concentrations to better understand why the meteoric $^{10}$Be erosion rates are incorrect. I also want to understand better the relationship between in situ and meteoric $^{10}$Be as another way to determine why the meteoric $^{10}$Be concentrations are not at the levels I expected. Because I collected 10 samples from USGS gauging stations, I am able to compare my $^{10}$Be concentrations and modeled erosion rates with sediment yields. I am also able to compare my meteoric $^{10}$Be concentration at one sample site with those of the previous study Brown et al. (1988).

## *Comparing In Situ vs. Meteoric $^{10}$Be Concentrations*

No correlation exists between standardized in situ and meteoric $^{10}$Be concentrations ($R^2$=0.08, $p$=0.03) (Figure 5.1). Many factors potentially cause this lack of correlation. First, the production curve of in situ $^{10}$Be is exponential with depth. Biota can churn the soil and mix the quartz grains so there is no depth dependence of in situ $^{10}$Be concentration to the depth at which stirring reaches (Jungers et al., 2009). Second,

meteoric $^{10}$Be typically has larger concentrations in the B horizon of well-developed soils than the A horizon (Jungers, et al., 2009; Graly, et al., 2010). If the erosion occurring in the basin is only stripping soil from the very top of the soil column the eroded soil could potentially be deficient in meteoric $^{10}$Be. All of the meteoric $^{10}$Be may not remain adhered to grains or may not attach to the grains at all. This does not appear true because the ratio between meteoric and in situ $^{10}$Be concentrations has no correlation with weight average, max or min soil pH in each basin ($R^2$=0.01, $p$=0.42; $R^2$=0.04, $p$=0.10; $R^2$<0.02, $p$=0.28) (Figure 5.2-Figure 5.4). These findings agree with the previous findings of Graly et al. (2010) who found no correlation between meteoric $^{10}$Be concentration and pH or CEC at pH above 4.

Another possibility for the difference between the standardized in situ and meteoric $^{10}$Be concentrations could be a sampling bias. I only sampled sediment that was between 250 and 850 µm and I potentially did not sample the sediment that had most of the meteoric $^{10}$Be. A sample with smaller sediment sizes would have more surface area therefore it could hold a larger amount of meteoric $^{10}$Be. If this is true for my samples than it contrasts with Brown et al. (1988) who found no relationship between meteoric $^{10}$Be concentrations and grain sizes but is consistent with the $^{10}$Be/grain size relationship reported in Willenbring and von Blanckenburg (2010).

Using the ratio I created to quantify the relationship between in situ and meteoric $^{10}$Be concentrations, based off of the data for Figure 5.1, I examined several variables to see if any were affecting the relationship between in situ and meteoric $^{10}$Be concentrations. With this ratio I can see that 53 basins, or 85%, fall below the one to one

line on Figure 5.1 indicating they have less meteoric $^{10}$Be than expected and 9 basins, or 14%, are above the line indicating they have more meteoric $^{10}$Be than expected. This shows me that a majority of the samples have less meteoric $^{10}$Be in them than expected.

The Coastal Plain is statistically different than the other physiographic provinces when looking at the difference between normalized in situ and meteoric $^{10}$Be concentrations ($p$=0.02). All of the other provinces are statistically similar ($p$=0.95) (Figure 5.5). In Figure 5.1 it is also possible to see that the all of the Coastal Plain samples are in a line across the bottom of the graph while the other physiographic provinces are spread around the graph. This is expected considering the Coastal Plain has the highest in situ concentrations and the lowest meteoric concentrations. There is also no correlation with the ratio between normalized meteoric and in situ $^{10}$Be concentrations and slope, effective elevation, basin area or annual precipitation ($R^2$=0.01, $p$=0.42; $R^2$=0.04, $p$=0.12; $R^2$<0.01, $p$=0.83; $R^2$<0.01, $p$=0.91) (Figure 5.6-Figure 5.9).

One factor does seem to have an effect on the ratio of meteoric $^{10}$Be to in situ $^{10}$Be, land use. I determined the dominate land use in each of the basins by calculating which land use was in the largest percentage of the basin (Figure 2.2) (NOAA, 2010). All of the basins fell into either agriculture, forest or urban. The ratio of meteoric $^{10}$Be to in situ $^{10}$Be in each of these land use categories are statistically dissimilar from one another ($p$<0.01) (Figure 5.10). The mean ratio of agriculture is 0.82, forest is 0.57 and urban is 0.20. This makes sense in agriculture regions because the farmers are probably plowing up meteoric $^{10}$Be from the B horizon while not changing the concentration of in situ $^{10}$Be.

The urban ratio could be explained by two factors. First, construction could be digging up soil below the B horizon with low meteoric $^{10}$Be but this would show up in the in situ $^{10}$Be concentrations also, but it does not (Figure 5.11). Another possibility is human activity decreasing the pH of the soil thereby making it more difficult for the soil to retain meteoric $^{10}$Be. Also, it is worth noting that all of the urban basins are in the Coastal Plain or very near the Coastal Plain which appears to naturally have relatively low concentrations on meteoric $^{10}$Be.

***Gaged basins***

For each of my basins, I converted my erosion rates into export rates of grams per year so that I could do a direct comparison between sediment yield, in situ $^{10}$Be erosion rates and meteoric $^{10}$Be erosion rates for the ten U.S. Geological Survey gauged sampling sites. Small basins have variable differences between sediment yield, in situ $^{10}$Be export rates and meteoric $^{10}$Be export rates. Large basins, specifically the six largest basins (440 km$^2$ to 29796 km$^2$); show less difference between sediment yield, in situ $^{10}$Be bases sediment export rates and meteoric $^{10}$Be based sediment export rates (Figure 5.12). Small basins naturally have more variability in sediment input and large basins have much less variability. Events, such as a land slide or a construction project, affect small basins much more because these events release a large percentage of the sediment leaving the basin. In larger basins these same events have much less affect because they release a much smaller percentage of the sediment from the basin.

The difference between in situ and meteoric $^{10}$Be sediment export rates when comparing them to modern sediment export rates could be explained by timescale difference. All of the differences between the long-term export rates, both in situ and meteoric, and the modern export rates are an order of magnitude or less. Gardner et al. (1987) showed the difference in timescale can explain up to an order of magnitude of difference between modern and long-term timescales.

A comparison of the standardized in situ and meteoric concentrations from the large basins shows that even in the large basins (440 km$^2$ to 29796 km$^2$) of the Potomac Watershed the standardized concentrations show no correlation ($R^2$=0.27, $p$=0.24) (Figure 5.13). This lack of correlation most likely is caused the different land uses in the basins potentially affecting the meteoric $^{10}$Be concentrations and acidic soils causing less than expected meteoric $^{10}$Be to stick to soils.

### *Variables Affecting In Situ $^{10}$Be Erosion Rates*

All statistical analyses of in situ $^{10}$Be erosion rates were done twice, once, with all of the data in a $\log_{10}$ transformation and a second time with the original data having samples POT20 and POT45 removed. I did the dual analysis to better understand how the outliers affect statistical inferences. The data, including the outliers, were $\log_{10}$ transformed to make the data more normally distributed, while the data excluding the outliers was not transformed because the original data was more normal than the transformation.

***Basin size***

Basin area seems to have no correlation with in situ $^{10}$Be erosion rates both including and excluding outliers ($R^2$=0.02, $p$=0.23; $R^2$=0.05, $p$=0.10) (Figure 4.7). Larger basins often show less variability in the in situ $^{10}$Be erosion rates (Duxbury, 2009; Matmon, et al., 2003; Reuter, et al., 2006; Sullivan, 2007) but it appears that the large basins in the Potomac Watershed contain as much variability as the small basins as long as you exclude the two statistical outliers at 29 and 39 m My$^{-1}$. Smaller basin erosion rates range from 4 to 21 m My$^{-1}$ while large basins range from 7 to 17 m My$^{-1}$. The slight difference in range is most likely caused by many more samples coming from small basins and mixing occurring in the larger basins. I believe that variability did not change with basin size for one main reason, the small basins show little variability, which makes it difficult, statistically, for the larger basins to show less variability.

***Slope and Elevation***

In situ $^{10}$Be erosion rates show no correlation with average basin slope and a weak positive correlation with the effective elevation of a basin when outliers are both included and excluded (Slope $R^2$=0.06, $p$>0.05; $R^2$=0.04, $p$=0.11; Elevation $R^2$=0.10, $p$=0.01; $R^2$=0.11, $p$=0.01) (Figure 4.5, Figure 4.6). There is no correlation between slope and in situ erosion rates for each physiographic province considered individually (CP, $R^2$=0.01, $p$=0.81; Pied, $R^2$=0.06, $p$=0.27; BR, $R^2$=0.01, $p$=0.81; VR, $R^2$=0.22, $p$>0.05; AP, $R^2$=0.07, $p$=0.61) (Figure 4.5). Also, there is no correlation between the average erosion rate of each physiographic province and the average slope ($R^2$=0.31, $p$=0.33) (Figure

5.14). The lack of a relationship between erosion rates and average slope contradicts some previous studies (DiBase, et al., 2009; Matmon, et al., 2003; Ouimet, et al., 2009; Palumbo, et al., 2009; von Blanckenburg, et al., 2004; Portenga & Bierman, 2011). The weak correlation between elevation and in situ $^{10}$Be erosion rates also contrast with some previous studies (Heimsath, et al., 2000; Palumbo, et al., 2009), but agrees with Portenga and Bierman (2011).

I believe that two factors cause this lack of correlation. First, the hills and mountains of the Potomac Watershed have had plenty of time to reach equilibrium. Looking at the contrasting views of Hack (1960) and Davis (1899) allows me to better understand the landscape evolution in the area. Hack's (1960) model suggests there should be very few areas of relatively high and low erosion rates in the sampled basin, which is what I measure in the Potomac River Basin. Hard to erode quartzites and quartz sandstone make up most of the steep areas and sediments and easily eroded shales make up the less sloped areas (Hack, 1960). The flattest and lowest area, the Coastal Plain, does have the lowest erosion rates and is statistically different when outliers are removed, most likely because the Coastal Plain has such a low slope making it extremely difficult to erode. On average, sampled basins from the Coastal Plain and the Piedmont both have statistically lower slopes than the other three provinces ($p$<0.01) and the Coastal Plain has a lower slope than the Piedmont ($p$=0.01) (Figure 5.15).

### *Physiographic provinces and spatial distribution*

When the in situ $^{10}$Be erosion rate outliers are left in, all five physiographic provinces have statistically similar erosion rates ($p$=0.13) (Figure 4.4). With outliers taken out the Coastal Plain is statistically different with its lower erosion rates ($p$<0.01). The other four provinces show statistical similarity ($p$=0.25) (Figure 4.4). As stated above, the very low slope and elevation of the Coastal Plain appears to cause the difference in in situ $^{10}$Be erosion rates.

Looking at Figure 5.16 it is possible to see the locations with the highest and lowest in situ $^{10}$Be erosion rates. As was previously determined all of the Coastal Plain samples are very low expect the outlier, POT20. The northern portion of the Piedmont has much larger erosion rates than the southern portion. Besides these patterns the only other pattern that sticks out is a line of low erosion rates in the Appalachian Plateau including POT56, POT57, POT59 and POT60.

### *Basin Soil pH*

In situ $^{10}$Be erosion rates, including outliers, show a weak correlation with weighted average and min soil pH, ($R^2$=0.06, $p$=0.049; $R^2$=0.07, $p$=0.04) (Figure 4.8, Figure 4.9) but no correlation with max soil pH ($R^2$=0.05, $p$=0.08) (Figure 4.10). The lack of correlation is to be expected because soil pH has never been shown to affect in situ $^{10}$Be erosion rates.

### *Erosion Rates from Past Studies*

Using the newly recalculated in situ $^{10}$Be erosion rates for Duxbury (2009), Matmon, et al. (2003), Reuter et al. (2006) and Sullivan (2007) from Portenga and Bierman (2011), I compared my data and these previous projects. For this analysis, I left the in situ $^{10}$Be erosion rate outliers in because previous studies left their outliers in. Using ANOVA, my data are statistically dissimilar to that of Matmon et al. (2003) from the Great Smokey Mountains National Park, Reuter et al. (2006) from the Susquehanna, and Sullivan (2007) from the Blue Ridge Escarpment ($p$<0.01) (Figure 5.17). My data does show statistical similarities with Duxbury's (2009) work from the Shenandoah using a t test ($p$=0.76) (Figure 5.17), which make sense because the Shenandoah is a tributary of the Potomac River.

### *Variables Affecting Meteoric $^{10}$Be Concentrations*

All statistical analyses done on my meteoric samples examined the normalized meteoric $^{10}$Be concentrations. I did not use erosion rates derived from the meteoric $^{10}$Be concentrations because the erosion rates modeled from meteoric $^{10}$Be were largely different than the in situ $^{10}$Be erosion rates. Because of this large difference, I sought to better understand what affects meteoric $^{10}$Be concentrations. All of my statistical analyses of the normalized meteoric $^{10}$Be concentrations were done on $\log_{10}$ transformed data because they are much closer to normally distributed than the original data.

***Basin size***

Basin area seems to have no correlation with meteoric $^{10}$Be concentrations ($R^2$<0.01, $p$=0.63) (Figure 4.16). Unlike the in situ data, the meteoric concentrations are more variable in small basins and less so in large basins. This is a common characteristic seen with in situ $^{10}$Be erosion rates (Duxbury, 2009; Matmon, et al., 2003; Reuter, et al., 2006; Sullivan, 2007). A small amount of this variability is explained by the large amount of samples coming from small basins. Most of the variability must result from the different land uses in the basins and the different soil types. The lack of variability in the large basins is most likely caused by mixing.

***Slope and Elevation***

It appears the normalized meteoric $^{10}$Be concentrations show a weak positive correlation with average slope and no correlation with the effective elevation of a basin ($R^2$=0.06, $p$=0.04; $R^2$<0.01, $p$=0.82) (Figure 4.14 and Figure 4.15).

***Physiographic provinces and spatial distribution***

Like in situ $^{10}$Be erosion rates, normalized meteoric $^{10}$Be concentrations are statistically different in the Coastal Plain ($p$<0.01), while the other four physiographic provinces are similar ($p$=0.08) (Figure 4.12). The normalized meteoric $^{10}$Be concentrations are much lower in the Coastal Plain then the other provinces; this is may be caused by acidic soils in the Coastal Plain causing less than expected meteoric $^{10}$Be to

be retained. Looking at how soil pH varies by physiographic province the data shows the Coastal Plain actually has some of the higher soil pHs (Figure 5.18).

Looking at Figure 5.19 it is possible to see the locations with the highest and lowest meteoric $^{10}$Be concentrations. As was previously determined all of the Coastal Plain samples are very low. All but one sample in the Appalachian Plateau has high meteoric $^{10}$Be concentrations. Also, the samples in the Piedmont that are closest to the Coastal Plain have low meteoric $^{10}$Be concentrations. The rest of the basin it is very difficult to see any patterns.

***Basin Soil pH***

Meteoric $^{10}$Be concentrations show a weak positive correlation with max soil pH and a weak negative correlation with min soil pH, ($R^2$=0.16, $p$<0.01; $R^2$=0.07, $p$=0.03) (Figure 4.17, Figure 4.18) and no correlation with weighted average soil pH ($R^2$=0.02, $p$=0.25) (Figure 4.19). These findings agree with the previous findings of Graly et al. (2010) who found no correlation between meteoric $^{10}$Be concentration and pH or CEC above a pH of 4.

***Land Use***

Using ANOVA, urban areas have statistically different concentration of $^{10}$Be than agriculture and forested areas ($p$<0.01). Agriculture and forested areas are statistically similar ($p$=0.18) (Figure 5.20). Mean normalized meteoric $^{10}$Be concentrations for each land use type are; urban 3.68 x $10^7$ atoms g sediment$^{-1}$, forest 1.39 x $10^8$ atoms g

sediment$^{-1}$ and, agriculture 1.84 x $10^8$ atoms g sediment$^{-1}$. Meteoric $^{10}$Be concentrations vary in the A and B horizon of the soil with most of the meteoric $^{10}$Be residing in the B horizon (Jungers, et al., 2009; Graly, et al., 2010). This causes meteoric $^{10}$Be concentrations to vary by land use because if a farmer or construction team is digging up the B horizon in the soil, higher concentration of meteoric $^{10}$Be will be transported to the stream than if just the A-horizon is being eroded. This may explain why agriculture-dominated basins have the highest normalized meteoric $^{10}$Be concentrations. Also all of the urban basins come from the Coastal Plain or very near the Coastal Plain which has much lower normalized meteoric $^{10}$Be concentrations than any of the other physiographic provinces.

### *Comparison of my Meteoric $^{10}$Be Concentrations to Brown et al.* (1988)

I went back to Brown et al.'s (1988) data and updated his meteoric $^{10}$Be delivery rates, meteoric $^{10}$Be concentrations, and erosion indexes (see methods chapter). With their concentrations updated, I am able to compare their data with my data. In my study I focused on smaller, for the most part ungauged stations. Brown et al. (1988), on the other hand, focused on larger gauged stations. This allows for a very interesting comparison (Figure 5.21) because it allows me to better see how basin area affects meteoric $^{10}$Be concentrations. Again, I see a wide range in concentrations in smaller basins and narrower range in larger basins; similar to what has been seen with in situ $^{10}$Be erosion rates (Duxbury, 2009; Matmon, et al., 2003; Reuter, et al., 2006; Sullivan, 2007).

While Brown et al. (1988) measured two samples from the Potomac Watershed; I was able to resample only one of the sites. At this one location, the Brown et al. (1988) corrected concentration is 9.79 x $10^7$ $^{10}$Be atoms g sediment$^{-1}$ and an erosion index of 0.67. My concentration at that location and erosion index, 6.49 x $10^7$ atoms g sediment$^{-1}$ and 0.47 are different than those of Brown et al. (1988).

Brown et al. (1988) collected 45 samples from the Chesapeake Bay Watershed. Brown et al. (1988) measured normalized meteoric $^{10}$Be concentrations ranging from 2.11 x $10^7$ atoms g sediment$^{-1}$ to 2.14 x $10^8$ atoms g sediment$^{-1}$, with a mean of 8.00 x $10^7$ atoms g sediment$^{-1}$, and a median of 6.57 x $10^7$ atoms g sediment$^{-1}$. A t-test shows that my data are statistically different than all of Brown et al. (1988) data ($p$<0.01) (Figure 5.22). This makes sense because Brown et al. (1988) only collected 2 samples from the Potomac Watershed. Also, because Brown et al. (1988) only sampled large basins, the range of their concentrations was smaller with a lot less basins with high normalized meteoric $^{10}$Be concentrations as seen in Figure 5.22, which greatly lowered their mean normalized meteoric $^{10}$Be concentration.

With the updated erosion indexes it appears that around two thirds, 29 of 45, of Browns original basins had more meteoric $^{10}$Be entering the basin than leaving. His average erosion index was 0.87. I analyzed the ten gauged basins from my data and discovered eight had more meteoric $^{10}$Be entering the basin than leaving. My average erosion index was 0.65. Using a t-test, my erosion indexes show statistical similarities with Brown et al.'s (1988) erosion indexes ($p$=0.44) (Figure 5.23).

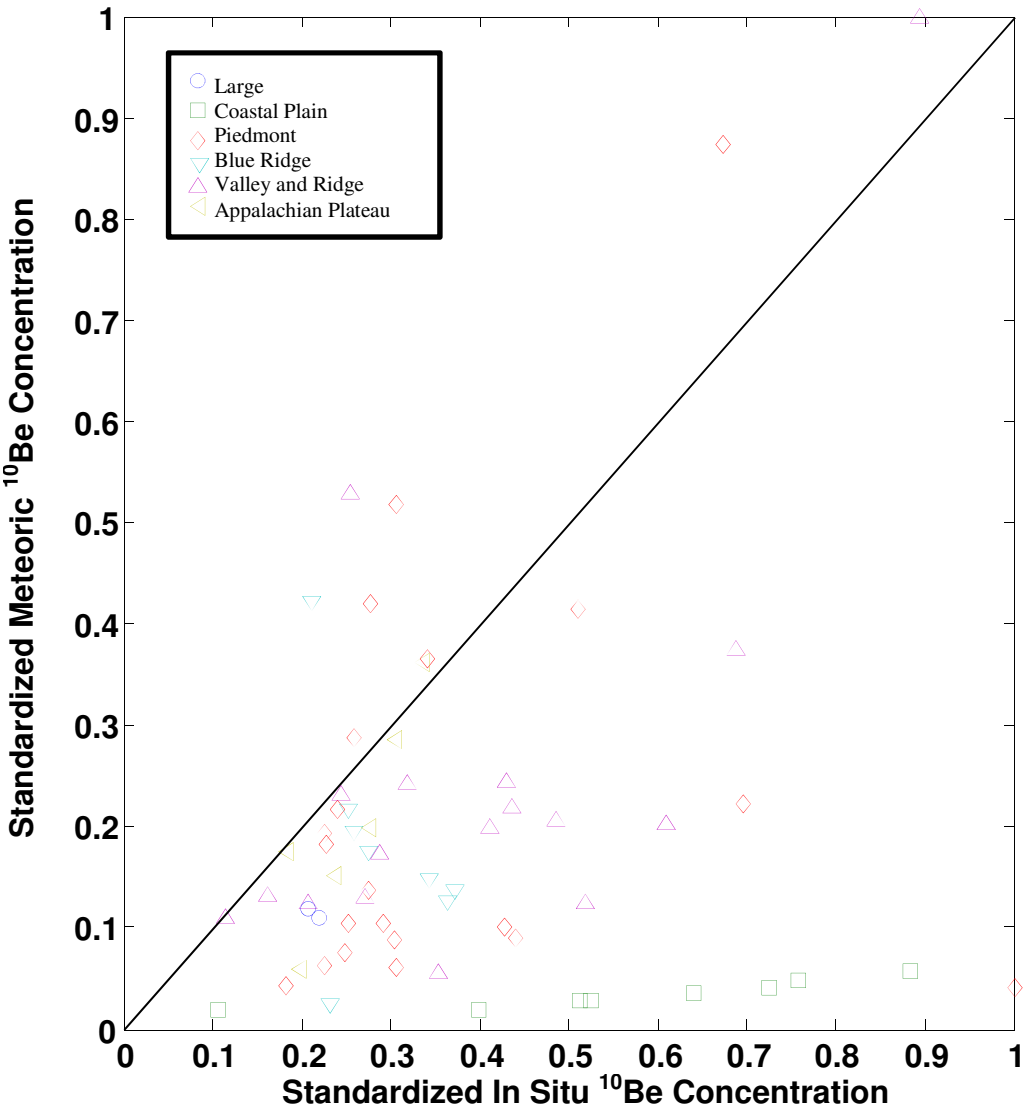


**Figure 5.1 - Standardized In Situ $^{10}$Be Concentrations against Standardized Meteoric $^{10}$Be Concentrations.**
The y-axis is the standardized meteoric $^{10}$Be concentrations. The x-axis is the standardized in situ $^{10}$Be concentrations. The line is a one to one relationship. The blue circles are samples from large basins that occupy many physiographic provinces. The green squares are from the Coastal Plain, red diamond, Piedmont, turquoise upside down triangle Blue Ridge, purple triangle Valley and Ridge, yellow sideways triangle Appalachian Plateau. Standardized in situ $^{10}$Be concentrations and standardized meteoric $^{10}$Be concentrations show no correlation ($r^2$=0.08, $p$=0.03).

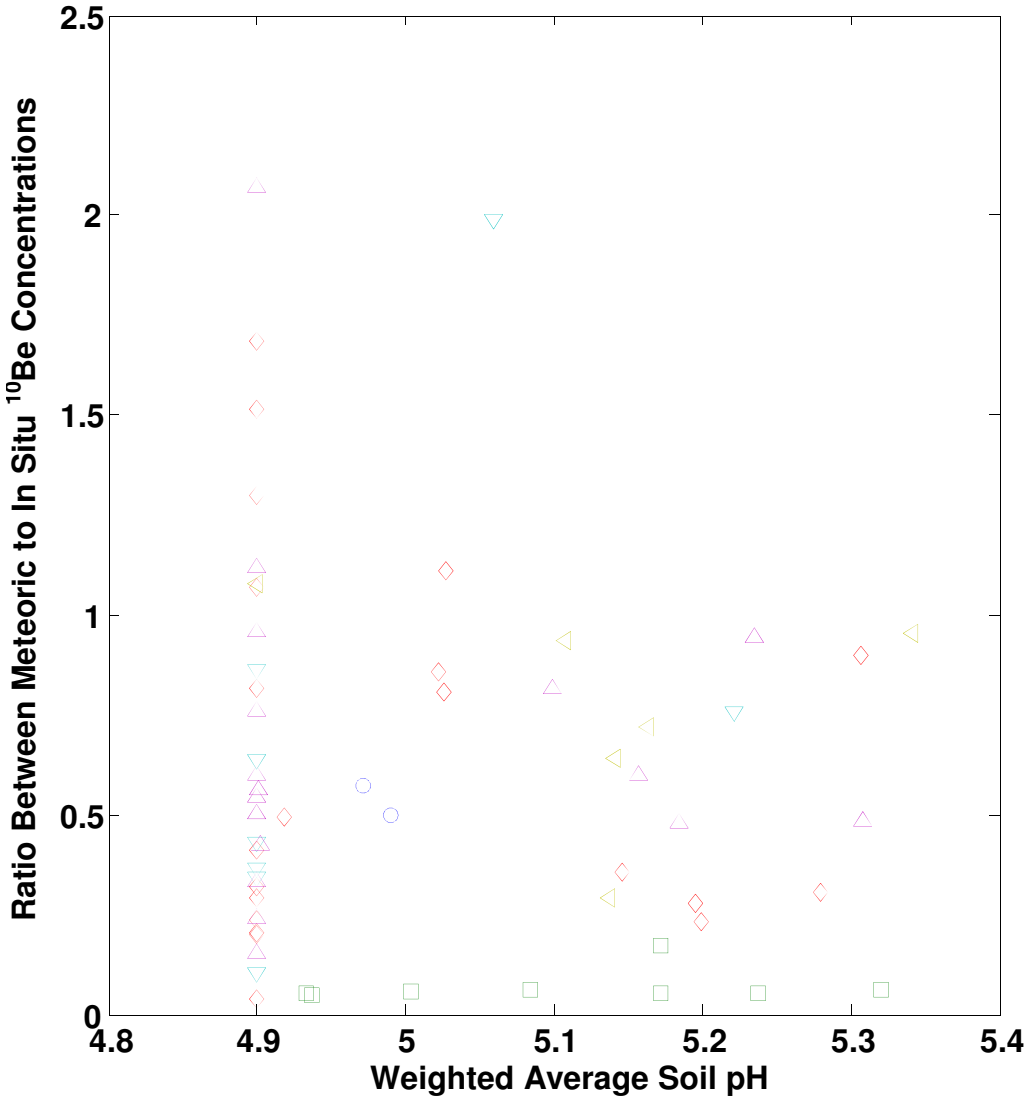


**Figure 5.2 - Ratio Between Meteoric to In Situ $^{10}$Be Concentrations against Weighted Average Soil pH.**
The y-axis is the ratio between meteoric to in situ $^{10}$Be concentrations. The x-axis is the weighted average soil pH. The blue circles are samples from large basins that occupy many physiographic provinces. The green squares are from the Coastal Plain, red diamond, Piedmont, turquoise upside down triangle Blue Ridge, purple triangle Valley and Ridge, yellow sideways triangle Appalachian Plateau. The ratio shows no correlation with weighted average soil pH ($R^2$=0.01, $p$=0.66). Data taken from http://soils.usda.gov/survey/geography/ssurgo/.

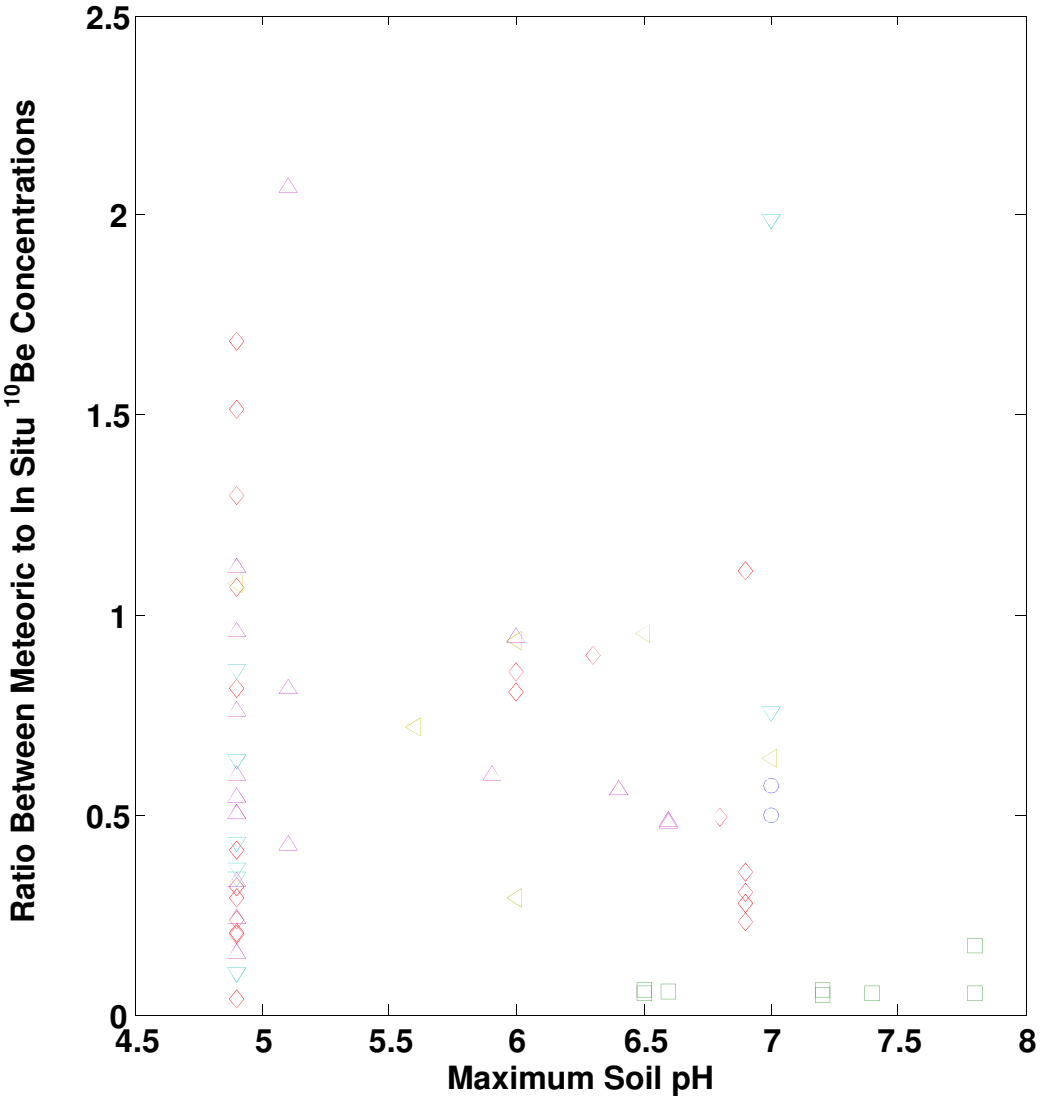


**Figure 5.3 - Ratio Between Meteoric to In Situ $^{10}$Be Concentrations against Maximum Soil pH.**
The y-axis is the ratio between meteoric to in situ $^{10}$Be concentrations. The x-axis is the maximum soil pH. The blue circles are samples from large basins that occupy many physiographic provinces. The green squares are from the Coastal Plain, red diamond, Piedmont, turquoise upside down triangle Blue Ridge, purple triangle Valley and Ridge, yellow sideways triangle Appalachian Plateau. The ratio shows no correlation with maximum soil pH ($R^2$=0.04, $p$=0.10). Data taken from http://soils.usda.gov/survey/geography/ssurgo/.

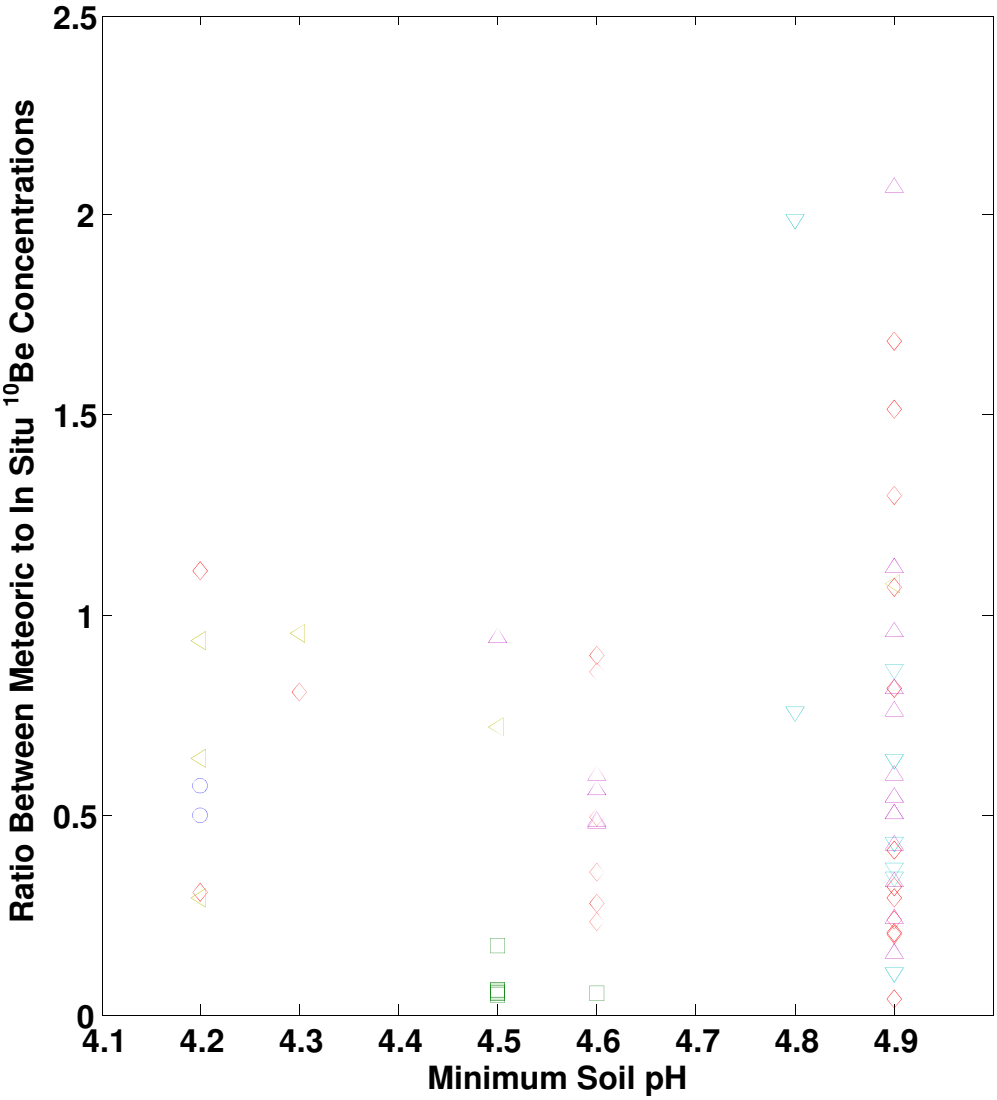


**Figure 5.4 - Ratio Between Meteoric to In Situ $^{10}$Be Concentrations against Minimum Soil pH.**
The y-axis is the ratio between meteoric to in situ $^{10}$Be concentrations. The x-axis is the minimum soil pH. The blue circles are samples from large basins that occupy many physiographic provinces. The green squares are from the Coastal Plain, red diamond, Piedmont, turquoise upside down triangle Blue Ridge, purple triangle Valley and Ridge, yellow sideways triangle Appalachian Plateau. The ratio shows no correlation with minimum soil pH ($R^2$=0.02, $p$=0.28). Data taken from http://soils.usda.gov/survey/geography/ssurgo/.

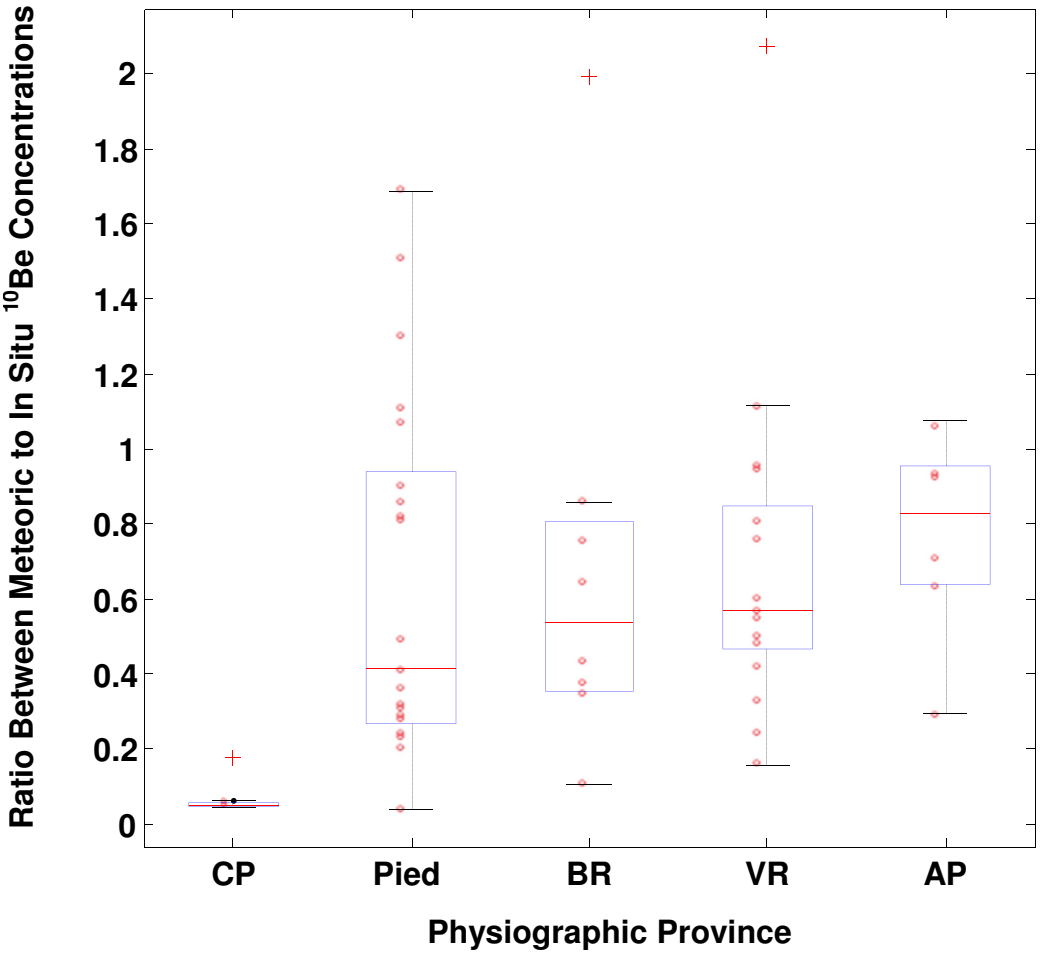


**Figure 5.5 - Ratio Between Meteoric to In Situ $^{10}$Be Concentrations against Physiographic Province.**
CP is the Coastal Plain, Pied is the Piedmont, BR is the Blue Ridge, VR is the Valley and Ridge, and AP is the Appalachian Plateau. The y-axis is the ratio between Meteoric to In Situ $^{10}$Be concentrations. The red line in the middle of the box is the median. The bottom of the box is the 25% quartile, and the top of the box is the 75% quartile. The bottom whisker is the 25% quartile - 1.5 * the interquartile range, the top whisker is the 75% quartile + 1.5 * the interquartile range. The interquartile range is equal to the 75% quartile - 25% quartile. All points out side of the whiskers, the red crosses, are statistical outliers if the data are normally distributed. All other data points are small red circles The Coastal Plain is statistically different than all other provinces ($p$=0.02). All of the other provinces are statistically similar ($p$=0.95).

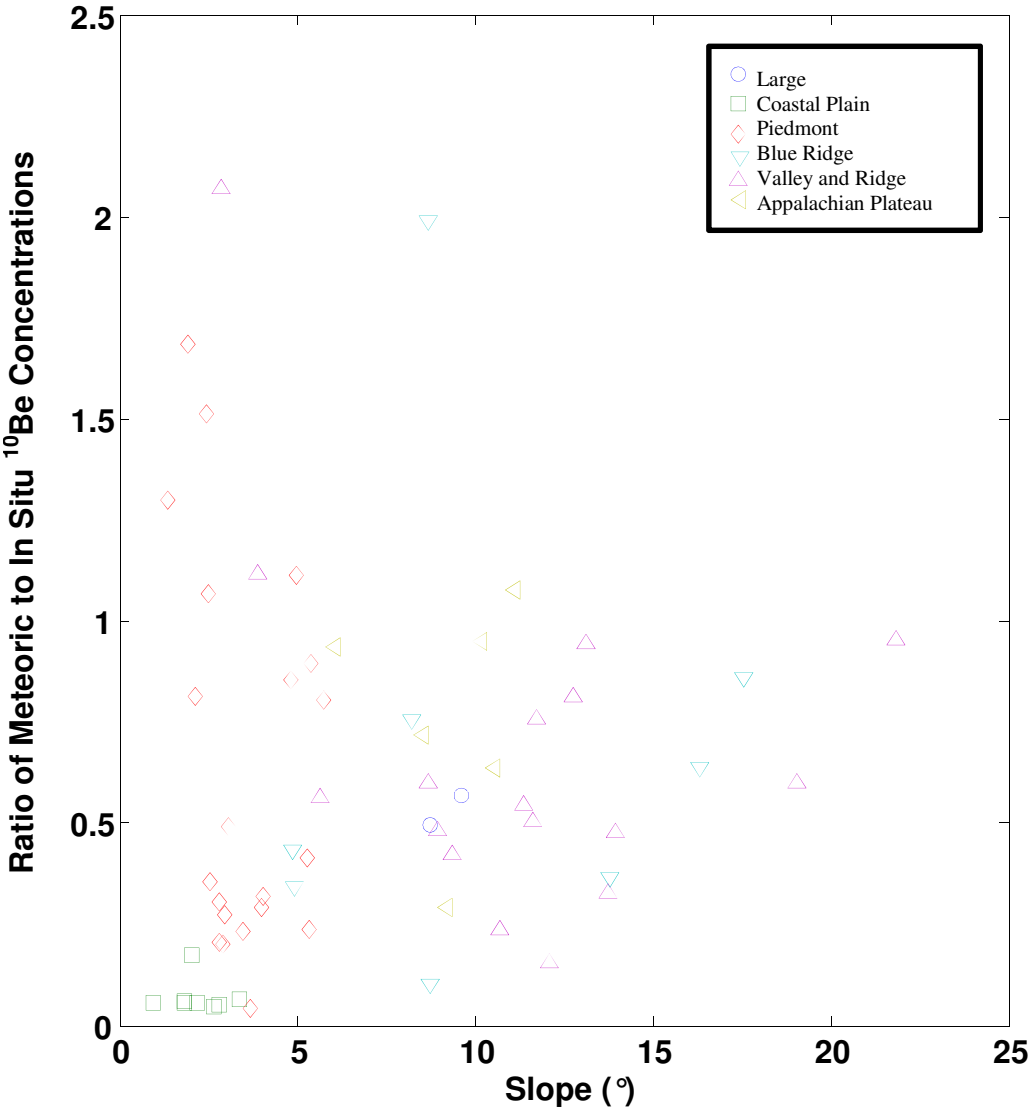


**Figure 5.6 - Ratio Between Meteoric to In Situ $^{10}$Be Concentrations against Average Slope.**
The y-axis is the ratio between meteoric to in situ $^{10}$Be concentrations. The x-axis is the average slope in degrees. The blue circles are samples from large basins that occupy many physiographic provinces. The green squares are from the Coastal Plain, red diamond, Piedmont, turquoise upside down triangle Blue Ridge, purple triangle Valley and Ridge, yellow sideways triangle Appalachian Plateau. The ratio between meteoric to in situ $^{10}$Be concentrations show no correlation with average slope ($R^2$=0.01, $p$=0.42).

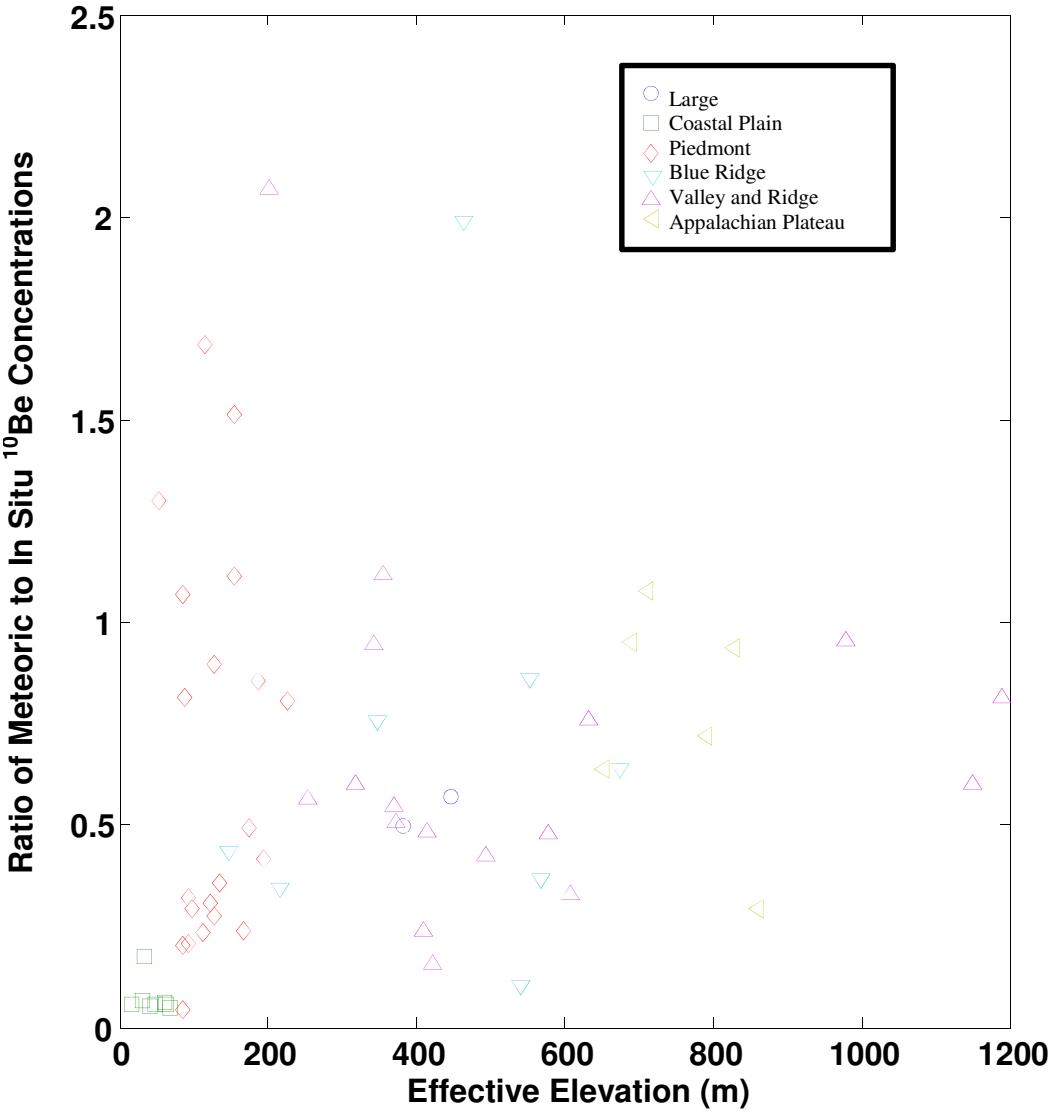


**Figure 5.7 - Ratio Between Meteoric to In Situ $^{10}$Be Concentrations against Effective Elevation.**
The y-axis is the ratio between meteoric to in situ $^{10}$Be concentrations. The x-axis is the effective elevation in m. The blue circles are samples from large basins that occupy many physiographic provinces. The green squares are from the Coastal Plain, red diamond, Piedmont, turquoise upside down triangle Blue Ridge, purple triangle Valley and Ridge, yellow sideways triangle Appalachian Plateau. The ratio between meteoric to in situ $^{10}$Be concentrations show no correlation with effective elevation ($R^2$=0.04, $p$=0.12).

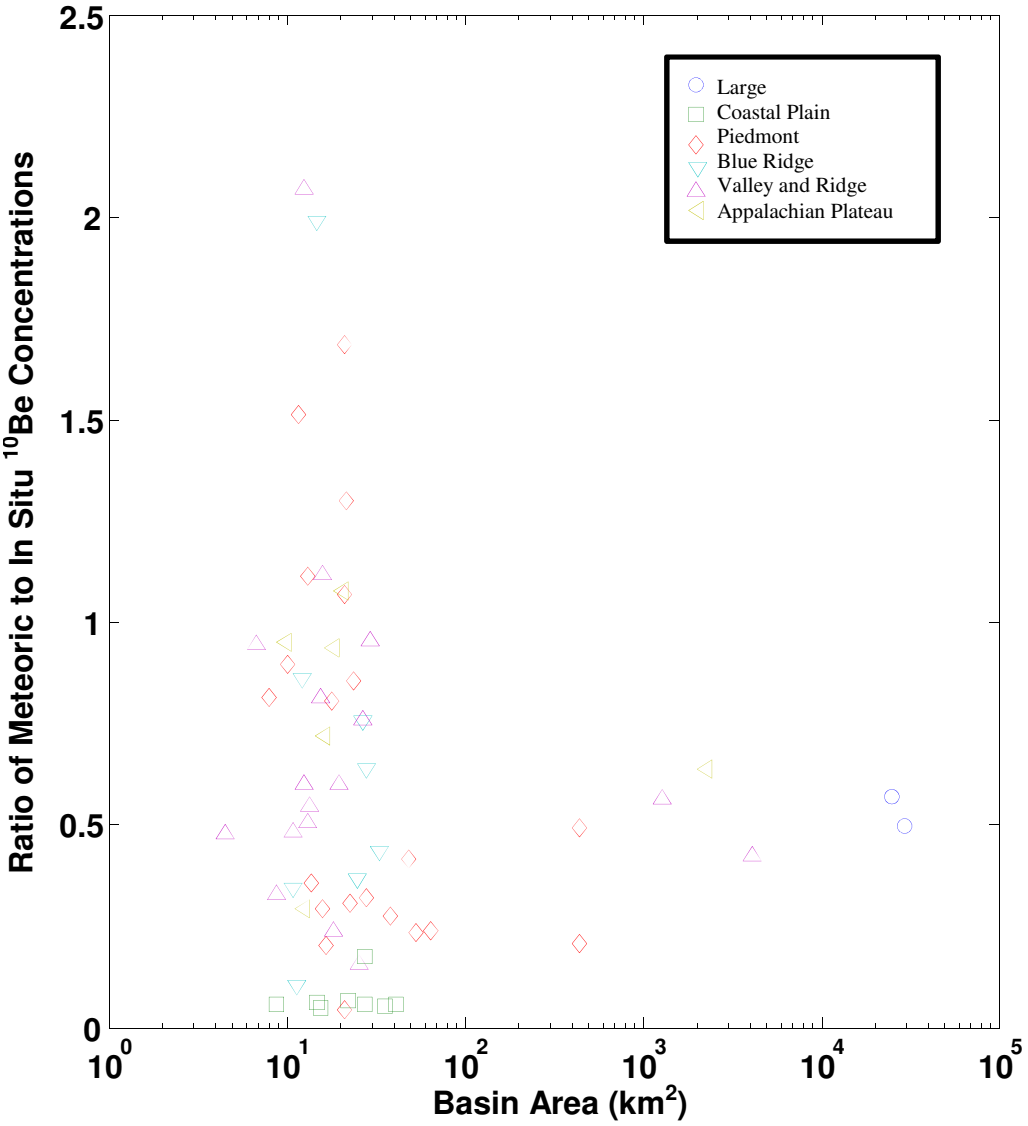


**Figure 5.8 - Ratio Between Meteoric to In Situ $^{10}$Be Concentrations against Basin Area.**

The y-axis is the ratio between meteoric to in situ $^{10}$Be concentrations. The x-axis is the basin area in km$^2$. The blue circles are samples from large basins that occupy many physiographic provinces. The green squares are from the Coastal Plain, red diamond, Piedmont, turquoise upside down triangle Blue Ridge, purple triangle Valley and Ridge, yellow sideways triangle Appalachian Plateau. The ratio between meteoric to in situ $^{10}$Be concentrations show no correlation with basin area ($R^2$<0.01, $p$=0.83).

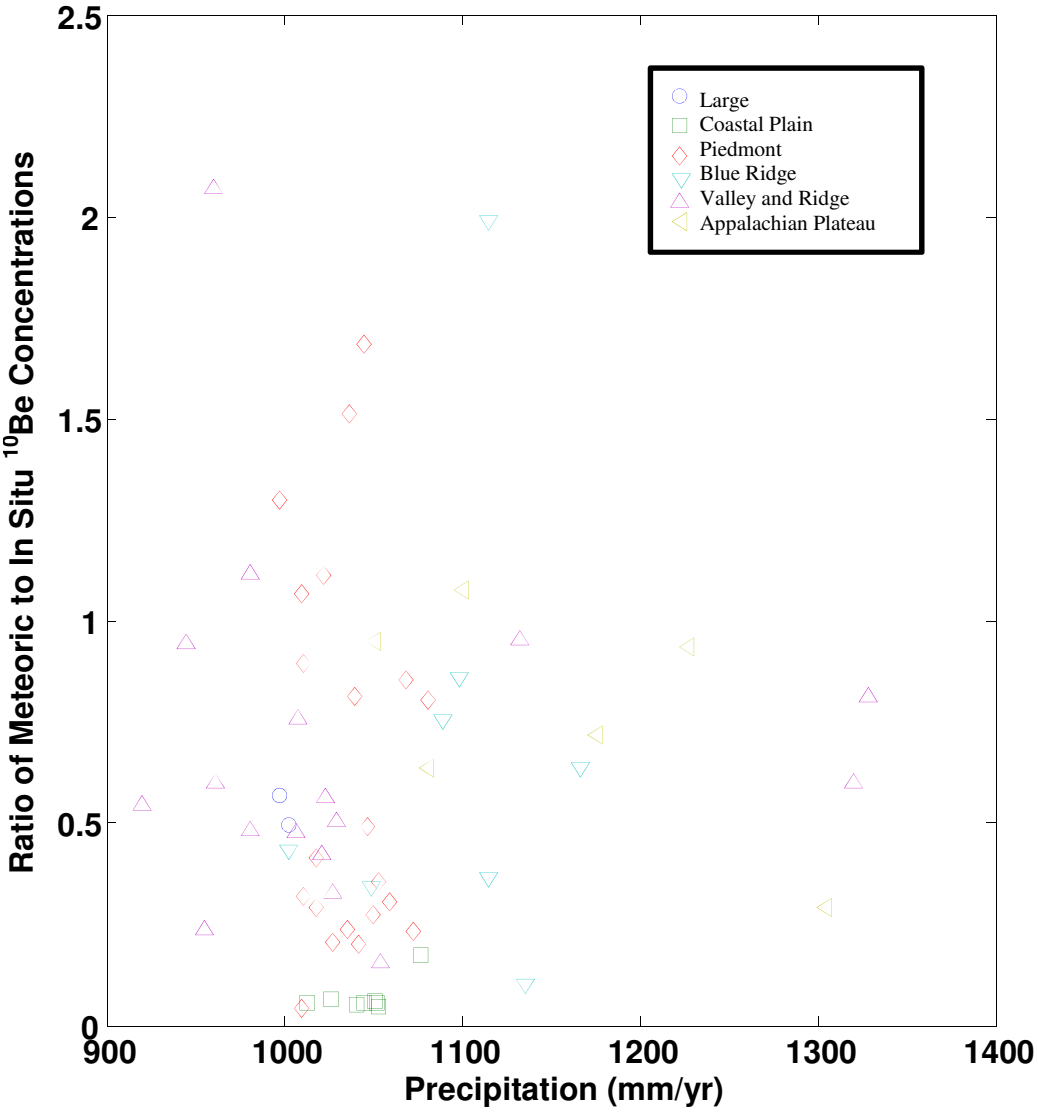


**Figure 5.9 - Ratio Between Meteoric to In Situ $^{10}$Be Concentrations against Precipitation.**
The y-axis is the ratio between meteoric to in situ $^{10}$Be concentrations. The x-axis is the precipitation in mm/yr. The blue circles are samples from large basins that occupy many physiographic provinces. The green squares are from the Coastal Plain, red diamond, Piedmont, turquoise upside down triangle Blue Ridge, purple triangle Valley and Ridge, yellow sideways triangle Appalachian Plateau. The ratio between meteoric to in situ $^{10}$Be concentrations show no correlation with precipitation ($R^2$<0.01, $p$=0.91).

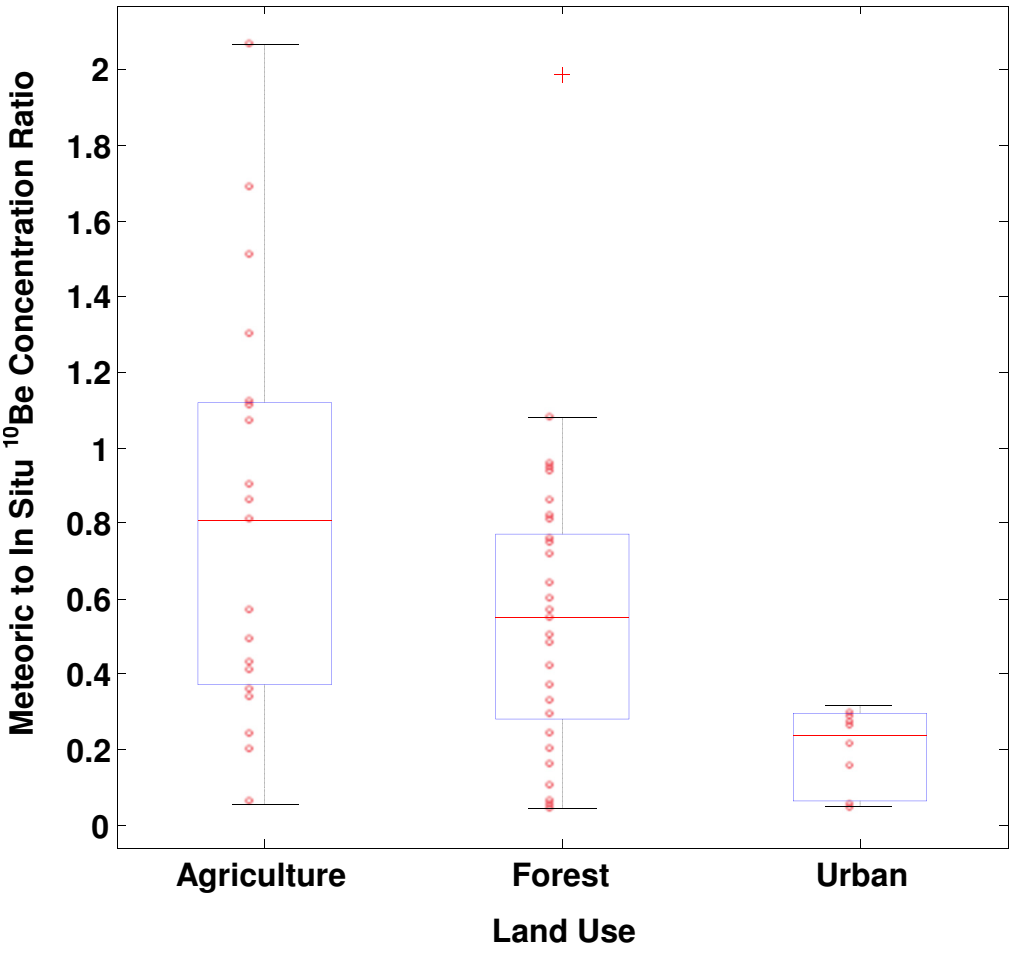


**Figure 5.10 - Ratio Between Meteoric to In Situ $^{10}$Be Concentrations against Land Use.**
Each land use group contains basins which contain a majority of that type of land use. The y-axis is the ratio between meteoric to in situ $^{10}$Be concentrations. The red line in the middle of the box is the median. The bottom of the box is the 25% quartile, and the top of the box is the 75% quartile. The bottom whisker is the 25% quartile - 1.5 * the interquartile range, the top whisker is the 75% quartile + 1.5 * the interquartile range. The interquartile range is equal to the 75% quartile - 25% quartile. All points out side of the whiskers, the red crosses, are statistical outliers if the data are normally distributed. All other data points are small red circles ($p$<0.01).

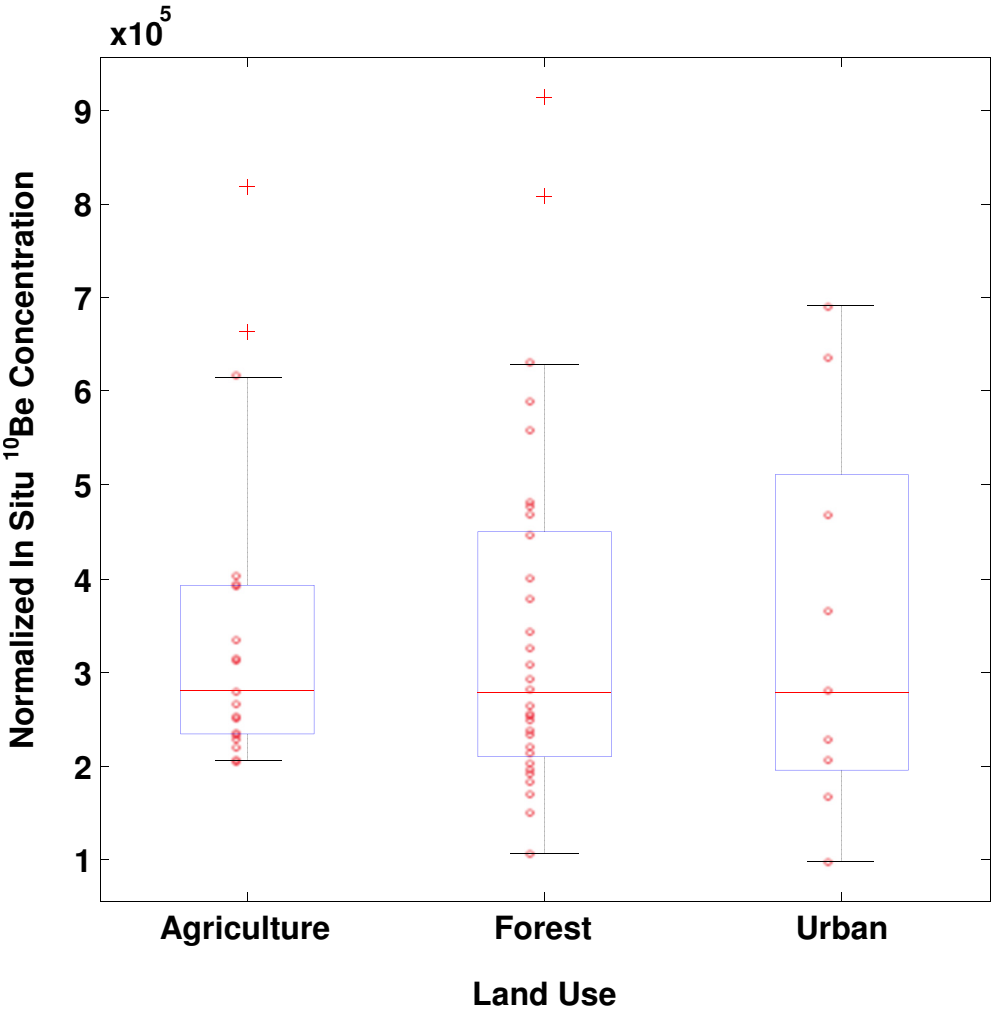


**Figure 5.11 - Normalized In Situ $^{10}$Be Concentrations against Land Use.**
Each land use group contains basins which contain a majority of that type of land use. The y-axis is the normalized in situ $^{10}$Be concentration in atoms g quartz$^{-1}$. The red line in the middle of the box is the median. The bottom of the box is the 25% quartile, and the top of the box is the 75% quartile. The bottom whisker is the 25% quartile - 1.5 * the interquartile range, the top whisker is the 75% quartile + 1.5 * the interquartile range. The interquartile range is equal to the 75% quartile - 25% quartile. All points out side of the whiskers, the red crosses, are statistical outliers if the data are normally distributed. All other data points are small red circles ($p$=0.98).

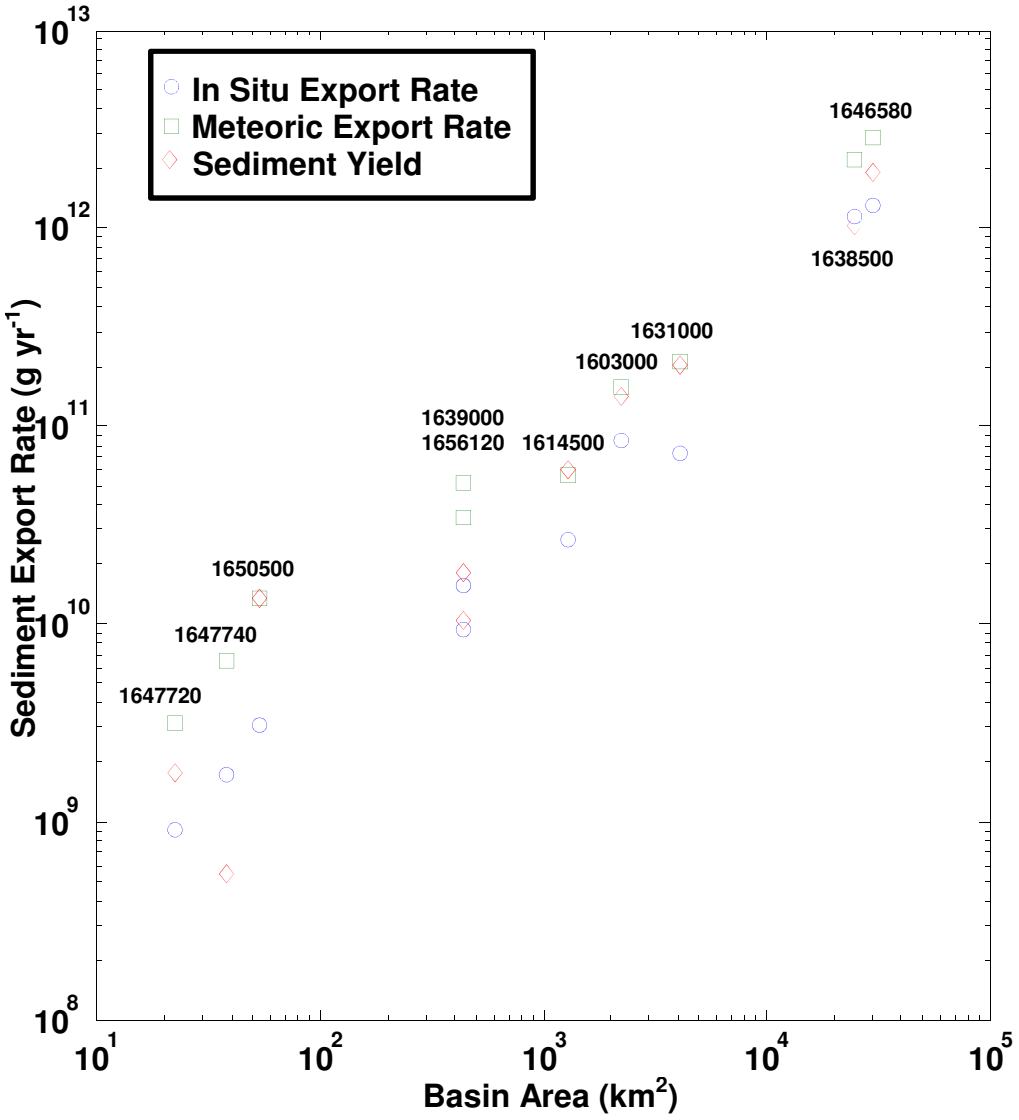


**Figure 5.12 - In Situ, Meteoric and Modern Sediment Export Rate at each Gaging Station**

This plot is a comparison of export rates of sediment determined by modern sediment yield calculations, and converting in situ and meteoric $^{10}$Be erosion rates into export rates. The y-axis is the export rates in g yr$^{-1}$ on a log scale. The x-axis is the basin area in km$^2$ on a log scale. The blue diamonds are the in situ $^{10}$Be export rates, the red squares are the meteoric $^{10}$Be export rate and the green triangles are the modern sediment export rates. The numbers above each set of points is the gaging station number.

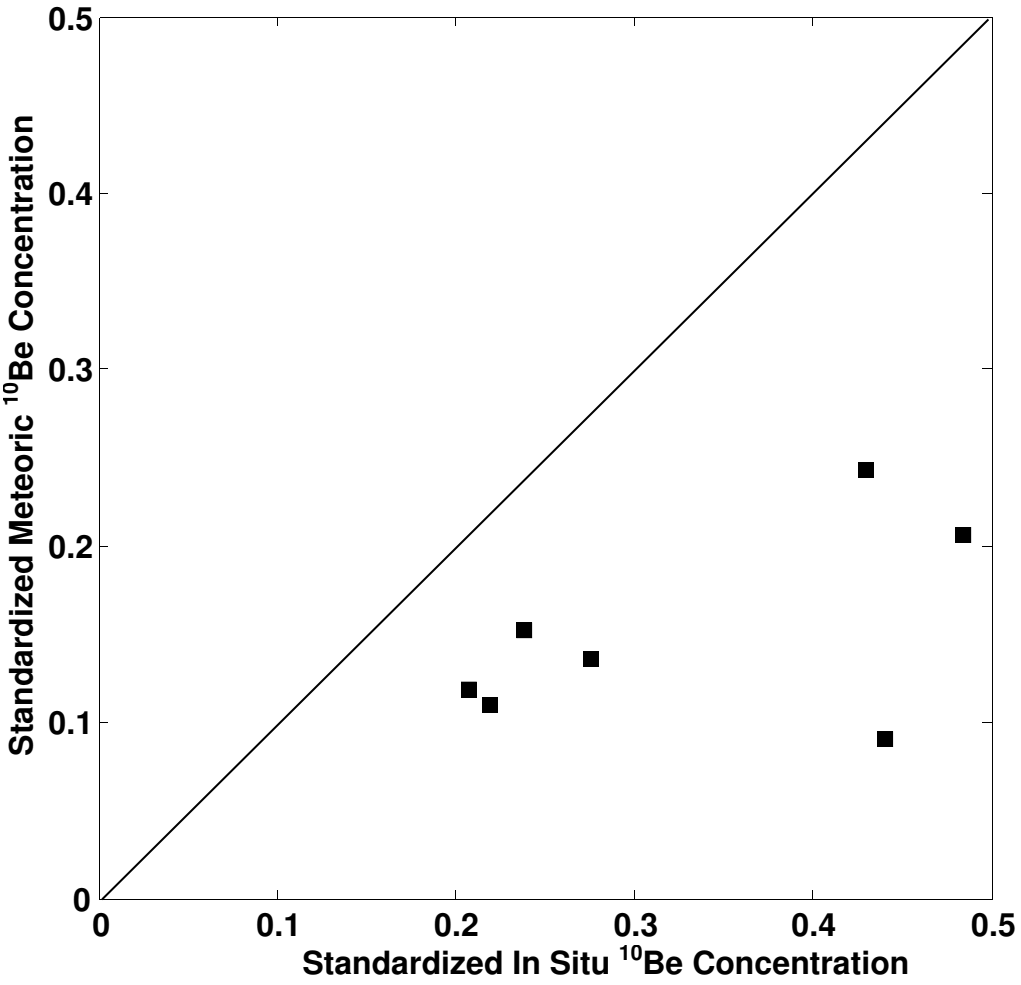


**Figure 5.13 - Standardized Meteoric $^{10}$Be Concentration against Standardized In Situ $^{10}$Be Concentration at Basins Greater than 400 km$^2$.**
The y-axis is the standardized in situ $^{10}$Be concentrations. The x-axis is the standardized meteoric $^{10}$Be concentrations. The line is a one to one relationship. Standardized in situ $^{10}$Be concentrations and standardized meteoric $^{10}$Be concentrations show no correlation ($R^2$=0.27, $p$=0.24).

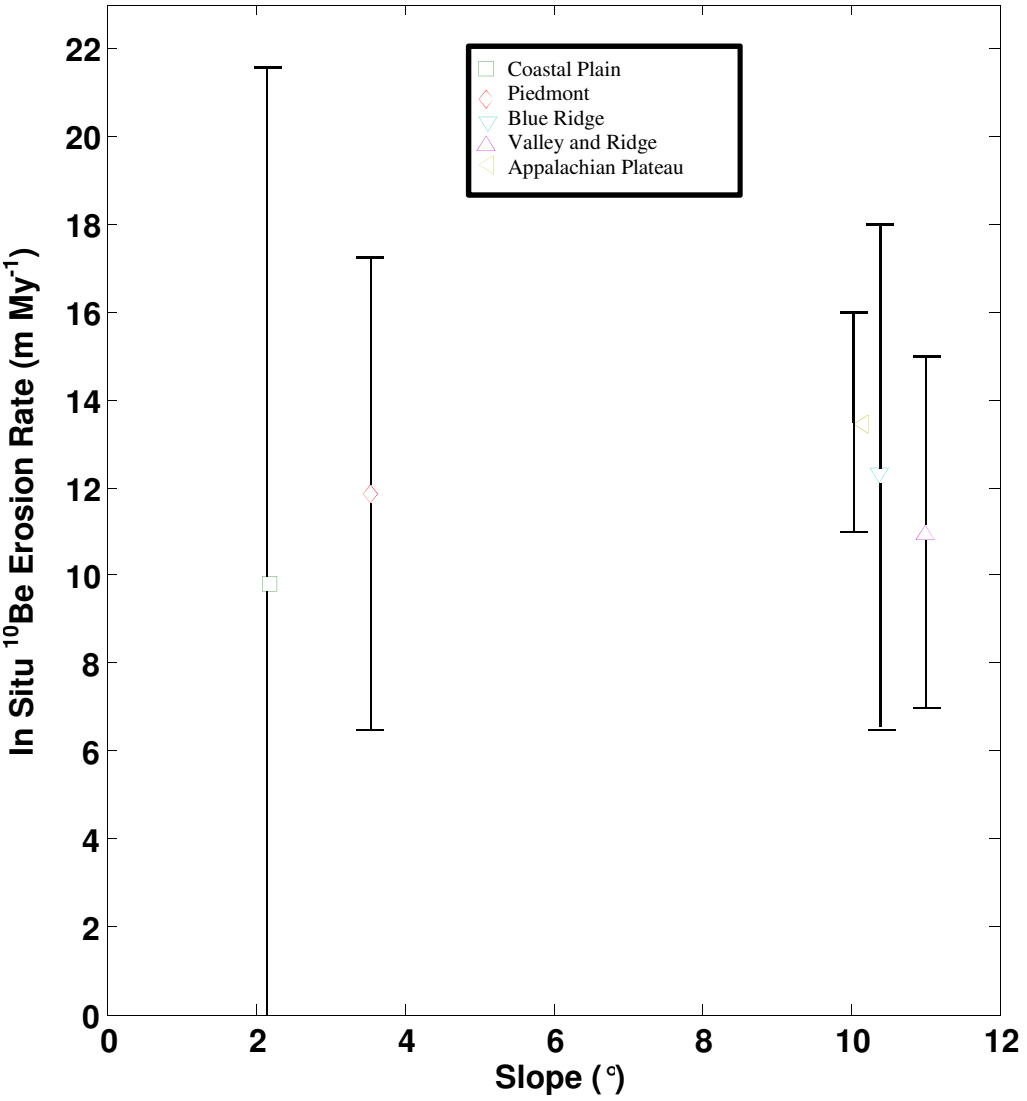


**Figure 5.14 – Average In Situ $^{10}$Be Erosion Rate in each Physiographic Province against Average Slope in each Province**
The y-axis is the in situ $^{10}$Be erosion rate in m My$^{-1}$. The x-axis is the average slope in degrees. The blue circles are samples from large basins that occupy many physiographic provinces. The green squares are from the Coastal Plain, red diamond, Piedmont, turquoise upside down triangle Blue Ridge, purple triangle Valley and Ridge, yellow sideways triangle Appalachian Plateau. The black lines coming off of each point are standard deviation error bars. Average in situ erosion rates from each physiographic province show no correlation with average slope ($R^2$=0.31, $p$=0.33).

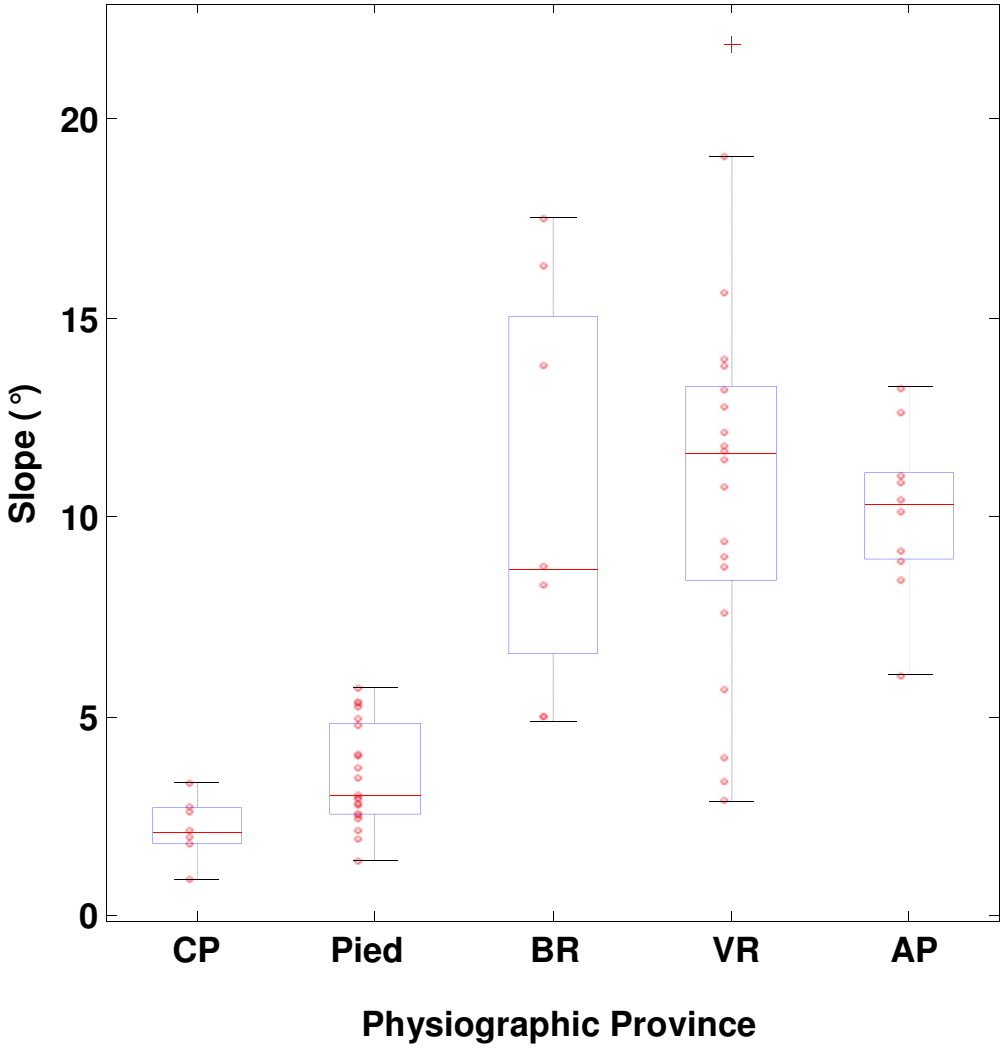


**Figure 5.15 - Average Slope against Physiographic Province.**
CP is the Coastal Plain, Pied is the Piedmont, BR is the Blue Ridge, VR is the Valley and Ridge, and AP is the Appalachian Plateau. The y-axis is the average slope in degrees. The red line in the middle of the box is the median. The bottom of the box is the 25% quartile, and the top of the box is the 75% quartile. The bottom whisker is the 25% quartile - 1.5 * the interquartile range, the top whisker is the 75% quartile + 1.5 * the interquartile range. The interquartile range is equal to the 75% quartile - 25% quartile. All points out side of the whiskers, the red crosses, are statistical outliers if the data are normally distributed. All other data points are small red circles. Slopes from the Coastal Plain and Piedmont are lower than the other provinces ($p$<0.01). The Coastal Plain is also lower than the Piedmont ($p$=0.01).

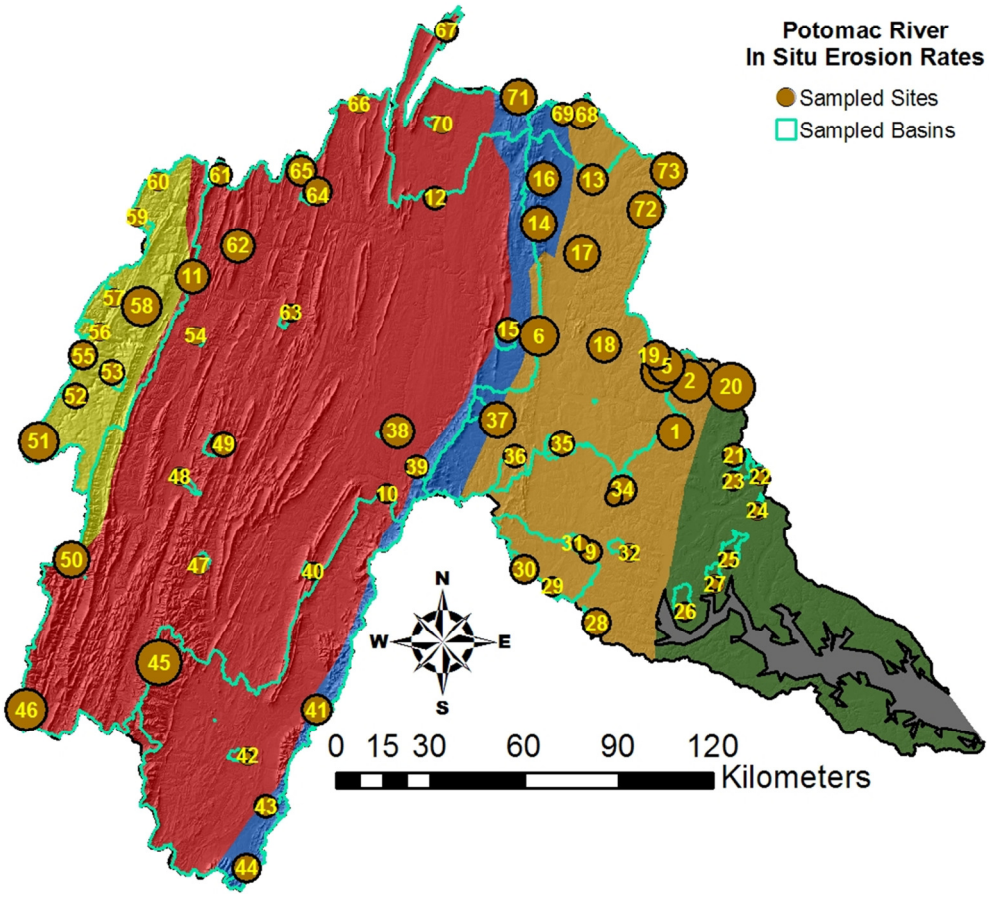


**Figure 5.16 – Spatial Distribution of In Situ $^{10}$Be Erosion Rates in the Potomac Basin**

The brown dots are the sampled sites, larger dots are higher erosion rates while the smaller dots are lower erosion rates. Each colored region on the map is a different physiographic province (from USGS). The green area is the Coastal Plain, the orange region is the Piedmont, and the blue portion is the Blue Ridge, the red area in the Valley and Ridge, and the yellow section is the Appalachian Plateau. The background is a shaded digital elevation model (USGS digital data, http://seamless.usgs.gov/).

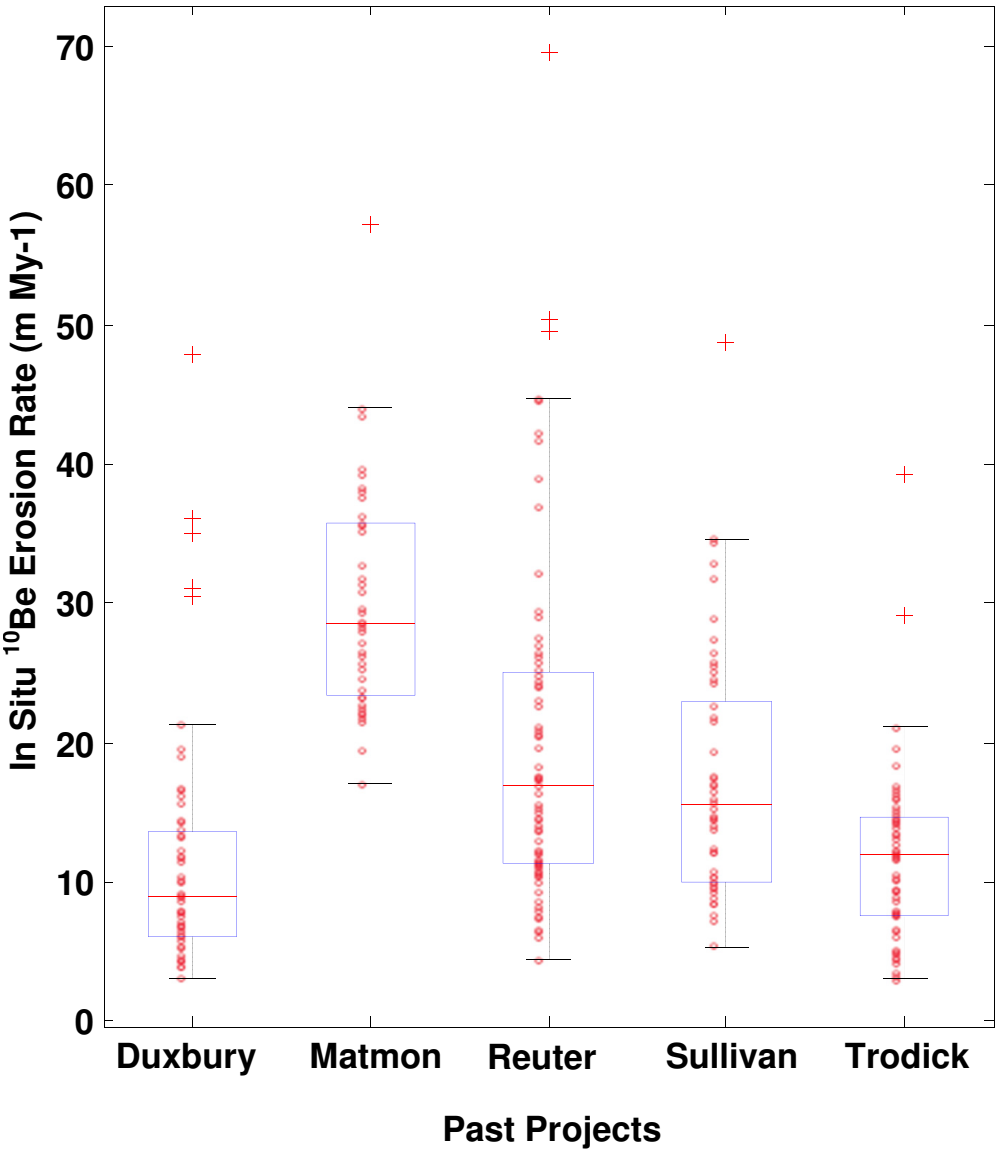


**Figure 5.17 - In Situ $^{10}$Be Erosion Rates of Past Projects.**
A series of box plots showing in situ $^{10}$Be erosion rates for my study against previous studies including Duxbury and others (2008), Matmon and others (2003), Reuter and others (2005) and Sullivan and others (2007) with the data taken from Portenga and others (2011. My data are statistically dissimilar than Matmon and others (2003) work from the Great Smokey Mountains National Park, Reuter and others (2005) work from the Susquehanna and Sullivan and others (2007) work from the Blue Ridge Escarpment ($p$<0.01). My data are similar to Duxbury and others (2008) work from the Shenandoah ($p$=0.76).

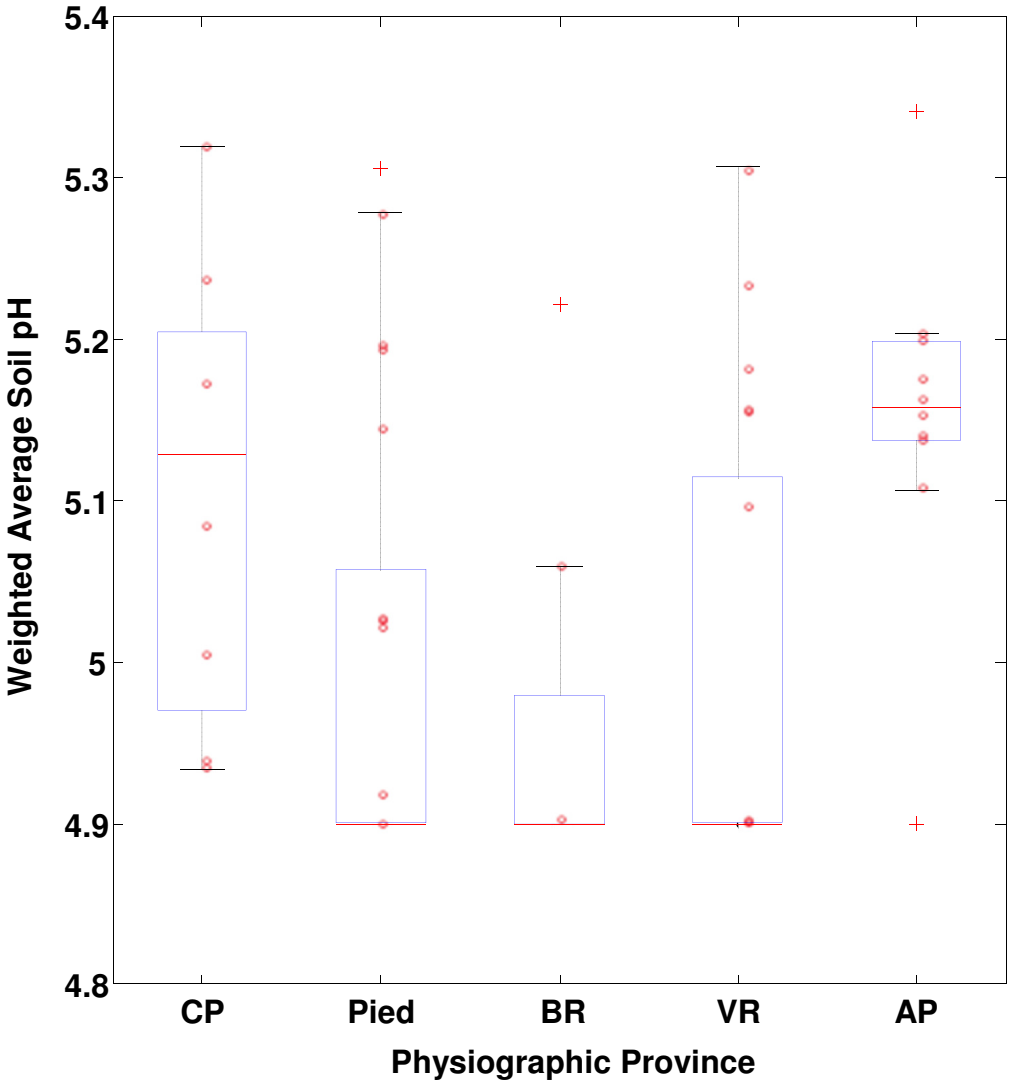


**Figure 5.18 – Weighted Average Soil pH against Physiographic Province.**
CP is the Coastal Plain, Pied is the Piedmont, BR is the Blue Ridge, VR is the Valley and Ridge, and AP is the Appalachian Plateau. The y-axis is the weighted average soil pH. The red line in the middle of the box is the median. The bottom of the box is the 25% quartile, and the top of the box is the 75% quartile. The bottom whisker is the 25% quartile - 1.5 * the interquartile range, the top whisker is the 75% quartile + 1.5 * the interquartile range. The interquartile range is equal to the 75% quartile - 25% quartile. All points out side of the whiskers, the red crosses, are statistical outliers if the data are normally distributed. All other data points are small red circles.

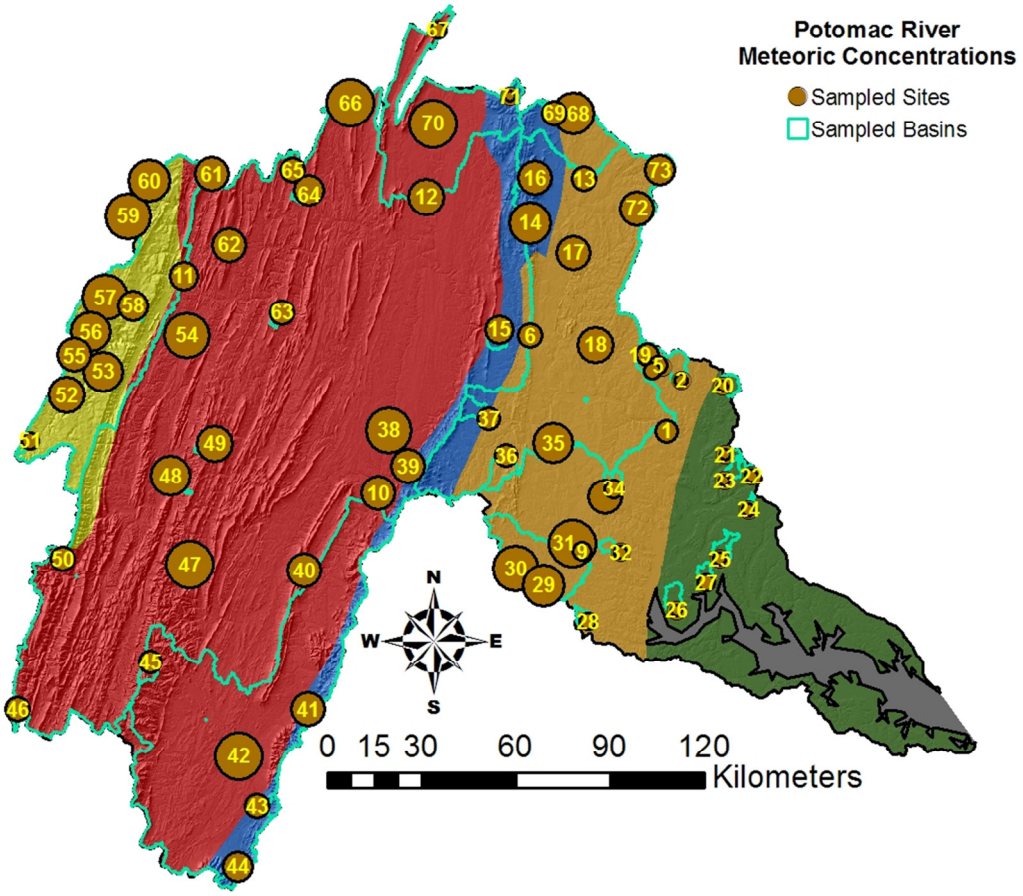


**Figure 5.19 – Spatial Distribution of Meteoric $^{10}$Be Concentrations in the Potomac Basin**

The brown dots are the sampled sites, larger dots are higher concentrations while the smaller dots are lower concentrations. Each colored region on the map is a different physiographic province (from USGS). The green area is the Coastal Plain, the orange region is the Piedmont, and the blue portion is the Blue Ridge, the red area in the Valley and Ridge, and the yellow section is the Appalachian Plateau. The background is a shaded digital elevation model (USGS digital data, http://seamless.usgs.gov/).

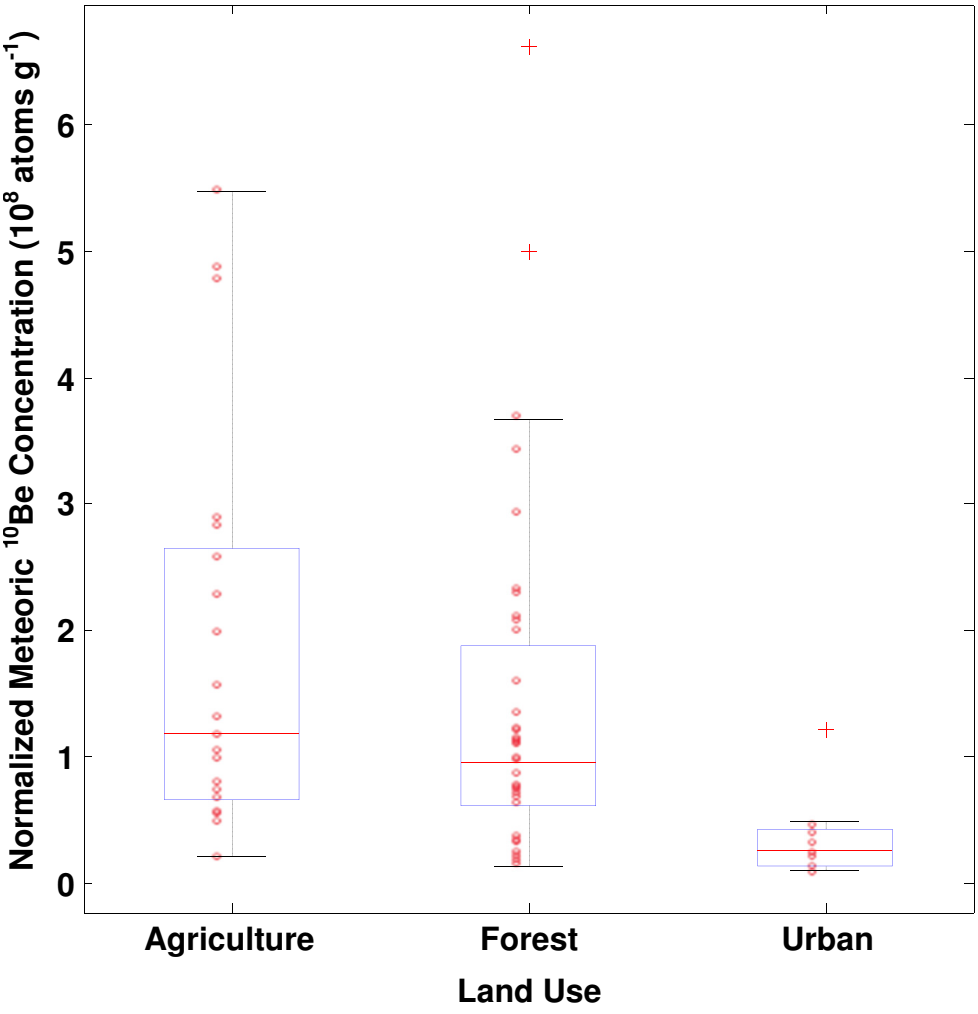


**Figure 5.20 – Normalized Meteoric $^{10}$Be Concentrations against Land Use.**
Each land use group contains basins which contain a majority of that type of land use. The y-axis is the normalized meteoric $^{10}$Be concentrations. The red line in the middle of the box is the median. The bottom of the box is the 25% quartile, and the top of the box is the 75% quartile. The bottom whisker is the 25% quartile - 1.5 * the interquartile range, the top whisker is the 75% quartile + 1.5 * the interquartile range. The interquartile range is equal to the 75% quartile - 25% quartile. All points out side of the whiskers, the red crosses, are statistical outliers if the data are normally distributed. All other data points are small red circles. The urban basins are statistically different ($p$<0.01), while the agriculture and forested basin are statistically similar ($p$=0.18).

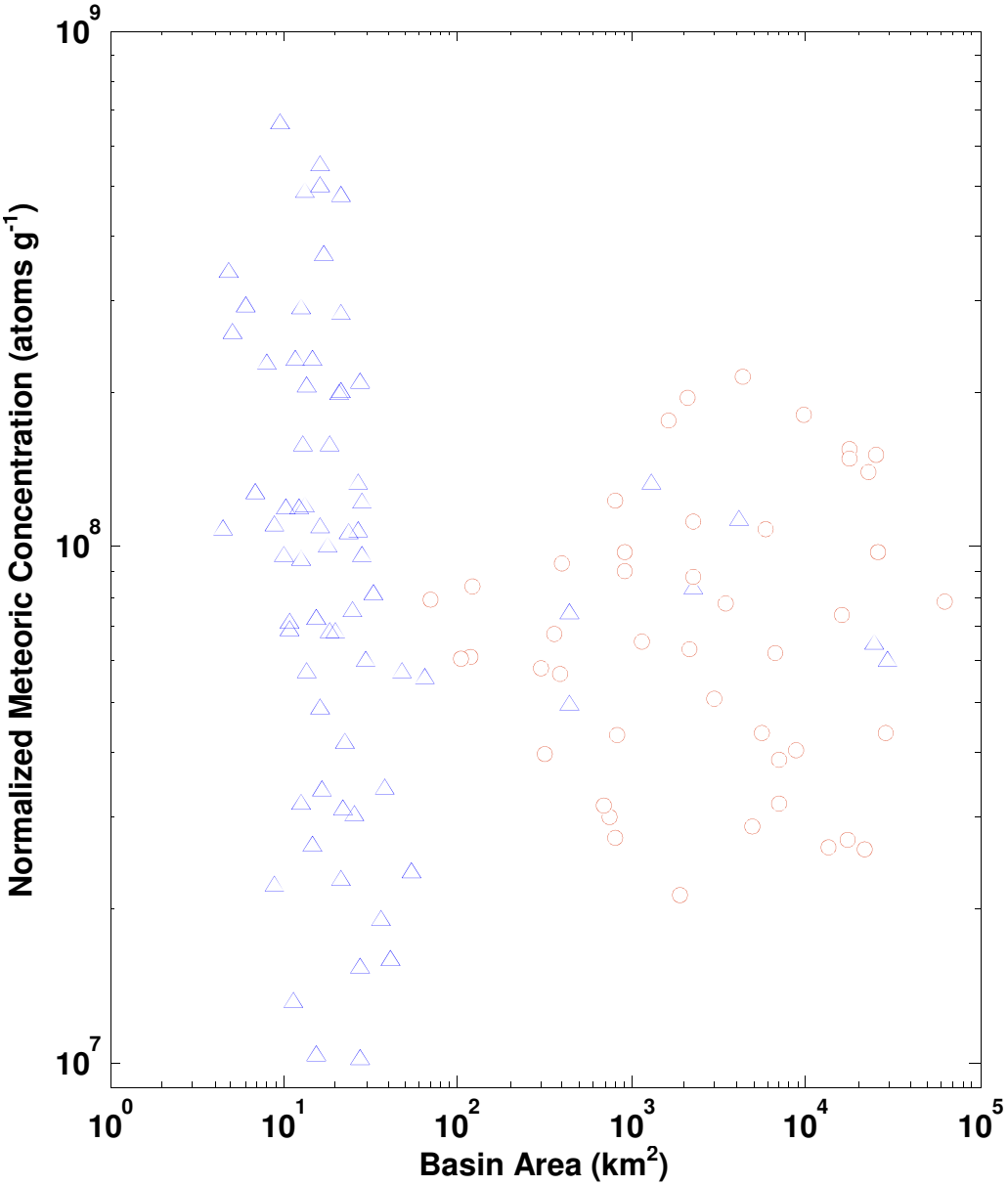


**Figure 5.21 - Brown et al. 1988 and My Normalized Meteoric $^{10}$Be Concentrations against Basin Area.**
A scatterplot showing my measured meteoric $^{10}$Be concentrations (atoms g$^{-1}$) and Brown and others' (1988) meteoric $^{10}$Be concentration (atoms g$^{-1}$) against basin area (km$^2$). The blue circles are my data and the red circles are Brown and others' (1988) data. The y-axis is the meteoric $^{10}$Be concentration in atoms g$^{-1}$ on a log scale and the x-axis is the basin area in km$^2$ on a log scale.

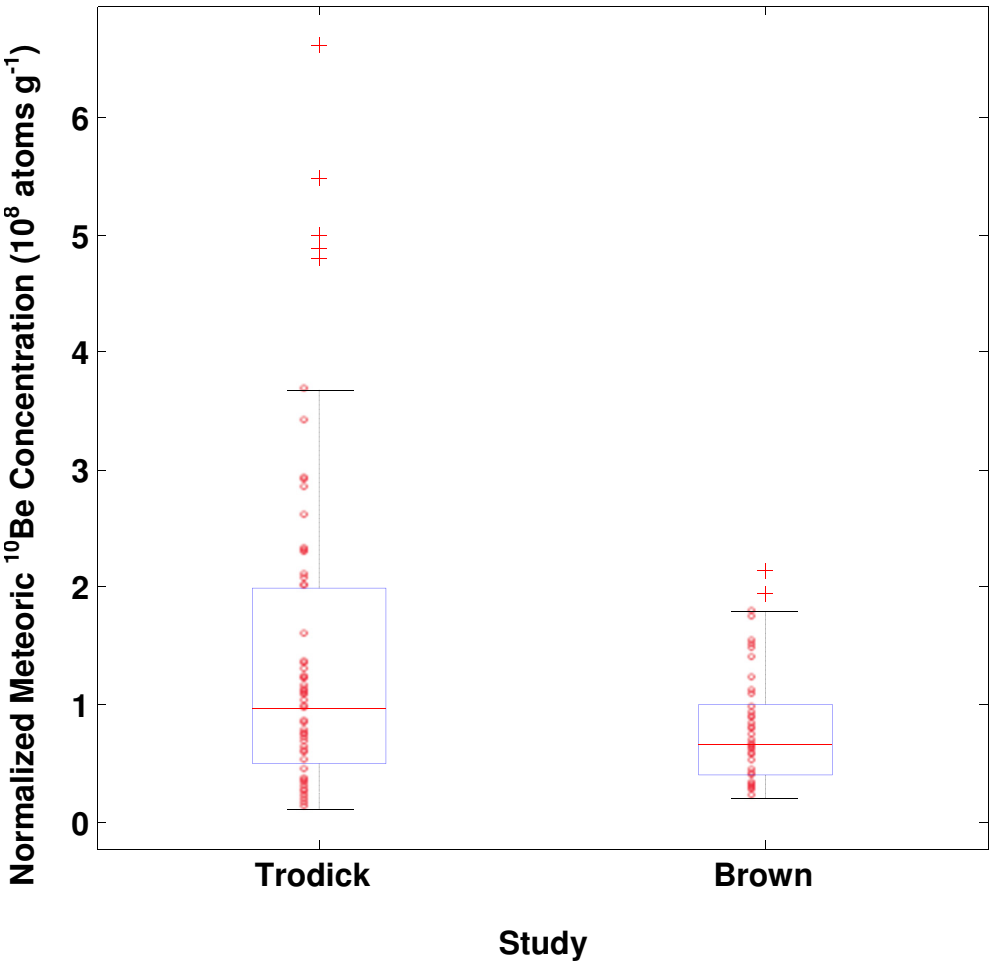


**Figure 5.22 - Normalized Meteoric $^{10}$Be Concentrations of Brown et al. 1988 and My Work.**
The y-axis is the normalized meteoric $^{10}$Be concentration in atoms g sediment$^{-1}$. The red line in the middle of the box is the median. The bottom of the box is the 25% quartile, and the top of the box is the 75% quartile. The bottom whisker is the 25% quartile - 1.5 * the interquartile range, the top whisker is the 75% quartile + 1.5 * the interquartile range. The interquartile range is equal to the 75% quartile - 25% quartile. All points out side of the whiskers, the red crosses, are statistical outliers if the data are normally distributed. All other data points are small red circles. Statistically they are different ($p$<0.01).

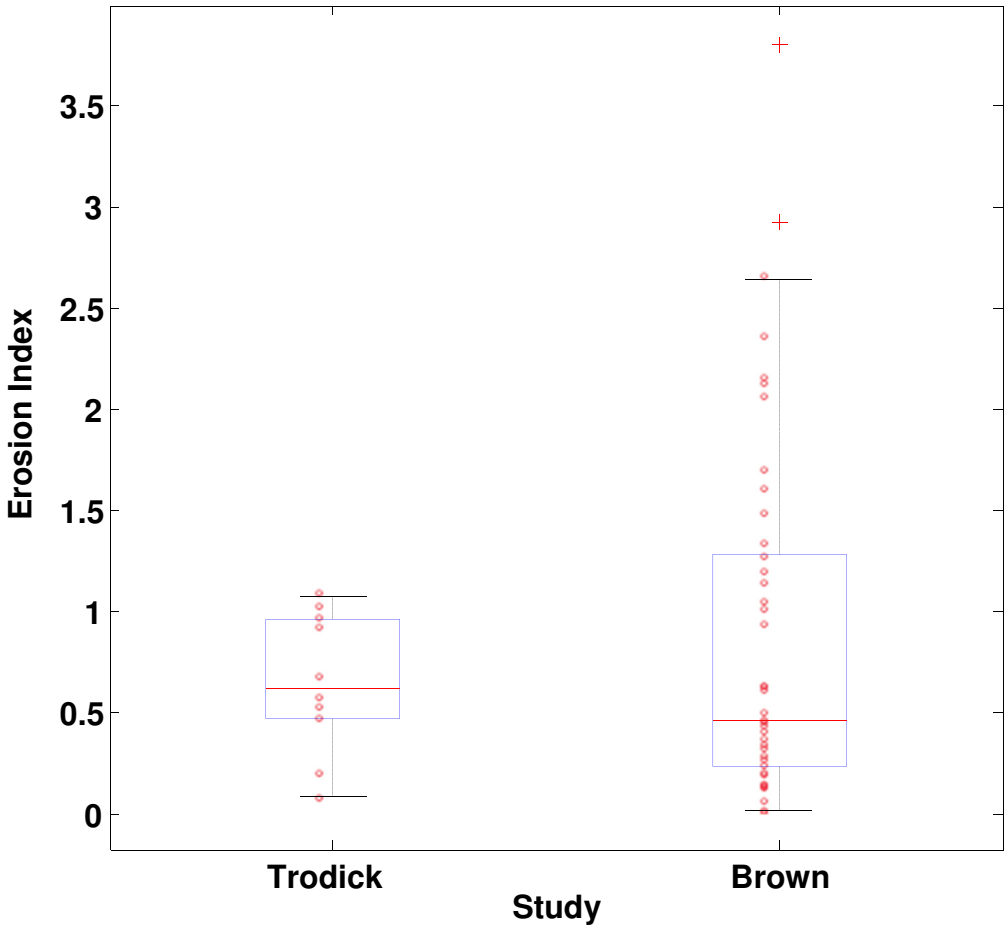


**Figure 5.23 - Erosion Indexes of Brown et al. (1988) and My Work.**
The y-axis is the erosion index. The red line in the middle of the box is the median. The bottom of the box is the 25% quartile, and the top of the box is the 75% quartile. The bottom whisker is the 25% quartile - 1.5 * the interquartile range, the top whisker is the 75% quartile + 1.5 * the interquartile range. The interquartile range is equal to the 75% quartile - 25% quartile. All points out side of the whiskers, the red crosses, are statistical outliers if the data are normally distributed. All other data points are small red circles. Statistically they are very similar ($p$=0.44).

## Chapter 6 – Conclusions and Recommendations

In situ, basin-scale, $^{10}$Be erosion rates range from 3 to 39 m My$^{-1}$ with a mean of 12 m My$^{-1}$ and a median of 12 m My$^{-1}$ (Figure 3.3 and Figure 3.5). The larger basins (29796 and 24851 km$^2$), which contain many of the physiographic provinces, have in situ $^{10}$Be erosion rates of 16 and 17 m My$^{-1}$. Meteoric, basin-scale, $^{10}$Be erosion rates using the approach of Willenbring and von Blanckenburg (2010) range from 3 to 212 m My$^{-1}$ with a mean of 40 m My$^{-1}$, median of 22 m My$^{-1}$ (Figure 3.4). The larger basins which flow through many of the physiographic provinces have meteoric $^{10}$Be erosion rates of 36 and 33 m My$^{-1}$.

When considering in situ $^{10}$Be erosion rates with outliers, all five physiographic provinces are similar ($p$=0.13) (Figure 4.4). The four physiographic provinces of the Piedmont, Blue Ridge, Valley and Ridge and the Appalachian Plateau are statistically similar for when looking at in situ $^{10}$Be erosion rates without outliers and normalized meteoric $^{10}$Be concentrations separately ($p$=0.25, $p$=0.06) (Figure 4.4 and Figure 4.12). This appears to agree with Hack's (1960) model of landscape evolution. The Coastal Plain is statistically separate from the other four physiographic provinces when analyzing both in situ $^{10}$Be erosion rates without outliers and normalized meteoric $^{10}$Be concentrations separately ($p$<0.01, $p$<0.01) (Figure 4.4 and Figure 4.12). In the case of in situ $^{10}$Be, the Coastal Plain erosion rates are much lower than the other physiographic provinces. This could be caused by the fact that the slope of the Coastal Plain is statistically lower than all of the other provinces ($p$<0.01, $p$=0.01) (Figure 5.15). The

slope, erosion rate relationship on the Coastal Plain agrees with Davis (1899). The normalized meteoric $^{10}$Be concentrations of the Coastal Plain are much lower than the other provinces. Most likely something is occurring on the Coastal Plain where an unexpectedly low amount of meteoric $^{10}$Be is sticking to the surface sediment, possibly acidified soil or could also be sandy, permeable soil trough which $^{10}$Be is deeply penetrating.

In situ $^{10}$Be erosion rates show no correlation with average slope and a weak positive correlation with the effective elevation of a basin when outliers are both included and excluded (Slope $R^2$=0.06, $p$>0.05; $R^2$=0.04, $p$=0.11; Elevation $R^2$=0.10, $p$=0.01; $R^2$=0.11, $p$=0.01) (Figure 4.5, Figure 4.6). There is also no correlation between slope and in situ erosion rates when each physiographic province is considered individually (CP, $R^2$=0.01, $p$=0.81; Pied, $R^2$=0.06, $p$=0.27; BR, $R^2$=0.01, $p$=0.81; VR, $R^2$=0.22, $p$>0.05; AP, $R^2$=0.07, $p$=0.61) (Figure 4.5). Although, as stated above, the Coastal Plain appears to have such a low slope that erosion is much slower. Again, this tends to agree with Hack (1960) except for the Coastal Plain. My sampled basins also show no correlation between normalized in situ and meteoric $^{10}$Be concentrations. Most likely this is occurring because of my poor understanding of where meteoric $^{10}$Be resides in the sediment of my basins which makes it difficult to properly normalize meteoric $^{10}$Be concentrations.

My in situ $^{10}$Be erosion rates are within the range of the past studies of Matmon et al. (2003), Reuter et al. (2006) and Sullivan (2007), but they are statistically different

($p$<0.01). On the other hand, my in situ $^{10}$Be erosion rates are statistically similar to Duxbury et al. (2009) work on the Shenandoah River, a tributary of the Potomac River ($p$=0.76) (Figure 5.7). Brown et al. (1988) meteoric $^{10}$Be concentrations that were collected from gaging stations in the Chesapeake Bay Watershed are statistically different than my meteoric $^{10}$Be concentrations ($p$<0.01). Their erosion indexes are statistically similar to mine ($p$=0.44) and most of their erosion indexes and mine are below 1 indicating that basins have slightly more meteoric $^{10}$Be entering than leaving the basin.

Finally, sediment export rates that I calculated from my in situ and meteoric $^{10}$Be erosion rates appear to line up with modern sediment export rates in large basins (>400 km$^2$) (Figure 5.12) but the lack of a correlation between the in situ and meteoric $^{10}$Be erosion rates in the large basins casts doubt on this finding (Figure 5.13). This finding which shows the meteoric $^{10}$Be concentration could potentially be used as a proxy for modern sediment yields, in large basins but much more work needs to be done to better understand the relationship between modern sediment yields and meteoric $^{10}$Be concentrations.

### *Recommendations for Future Work*

My research has continued the recent work on in situ $^{10}$Be erosion rates from around the world. Clearly these studies should continue so that we can better understand how the earth is eroding. While there have been many studies on in situ $^{10}$Be, there have been very few studies using meteoric $^{10}$Be. I think someone could get samples from basins used for previous studies on in situ $^{10}$Be and future in situ $^{10}$Be studies should also

include meteoric $^{10}$Be so that the relationship between in situ and meteoric $^{10}$Be can be better understood along with the variables that affect meteoric $^{10}$Be concentration. As of right now it appears that meteoric $^{10}$Be does not work well in the Potomac Basin, so I would suggest trying it in new areas that have noticeably different landscapes than the Potomac Basin.

Finally, to properly use meteoric $^{10}$Be, soil cores need to be taken from representative points in each sampled basin. These soil cores can have specific parts analyzed for meteoric $^{10}$Be to allow for a better understanding of how the meteoric $^{10}$Be is distributed in the soil of the basin with depth. Knowing how the meteoric $^{10}$Be is distributed in the soil would allow for a better determination of erosion rates using meteoric $^{10}$Be. Future studies would benefit from comparing in situ $^{10}$Be erosion rates, meteoric $^{10}$Be erosion rates, and modern sediment yields. To do this, future studies need to sample near gaging stations so that there is a record of modern sediment export.

## Bibliography


Balco, G. et al., 2008. A complete and eassily accessible means of calculating surface exposure ages or erosion rates from $^{10}$Be and $^{26}$Al measurements. *Quaternary Geochronology,* Issue 3, pp. 174-195.

Barg, E. et al., 1997. Beryllium geochemistry in soils; evaluation of $^{10}$Be/$^{9}$Be ratios in authigenic minerals as a basis for age models. *Chemical Geology,* Volume 140, pp. 237-258.

Bierman, P. R., 1994. Using in situ produced cosmogenic isotopes to estimate rates of landscape evolution; a review from the geomorphic perspective.. *Journal of Geophysical Research,* Issue 99, pp. 13885-13896.

Bierman, P. R., Jungers, M. C., Reusser, L. J. & Pavich, M. J., 2008. Look Again: Meteoric $^{10}$Be is a Useful Tracer of Hillslope and Basin-Scale Process. *Geological Society of America Abstracts with Programs,* pp. 165-6.

Bierman, P. R. & Nichols, K., 2004. Rock to sediment - Slope to sea with $^{10}$Be - Rates of landscape change.. *Annual review of Earth and Planetary Sciences,* Issue 32, pp. 214-255.

Bierman, P. R. & Steig, E., 1996. Estimating rates of denudation and sediment transport using cosmogenic isotope abundances in sediment. *Earth Surface Processes and Landforms,* Issue 21, pp. 125-139.

Birkeland, P. W., 1999. *Soils and Geomorphology.* 3rd ed. Oxford: University Press.

Brown, E. T. et al., 1995. Denudation rates determined from the accumilation of in situ-produced $^{10}$Be in the Luquillo Experimental Forest, Puerto Rico. *Earth and Planetary Science Letters,* Issue 129, pp. 193-202.

Brown, L. et al., 1988. Erosion of the Eastern United States Observed with $^{10}$Be. *Earth Surface Processes and Landforms,* Volume 13, pp. 441-457.

Brown, R. H., 1943. *Mirror for Americans: Likeness of the Eastern Seaboard, 1810.*. New York: American Geographical Society.

Costa, J. E., 1975. Effects of agriculture on erosion and sedimentation in the Piedmont province, Maryland. *Geological Society of America Bulletin,* Issue 86, pp. 1281-1286.

Davis, W. M., 1899. The geographical cycle. *Geographical Journal,* Volume 14, pp. 481-504.

Desilets, D. & Zreda, M., 2000. Scaling production rates of terrestrial cosmogenic nuclides for altitude and geomagnetic effects. *Geological Society of America Abstracts with Programs,* 7(31), pp. A-400.

DiBase, R. A., Whipple, K. X., Heimsath, A. M. & Ouimet, W. B., 2009. Landscape form and millennial erosion rates in the San Gabriel Mountains, CA. *Earth and Planetary Science Letters,* Volume 289, pp. 134-144.

Dunai, T. J., 2000. Scaling factors for production rates of in situ produced cosmogenic nuclides: a critical reevaluation. *Earth and Plantary Science Letters,* Issue 176, pp. 157-169.

Duxbury, J. P., 2009. *Erosion rates in and around Shenandoah National Park, VA, determined using analysis of cosmogenic $^{10}$Be,* Burlington: University of Vermont.

EPA, US, 2001. *State of the River 2001.* [Online]
Available at:
http://water.epa.gov/type/watersheds/named/heritage/upload/2001_06_25_heritage_sor_sorpotomac.pdf
[Accessed 17 May 2011].

Evans, J. K., Gottgens, J. F., Gill, W. M. & Mackey, S. D., 2000. Sediment Yields Controlled by Intrabasinal Storage and Sediment Conveyance over the Interval 1842-1994: Chargin River, Northeast Ohio, U.S.A.. *Journal of Soil and Water Conservation,* 3(55), p. 264.

Fenneman, N. M., 1938. *Physiography of Eastern United States.* New York: McGraw-Hill.

Gardner, T. W., Jorgensen, D. W., Shuman, C. & Lemieux, C. R., 1987. Geomorphic and tectonic process rates: Effects of measured time interval. *Geology,* Volume 15, pp. 259-261.

Gellis, A. C., Banks, W. S. L., Langland, M. J. & Martucci, S. K., 2004. *Summary of suspended-sediment data for streams draining the Chesapeake Bay watershed, water years 1952-2002,* Reston: USGS.

Gerhart, J. M., 1991. *National Water-Quality Assessment--Potomac River Basin,* Baltimore: USGS.

Graly, J. A., Bierman, P. R., Reusser, L. J. & Pavich, M. J., 2010. Meteoric $^{10}$Be in soil profiles - a global meta-analysis. *Geochimica et Cosmochimica Acta,* Issue 74, pp. 6814-6829.

Granger, D. E., Fabel, D. & Palmer, A. N., 2001. Pliocene-Pleistocene incision of the Green River, Kentucky, determined from radioactive decay of cosmogenic $^{26}$Al and $^{10}$Be in Mammoth Cave sediments. *Geological Society of America Bulletin,* Volume 113, pp. 825-836.

Granger, D. E., Kirchner, J. W. & Finkel, R., 1996. Spatially averaged long-term erosion rates measured from in situ-produced cosmogenic nuclides in alluvial sediments. *Journal of Geology,* 3(104), pp. 249-257.

Hack, J. T., 1960. Interpretation of erosional topography in humid temperate regions. *American Journal of Science,* Volume 258A, pp. 80-97.

Hancock, G. & Kirwan, M., 2007. Summit erosion rates deduced from $^{10}$Be: Implications for relief production in the central Appalachians. *Geology,* Volume 35, pp. 89-92.

Heimsath, A. M. et al., 2000. Soil production on a retreating escarpment in southeastern Australia. *Geology,* Volume 28, pp. 787-790.

Hewawasam, T., von Blanckenburg, F. & Kubik, P., 2002. Ancient landscapes in wet tropical Highlands, Sri Lanka.. *Geochimica et Cosmochimica Acta,* S1(66), p. A237.

Holeman, J. N., 1968. The sediment yield of the major rivers of the world. *Water Resources Research,* Issue 4, pp. 737-747.

ICPRB, 2011. *Interstate Commission on the Potomac River Basin.* [Online] Available at: http://www.potomacriver.org/cms/ [Accessed 17 May 2011].

Jennings, K., Bierman, P. R. & Southon, J., 2003. Timing and style of deposition on humid-temperate fans, Vermont, United States. *Geological Society of America Bulletin,* 2(115), pp. 182-199.

Judson, S., 1968. Erosion of the land or what's happening to my continents. *American Scientist,* Issue 56, pp. 356-374.

Judson, S. & Ritter, D., 1964. Rates of regional denudation in the United States. *Journal of Geophysical Research,* 16(69), pp. 3395-3401.

Jungers, M. C. et al., 2009. Tracing hillslope sediment production and transport with in situ and meteoric $^{10}$Be. *Journal of Geophysical Research-Earth Surface,* Volume 114.

Kirchner, J. W. et al., 2001. Moutain erosion over 10 yr., 10 k.y., and 10 m.y. timescales. *Geology,* 29(7), pp. 591-594.

Kohl, C. P. & Nishiizumi, K., 1992. CHemical isolation of quartz for measurement of in-situ-produced cosmogenic nuclides. *Geochimica et Cosmochimica Acta,* Volume 56, pp. 3583-3587.

Kottek, M. et al., 2006. World Map of the Koppen-Geiger climate classification updated. *Meteorol. Z.,* Volume 15, pp. 259-263.

Lal, D., 1988. In situ-produced cosmogenic isotopes in terrestrial rocks. *Annual Reviews of Earth and Planetary Science,* Volume 16, pp. 355-388.

Lal, D., 1991. Cosmic ray labeling of erosion surface; in situ nuclide production rates and erosion models. *Earth and Plantary Science Letters,* Volume 104, pp. 424-439.

Lal, D., 1998. *Cosmic ray produced isotopes in terrestrial systems. Isotopes in the solar system.* Bangalore, Indian Academy of Sciences, pp. 241-249.

Lal, D. & Arnold, J. R., 1985. Geophysical records of a tree: new applications for studying geomagnetic field and solar activity changes during the past $10^4$ years. *Meteoritics,* Volume 20, pp. 403-414.

Lal, D., Pavich, M. J., Gu, Z. Y. & Jull, A. J. T., 1996. Recent Erosional History of a Soil Profile Based on Cosmogenic In Situ Radionuclides $^{14}$C and $^{10}$Be. *Geophysical monograph,* Volume 95, pp. 371-376.

Lifton, N., Smart, D. F. & Shea, M. A., 2008. Scaling time-intergrated in situ cosmogenic nuclide production rates using a continuous geomagnetic model. *Earth and Planetary Science Letters,* Volume 268, pp. 190-201.

Matmon, A. S. et al., 2003. Erosion of an ancient mountain range, the Great Smoky Mountains, North Carolina and Tennessee. *American Journal of Science,* Volume 303, pp. 817-855.

Meade, R. H., 1969. Errors in using modern stream-load data to estimate natural rates of denudation. *Geological Society of America Bulletin,* Volume 80, pp. 1265-1274.

Merritts, D. & Walter, R., 2003. *Colonial millponds of Lancaster County, Pennsylvania as a major source of pollution to the Susquehanna River and Chesapeake Bay..* Lancaster: Franklin and Marshall College.

Merritts, et al., 2006. High Erosion Rates in Early America Estimated from Widespread Sediment Trapping in Thousands of 18th-20th Century Mill Dam Reservoirs, Appalachian Piedmont, USA. *Geological Society of America Abstract with Programs.*

Milici, R. C., 1995. Blue Ridge thrust belt (068), Piedmont Province (069), Atlantic Coastal Plain Province (071), and New England Province (072). In: *1995 National Assessment of United States Oil and Gas Resources--Results, methodology, and supporting data.* DDS-30 ed. s.l.:U.S. Geological Survey Digital Data Series.

Monaghan, M. C., Krishnaswami, S. & Turekian, K. K., 1986. The global-average production rate of $^{10}$Be. *Earth and Planetary Science Letters,* Volume 76, pp. 279-287.

Naeser, N. D. et al., 2004. Paleozoic to Recent Tectonic and Denudation History of Rocks in the Blue Ridge Province, Central and Southern Appalachians-Evidence from Fission-Track Thermochronology. *Geological Society of America Abstracts with Programs.*

NCDC, 2004. *Climatography of the United States 1971-2000.* [Online] Available at: http://cdo.ncdc.noaa.gov/climatenormals/clim20/va/448906.pdf [Accessed 17 May 2011].

Nishiizumi, K. et al., 2007. Absolute calibration of $^{10}$Be AMS standards. *Nuclear Instruments and Methods in Physics Research,* 258(2), pp. 403-413.

Nishiizumi, K. et al., 1989. Cosmic ray production rates of $^{10}$Be and $^{26}$Al in quartz from glacially polished rocks. *Journal of Geophysical Research, B, Solid Earth and Planets,* 94(12), pp. 17907-17915.

NOAA, 2010. *NOAA's Coastal Geospatial Data Project.* [Online] Available at: http://coastalgeospatial.noaa.gov/data_gis.html [Accessed 21 July 2011].

Noren, A. J. et al., 2002. Millennial-scale storminess variability in the northeastern United States during the Holocene epoch. *Nature,* Volume 419, pp. 821-824.

Ouimet, W. B., Whipple, K. X. & Granger, D. E., 2009. Beyond threshold hill slopes: Channel adjustments to base-level fall in tectonically active mountain ranges. *Geology,* 37(7), pp. 579-582.

Palumbo, L., Hetzel, R., Tao, M. & Li, X., 2009. Topographic and lithologic control on catchment-wide denudation rates derived from cosmogenic $^{10}$Be in two mountain ranges at the margin of NE Tibet. *Geomorphology,* Volume 117, pp. 120-142.

Pavich, M. J. et al., 1986. 10Be distribution in soils from Merced River terraces, Calfornia. *Geochimica et Cosmochimica Acta,* Volume 50, pp. 1727-1735.

Pavich, M. J., Brown, L., Klein, J. & Middleton, R., 1984. $^{10}$Be accumulation in a soil chronosequence. *Earth and Planetary Science Letters,* Volume 68, pp. 198-204.

Pazzaglia, F. J. & Brandon, M. T., 1996. Macrogeomorphic evolution of the post-Triassic Appalachian Mountains determined by deconvolution of the offshore basin sedimentary record. *Basin Research,* Volume 8, pp. 255-278.

Portenga, E. W. & Bierman, P. R., 2011. Understanding Earth's Eroding Surface with 10Be. *GSA Today.*

Portenga, E. W., Bierman, P. R., Trodick Jr., C. D. & Rood, D. H., 2010. Low Rates of Bedrock Outcrop Erosion in the Contral Appalachian Mountain Inferred from In Situ $^{10}$Be Concentrations. *Geological Society of America Abstracts with Programs,* pp. 4-12.

Reed, J. C., Sigafoos, R. S. & Fisher, G. W., 1980. *The river and the rock: the geologic story of Great Falls and the Potomac River gorge..* Reston: USGPO.

Reusser, L. J., Bierman, P. R. & Finkel, R., 2008. Estimating Pre-Disturbance Rates of Sedimanet Generation with In Situ and Meteoric $^{10}$Be: Waipaoa River Basin New Zealand. *Geological Society of America Abstracts with Programs,* pp. 299-7.

Reusser, L. J. et al., 2004. Rapid Late Pleistocene Incision of Atlantic Passive-Margin River Gorges. *Science,* Volume 305, pp. 499-502.

Reuter, J. M. et al., 2006. $^{10}$Be estimates of erosion rates in the Susquehanna River basin: Implications for models of Appalachian geomorphology and consideration of rates in a global context. *Geological Society of America Abstracts with Programs,* 38(7), p. 278.

Roden, M. K., 1991. Apatite fission-track thermochronology of the southern Appalachian basin: Maryland, West Virginia, and Virginia. *Journal of Geology,* 99(1), pp. 41-53.

Scaller, M., von Blanckenburg, F., Hovius, H. & Kubik, P. W., 2001. Large-scale erosion rates from in situ-produced cosmogenic nuclides in Eropean river sediments. *Earth and Planetary Science Letters,* Volume 188, pp. 441-458.

Schumm, S. A., 1977. *The fluvial system.* New York: Wiley-Interscience.

Spotila, J. A. et al., 2004. Origin of the Blue Ridge escarpment along the passive margin of Eastern North America. *Basin Research,* Volume 16, pp. 41-63.

Stanton, R. L., 1993. *Potomac Journey.* Washington and London: Smithsonian Institution Press.

Stone, J., 1998. A rapid fusion method for seperation of beryllium-10 from soils and silicates. *Geochimica et Cosmochimica Acta,* 62(3), pp. 555-561.

Stone, J., 2000. Air pressure and cosmogenic isotope production. *Journal of Geophysical Research,* 105(b10), pp. 23753-23759.

Sullivan, C. L., 2007. *$^{10}$Be erosion rates and landscape evolution of the Blue Ridge Escarpment, southern Appalachian Mountains,* Burlington: University of Vermont.

Tomkins, K. M. et al., 2007. Contemporary versus long-term denudation along a passive plate margin: the role of extreme events. *Earth Surface Processes and Landforms,* Volume 32, p. 1013.

Trapp, H. & Horn, M. A., 1997. *Ground Water Atlas of the United States: Segment 11, Delaware, Maryland, New Jersey, North Carolina, Pennsyvania, Virginia, West Virginia,* s.l.: U. S. Geological Survey.

Trimble, S. W., 1977. The fallacy of stream equilibrium in contemporary denudation studies. *American Journal of Science,* Volume 277, pp. 876-887.

Trimble, S. W., 1999. Decreased rates of alluvial sediment storage in the Coon Creek Basin, Wisconsin, 1975-93. *Science,* 285(5431), pp. 1244-1246.

Valette-Silver, J. N., Tera, F., Klein, J. & Middleton, R., 1986. $^{10}$Be in geothermal systems. *Geothermal Resources Council, Transactions,* Volume 10, pp. 161-166.

von Blanckenburg, F., 2005. The control mechanisms of erosion and weathering at basin scale from cosmogenic nuclides in river sediment. *Earth and Planetary Science Letters,* 237(3-4), pp. 462-479.

von Blanckenburg, F., Hewawasam, T. & Kubik, P. W., 2004. Cosmogenic nuclide evidence for low weathering and denudation in the wet, tropical highlands of Sri Lanka. *Journal of Geophysical Research,* 109(F3).

Walling, D. E., 1983. The sediment delivery problem. *Journal of Hydrology,* 65(1-3), pp. 209-237.

Walter, R. C. & Merritts, D. J., 2008. Natural Streams and the Legacy of Water-Powered Mills. *Science,* Volume 319, pp. 299-304.

Ward, D. J., Spotila, A. J., Hancock, G. S. & Galbraith, J. M., 2005. New constraints on the late Cenozoic incision history of the New River, Virginia. *Geomorphology,* Issue 72, pp. 54-72.

Wilkinson, B. H. & McElroy, B. J., 2007. The impact of humans on continental erosion and sedimentation. *Geological Society of America Bulletin,* 119(1), pp. 140-156.

Willenbring, J. K. & von Blanckenburg, F., 2010. Meteoric cosmogenic Beryllium-10 absorbed to river sediment and soil. *Earth Science Reviews,* 98(1-2), pp. 105-122.

Wolman, M. G. & Schick, A. P., 1967. Effects of construction on fluvial sediment, urban and suburban areas of Maryland. *Water Resources Research,* 3(2), pp. 451-464.

# Appendix A - Tables

## Table A.1 - Sample Location

| Sample Name | Stream Name/Gaging Station | Physiographic Province | Latitude (DD) | Longitude (DD) | In Situ $^{10}$Be Concentration[1] (atoms/g) | In Situ $^{10}$Be Error[1] (atoms/g) | Meteoric $^{10}$Be Concentration[1] (atoms/g) | Meteoric $^{10}$Be Error[1] (atoms/g) |
|---|---|---|---|---|---|---|---|---|
| POT01 | 1646580 | Main Branch | 38.930571 | -77.116148 | 2.83E+05 | 5.14E+03 | 1.94E+08 | 4.24E+06 |
| POT02 | 1650500 | Piedmont | 39.064727 | -77.028419 | 1.84E+05 | 4.11E+03 | 8.07E+07 | 1.17E+06 |
| POT04 | 1647740 | Piedmont | 39.105904 | -77.125032 | 2.31E+05 | 5.93E+03 | 1.15E+08 | 1.96E+06 |
| POT05 | 1647720 | Piedmont | 39.117900 | -77.100871 | 2.54E+05 | 5.67E+03 | 1.42E+08 | 2.06E+06 |
| POT06 | 1638500 | Main Branch | 39.272350 | -77.546222 | 2.81E+05 | 6.27E+03 | 2.09E+08 | 2.27E+06 |
| POT09 | 1656120 | Piedmont | 38.640112 | -77.512321 | 4.34E+05 | 1.15E+04 | 1.62E+08 | 2.33E+06 |
| POT10 | 1631000 | Valley and Ridge | 38.914248 | -78.209969 | 6.76E+05 | 1.22E+04 | 3.65E+08 | 5.15E+06 |
| POT11 | 1603000 | Appalachian Plateau | 39.621466 | -78.773700 | 3.88E+05 | 8.63E+03 | 2.93E+08 | 2.95E+06 |
| POT12 | 1614500 | Valley and Ridge | 39.715704 | -77.824155 | 5.00E+05 | 9.07E+03 | 4.46E+08 | 5.62E+06 |
| POT13 | 1639000 | Piedmont | 39.715704 | -77.824155 | 2.98E+05 | 5.43E+03 | 2.55E+08 | 2.57E+06 |
| POT14 | No Name | Blue Ridge | 39.586971 | -77.464085 | 2.96E+05 | 6.56E+03 | 8.39E+08 | 1.04E+07 |
| POT15 | Dutchman Creek | Blue Ridge | 39.306916 | -77.651142 | 3.60E+05 | 8.01E+03 | 2.63E+08 | 2.39E+06 |
| POT16 | Friends Creek | Blue Ridge | 39.708375 | -77.411599 | 3.26E+05 | 7.26E+03 | 3.80E+08 | 5.18E+06 |
| POT17 | Above Israel Creek | Piedmont | 39.479666 | -77.327614 | 2.48E+05 | 5.54E+03 | 3.89E+08 | 4.60E+06 |
| POT18 | Ten Mile Creek | Piedmont | 39.210672 | -77.310759 | 2.72E+05 | 6.06E+03 | 5.21E+08 | 4.27E+06 |
| POT19 | Rock Creek | Piedmont | 39.154325 | -77.131963 | 3.03E+05 | 5.50E+03 | 1.94E+08 | 1.77E+06 |
| POT20 | Beaver Dam Creek | Coastal Plain | 39.021751 | -76.860352 | 9.94E+04 | 2.22E+03 | 3.52E+07 | 4.72E+05 |
| POT21 | Henson Creek | Coastal Plain | 38.831217 | -76.919746 | 3.85E+05 | 8.56E+03 | 3.49E+07 | 4.86E+05 |
| POT22 | No Name | Coastal Plain | 38.755388 | -76.841726 | 7.25E+05 | 1.32E+04 | 8.86E+07 | 9.75E+05 |
| POT23 | Tinkers Creek | Coastal Plain | 38.759003 | -76.941934 | 4.92E+05 | 1.03E+04 | 5.12E+07 | 7.56E+05 |
| POT24 | Timothy Creek | Coastal Plain | 38.664503 | -76.879363 | 6.85E+05 | 1.08E+04 | 7.41E+07 | 8.47E+05 |
| POT25 | Port Tobacco Creek | Coastal Plain | 38.542057 | -77.017593 | 6.00E+05 | 9.41E+03 | 6.29E+07 | 1.08E+06 |
| POT26 | Beaver Dam Creek | Coastal Plain | 38.422865 | -77.213202 | 4.79E+05 | 1.07E+04 | 5.08E+07 | 7.96E+05 |
| POT27 | Burgess Creek | Coastal Plain | 38.483023 | -77.084112 | 8.18E+05 | 1.29E+04 | 1.01E+08 | 1.08E+06 |

| Sample Name | Stream Name/Gaging Station | Physiographic Province | Latitude (DD) | Longitude (DD) | In Situ $^{10}$Be Concentration[1] (atoms/g) | In Situ $^{10}$Be Error[1] (atoms/g) | Meteoric $^{10}$Be Concentration[1] (atoms/g) | Meteoric $^{10}$Be Error[1] (atoms/g) |
|---|---|---|---|---|---|---|---|---|
| POT28 | Potomac Run Creek | Piedmont | 38.441724 | -77.540603 | 2.98E+05 | 9.04E+03 | 1.12E+08 | 1.52E+06 |
| POT29 | Elk Run | Piedmont | 38.566422 | -77.672696 | 4.98E+05 | 1.11E+04 | 7.54E+08 | 1.15E+07 |
| POT30 | Licking Run | Piedmont | 38.629276 | -77.764106 | 3.09E+05 | 6.90E+03 | 9.46E+08 | 5.51E+06 |
| POT31 | Slate Run | Piedmont | 38.668758 | -77.537427 | 6.38E+05 | 1.42E+04 | 1.53E+09 | 2.01E+07 |
| POT32 | Powells Creek | Piedmont | 38.617440 | -77.372117 | 9.80E+05 | 1.54E+04 | 7.28E+07 | 7.89E+05 |
| POT33 | Popes Head Creek | Piedmont | 38.781789 | -77.387953 | 6.88E+05 | 1.08E+04 | 3.93E+08 | 2.73E+06 |
| POT34 | Head Creek East Fork | Piedmont | 38.797979 | -77.351861 | 3.03E+05 | 6.74E+03 | 1.58E+08 | 1.22E+06 |
| POT35 | Lenah Run | Piedmont | 38.959309 | -77.538328 | 3.36E+05 | 7.47E+03 | 6.49E+08 | 4.50E+06 |
| POT36 | Little Creek | Piedmont | 38.950832 | -77.719560 | 4.53E+05 | 8.66E+03 | 1.85E+08 | 1.98E+06 |
| POT37 | North Fork Beaver Dam Creek | Piedmont | 39.061616 | -77.754321 | 2.74E+05 | 6.12E+03 | 1.87E+08 | 1.76E+06 |
| POT38 | Opequon Creek | Valley and Ridge | 39.082839 | -78.126397 | 2.80E+05 | 6.22E+03 | 8.95E+08 | 8.88E+06 |
| POT39 | Howellsville Branch | Valley and Ridge | 38.973523 | -78.082023 | 5.54E+05 | 1.23E+04 | 3.98E+08 | 2.56E+06 |
| POT40 | No Name | Valley and Ridge | 38.735808 | -78.530574 | 9.41E+05 | 1.47E+04 | 3.63E+08 | 3.36E+06 |
| POT41 | Hawksbill Creek | Blue Ridge | 38.347143 | -78.612027 | 3.70E+05 | 8.24E+03 | 4.14E+08 | 2.22E+06 |
| POT42 | No Name | Valley and Ridge | 38.250988 | -78.892007 | 1.11E+06 | 1.74E+04 | 1.70E+09 | 1.75E+07 |
| POT43 | Sawmill Run | Blue Ridge | 38.101435 | -78.860335 | 5.50E+05 | 1.21E+04 | 2.63E+08 | 3.92E+06 |
| POT44 | Back Creek | Blue Ridge | 37.940339 | -78.968182 | 4.40E+05 | 7.67E+03 | 3.51E+08 | 3.38E+06 |
| POT45 | Skidmore Fork | Valley and Ridge | 38.558167 | -79.152031 | 2.39E+05 | 5.74E+03 | 2.18E+08 | 1.44E+06 |
| POT46 | Laurel Fork | Valley and Ridge | 38.492563 | -79.665341 | 3.96E+05 | 8.81E+03 | 3.06E+08 | 2.79E+06 |
| POT47 | Crab Run | Valley and Ridge | 38.809617 | -78.945694 | | | 5.19E+08 | 5.49E+06 |
| POT48 | Dumpling Run | Valley and Ridge | 39.070046 | -78.957539 | 8.73E+05 | 1.59E+04 | 6.08E+08 | 4.68E+06 |
| POT49 | North River | Valley and Ridge | 39.137350 | -78.771715 | 5.06E+05 | 9.19E+03 | 4.30E+08 | 4.77E+06 |
| POT50 | Roaring Creek | Valley and Ridge | 38.889463 | -79.403086 | 4.95E+05 | 9.88E+03 | 2.90E+08 | 4.76E+06 |
| POT51 | Laural Run | Appalachian Plateau | 39.237272 | -79.449005 | 3.79E+05 | 6.90E+03 | 1.34E+08 | 1.16E+06 |
| POT52 | Laural Run | Appalachian Plateau | 39.348403 | -79.285069 | 5.74E+05 | 9.02E+03 | 6.24E+08 | 9.58E+06 |
| POT53 | Deep Run Cranberry Run | Appalachian Plateau | 39.398563 | -79.133406 | 5.72E+05 | 9.02E+03 | 7.08E+08 | 7.71E+06 |
| POT54 | Rienhart Run | Valley and Ridge | 39.455182 | -78.804073 | | | 3.42E+08 | 2.64E+06 |
| POT55 | Crabtree Creek | Appalachian Plateau | 39.457833 | -79.228077 | 5.03E+05 | 1.12E+04 | 4.15E+08 | 3.20E+06 |
| POT56 | Middle Fork | Appalachian Plateau | 39.513378 | -79.154863 | | | 2.56E+08 | 1.98E+06 |
| POT57 | Blacklick Run | Appalachian Plateau | 39.603374 | -79.079118 | | | 3.50E+08 | 4.17E+06 |

| Sample Name | Stream Name/Gaging Station | Physiographic Province | Latitude (DD) | Longitude (DD) | In Situ $^{10}$Be Concentration[1] (atoms/g) | In Situ $^{10}$Be Error[1] (atoms/g) | Meteoric $^{10}$Be Concentration[1] (atoms/g) | Meteoric $^{10}$Be Error[1] (atoms/g) |
|---|---|---|---|---|---|---|---|---|
| POT58 | George's Creek | Appalachian Plateau | 39.565669 | -78.979940 | 3.06E+05 | 6.82E+03 | 3.29E+08 | 3.01E+06 |
| POT59 | Willis Creek | Appalachian Plateau | 39.819052 | -78.937583 | | | 4.28E+08 | 7.10E+06 |
| POT60 | No Name | Appalachian Plateau | 39.905885 | -78.835487 | | | 3.04E+08 | 2.35E+06 |
| POT61 | Sand Spring Run | Valley and Ridge | 39.893341 | -78.601899 | 6.35E+05 | 1.00E+04 | 3.57E+08 | 4.53E+06 |
| POT62 | No Name | Valley and Ridge | 39.687011 | -78.585806 | 3.07E+05 | 7.83E+03 | 3.91E+08 | 5.29E+06 |
| POT63 | Critton Run | Valley and Ridge | 39.471218 | -78.437963 | 6.86E+05 | 1.10E+04 | 2.12E+08 | 3.55E+06 |
| POT64 | McKee's Run | Valley and Ridge | 39.795513 | -78.254671 | 3.50E+05 | 7.81E+03 | 2.97E+08 | 1.98E+06 |
| POT65 | Branch of East Branch | Valley and Ridge | 39.861461 | -78.301706 | 3.62E+05 | 8.93E+03 | 2.29E+08 | 1.25E+06 |
| POT66 | Liching Fortune Teller Creek | Valley and Ridge | 40.017985 | -78.040094 | | | 7.14E+08 | 3.87E+06 |
| POT67 | No Name | Valley and Ridge | 40.177332 | -77.663040 | 4.80E+05 | 7.56E+03 | 1.05E+08 | 7.04E+05 |
| POT68 | Branch of Rock Creek | Piedmont | 39.867126 | -77.222729 | 2.94E+05 | 6.56E+03 | 7.79E+08 | 4.82E+06 |
| POT69 | Mummasburg Run | Blue Ridge | 39.879445 | -77.293582 | 4.11E+05 | 7.46E+03 | 2.36E+08 | 1.61E+06 |
| POT70 | Branch of Back Creek | Valley and Ridge | 39.916254 | -77.748227 | | | 5.35E+08 | 5.83E+06 |
| POT71 | Birch Run | Blue Ridge | 39.950477 | -77.444472 | 3.48E+05 | 6.32E+03 | 4.88E+07 | 4.23E+05 |
| POT72 | Turkeyfoot Run | Piedmont | 39.567456 | -77.059822 | 2.46E+05 | 5.49E+03 | 3.68E+08 | 4.18E+06 |
| POT73 | Big Pipe Creek | Piedmont | 39.660970 | -76.948189 | 2.58E+05 | 5.73E+03 | 3.53E+08 | 2.41E+06 |

[1]Measured concentrations from Lawrence Livermore National Laboratory, normalized to standard 07KNSTD3110 with a reported ratio of 2850 x $10^{-15}$ (Nishiizumi, et al., 2007) and blank corrected.

**Table A.2 - Data for Cronus Calculator**

| Sample name | Effective Latitude[1] (DD) | Effective Longitude[1] (DD) | Effective Elevation[1] (m) | Measured Concentration[2] (atoms/g) | Error[2] (atoms/g) |
|---|---|---|---|---|---|
| POT01 | 39.1646 | -78.3821 | 383.4 | 2.83E+05 | 5.14E+03 |
| POT02 | 39.1077 | -77.0333 | 112.7 | 1.84E+05 | 4.11E+03 |
| POT04 | 39.1480 | -77.1409 | 126.5 | 2.31E+05 | 5.93E+03 |
| POT05 | 39.1463 | -77.0953 | 121.8 | 2.54E+05 | 5.67E+03 |
| POT06 | 39.1331 | -78.5789 | 445.8 | 2.81E+05 | 6.27E+03 |
| POT09 | 38.6458 | -77.6740 | 92.4 | 4.34E+05 | 1.15E+04 |
| POT10 | 38.3639 | -78.8516 | 492.6 | 6.76E+05 | 1.22E+04 |
| POT11 | 39.5320 | -79.0409 | 651.4 | 3.88E+05 | 8.63E+03 |
| POT12 | 39.9156 | -77.7381 | 253.5 | 5.00E+05 | 9.07E+03 |
| POT13 | 39.8122 | -77.2481 | 174.0 | 2.98E+05 | 5.43E+03 |
| POT14 | 39.5889 | -77.4863 | 463.9 | 2.96E+05 | 6.56E+03 |
| POT15 | 39.2838 | -77.6720 | 148.0 | 3.60E+05 | 8.01E+03 |
| POT16 | 39.7046 | -77.4442 | 346.4 | 3.26E+05 | 7.26E+03 |
| POT17 | 39.4753 | -77.2971 | 128.5 | 2.48E+05 | 5.54E+03 |
| POT18 | 39.2305 | -77.3077 | 154.2 | 2.72E+05 | 6.06E+03 |
| POT19 | 39.1742 | -77.1376 | 135.1 | 3.03E+05 | 5.50E+03 |
| POT20 | 39.0238 | -76.8481 | 33.2 | 9.94E+04 | 2.22E+03 |
| POT21 | 38.8347 | -76.9004 | 67.5 | 3.85E+05 | 8.56E+03 |
| POT22 | 38.7840 | -76.8573 | 60.6 | 7.25E+05 | 1.32E+04 |
| POT23 | 38.7815 | -76.9091 | 62.2 | 4.92E+05 | 1.03E+04 |
| POT24 | 38.6820 | -76.8701 | 49.0 | 6.85E+05 | 1.08E+04 |
| POT25 | 38.5761 | -76.9937 | 40.2 | 6.00E+05 | 9.41E+03 |
| POT26 | 38.4612 | -77.2141 | 16.7 | 4.79E+05 | 1.07E+04 |
| POT27 | 38.5142 | -77.0821 | 29.9 | 8.18E+05 | 1.29E+04 |
| POT28 | 38.4614 | -77.5592 | 86.0 | 2.98E+05 | 9.04E+03 |
| POT29 | 38.5507 | -77.6748 | 87.1 | 4.98E+05 | 1.11E+04 |
| POT30 | 38.6472 | -77.7873 | 115.6 | 3.09E+05 | 6.90E+03 |

| Sample name | Effective Latitude[1] (DD) | Effective Longitude[1] (DD) | Effective Elevation[1] (m) | Measured Concentration[2] (atoms/g) | Error[2] (atoms/g) |
|---|---|---|---|---|---|
| POT31 | 38.6784 | -77.5692 | 53.2 | 6.38E+05 | 1.42E+04 |
| POT32 | 38.6389 | -77.4061 | 86.5 | 9.80E+05 | 1.54E+04 |
| POT33 | 38.8084 | -77.3677 | 91.8 | 6.88E+05 | 1.08E+04 |
| POT34 | 38.8216 | -77.3337 | 98.1 | 3.03E+05 | 6.74E+03 |
| POT35 | 38.9644 | -77.5740 | 86.5 | 3.36E+05 | 7.47E+03 |
| POT36 | 38.9100 | -77.7497 | 167.7 | 4.53E+05 | 8.66E+03 |
| POT37 | 39.0953 | -77.8036 | 194.2 | 2.74E+05 | 6.12E+03 |
| POT38 | 39.0804 | -78.1632 | 202.0 | 2.80E+05 | 6.22E+03 |
| POT39 | 38.9555 | -78.0571 | 373.3 | 5.54E+05 | 1.23E+04 |
| POT40 | 38.7440 | -78.5545 | 607.6 | 9.41E+05 | 1.47E+04 |
| POT41 | 38.3203 | -78.6222 | 553.4 | 3.70E+05 | 8.24E+03 |
| POT42 | 38.2594 | -78.9283 | 355.0 | 1.11E+06 | 1.74E+04 |
| POT43 | 38.0935 | -78.8106 | 567.1 | 5.50E+05 | 1.21E+04 |
| POT44 | 37.9132 | -79.0043 | 674.3 | 4.40E+05 | 7.67E+03 |
| POT45 | 38.5328 | -79.1694 | 977.5 | 2.39E+05 | 5.74E+03 |
| POT46 | 38.4727 | -79.6798 | 1189.7 | 3.96E+05 | 8.81E+03 |
| POT48 | 39.0436 | -78.9278 | 370.1 | 8.73E+05 | 1.59E+04 |
| POT49 | 39.1385 | -78.8125 | 633.2 | 5.06E+05 | 9.19E+03 |
| POT50 | 38.9115 | -79.4140 | 1148.5 | 4.95E+05 | 9.88E+03 |
| POT51 | 39.2320 | -79.4714 | 860.7 | 3.79E+05 | 6.90E+03 |
| POT52 | 39.3621 | -79.3090 | 828.0 | 5.74E+05 | 9.02E+03 |
| POT53 | 39.3709 | -79.1249 | 710.6 | 5.72E+05 | 9.02E+03 |
| POT55 | 39.4464 | -79.2536 | 790.4 | 5.03E+05 | 1.12E+04 |
| POT58 | 39.5436 | 78.9634 | 689.7 | 3.06E+05 | 6.82E+03 |
| POT61 | 39.8905 | -78.6265 | 577.7 | 6.35E+05 | 1.00E+04 |
| POT62 | 39.6955 | -78.6093 | 343.7 | 3.07E+05 | 7.83E+03 |
| POT63 | 39.4651 | -78.4584 | 409.8 | 6.86E+05 | 1.10E+04 |
| POT64 | 39.7878 | 78.2925 | 318.9 | 3.50E+05 | 7.81E+03 |
| POT65 | 39.8874 | -78.2867 | 415.4 | 3.62E+05 | 8.93E+03 |

| Sample name | Effective Latitude[1] (DD) | Effective Longitude[1] (DD) | Effective Elevation[1] (m) | Measured Concentration[2] (atoms/g) | Error[2] (atoms/g) |
|---|---|---|---|---|---|
| POT67 | 40.2034 | -77.6386 | 421.0 | 4.80E+05 | 7.56E+03 |
| POT68 | 39.8900 | -77.2197 | 154.1 | 2.94E+05 | 6.56E+03 |
| POT69 | 39.9043 | -77.3101 | 217.0 | 4.11E+05 | 7.46E+03 |
| POT71 | 39.9720 | -77.4291 | 540.8 | 3.48E+05 | 6.32E+03 |
| POT72 | 39.5648 | -77.0250 | 186.7 | 2.46E+05 | 5.49E+03 |
| POT73 | 39.6687 | -76.9185 | 226.8 | 2.58E+05 | 5.73E+03 |

[1]Created by model in ArcGIS that exports elevation, longitude, and latitude, ASCII grid files for each cell in any sized watershed and elevation datasets of any resolution. The ASCII grid files were fed directly into a Matlab script which determined the effective elevation longitude and latitude needed by the CRONUS calculator. The Matlab script reduces the ASCII grid files of elevation and latitude to a single point representing the entire basin. The elevation and latitude grids are used to calculate the ELD scaling factor for each cell. The average scaling factor for all cells, or the effective ELD, is used in conjunction with the actual effective latitude for the basin to back calculate the corresponding effective elevation (Portenga & Bierman, 2011).

[2] Measured concentrations from Lawrence Livermore National Laboratory, normalized to standard 07KNSTD3110 and blank corrected.

## Table A.3 - In Situ $^{10}$Be Information

| Sample | LLNL BE# | Batch# | 10Be/9Be Ratio[1] (blank corrected) | Ratio Error[1] | Sample Mass (g) | Carrier Mass[2] (ug) | Prod Rate[3] (atoms/(g*y)) | Erosion Rate[4] (m/My) | Error[4] (m/My) | Normalized Concentration[5] (atoms/g) | Standardized Concentration[6] | Log Trans ER[7] |
|---|---|---|---|---|---|---|---|---|---|---|---|---|
| POT01 | BE29062 | B433 | 3.44E-13 | 6.74E-15 | 20.28 | 249.1 | 5.72 | 16.14 | 1.19 | 2.42E+05 | 0.26 | 1.21 |
| POT02 | BE29063 | B433 | 2.36E-13 | 5.80E-15 | 21.30 | 248.8 | 4.49 | 21.21 | 1.52 | 2.01E+05 | 0.17 | 1.33 |
| POT04 | BE29064 | B433 | 2.84E-13 | 7.30E-15 | 20.47 | 248.8 | 4.55 | 16.66 | 1.24 | 2.48E+05 | 0.21 | 1.22 |
| POT05 | BE29066 | B433 | 3.11E-13 | 7.55E-15 | 20.33 | 248.1 | 4.53 | 14.93 | 1.10 | 2.74E+05 | 0.23 | 1.17 |
| POT06 | BE29067 | B433 | 3.41E-13 | 8.23E-15 | 20.33 | 250.9 | 6.03 | 17.02 | 1.27 | 2.29E+05 | 0.25 | 1.23 |
| POT09 | BE29068 | B433 | 5.24E-13 | 1.49E-14 | 20.11 | 249.2 | 4.37 | 7.88 | 0.64 | 4.86E+05 | 0.39 | 0.90 |
| POT10 | BE29069 | B433 | 8.15E-13 | 1.60E-14 | 20.20 | 250.5 | 6.19 | 6.55 | 0.53 | 5.35E+05 | 0.61 | 0.82 |
| POT11 | BE29070 | B433 | 4.83E-13 | 1.14E-14 | 20.68 | 248.3 | 7.22 | 13.99 | 1.08 | 2.63E+05 | 0.35 | 1.15 |
| POT12 | BE29071 | B433 | 6.18E-13 | 1.19E-14 | 20.49 | 248.1 | 5.16 | 7.79 | 0.61 | 4.75E+05 | 0.45 | 0.89 |
| POT13 | BE29072 | B433 | 3.66E-13 | 7.17E-15 | 20.41 | 248.7 | 4.80 | 13.11 | 0.97 | 3.04E+05 | 0.27 | 1.12 |
| POT14 | BE29073 | B433 | 3.65E-13 | 8.63E-15 | 20.55 | 249.2 | 6.18 | 16.41 | 1.23 | 2.34E+05 | 0.27 | 1.22 |
| POT15 | BE29074 | B434 | 4.83E-13 | 1.14E-14 | 22.24 | 247.9 | 4.65 | 10.30 | 0.79 | 3.79E+05 | 0.33 | 1.01 |
| POT16 | BE29086 | B435 | 2.45E-13 | 5.96E-15 | 12.49 | 248.7 | 5.59 | 13.54 | 1.03 | 2.86E+05 | 0.29 | 1.13 |
| POT17 | BE29075 | B434 | 3.35E-13 | 7.98E-15 | 22.48 | 249.5 | 4.58 | 15.47 | 1.14 | 2.66E+05 | 0.22 | 1.19 |
| POT18 | BE29077 | B434 | 3.15E-13 | 7.50E-15 | 19.21 | 249.0 | 4.67 | 14.20 | 1.06 | 2.86E+05 | 0.25 | 1.15 |
| POT19 | BE29078 | B434 | 4.08E-13 | 7.95E-15 | 22.46 | 249.5 | 4.59 | 12.38 | 0.92 | 3.23E+05 | 0.27 | 1.09 |
| POT20 | BE29079 | B434 | 1.37E-13 | 3.52E-15 | 23.05 | 249.8 | 4.15 | 39.20 | 2.67 | 1.17E+05 | 0.09 | 1.59 |
| POT21 | BE29080 | B434 | 5.19E-13 | 1.23E-14 | 22.37 | 248.6 | 4.28 | 8.89 | 0.69 | 4.41E+05 | 0.35 | 0.95 |
| POT22 | BE29081 | B434 | 9.86E-13 | 1.94E-14 | 22.51 | 247.7 | 4.25 | 4.20 | 0.36 | 8.36E+05 | 0.66 | 0.62 |
| POT23 | BE29088 | B435 | 6.68E-13 | 1.31E-14 | 22.73 | 250.4 | 4.26 | 6.65 | 0.53 | 5.66E+05 | 0.44 | 0.82 |
| POT24 | BE29089 | B435 | 8.51E-13 | 1.45E-14 | 20.63 | 248.6 | 4.20 | 4.44 | 0.37 | 8.00E+05 | 0.62 | 0.65 |
| POT25 | BE29090 | B435 | 7.50E-13 | 1.28E-14 | 20.78 | 248.6 | 4.16 | 5.15 | 0.42 | 7.07E+05 | 0.54 | 0.71 |
| POT26 | BE29091 | B435 | 6.04E-13 | 1.42E-14 | 21.03 | 249.7 | 4.06 | 6.57 | 0.53 | 5.78E+05 | 0.43 | 0.82 |
| POT27 | BE29082 | B434 | 1.11E-12 | 1.94E-14 | 22.48 | 247.9 | 4.11 | 3.51 | 0.30 | 9.76E+05 | 0.74 | 0.55 |
| POT28 | BE29083 | B434 | 4.04E-13 | 6.80E-15 | 22.39 | 247.4 | 4.33 | 12.03 | 0.95 | 3.38E+05 | 0.27 | 1.08 |
| POT29 | BE29092 | B435 | 6.87E-13 | 1.61E-14 | 22.22 | 241.1 | 4.34 | 6.68 | 0.54 | 5.63E+05 | 0.45 | 0.82 |
| POT30 | BE29093 | B435 | 3.82E-13 | 9.12E-15 | 20.54 | 249.0 | 4.47 | 11.85 | 0.89 | 3.39E+05 | 0.28 | 1.07 |
| POT31 | BE29094 | B435 | 5.05E-13 | 1.17E-14 | 13.17 | 249.1 | 4.21 | 4.85 | 0.41 | 7.42E+05 | 0.58 | 0.69 |
| POT32 | BE29095 | B435 | 1.22E-12 | 2.03E-14 | 20.62 | 248.3 | 4.35 | 2.98 | 0.26 | 1.10E+06 | 0.89 | 0.47 |
| POT33 | BE29084 | B434 | 9.41E-13 | 1.44E-14 | 22.72 | 248.4 | 4.38 | 4.60 | 0.38 | 7.69E+05 | 0.62 | 0.66 |
| POT34 | BE29085 | B434 | 4.11E-13 | 9.82E-15 | 22.77 | 251.0 | 4.41 | 11.97 | 0.90 | 3.37E+05 | 0.27 | 1.08 |
| POT35 | BE29096 | B435 | 4.05E-13 | 9.49E-15 | 20.06 | 249.3 | 4.37 | 10.56 | 0.81 | 3.77E+05 | 0.30 | 1.02 |
| POT36 | BE29097 | B435 | 5.12E-13 | 9.36E-15 | 18.97 | 251.0 | 4.70 | 8.02 | 0.63 | 4.72E+05 | 0.41 | 0.90 |
| POT37 | BE29099 | B436 | 3.03E-13 | 7.21E-15 | 18.42 | 249.1 | 4.83 | 14.50 | 1.08 | 2.78E+05 | 0.25 | 1.16 |

| Sample | LLNL BE# | Batch# | 10Be/9Be Ratio[1] (blank corrected) | Ratio Error[1] | Sample Mass (g) | Carrier Mass[2] (ug) | Prod Rate[3] (atoms/(g*y)) | Erosion Rate[4] (m $My^{-1}$) | Error[4] (m $My^{-1}$) | Normalized Concentration[5] (atoms/g) | Standardized Concentration[6] | Log Trans ER[7] |
|---|---|---|---|---|---|---|---|---|---|---|---|---|
| POT38 | BE29100 | B436 | 3.12E-13 | 7.39E-15 | 18.51 | 248.3 | 4.86 | 14.23 | 1.06 | 2.82E+05 | 0.25 | 1.15 |
| POT39 | BE29101 | B436 | 6.72E-13 | 1.56E-14 | 20.11 | 248.2 | 5.65 | 7.54 | 0.61 | 4.81E+05 | 0.50 | 0.88 |
| POT40 | BE29102 | B436 | 1.03E-12 | 1.68E-14 | 18.21 | 250.0 | 6.86 | 4.96 | 0.42 | 6.72E+05 | 0.85 | 0.70 |
| POT41 | BE29103 | B436 | 4.11E-13 | 9.61E-15 | 18.67 | 251.2 | 6.50 | 13.45 | 1.03 | 2.79E+05 | 0.33 | 1.13 |
| POT42 | BE29104 | B436 | 1.24E-12 | 2.05E-14 | 18.53 | 247.8 | 5.49 | 3.27 | 0.29 | 9.87E+05 | 1.00 | 0.51 |
| POT43 | BE29105 | B436 | 6.73E-13 | 1.62E-14 | 20.48 | 250.5 | 6.55 | 8.72 | 0.70 | 4.11E+05 | 0.50 | 0.94 |
| POT44 | BE29106 | B436 | 4.93E-13 | 8.35E-15 | 18.60 | 248.4 | 7.12 | 12.06 | 0.92 | 3.03E+05 | 0.40 | 1.08 |
| POT45 | BE29107 | B436 | 2.46E-13 | 5.66E-15 | 17.16 | 249.1 | 9.19 | 29.10 | 2.20 | 1.27E+05 | 0.22 | 1.46 |
| POT46 | BE29108 | B436 | 4.07E-13 | 9.52E-15 | 17.21 | 250.1 | 10.82 | 19.68 | 1.54 | 1.79E+05 | 0.36 | 1.29 |
| POT48 | BE29109 | B436 | 9.68E-13 | 1.83E-14 | 18.66 | 251.7 | 5.64 | 4.46 | 0.38 | 7.58E+05 | 0.79 | 0.65 |
| POT49 | BE29110 | B437 | 6.59E-13 | 1.26E-14 | 21.63 | 248.5 | 7.06 | 10.24 | 0.80 | 3.51E+05 | 0.46 | 1.01 |
| POT50 | BE29111 | B437 | 6.44E-13 | 1.42E-14 | 21.64 | 249.1 | 10.60 | 15.21 | 1.20 | 2.29E+05 | 0.45 | 1.18 |
| POT51 | BE29112 | B437 | 4.88E-13 | 9.37E-15 | 21.40 | 249.0 | 8.50 | 16.61 | 1.26 | 2.19E+05 | 0.34 | 1.22 |
| POT52 | BE29113 | B437 | 7.54E-13 | 1.25E-14 | 21.89 | 249.2 | 8.31 | 10.36 | 0.81 | 3.38E+05 | 0.52 | 1.02 |
| POT53 | BE29114 | B437 | 4.98E-13 | 8.33E-15 | 14.50 | 249.6 | 7.55 | 9.52 | 0.75 | 3.71E+05 | 0.52 | 0.98 |
| POT55 | BE29115 | B437 | 2.68E-13 | 6.39E-15 | 8.93 | 250.8 | 8.07 | 11.66 | 0.92 | 3.05E+05 | 0.45 | 1.07 |
| POT58 | BE29116 | B437 | 3.98E-13 | 9.34E-15 | 21.65 | 248.7 | 7.36 | 18.43 | 1.39 | 2.04E+05 | 0.28 | 1.27 |
| POT61 | BE29117 | B437 | 8.27E-13 | 1.37E-14 | 21.66 | 249.1 | 6.84 | 7.72 | 0.61 | 4.55E+05 | 0.57 | 0.89 |
| POT62 | BE29118 | B437 | 1.82E-13 | 4.47E-15 | 9.81 | 248.3 | 5.57 | 14.42 | 1.10 | 2.70E+05 | 0.28 | 1.16 |
| POT63 | BE29119 | B437 | 8.99E-13 | 1.48E-14 | 21.70 | 248.0 | 5.88 | 6.13 | 0.50 | 5.72E+05 | 0.62 | 0.79 |
| POT64 | BE29120 | B437 | 4.22E-13 | 9.86E-15 | 20.05 | 249.3 | 5.41 | 12.15 | 0.93 | 3.17E+05 | 0.32 | 1.08 |
| POT65 | BE29122 | B438 | 4.39E-13 | 1.13E-14 | 20.15 | 248.7 | 5.95 | 12.73 | 0.99 | 2.98E+05 | 0.33 | 1.10 |
| POT67 | BE29123 | B438 | 6.42E-13 | 1.07E-14 | 22.16 | 248.0 | 6.02 | 9.38 | 0.72 | 3.91E+05 | 0.43 | 0.97 |
| POT68 | BE29124 | B438 | 3.82E-13 | 8.98E-15 | 21.58 | 249.0 | 4.71 | 13.11 | 0.98 | 3.06E+05 | 0.27 | 1.12 |
| POT69 | BE29125 | B438 | 5.43E-13 | 1.03E-14 | 21.99 | 249.1 | 5.00 | 9.45 | 0.73 | 4.03E+05 | 0.37 | 0.98 |
| POT71 | BE29126 | B438 | 4.61E-13 | 8.79E-15 | 21.98 | 248.6 | 6.64 | 14.64 | 1.10 | 2.57E+05 | 0.31 | 1.17 |
| POT72 | BE29127 | B438 | 3.26E-13 | 7.73E-15 | 22.13 | 249.8 | 4.84 | 16.35 | 1.20 | 2.49E+05 | 0.22 | 1.21 |
| POT73 | BE29128 | B438 | 3.52E-13 | 8.29E-15 | 22.70 | 248.6 | 5.03 | 16.01 | 1.18 | 2.51E+05 | 0.23 | 1.20 |

[1]Measured ratios from Lawrence Livermore National Laboratory, blank corrected.

[2]Mass of $^{9}Be$ added to a sample from the SPEX Be Carrier.

[3]Calculated using the Cronus Calculator. Basin-scale erosion rates were modeled using the interpretive model of Bierman and Steig (1996) with a normalized sea level, high latitude in situ $^{10}Be$ production rate of 4.9 atoms g $quartz^{-1}$ $yr^{-1}$, an attenuation depth of 160 g $cm^{-2}$, and assuming a rock density of 2.7 g $cm^{-3}$

[4]Calculated using the Cronus Calculator based off the effective elevation and latitude of each basin.

[5]To normalize each measured in situ $^{10}Be$ concentration, each production rate was divided by 4.9 atoms g $quartz^{-1}$ $yr^{-1}$, the normalized sea level, high latitude in situ $^{10}Be$ production rate, to get a normalized production rate. Next, I divided each measured in situ $^{10}Be$ concentration by my newly normalized production rate for that basin.

[6]Divided each normalized concentration by the highest normalized concentration.

[7]A $\log_{10}$ transformation of each in situ $^{10}Be$ erosion rate.

## Table A.4 - Meteoric $^{10}$Be Information

| Sample | LLNLBE# | Batch# | 10Be/9Be Ratio[1] (Blank Corrected) | Ratio Error[1] | Sample Mass (g) | Carrier Mass[2] (ug) | Deposition Rate[3] (atoms/(cm$^3$*y)) | Erosion Rates[4] (m/My) | Normalized Concentration[5] (atoms/g) | Standardized Concentration[6] | Log Trans Conc.[7] |
|---|---|---|---|---|---|---|---|---|---|---|---|
| POT01 | BE27095 | MB9 | 5.31E-12 | 1.16E-13 | 0.551 | 300.99 | 1.87E+06 | 36 | 6.00E+07 | 0.11 | 7.78 |
| POT02 | BE27096 | MB9 | 2.08E-12 | 3.03E-14 | 0.519 | 300.99 | 2.00E+06 | 92 | 2.34E+07 | 0.04 | 7.37 |
| POT04 | BE27097 | MB9 | 3.31E-12 | 5.63E-14 | 0.581 | 301.98 | 1.96E+06 | 63 | 3.40E+07 | 0.06 | 7.53 |
| POT05 | BE27098 | MB9 | 4.07E-12 | 5.88E-14 | 0.575 | 300.99 | 1.98E+06 | 52 | 4.17E+07 | 0.08 | 7.62 |
| POT06 | BE27778 | MB15 | 5.31E-12 | 5.78E-14 | 0.456 | 300.99 | 1.86E+06 | 33 | 6.49E+07 | 0.12 | 7.81 |
| POT09 | BE27100 | MB9 | 4.17E-12 | 6.01E-14 | 0.517 | 300.00 | 1.90E+06 | 44 | 4.94E+07 | 0.09 | 7.69 |
| POT10 | BE27101 | MB9 | 1.04E-11 | 1.47E-13 | 0.574 | 300.99 | 1.88E+06 | 19 | 1.13E+08 | 0.21 | 8.05 |
| POT11 | BE27779 | MB15 | 8.55E-12 | 8.61E-14 | 0.459 | 300.99 | 2.04E+06 | 26 | 8.34E+07 | 0.15 | 7.92 |
| POT12 | BE27780 | MB15 | 1.18E-11 | 1.49E-13 | 0.486 | 300.99 | 1.94E+06 | 16 | 1.33E+08 | 0.24 | 8.12 |
| POT13 | BE27781 | MB15 | 6.55E-12 | 6.61E-14 | 0.495 | 300.00 | 1.98E+06 | 29 | 7.47E+07 | 0.14 | 7.87 |
| POT14 | BE27782 | MB15 | 1.82E-11 | 2.25E-13 | 0.475 | 327.72 | 2.10E+06 | 9 | 2.31E+08 | 0.42 | 8.36 |
| POT15 | BE27762 | MB16 | 7.55E-12 | 6.84E-14 | 0.577 | 300.99 | 1.88E+06 | 26 | 8.12E+07 | 0.15 | 7.91 |
| POT16 | BE27763 | MB16 | 8.78E-12 | 1.20E-13 | 0.463 | 300.00 | 2.06E+06 | 20 | 1.07E+08 | 0.20 | 8.03 |
| POT17 | BE27764 | MB16 | 9.18E-12 | 1.09E-13 | 0.474 | 300.00 | 1.90E+06 | 18 | 1.18E+08 | 0.22 | 8.07 |
| POT18 | BE27765 | MB16 | 1.22E-11 | 1.00E-13 | 0.471 | 300.99 | 1.92E+06 | 14 | 1.58E+08 | 0.29 | 8.20 |
| POT19 | BE27766 | MB16 | 4.65E-12 | 4.23E-14 | 0.481 | 300.99 | 1.97E+06 | 38 | 5.72E+07 | 0.10 | 7.76 |
| POT20 | BE27767 | MB16 | 8.21E-13 | 1.10E-14 | 0.462 | 296.04 | 2.01E+06 | 212 | 1.02E+07 | 0.02 | 7.01 |
| POT21 | BE27768 | MB16 | 7.59E-13 | 1.06E-14 | 0.443 | 304.95 | 1.96E+06 | 208 | 1.03E+07 | 0.02 | 7.01 |
| POT22 | BE27769 | MB16 | 2.12E-12 | 2.34E-14 | 0.479 | 299.01 | 1.95E+06 | 82 | 2.64E+07 | 0.05 | 7.42 |
| POT23 | BE27770 | MB16 | 1.21E-12 | 1.79E-14 | 0.479 | 301.98 | 1.94E+06 | 140 | 1.53E+07 | 0.03 | 7.18 |
| POT24 | BE27771 | MB16 | 1.68E-12 | 1.93E-14 | 0.459 | 301.98 | 1.95E+06 | 97 | 2.21E+07 | 0.04 | 7.34 |
| POT25 | BE27105 | MB9 | 1.64E-12 | 2.82E-14 | 0.526 | 301.98 | 1.92E+06 | 113 | 1.90E+07 | 0.03 | 7.28 |
| POT26 | BE27772 | MB16 | 1.24E-12 | 1.94E-14 | 0.491 | 300.99 | 1.87E+06 | 136 | 1.58E+07 | 0.03 | 7.20 |
| POT27 | BE27773 | MB16 | 2.52E-12 | 2.69E-14 | 0.497 | 299.01 | 1.89E+06 | 69 | 3.11E+07 | 0.06 | 7.49 |
| POT28 | BE27774 | MB16 | 2.84E-12 | 3.86E-14 | 0.510 | 300.99 | 1.92E+06 | 64 | 3.38E+07 | 0.06 | 7.53 |
| POT29 | BE27775 | MB16 | 1.78E-11 | 2.72E-13 | 0.474 | 300.00 | 1.92E+06 | 9 | 2.28E+08 | 0.42 | 8.36 |
| POT30 | BE27776 | MB16 | 2.55E-11 | 1.48E-13 | 0.542 | 300.99 | 1.93E+06 | 8 | 2.84E+08 | 0.52 | 8.45 |
| POT31 | BE28973 | MB20 | 3.80E-11 | 5.00E-13 | 0.498 | 299.41 | 1.85E+06 | 4 | 4.79E+08 | 0.87 | 8.68 |
| POT32 | BE28974 | MB20 | 1.99E-12 | 2.16E-14 | 0.545 | 298.42 | 1.87E+06 | 95 | 2.26E+07 | 0.04 | 7.35 |
| POT33 | BE28975 | MB20 | 1.05E-11 | 7.30E-14 | 0.536 | 300.40 | 1.88E+06 | 18 | 1.22E+08 | 0.22 | 8.08 |
| POT34 | BE28976 | MB20 | 4.23E-12 | 3.26E-14 | 0.532 | 298.42 | 1.89E+06 | 44 | 4.86E+07 | 0.09 | 7.69 |
| POT35 | BE28977 | MB20 | 1.73E-11 | 1.20E-13 | 0.533 | 299.41 | 1.88E+06 | 11 | 2.00E+08 | 0.37 | 8.30 |
| POT36 | BE29391 | MB20 | 5.02E-12 | 5.39E-14 | 0.546 | 300.40 | 1.93E+06 | 39 | 5.56E+07 | 0.10 | 7.75 |
| POT37 | BE29392 | MB20 | 4.88E-12 | 4.58E-14 | 0.522 | 299.41 | 1.90E+06 | 38 | 5.70E+07 | 0.10 | 7.76 |
| POT38 | BE29393 | MB20 | 2.31E-11 | 2.30E-13 | 0.514 | 297.43 | 1.79E+06 | 7 | 2.90E+08 | 0.53 | 8.46 |
| POT39 | BE29394 | MB20 | 1.15E-11 | 7.44E-14 | 0.581 | 299.41 | 1.92E+06 | 18 | 1.20E+08 | 0.22 | 8.08 |
| POT40 | BE29395 | MB20 | 9.30E-12 | 8.60E-14 | 0.511 | 298.42 | 1.90E+06 | 19 | 1.10E+08 | 0.20 | 8.04 |
| POT41 | BE29396 | MB20 | 1.08E-11 | 5.80E-14 | 0.524 | 300.40 | 2.02E+06 | 18 | 1.19E+08 | 0.22 | 8.08 |
| POT42 | BE29397 | MB20 | 4.34E-11 | 4.46E-13 | 0.513 | 300.40 | 1.80E+06 | 4 | 5.48E+08 | 1.00 | 8.74 |
| POT43 | BE27106 | MB9 | 7.54E-12 | 1.12E-13 | 0.575 | 300.00 | 2.04E+06 | 29 | 7.48E+07 | 0.14 | 7.87 |
| POT44 | BE29398 | MB20 | 9.58E-12 | 9.23E-14 | 0.546 | 299.41 | 2.12E+06 | 22 | 9.59E+07 | 0.18 | 7.98 |

| Sample | LLNLBE# | Batch# | 10Be/9Be Ratio[1] (Blank Corrected) | Ratio Error[1] | Sample Mass (g) | Carrier Mass[2] (ug) | Deposition Rate[3] (atms/(cm$^3$*y)) | Erosion Rates[4] (m My$^{-1}$) | Normalized Concentration[5] (atoms/g) | Standardized Concentration[6] | Log Trans Conc.[7] |
|---|---|---|---|---|---|---|---|---|---|---|---|
| POT45 | BE29399 | MB20 | 5.52E-12 | 3.65E-14 | 0.507 | 299.41 | 2.09E+06 | 36 | 6.04E+07 | 0.11 | 7.78 |
| POT46 | BE29401 | MB21 | 8.40E-12 | 7.65E-14 | 0.549 | 299.41 | 2.45E+06 | 30 | 7.25E+07 | 0.13 | 7.86 |
| POT47 | BE29402 | MB21 | 1.44E-11 | 1.52E-13 | 0.554 | 298.42 | 6.02E+05 | 4 | 5.00E+08 | 0.91 | 8.70 |
| POT48 | BE29403 | MB21 | 1.60E-11 | 1.23E-13 | 0.530 | 302.37 | 1.72E+06 | 10 | 2.06E+08 | 0.38 | 8.31 |
| POT49 | BE29404 | MB21 | 1.16E-11 | 1.29E-13 | 0.539 | 298.42 | 1.88E+06 | 16 | 1.32E+08 | 0.24 | 8.12 |
| POT50 | BE27107 | MB9 | 7.28E-12 | 1.20E-13 | 0.506 | 300.99 | 2.46E+06 | 31 | 6.83E+07 | 0.12 | 7.83 |
| POT51 | BE29405 | MB21 | 3.98E-12 | 3.45E-14 | 0.594 | 299.41 | 2.44E+06 | 67 | 3.18E+07 | 0.06 | 7.50 |
| POT52 | BE29406 | MB21 | 1.71E-11 | 2.62E-13 | 0.551 | 301.38 | 2.30E+06 | 14 | 1.57E+08 | 0.29 | 8.20 |
| POT53 | BE29407 | MB21 | 1.79E-11 | 1.96E-13 | 0.509 | 300.40 | 2.07E+06 | 11 | 1.99E+08 | 0.36 | 8.30 |
| POT54 | BE29408 | MB21 | 9.26E-12 | 7.16E-14 | 0.539 | 297.43 | 5.80E+05 | 6 | 3.42E+08 | 0.62 | 8.53 |
| POT55 | BE29409 | MB21 | 1.05E-11 | 8.07E-14 | 0.506 | 300.40 | 2.21E+06 | 20 | 1.09E+08 | 0.20 | 8.04 |
| POT56 | BE29410 | MB21 | 7.10E-12 | 5.49E-14 | 0.555 | 299.41 | 7.12E+05 | 10 | 2.09E+08 | 0.38 | 8.32 |
| POT57 | BE29411 | MB21 | 9.34E-12 | 1.11E-13 | 0.518 | 290.51 | 6.95E+05 | 7 | 2.92E+08 | 0.53 | 8.47 |
| POT58 | BE27108 | MB9 | 8.92E-12 | 8.18E-14 | 0.544 | 300.00 | 1.98E+06 | 22 | 9.63E+07 | 0.18 | 7.98 |
| POT59 | BE29412 | MB21 | 1.12E-11 | 1.86E-13 | 0.523 | 299.41 | 6.76E+05 | 6 | 3.68E+08 | 0.67 | 8.57 |
| POT60 | BE29413 | MB21 | 8.26E-12 | 6.38E-14 | 0.545 | 300.40 | 6.80E+05 | 8 | 2.60E+08 | 0.47 | 8.41 |
| POT61 | BE29414 | MB21 | 9.51E-12 | 1.21E-13 | 0.533 | 299.41 | 1.91E+06 | 20 | 1.09E+08 | 0.20 | 8.04 |
| POT62 | BE29416 | MB22 | 1.06E-11 | 1.43E-13 | 0.539 | 298.42 | 1.79E+06 | 17 | 1.27E+08 | 0.23 | 8.10 |
| POT63 | BE27109 | MB9 | 5.45E-12 | 9.14E-14 | 0.518 | 300.99 | 1.80E+06 | 31 | 6.83E+07 | 0.12 | 7.83 |
| POT64 | BE29417 | MB22 | 7.53E-12 | 5.03E-14 | 0.511 | 301.38 | 1.82E+06 | 23 | 9.47E+07 | 0.17 | 7.98 |
| POT65 | BE29418 | MB22 | 5.82E-12 | 3.16E-14 | 0.508 | 299.41 | 1.86E+06 | 30 | 7.15E+07 | 0.13 | 7.85 |
| POT66 | BE29419 | MB22 | 1.89E-11 | 1.03E-13 | 0.530 | 299.41 | 6.26E+05 | 3 | 6.62E+08 | 1.21 | 8.82 |
| POT67 | BE29420 | MB22 | 2.70E-12 | 1.82E-14 | 0.519 | 300.40 | 2.01E+06 | 71 | 3.02E+07 | 0.06 | 7.48 |
| POT68 | BE29421 | MB22 | 2.04E-11 | 1.26E-13 | 0.523 | 299.41 | 1.96E+06 | 9 | 2.30E+08 | 0.42 | 8.36 |
| POT69 | BE29422 | MB22 | 6.27E-12 | 4.28E-14 | 0.533 | 300.40 | 1.99E+06 | 31 | 6.88E+07 | 0.13 | 7.84 |
| POT70 | BE29423 | MB22 | 1.33E-11 | 1.45E-13 | 0.510 | 306.32 | 6.36E+05 | 4 | 4.88E+08 | 0.89 | 8.69 |
| POT71 | BE29424 | MB22 | 1.26E-12 | 1.09E-14 | 0.516 | 300.40 | 2.16E+06 | 164 | 1.31E+07 | 0.02 | 7.12 |
| POT72 | BE29425 | MB22 | 9.68E-12 | 1.10E-13 | 0.530 | 301.38 | 2.01E+06 | 20 | 1.06E+08 | 0.19 | 8.03 |
| POT73 | BE29426 | MB22 | 9.24E-12 | 6.31E-14 | 0.525 | 300.40 | 2.04E+06 | 21 | 1.00E+08 | 0.18 | 8.00 |

[1]Measured ratios from Lawrence Livermore National Laboratory, blank corrected.

[2]Mass of $^9$Be added to a sample from the SPEX Be Carrier.

[3]Deposition rate calculated using equation 2 from Graley et al. (2010).

[4]Calculated with equation 21 from Willenbring and von Blanckenburg (2010).

[5] To normalize each measured meteoric $^{10}$Be concentration, each deposition rate was divided by the highest deposition rate for both the Potomac River Basin Data and the Brown et al (1988) data to get a normalized deposition rate. Next, I divided each measured meteoric $^{10}$Be concentration by my newly normalized deposition rate for that basin.

[6]Divided each normalized concentration by the highest normalized concentration.

[7]A $\log_{10}$ transformation of each meteoric $^{10}$Be concentration.

## Table A.5 - Basin Information

| Sample | Physiographic Province | Average Elevation[1] (m) | Average Slope[2] (°) | Basin Area ($km^2$) | Mean Precip.[3] (cm/y) | Weighted Average pH[4] | Maximum pH[4] | Minimum pH[4] | Land Use[5] | Met. And In Situ Ratio[6] |
|---|---|---|---|---|---|---|---|---|---|---|
| POT01 | Main Branch | 387 | 8.75 | 29796 | 100 | 5.0 | 7.0 | 4.2 | Forest | 0.50 |
| POT02 | Piedmont | 130 | 3.46 | 54 | 107 | 5.2 | 6.9 | 4.6 | Urban | 0.23 |
| POT04 | Piedmont | 143 | 2.97 | 38 | 105 | 5.2 | 6.9 | 4.6 | Urban | 0.28 |
| POT05 | Piedmont | 140 | 2.83 | 23 | 106 | 5.3 | 6.9 | 4.2 | Urban | 0.31 |
| POT06 | Main Branch | 432 | 9.63 | 24851 | 100 | 5.0 | 7.0 | 4.2 | Forest | 0.57 |
| POT09 | Piedmont | 113 | 2.80 | 436 | 103 | 4.9 | 4.9 | 4.9 | Agriculture | 0.20 |
| POT10 | Valley and Ridge | 494 | 9.36 | 4136 | 102 | 4.9 | 5.1 | 4.9 | Forest | 0.42 |
| POT11 | Appalachian Plateau | 658 | 10.52 | 2254 | 108 | 5.1 | 7.0 | 4.2 | Forest | 0.64 |
| POT12 | Valley and Ridge | 266 | 5.63 | 1281 | 102 | 4.9 | 6.4 | 4.6 | Agriculture | 0.57 |
| POT13 | Piedmont | 192 | 3.06 | 440 | 105 | 4.9 | 6.8 | 4.6 | Agriculture | 0.49 |
| POT14 | Blue Ridge | 477 | 8.71 | 15 | 111 | 5.1 | 7.0 | 4.8 | Forest | 1.99 |
| POT15 | Blue Ridge | 167 | 4.88 | 33 | 100 | 4.9 | 4.9 | 4.9 | Agriculture | 0.43 |
| POT16 | Blue Ridge | 361 | 8.22 | 27 | 109 | 5.2 | 7.0 | 4.8 | Forest | 0.75 |
| POT17 | Piedmont | 152 | 5.38 | 10 | 101 | 5.3 | 6.3 | 4.6 | Agriculture | 0.90 |
| POT18 | Piedmont | 173 | 4.97 | 13 | 102 | 5.0 | 6.9 | 4.2 | Agriculture | 1.11 |
| POT19 | Piedmont | 155 | 2.57 | 14 | 105 | 5.1 | 6.9 | 4.6 | Agriculture | 0.36 |
| POT20 | Coastal Plain | 53 | 2.01 | 28 | 108 | 5.2 | 7.8 | 4.5 | Urban | 0.17 |
| POT21 | Coastal Plain | 79 | 2.65 | 16 | 105 | 4.9 | 7.2 | 4.5 | Urban | 0.05 |
| POT22 | Coastal Plain | 73 | 1.82 | 15 | 105 | 5.1 | 7.2 | 4.5 | Urban | 0.06 |
| POT23 | Coastal Plain | 76 | 2.17 | 28 | 105 | 4.9 | 7.8 | 4.5 | Urban | 0.05 |
| POT24 | Coastal Plain | 69 | 0.93 | 9 | 105 | 5.0 | 6.6 | 4.5 | Agriculture | 0.06 |
| POT25 | Coastal Plain | 57 | 2.79 | 36 | 104 | 5.2 | 6.5 | 4.5 | Forest | 0.05 |
| POT26 | Coastal Plain | 33 | 1.83 | 41 | 101 | 5.2 | 7.4 | 4.6 | Forest | 0.05 |
| POT27 | Coastal Plain | 47 | 3.37 | 22 | 103 | 5.3 | 6.5 | 4.5 | Forest | 0.06 |
| POT28 | Piedmont | 99 | 2.94 | 17 | 104 | 4.9 | 4.9 | 4.9 | Forest | 0.20 |
| POT29 | Piedmont | 109 | 2.16 | 8 | 104 | 4.9 | 4.9 | 4.9 | Forest | 0.82 |
| POT30 | Piedmont | 140 | 1.94 | 21 | 105 | 4.9 | 4.9 | 4.9 | Agriculture | 1.69 |
| POT31 | Piedmont | 74 | 1.39 | 21 | 100 | 4.9 | 4.9 | 4.9 | Agriculture | 1.30 |
| POT32 | Piedmont | 108 | 3.71 | 21 | 101 | 4.9 | 4.9 | 4.9 | Forest | 0.04 |
| POT33 | Piedmont | 110 | 4.06 | 28 | 101 | 4.9 | 4.9 | 4.9 | Urban | 0.32 |
| POT34 | Piedmont | 121 | 4.01 | 16 | 102 | 4.9 | 4.9 | 4.9 | Urban | 0.29 |
| POT35 | Piedmont | 110 | 2.51 | 21 | 101 | 4.9 | 4.9 | 4.9 | Agriculture | 1.07 |
| POT36 | Piedmont | 184 | 5.36 | 64 | 104 | 4.9 | 4.9 | 4.9 | Agriculture | 0.24 |
| POT37 | Piedmont | 210 | 5.27 | 48 | 102 | 4.9 | 4.9 | 4.9 | Agriculture | 0.41 |
| POT38 | Valley and Ridge | 216 | 2.85 | 12 | 96 | 4.9 | 5.1 | 4.9 | Agriculture | 2.07 |
| POT39 | Valley and Ridge | 377 | 11.60 | 13 | 103 | 4.9 | 4.9 | 4.9 | Forest | 0.50 |
| POT40 | Valley and Ridge | 605 | 13.75 | 9 | 103 | 4.9 | 4.9 | 4.9 | Forest | 0.33 |
| POT41 | Blue Ridge | 602 | 17.53 | 12 | 110 | 4.9 | 4.9 | 4.9 | Forest | 0.86 |
| POT42 | Valley and Ridge | 369 | 3.91 | 16 | 98 | 4.9 | 4.9 | 4.9 | Agriculture | 1.12 |
| POT43 | Blue Ridge | 575 | 13.79 | 25 | 111 | 4.9 | 4.9 | 4.9 | Forest | 0.37 |
| POT44 | Blue Ridge | 693 | 16.34 | 28 | 117 | 4.9 | 4.9 | 4.9 | Forest | 0.64 |

| Sample | Physiographic Province | Average Elevation[1] (m) | Average Slope[2] (°) | Basin Area (km$^2$) | Mean Precip.[3] (cm/y) | Weighted Average pH[4] | Maximum pH[4] | Minimum pH[4] | Land Use[5] | Met. And In Situ Ratio[6] |
|---|---|---|---|---|---|---|---|---|---|---|
| POT45 | Valley and Ridge | 990 | 21.85 | 29 | 113 | 4.9 | 4.9 | 4.9 | Forest | 0.96 |
| POT46 | Valley and Ridge | 1198 | 12.74 | 15 | 133 | 5.1 | 5.1 | 4.9 | Forest | 0.81 |
| POT47 | Valley and Ridge | 595 | 13.14 | 16 | 95 | 4.9 | 4.9 | 4.9 | Forest | |
| POT48 | Valley and Ridge | 391 | 11.39 | 13 | 92 | 4.9 | 4.9 | 4.9 | Forest | 0.55 |
| POT49 | Valley and Ridge | 651 | 11.74 | 27 | 101 | 4.9 | 4.9 | 4.9 | Forest | 0.76 |
| POT50 | Valley and Ridge | 1150 | 19.04 | 20 | 132 | 4.9 | 4.9 | 4.9 | Forest | 0.60 |
| POT51 | Appalachian Plateau | 868 | 9.22 | 13 | 131 | 5.1 | 6 | 4.2 | Forest | 0.29 |
| POT52 | Appalachian Plateau | 844 | 6.07 | 19 | 123 | 5.1 | 6 | 4.2 | Forest | 0.94 |
| POT53 | Appalachian Plateau | 720 | 11.12 | 21 | 110 | 4.9 | 4.9 | 4.9 | Forest | 1.08 |
| POT54 | Valley and Ridge | 324 | 15.61 | 5 | 92 | 4.9 | 4.9 | 4.9 | Forest | |
| POT55 | Appalachian Plateau | 804 | 8.51 | 16 | 118 | 5.2 | 5.6 | 4.5 | Forest | 0.72 |
| POT56 | Appalachian Plateau | 716 | 13.29 | 28 | 113 | 5.2 | 6 | 4.2 | Forest | |
| POT57 | Appalachian Plateau | 740 | 12.70 | 6 | 110 | 5.2 | 6 | 4.5 | Forest | |
| POT58 | Appalachian Plateau | 704 | 10.18 | 10 | 105 | 5.3 | 6.5 | 4.3 | Forest | 0.95 |
| POT59 | Appalachian Plateau | 734 | 8.97 | 17 | 107 | 5.2 | 6.3 | 4.6 | Forest | |
| POT60 | Appalachian Plateau | 707 | 10.93 | 5 | 108 | 5.2 | 6.3 | 4.7 | Agriculture | |
| POT61 | Valley and Ridge | 602 | 13.94 | 5 | 101 | 5.2 | 6.6 | 4.6 | Forest | 0.48 |
| POT62 | Valley and Ridge | 367 | 13.14 | 7 | 95 | 5.2 | 6 | 4.5 | Forest/Agriculture | 0.95 |
| POT63 | Valley and Ridge | 424 | 10.71 | 18 | 96 | 4.9 | 4.9 | 4.9 | Forest | 0.24 |
| POT64 | Valley and Ridge | 341 | 8.70 | 13 | 96 | 5.2 | 5.9 | 4.6 | Forest | 0.60 |
| POT65 | Valley and Ridge | 430 | 8.95 | 11 | 98 | 5.3 | 6.6 | 4.6 | Forest | 0.48 |
| POT66 | Valley and Ridge | 309 | 7.54 | 10 | 99 | 5.2 | 5.9 | 4.9 | Forest | |
| POT67 | Valley and Ridge | 438 | 12.09 | 25 | 105 | 4.9 | 4.9 | 4.9 | Forest | 0.16 |
| POT68 | Piedmont | 171 | 2.43 | 12 | 104 | 4.9 | 4.9 | 4.9 | Agriculture | 1.51 |
| POT69 | Blue Ridge | 237 | 4.91 | 11 | 105 | 4.9 | 4.9 | 4.9 | Agriculture | 0.34 |
| POT70 | Valley and Ridge | 196 | 3.30 | 13 | 101 | 4.9 | 4.9 | 4.9 | Agriculture | |
| POT71 | Blue Ridge | 558 | 8.71 | 11 | 114 | 4.9 | 4.9 | 4.9 | Forest | 0.10 |
| POT72 | Piedmont | 205 | 4.79 | 24 | 107 | 5.0 | 6 | 4.6 | Agriculture | 0.86 |
| POT73 | Piedmont | 247 | 5.72 | 18 | 108 | 5.0 | 6 | 4.3 | Agriculture | 0.81 |

[1]Data from USGS digital data at http://seamless.usgs.gov/.
[2]Data interpolated using USGS digital data at http://seamless.usgs.gov/.
[3]Data taken from a raster dataset from http://worldclim.org/.
[4]Data taken from http://soils.usda.gov/survey/geography/ssurgo/
[5]From USGS raster dataset.
[6]Divided the standardized meteoric $^{10}$Be concentration by the standardized in situ $^{10}$Be concentration

**Table A.6 - Gaging Station Information**

| Sample | Gaging Station | In Situ Export Rate[1] (g/y) | Meteoric Export Rate[1] (g/y) | Average Sediment Load[2] (g/y) | Erosion Index[3] |
|---|---|---|---|---|---|
| POT01 | 1646580 | 1.30E+12 | 2.88E+12 | 1.93E+12 | 0.67 |
| POT02 | 1650500 | 3.07E+09 | 1.33E+10 | 1.34E+10 | 1.01 |
| POT04 | 1647740 | 1.72E+09 | 6.51E+09 | 5.45E+08 | 0.08 |
| POT05 | 1647720 | 9.08E+08 | 3.13E+09 | 1.77E+09 | 0.57 |
| POT06 | 1638500 | 1.14E+12 | 2.22E+12 | 1.03E+12 | 0.47 |
| POT09 | 1656120 | 9.28E+09 | 5.13E+10 | 1.04E+10 | 0.20 |
| POT10 | 1631000 | 7.31E+10 | 2.13E+11 | 2.04E+11 | 0.96 |
| POT11 | 1603000 | 8.52E+10 | 1.57E+11 | 1.42E+11 | 0.91 |
| POT12 | 1614500 | 2.69E+10 | 5.57E+10 | 5.98E+10 | 1.07 |
| POT13 | 1639000 | 1.56E+10 | 3.42E+10 | 1.80E+10 | 0.53 |

[1]Calculated using Equation 3-3

[2]From Gellis et al. (2004)

[3]Calculated using Equation **2-1** taken from Brown et al. (1988)

## Table A.7 - Brown et al. (1988) Data

| Station | River | Location | Basin Area ($km^2$) | Altitude (m) | Gradient | Rainfall (cm/y) | Original Concentration (atoms/g) | Error (%) | Original EI | Sed. Load (g/y) | Latitude (DD) | New Concentration (atoms/g) | Deposition Rate[1] (atms/cm3*y) | New Index[2] | Normalized Concentration[3] (atoms/g) |
|---|---|---|---|---|---|---|---|---|---|---|---|---|---|---|---|
| 1463500 | Delaware | Trenton | 17560 | 2 | 0.00E+00 | 113 | 1.21E+08 | 5 | 0.26 | 5.44E+11 | 40.2217 | 1.09E+08 | 2.34E+06 | 0.14 | 2.71E+07 |
| 1474505 | Schuylkill | Philadelphia | 4903 | 2 | 0.00E+00 | 108 | 1.22E+08 | 12 | 0.81 | 4.56E+11 | 39.9208 | 1.10E+08 | 2.24E+06 | 0.46 | 2.86E+07 |
| 2083500 | Tar | Tarboro | 5654 | 3 | 1.60E-04 | 112 | 1.93E+08 | 21 | 0.27 | 1.13E+11 | 35.8944 | 1.75E+08 | 2.32E+06 | 0.15 | 4.37E+07 |
| 2084160 | Chicod | Road 1769 | 117 | 2 | 5.90E-04 | 128 | 3.09E+08 | 16 | 0.48 | 3.04E+09 | 35.5617 | 2.79E+08 | 2.65E+06 | 0.27 | 6.12E+07 |
| 2089500 | Neuse | Kinston | 6972 | 3 | 1.60E-04 | 127 | 1.93E+08 | 4 | 0.13 | 7.67E+10 | 35.2578 | 1.75E+08 | 2.62E+06 | 0.07 | 3.86E+07 |
| 2091500 | Contentnea | Hookerton | 1888 | 5 | 1.40E-04 | 112 | 9.30E+07 | 5 | 0.05 | 1.51E+10 | 35.4289 | 8.41E+07 | 2.32E+06 | 0.03 | 2.11E+07 |
| 2091970 | Creeping Swamp | Vanceboro | 70 | 5 | 6.90E-04 | 128 | 4.00E+08 | 44 | 0.24 | 7.00E+08 | 35.3900 | 3.62E+08 | 2.65E+06 | 0.14 | 7.93E+07 |
| 2105769 | Cape Fear | Lock 1 | 13610 | -1 | 6.00E-05 | 117 | 1.20E+08 | 9 | 0.13 | 2.31E+11 | 34.4044 | 1.09E+08 | 2.41E+06 | 0.08 | 2.61E+07 |
| 2131000 | Pee Dee | Pee Dee | 22870 | 8 | 2.00E-04 | 116 | 6.36E+08 | 13 | 0.89 | 4.80E+11 | 34.2042 | 5.75E+08 | 2.39E+06 | 0.51 | 1.40E+08 |
| 2175000 | Edisto | Givhans | 7070 | 6 | 1.40E-04 | 114 | 1.41E+08 | 21 | 0.03 | 2.12E+10 | 33.0278 | 1.27E+08 | 2.32E+06 | 0.02 | 3.18E+07 |
| 2198500 | Savannah | Clyo | 25510 | 2 | 1.00E-04 | 120 | 6.96E+08 | 28 | 0.27 | 1.53E+11 | 32.5281 | 6.29E+08 | 2.42E+06 | 0.16 | 1.51E+08 |
| 1470500 | Schuyikill | Berne | 919 | 95 | 1.33E-03 | 116 | 4.11E+08 | 39 | 2.1 | 7.08E+10 | 40.5225 | 3.72E+08 | 2.40E+06 | 1.19 | 8.98E+07 |
| 1481000 | Brandywine Cr. | Chadds Ford | 743 | 46 | 5.45E-03 | 111 | 1.31E+08 | 8 | 0.67 | 5.50E+10 | 39.8697 | 1.18E+08 | 2.30E+06 | 0.38 | 2.99E+07 |
| 1481500 | Brandywine Cr. | Wilmington | 813 | 21 | 5.45E-03 | 113 | 5.46E+08 | 53 | 2.6 | 5.69E+10 | 39.7694 | 4.94E+08 | 2.34E+06 | 1.48 | 1.22E+08 |
| 1570500 | Susquehanna | Harrisburg | 62400 | 88 | 3.20E-04 | 101 | 3.11E+08 | 23 | 1.11 | 2.93E+12 | 40.2547 | 2.81E+08 | 2.09E+06 | 0.63 | 7.80E+07 |
| 1638500 | Potomac | Point of Rocks | 25996 | 61 | 4.80E-04 | 109 | 4.21E+08 | 4 | 0.77 | 6.76E+11 | 39.2736 | 3.81E+08 | 2.26E+06 | 0.44 | 9.79E+07 |
| 1643000 | Monocay | Fredrick | 2116 | 71 | 4.60E-04 | 111 | 8.50E+08 | 4 | 3.77 | 1.35E+11 | 39.7695 | 7.69E+08 | 2.30E+06 | 2.14 | 1.94E+08 |
| 1664000 | Rappahannock | Remington | 1606 | 77 | 4.90E-04 | 105 | 7.26E+08 | 1 | 3.62 | 1.09E+11 | 38.5306 | 6.56E+08 | 2.17E+06 | 2.05 | 1.75E+08 |
| 2035000 | James | Cartersville | 16206 | 50 | 2.80E-04 | 110 | 3.20E+08 | 19 | 0.58 | 4.21E+11 | 37.6708 | 2.89E+08 | 2.28E+06 | 0.33 | 7.37E+07 |
| 2075500 | Dan | Paces | 6604 | 98 | 3.60E-04 | 112 | 2.76E+08 | 67 | 1.84 | 6.41E+11 | 36.6422 | 2.50E+08 | 2.32E+06 | 1.04 | 6.25E+07 |
| 2080500 | Roanoke | Roanoke Rapids | 21720 | 13 | 4.10E-04 | 114 | 1.17E+08 | 13 | 0.02 | 6.52E+10 | 36.4600 | 1.06E+08 | 2.36E+06 | 0.01 | 2.60E+07 |
| 2087500 | Neuse | Clayton | 2978 | 39 | 3.80E-04 | 128 | 2.57E+08 | 18 | 0.82 | 1.58E+11 | 35.6472 | 2.32E+08 | 2.65E+06 | 0.47 | 5.09E+07 |
| 2098198 | Haw | Moncure | 4375 | 47 | 4.40E-04 | 124 | 1.05E+09 | 4 | 2.01 | 1.36E+11 | 35.6494 | 9.46E+08 | 2.56E+06 | 1.14 | 2.14E+08 |
| 2100500 | Deep | Ramseur | 904 | 128 | 1.40E-03 | 124 | 4.76E+08 | 67 | 1.77 | 5.42E+10 | 35.7264 | 4.30E+08 | 2.56E+06 | 1.01 | 9.74E+07 |
| 2116500 | Yadkin | Yadkin College | 5900 | 195 | 3.10E-04 | 123 | 5.23E+08 | 32 | 4.64 | 8.38E+11 | 35.8567 | 4.73E+08 | 2.54E+06 | 2.64 | 1.08E+08 |
| 2129000 | Pee Dee | Rockingham | 17780 | 37 | 6.10E-04 | 119 | 7.23E+08 | 11 | 0.61 | 2.31E+11 | 34.9458 | 6.54E+08 | 2.46E+06 | 0.35 | 1.54E+08 |
| 2151500 | Broad | Boiling Springs | 2266 | 195 | 1.08E-03 | 130 | 5.74E+08 | 34 | 6.69 | 4.46E+11 | 35.2108 | 5.19E+08 | 2.69E+06 | 3.81 | 1.12E+08 |
| 1540500 | Susquehanna | Danville | 29060 | 131 | 2.70E-04 | 103 | 1.77E+08 | 10 | 0.48 | 1.60E+12 | 40.9581 | 1.60E+08 | 2.13E+06 | 0.41 | 4.35E+07 |
| 1545600 | Young Womans | Renovo | 120 | 238 | 1.01E-02 | 103 | 3.40E+08 | 86 | 0.36 | 1.68E+09 | 41.3894 | 3.07E+08 | 2.13E+06 | 0.20 | 8.36E+07 |
| 1553500 | Susquehanna | West Branch | 17734 | 130 | 2.80E-04 | 103 | 6.01E+08 | 20 | 1.12 | 4.43E+11 | 40.9675 | 5.43E+08 | 2.13E+06 | 0.64 | 1.48E+08 |
| 1567000 | Juniata | Newport | 8687 | 111 | 4.90E-04 | 103 | 1.64E+08 | 8 | 0.37 | 2.61E+11 | 40.4783 | 1.48E+08 | 2.13E+06 | 0.21 | 4.03E+07 |
| 3068000 | Shavers Fork | Bemis | 298 | 785 | 9.61E-03 | 125 | 2.87E+08 | 19 | 0.44 | 7.45E+09 | 38.8075 | 2.60E+08 | 2.59E+06 | 0.25 | 5.82E+07 |
| 3068600 | Shavers Fork | above Bowden | 357 | 683 | 5.19E-03 | 125 | 3.35E+08 | 18 | 0.72 | 1.25E+10 | 38.9028 | 3.03E+08 | 2.59E+06 | 0.41 | 6.79E+07 |
| 3068800 | Shavers Fork | below Bowden | 391 | 645 | 3.69E-03 | 125 | 2.79E+08 | 27 | 0.89 | 2.03E+10 | 38.9131 | 2.52E+08 | 2.59E+06 | 0.51 | 5.66E+07 |
| 3202400 | Guyandotte | Baileysville | 798 | 347 | 1.15E-03 | 115 | 1.24E+08 | 22 | 1.08 | 1.04E+11 | 37.6039 | 1.12E+08 | 2.38E+06 | 0.61 | 2.73E+07 |
| 3202490 | Indian Cr. | Fanrock | 105 | 369 | 2.44E-03 | 115 | 2.76E+08 | 32 | 0.52 | 2.94E+09 | 37.5669 | 2.50E+08 | 2.38E+06 | 0.29 | 6.08E+07 |
| 3202750 | Clear Fork | Clear Fork | 319 | 354 | 2.13E-03 | 115 | 1.80E+08 | 30 | 1.65 | 4.37E+10 | 37.6231 | 1.63E+08 | 2.38E+06 | 0.94 | 3.97E+07 |
| 3198550 | Big Coal | Alum | 1145 | 180 | 4.90E-04 | 120 | 3.11E+08 | 24 | 3.73 | 2.14E+11 | 38.2500 | 2.81E+08 | 2.48E+06 | 2.12 | 6.57E+07 |
| 3199000 | Little Coal | Danville | 699 | 201 | 1.24E-03 | 120 | 1.50E+08 | 37 | 2.36 | 1.71E+11 | 38.0769 | 1.36E+08 | 2.48E+06 | 1.34 | 3.17E+07 |
| 3199400 | Little Coal | Julian | 826 | 193 | 4.90E-04 | 120 | 2.05E+08 | 52 | 2.83 | 1.78E+11 | 38.1547 | 1.85E+08 | 2.48E+06 | 1.60 | 4.33E+07 |
| 3199700 | Coal | Alum | 2163 | 180 | 3.40E-04 | 120 | 3.01E+08 | 30 | 4.13 | 4.63E+11 | 38.2867 | 2.72E+08 | 2.48E+06 | 2.34 | 6.36E+07 |

| Station | River | Location | Basin Area ($km^2$) | Altitude (m) | Gradient | Rainfall (cm/y) | Original Concentration (atms/g) | Error (%) | Original EI | Sed. Load (g/y) | Latitude (DD) | New Concentration[1] (atoms/g) | Deposition Rate[2] (atms/cm3*y) | New Index[3] | Normalized Concentration[4] |
|---|---|---|---|---|---|---|---|---|---|---|---|---|---|---|---|
| 3200500 | Coal | Tornado | 2230 | 174 | 3.30E-04 | 120 | 4.14E+08 | 5 | 5.15 | 4.33E+11 | 38.3389 | 3.74E+08 | 2.48E+06 | 2.92 | 8.74E+07 |
| 1610200 | Lost | McMauley | 401 | 384 | 2.89E-03 | 125 | 4.58E+08 | 24 | 2.23 | 3.17E+10 | 39.0550 | 4.14E+08 | 2.59E+06 | 1.26 | 9.28E+07 |
| 3176500 | New River | Glen Lyn | 9759 | 454 | 1.01E-03 | 102 | 7.25E+08 | 25 | 0.44 | 7.81E+10 | 37.3728 | 6.56E+08 | 2.11E+06 | 0.25 | 1.80E+08 |
| 3453500 | Franch Broad | Marshall | 3450 | 502 | 3.03E-03 | 132 | 4.03E+08 | 9 | 2.89 | 4.38E+11 | 35.7864 | 3.64E+08 | 2.73E+06 | 1.70 | 7.74E+07 |

Unless otherwise noted all data are original.

[1]Updated from KNSTD to 07KNSTD by multiplying each original meteoric $^{10}Be$ concentration by 0.9042.

[2]Deposition rate calculated using equation 2 from Graley et al. (2010).

[3]Calculated using Equation **2-1** taken from Brown et al. (1988)

[4]To normalize each measured meteoric $^{10}Be$ concentration, each deposition rate was divided by the highest deposition rate for both the Potomac River Basin Data and the Brown et al (1988) data to get a normalized production rate. Next, I divided each measured meteoric $^{10}Be$ concentration by my newly normalized deposition rate for that basin.

## Appendix B – Sampled Sites

| Sample Site | **POT-01** | Sampler **Charles Trodick** | | Gaging Station # | **1646580** |
|---|---|---|---|---|---|
| Elevation | **8m** | Latitude | **38.930571** | Longitude | **-77.116148** |
| Description | | | | | |
| **80 meters upstream from Chain Bridge on VA side between 2nd and 3rd pylon. Sediment trap on downstream side of rock pile next to river near low flood area** | | | | | |

| Sample Site | **POT-02** | Sampler **Charles Trodick** | | Gaging Station # | **1650500** |
|---|---|---|---|---|---|
| Elevation | **79m** | Latitude | **39.064727** | Longitude | **-77.028419** |
| Description | | | | | |
| **Northwest Branch off abandon portion of Old Randolph Road Bridge. Near corner of Randolph and Old Randolph. Old Gaging station. Sample just downstream from bridge. Bar in middle of stream.** | | | | | |

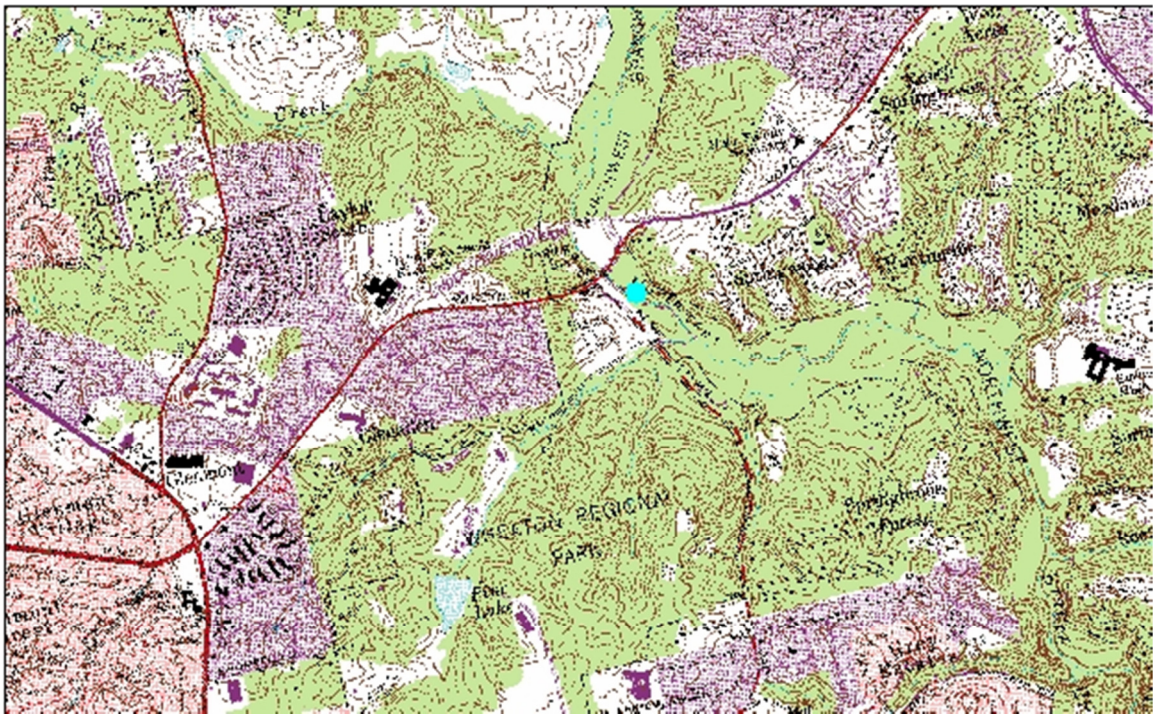

| Sample Site | **POT-04** | Sampler **Charles Trodick** | | Gaging Station # | **1647740** |
|---|---|---|---|---|---|
| Elevation | **143m** | Latitude | **39.105904** | Longitude | **-77.125032** |
| Description | | | | | |
| **North Branch of Rock Creek near Rockville, MD. Near Avery St. and Southlawn. Upstream from Avery Bridge and downstream from Southlawn. Off walking path.** | | | | | |

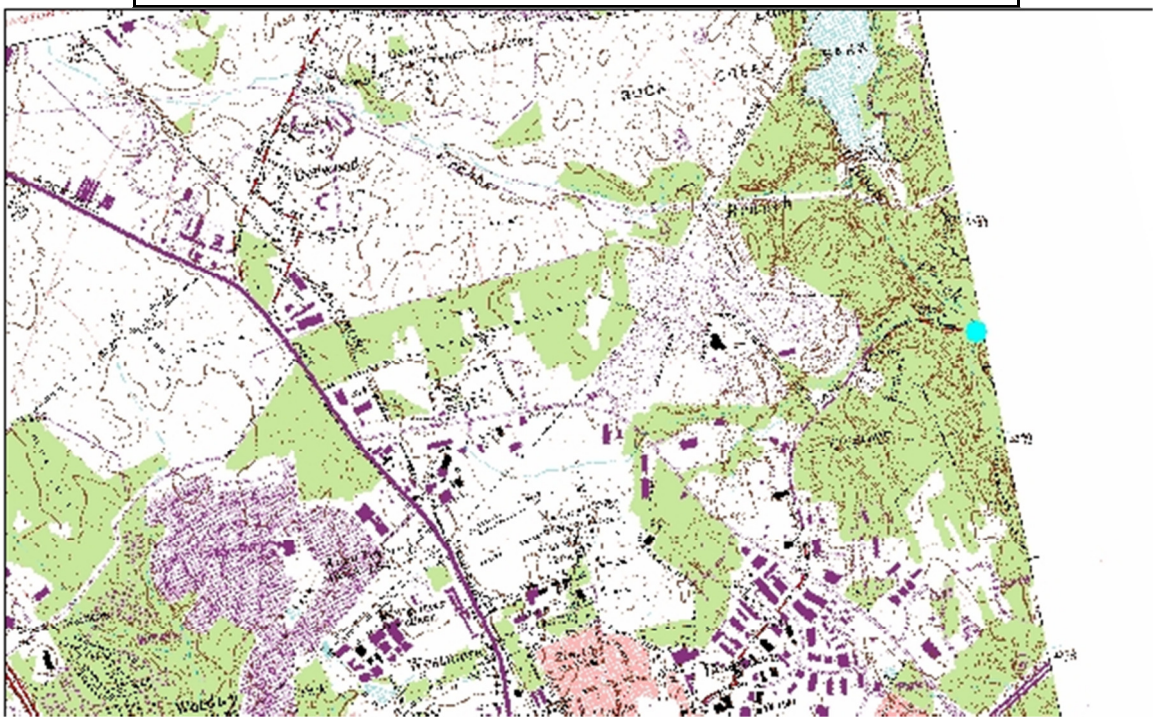

| Sample Site | **POT-05** | Sampler **Charles Trodick** | | Gaging Station # | **1647720** |
|---|---|---|---|---|---|
| Elevation | **120m** | Latitude | **39.1179** | Longitude | **-77.100871** |
| Description | | | | | |
| **Near Mancaster Road. North Branch of Rock Creek near Norbeck, MD. Upstream from bridge, bar on outside of turn.** | | | | | |

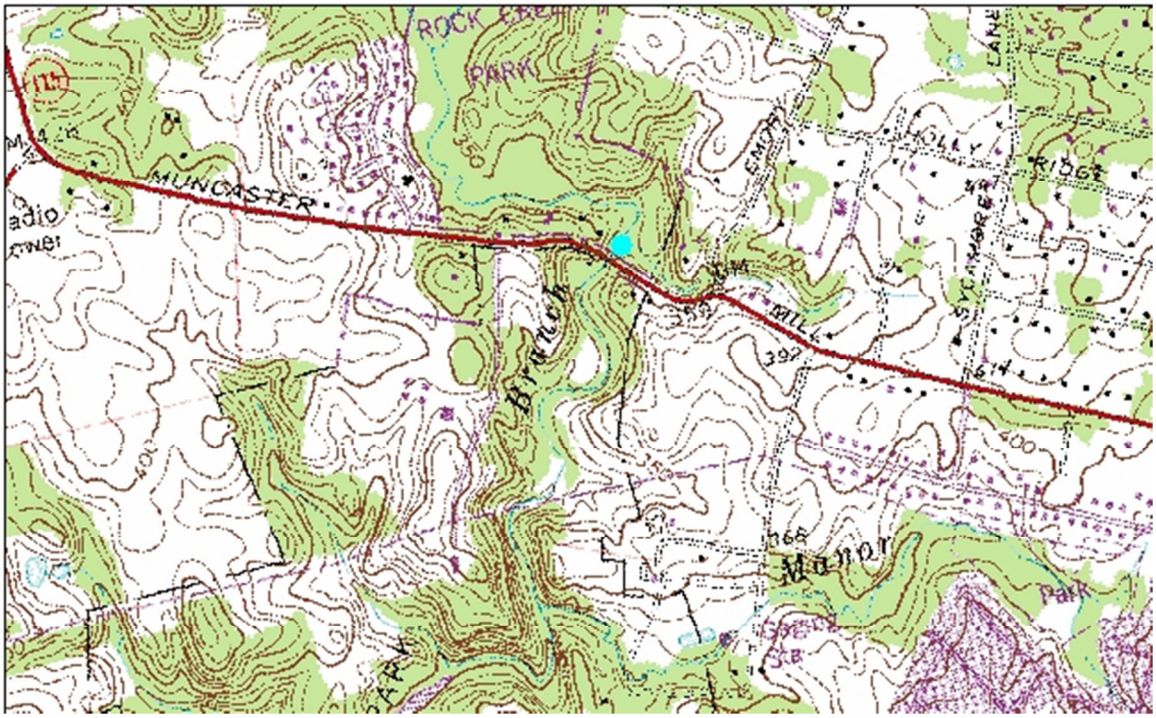

| Sample Site | **POT-06** | Sampler **Charles Trodick** | | Gaging Station # | **1638500** |
|---|---|---|---|---|---|
| Elevation | **105m** | Latitude | **39.27235** | Longitude | **-77.546222** |
| Description | | | | | |
| **Potomac River at Point of Rocks. VA side, under bridge. River side, up stream of 3rd pylon. Boat ramp area. Second sample collected downstream.** | | | | | |

| Sample Site | **POT-09** | Sampler **Charles Trodick** | | Gaging Station # | **1656120** |
|---|---|---|---|---|---|
| Elevation | **63m** | Latitude | **38.640112** | Longitude | **-77.512321** |
| Description | | | | | |
| **Cedar Run, NW corner of Quantico. Where Aden Road crosses over Cedar Run. Upstream from bridge. Past two small tributaries. Bar in middle of stream.** | | | | | |

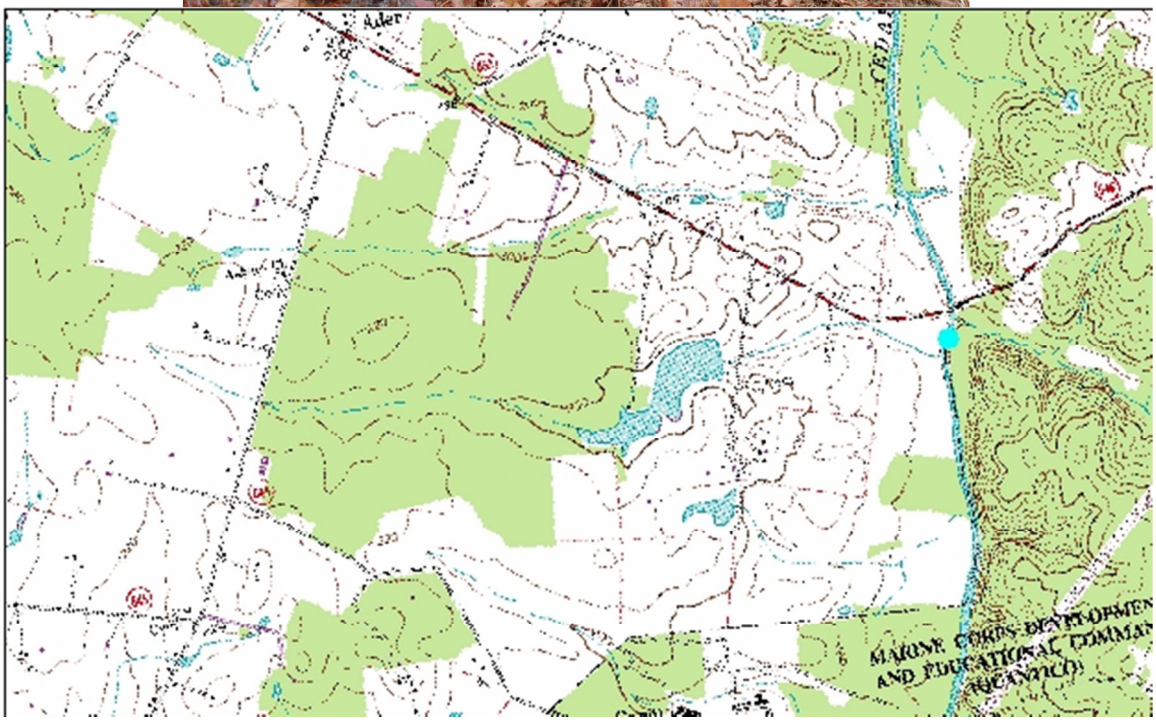

| Sample Site | **POT-10** | Sampler **Charles Trodick** | | Gaging Station # | **1631000** |
|---|---|---|---|---|---|
| Elevation | **148m** | Latitude | **38.914248** | Longitude | **-78.209969** |
| Description | | | | | |
| **South Fork Shenandoah at Front Royal. At boat landing downstream from bridge. Path downstream from boat landing. Town side of river across from house. Forested at sample site.** | | | | | |

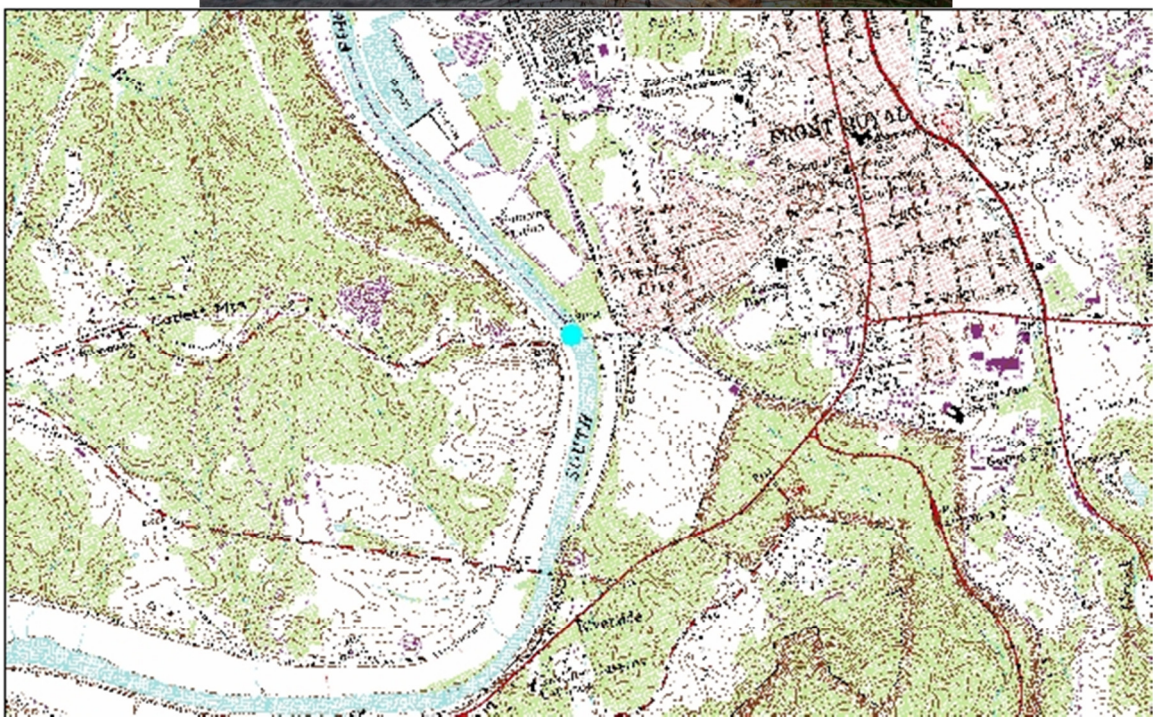

| Sample Site | **POT-11** | Sampler **Charles Trodick** | | Gaging Station # | **1603000** |
|---|---|---|---|---|---|
| Elevation | | Latitude | **39.621466** | Longitude | **-78.7737** |
| Description | | | | | |
| **Potomac at Cumberland, MD. Highway 28 bridge, south end. Riffle just upstream from bridge. Between land and first pylon.** | | | | | |

| Sample Site | **POT-12** | Sampler **Charles Trodick** | | Gaging Station # | **1614500** |
|---|---|---|---|---|---|
| Elevation | **132m** | Latitude | **39.715704** | Longitude | **-77.824155** |
| Description | | | | | |
| **Gaging station down Wishand Road in southern Pennsylvania. Shack with platform near old dam. Upstream from station past a metal pole sticking out of a tree. Sediment from near side of stream, downstream from island.** | | | | | |

| Sample Site | **POT-13** | Sampler **Charles Trodick** | | Gaging Station # | **1639000** |
|---|---|---|---|---|---|
| Elevation | **118m** | Latitude | **39.715704** | Longitude | **-77.824155** |
| Description | | | | | |
| **Creek near Taneytown. Border with Carroll County, MD. On same side as gaging station, just in front of gaging station past the wall. A little difficult to determine sediment source.** | | | | | |

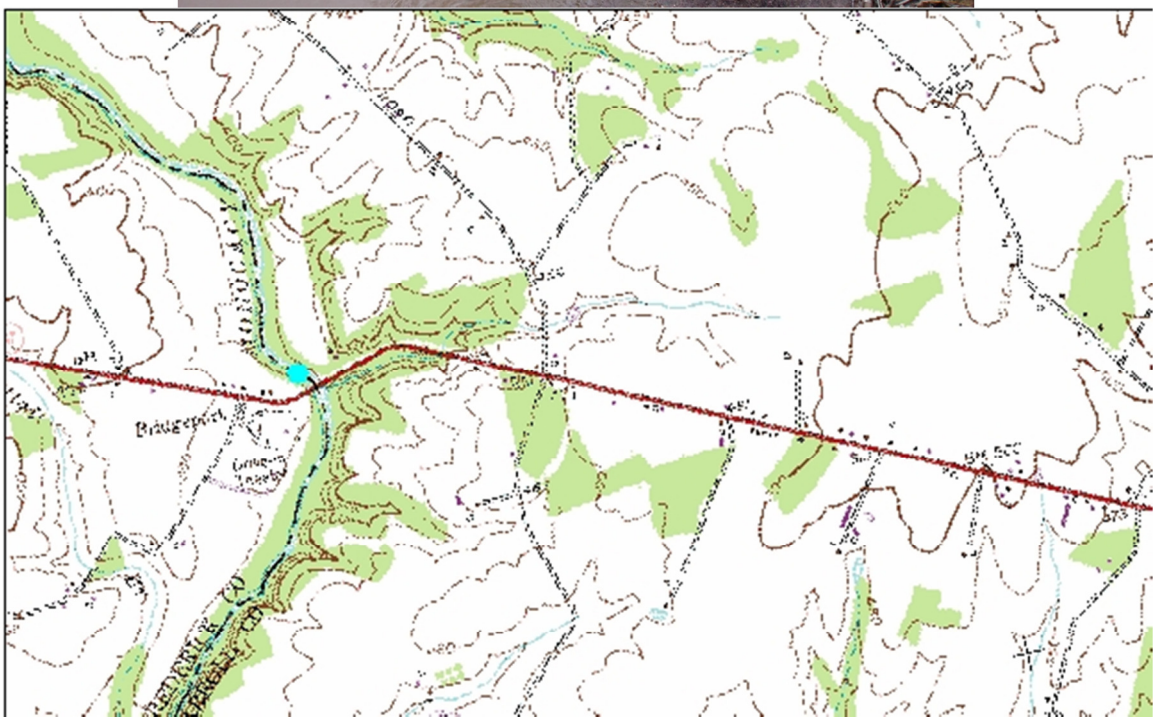

| Sample Site | **POT-14** | Sampler **Charles Trodick** | | Stream Name | |
|---|---|---|---|---|---|
| Elevation | **288m** | Latitude | **39.586971** | Longitude | **-77.464085** |
| Description | | | | | |
| **Near Cunningham Falls State Park Road. Just off road. Private land upstream from small bridge and two manmade log dams past previous dredging. Small rich community with some construction but land seems natural.** | | | | | |

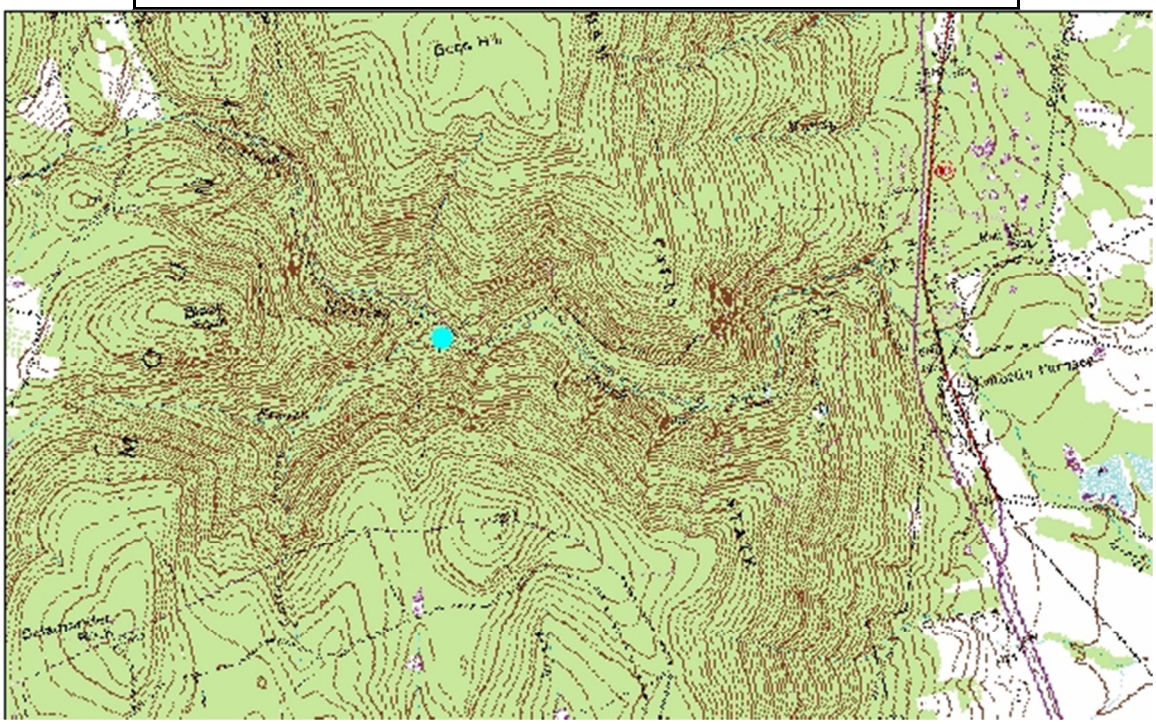

| Sample Site | **POT-15** | Sampler **Charles Trodick** | | Stream Name | **Dutchman Creek** |
|---|---|---|---|---|---|
| Elevation | | Latitude | **39.306916** | Longitude | **-77.651142** |
| Description | | | | | |
| **Just upstream from Dutchman Creek Bridge. Gravel bedded stream. Sampled 4 different locations because of very little sand. Tall shinny rock uphill from site. Forested region. Just up from Potomac.** | | | | | |

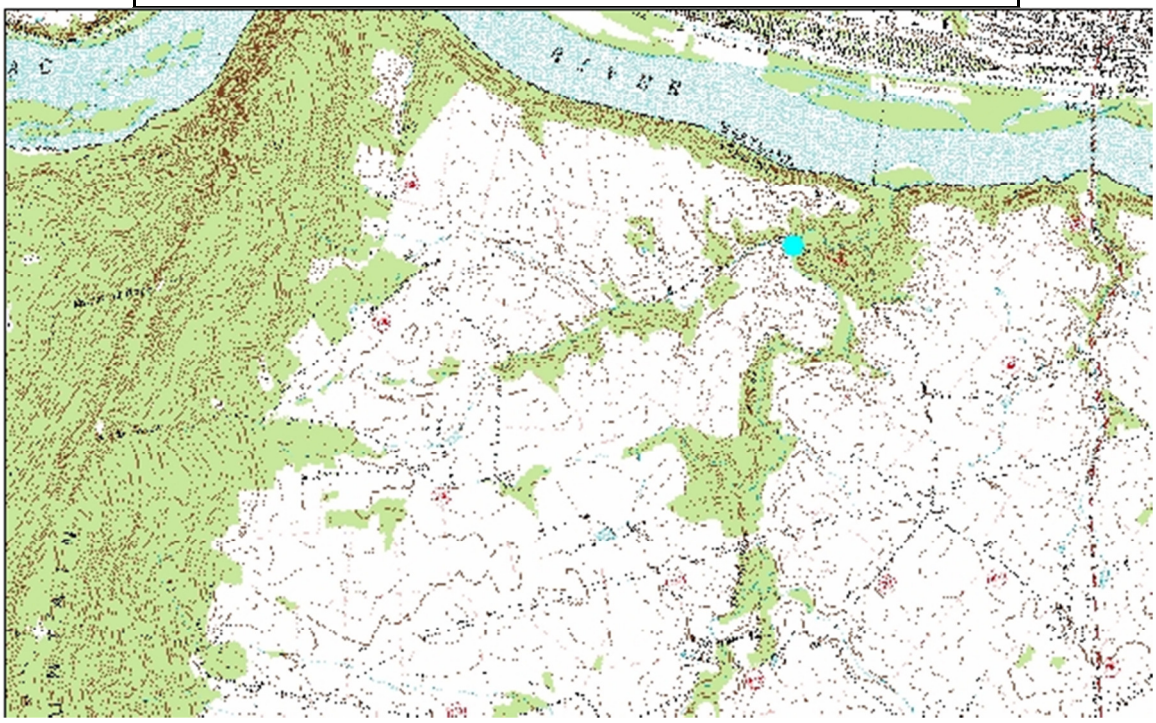

| Sample Site | **POT-16** | Sampler **Charles Trodick** | | Stream Name | **Friends Creek** |
|---|---|---|---|---|---|
| Elevation | | Latitude | **39.708375** | Longitude | **-77.411599** |
| Description | | | | | |
| **Just off Friends Creek Road. Down cut bank, upstream from tributary. Sampled at inlet and edge of stream 40m from road. Completely forested area.** | | | | | |

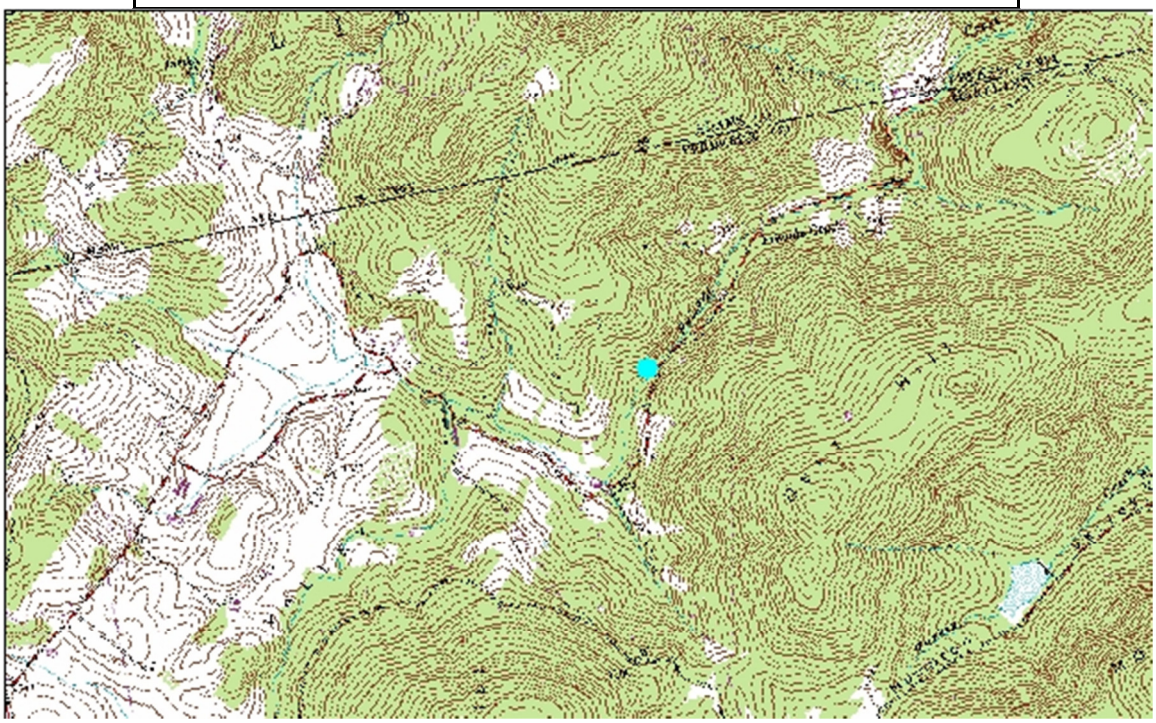

| Sample Site | **POT-17** | Sampler **Charles Trodick** | | Stream Name | **Above Israel Creek** |
|---|---|---|---|---|---|
| Elevation | | Latitude | **39.479666** | Longitude | **-77.327614** |
| Description | | | | | |
| **Just off Water Street Road on Stauffer Road upstream from bridge near pasture land. Very few trees. Sample taken from some grasses across from an inlet near a big tree.** | | | | | |

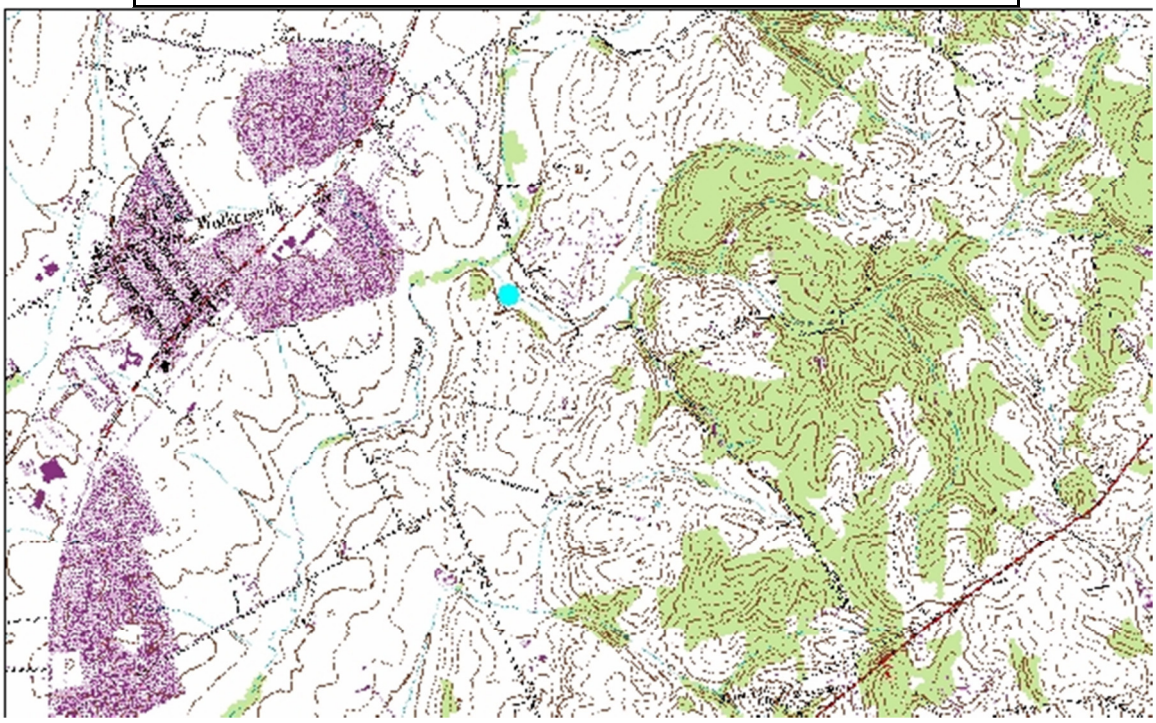

| Sample Site | **POT-18** | Sampler **Charles Trodick** | | Stream Name | **Ten Mile Creek** |
|---|---|---|---|---|---|
| Elevation | | Latitude | **39.210672** | Longitude | **-77.310759** |
| Description | | | | | |
| **Just past gate on Ten Mile Creek Road. Small point bar upstream from bridge. Black Hill Regional Park upstream from Little Seneca Lake, Reservoir.** | | | | | |

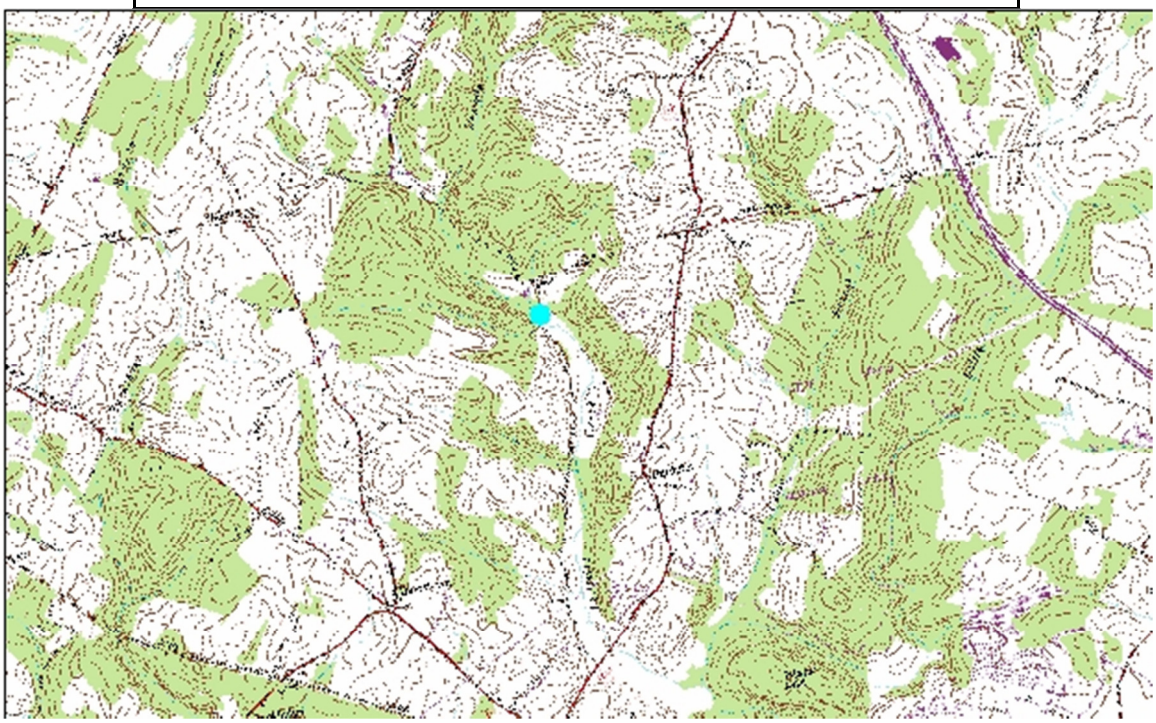

| Sample Site | **POT-19** | Sampler **Charles Trodick** | | Stream Name | **Rock Creek** |
|---|---|---|---|---|---|
| Elevation | | Latitude | **39.154325** | Longitude | **-77.131963** |
| Description | | | | | |
| **Upstream from Munster Road Bridge and confluence. Tried sampling under bridge but sediment was to fine. Found point bar upstream with gravel and fine sand. Near horse trail. Some trees. Rich suburban neighborhood.** | | | | | |

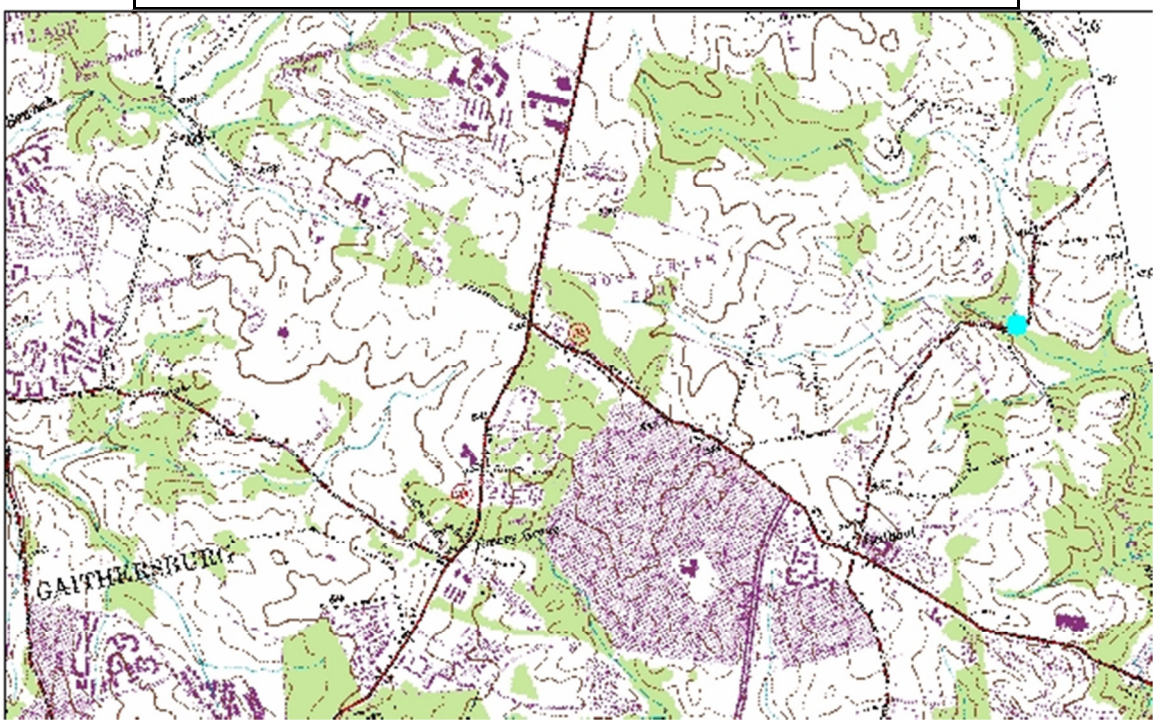

| Sample Site | **POT-20** | Sampler **Charles Trodick** | | Stream Name | **Beaver Dam Creek** |
|---|---|---|---|---|---|
| Elevation | | Latitude | **39.021751** | Longitude | **-76.860352** |
| Description | | | | | |
| **At edge of ME agriculture land on Beaver Dam Road. Point bar upstream from bridge.** | | | | | |

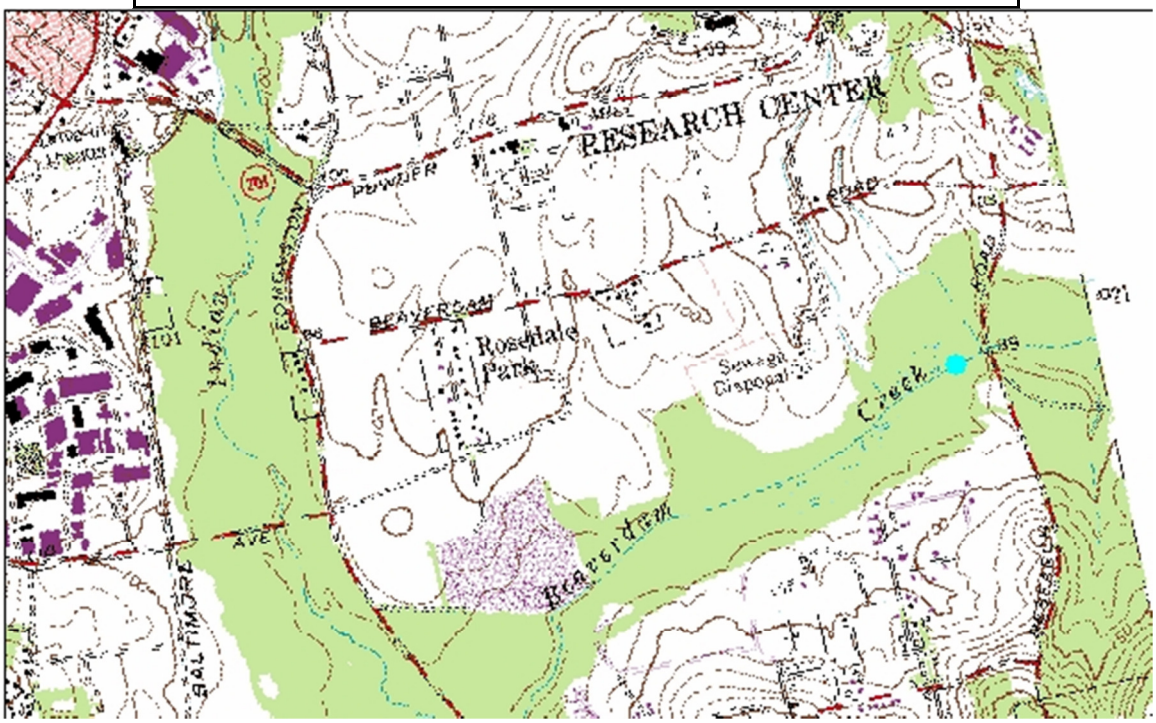

| Sample Site | **POT-21** | Sampler **Charles Trodick** | | Stream Name | **Henson Creek** |
|---|---|---|---|---|---|
| Elevation | | Latitude | **38.831217** | Longitude | **-76.919746** |
| Description | | | | | |
| **Parked at church on loop to south of Suitland Parkway. Residential area. Stream in woods. Behind church, follow small stream south to confluence with Henson Creek.** | | | | | |

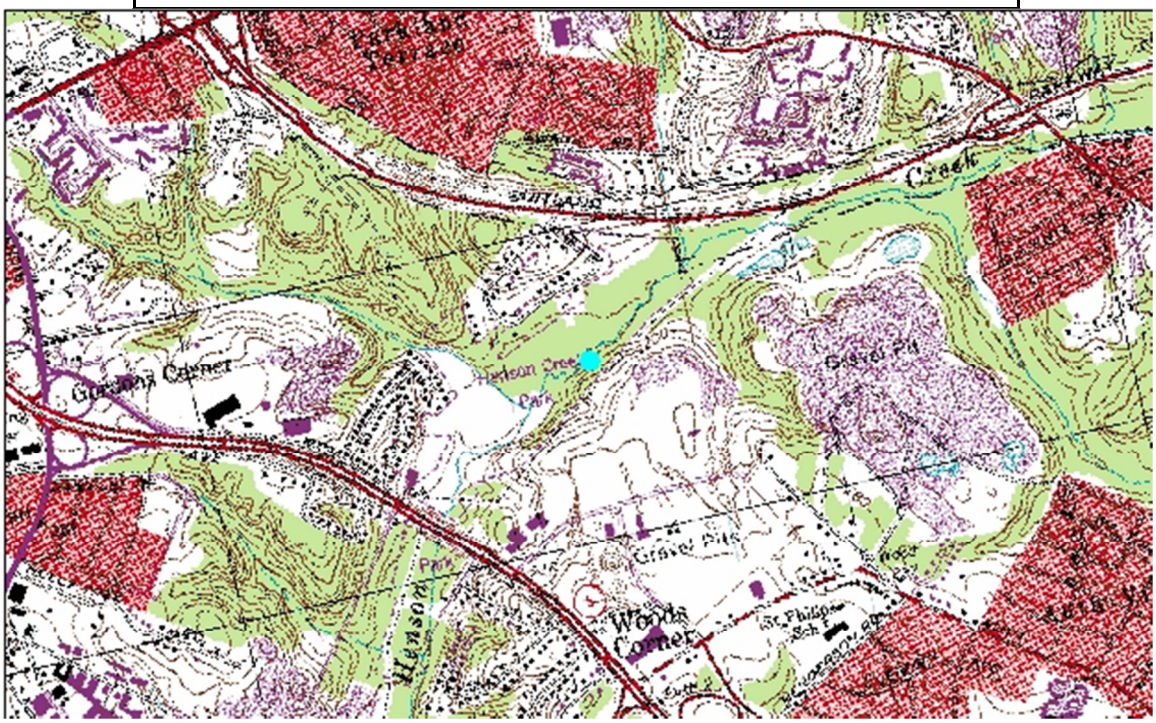

| Sample Site | **POT-22** | Sampler **Charles Trodick** | | Stream Name | |
|---|---|---|---|---|---|
| Elevation | | Latitude | **38.755388** | Longitude | **-76.841726** |
| Description | | | | | |
| **Next to Homeland Security, across stream. Stopped at back of housing development. Hiked upstream from small confluence.** | | | | | |

| Sample Site | **POT-23** | Sampler **Charles Trodick** | | Stream Name | **Tinkers Creek** |
|---|---|---|---|---|---|
| Elevation | | Latitude | **38.759003** | Longitude | **-76.941934** |
| Description | | | | | |
| **Point bar upstream from on Steed Road. Perfect sample.** | | | | | |

| Sample Site | **POT-24** | Sampler **Charles Trodick** | | Stream Name | **Timothy Creek** |
|---|---|---|---|---|---|
| Elevation | | Latitude | **38.664503** | Longitude | **-76.879363** |
| Description | | | | | |
| **Just upstream from bridge on Mckendree Road. Just downstream from confluence. Swampy area, near new housing development.** | | | | | |

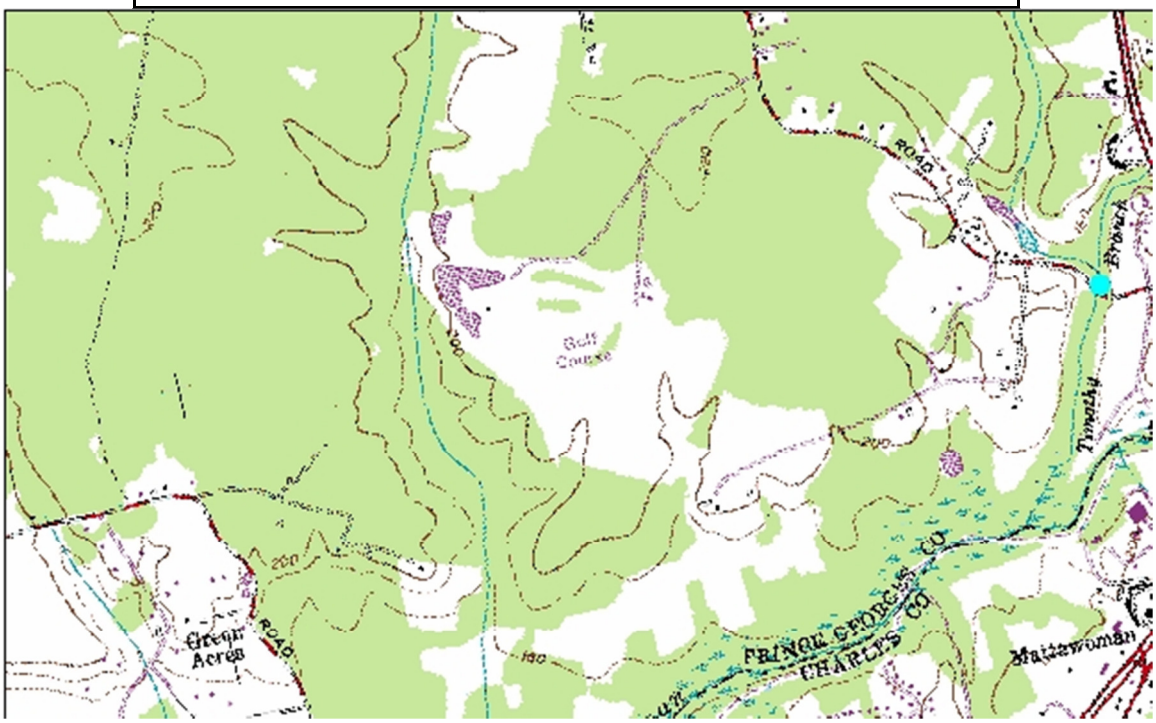

| Sample Site | **POT-25** | Sampler **Charles Trodick** | | Stream Name | **Port Tobacco Creek** |
|---|---|---|---|---|---|
| Elevation | | Latitude | **38.542057** | Longitude | **-77.017593** |
| Description | | | | | |
| **Downstream from bridge, Indian Head and La Plata Road. Further downstream then planned, need to include more basins. Stream bed gravel and fine sand.** | | | | | |

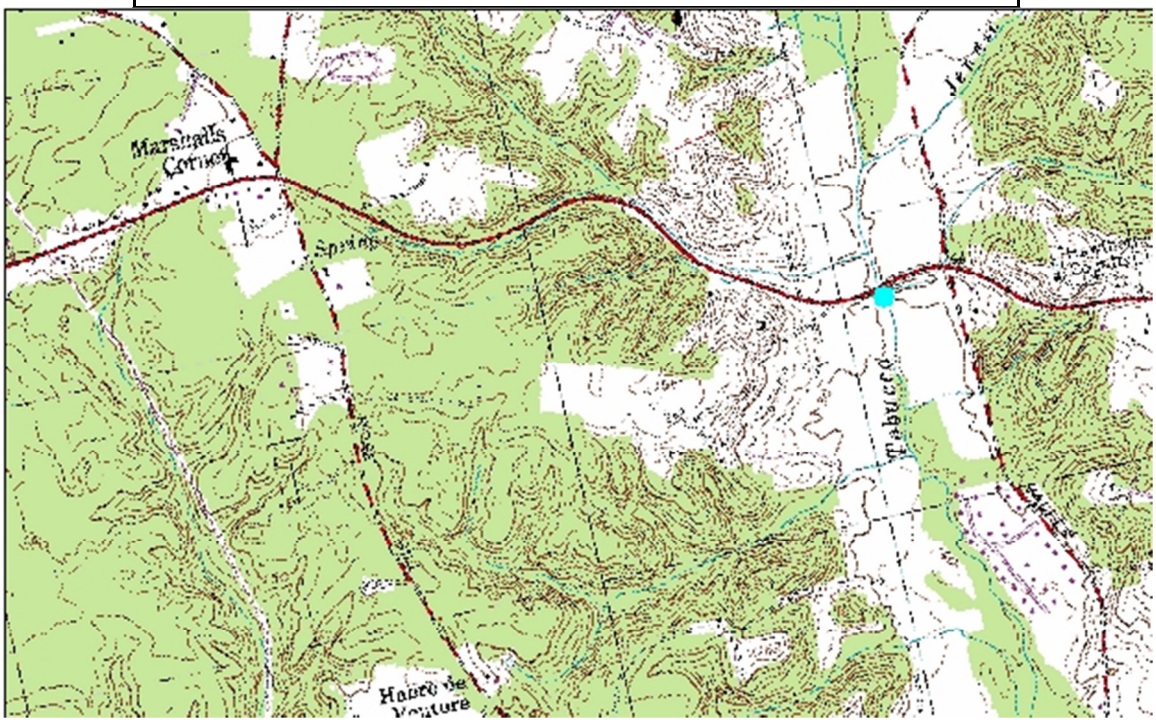

| Sample Site | **POT-26** | Sampler **Charles Trodick** | | Stream Name | **Beaver Dam Creek** |
|---|---|---|---|---|---|
| Elevation | | Latitude | **38.422865** | Longitude | **-77.213202** |
| Description | | | | | |
| **Just downstream from Hancock Run Road. Small point bar. Rural area. Surrounded by trees. Lots of sand and gravel on road side.** | | | | | |

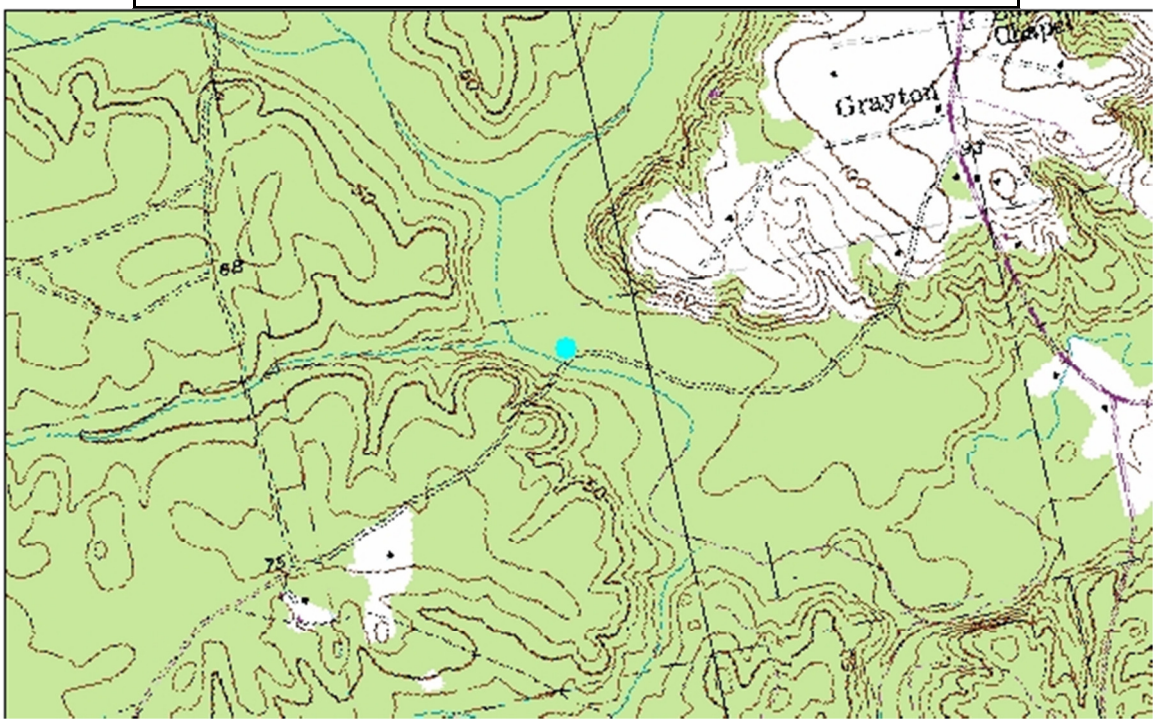

| Sample Site | **POT-27** | Sampler **Charles Trodick** | | Stream Name | **Burgess Creek** |
|---|---|---|---|---|---|
| Elevation | | Latitude | **38.483023** | Longitude | **-77.084112** |
| Description | | | | | |
| **Just upstream from La Plata (6) Road Bridge on east side only visible shallow spot. Tree in water. Tire. Perfect Sand. Parked on Mill Swamp Road.** | | | | | |

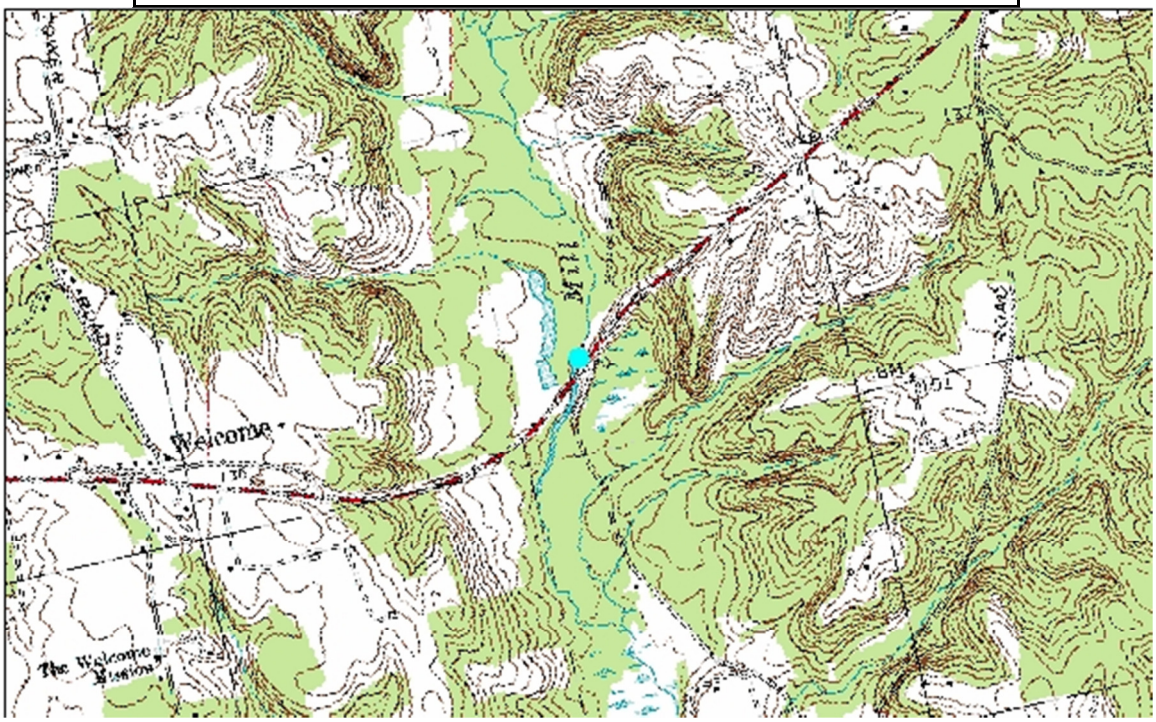

| Sample Site | **POT-28** | Sampler **Charles Trodick** | | Stream Name | **Potomac Run Creek** |
|---|---|---|---|---|---|
| Elevation | | Latitude | **38.441724** | Longitude | **-77.540603** |
| Description | | | | | |
| **Just downstream from Poplar Road Bridge. Sand bar on north side of stream. Forested with new development.** | | | | | |

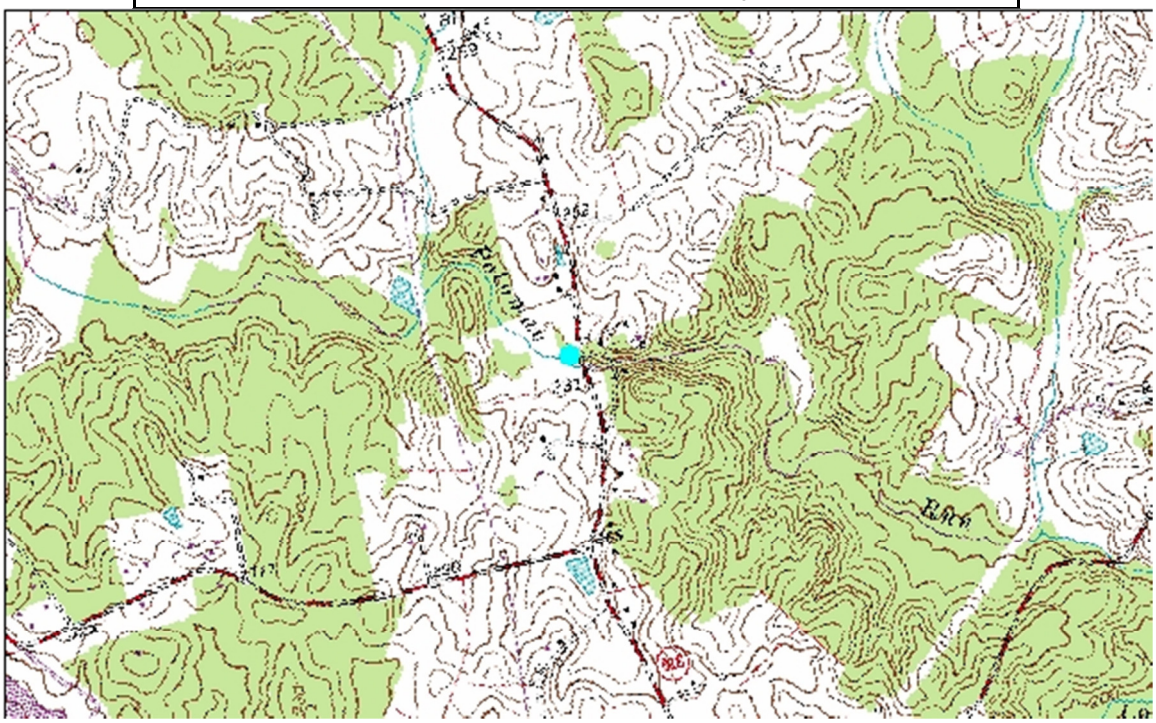

| Sample Site | **POT-29** | Sampler **Charles Trodick** | | Stream Name | **Elk Run** |
|---|---|---|---|---|---|
| Elevation | | Latitude | **38.566422** | Longitude | **-77.672696** |
| Description | | | | | |
| **Just off Poplar Road Bridge on farm road, upstream of confluence. Appears farmer is removing gravel.** | | | | | |

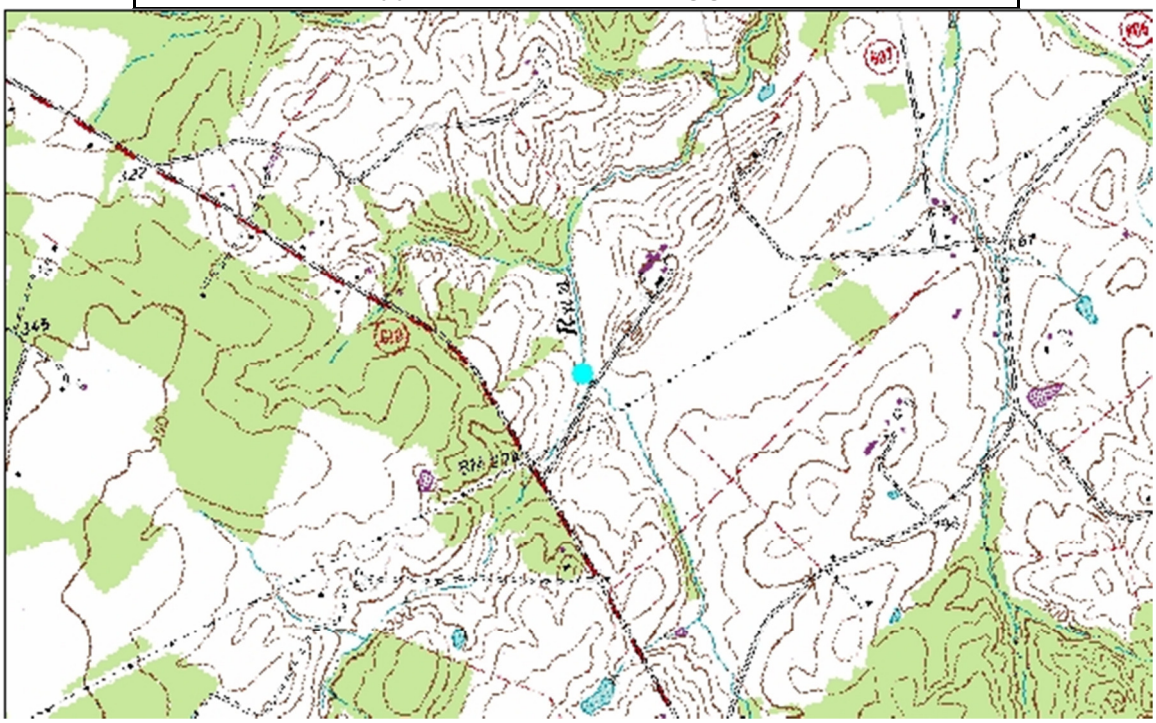

| Sample Site | **POT-30** | Sampler **Charles Trodick** | | Stream Name | **Licking Run** |
|---|---|---|---|---|---|
| Elevation | | Latitude | **38.629276** | Longitude | **-77.764106** |
| Description | | | | | |
| **Upstream from bridge on Green Road. Surrounded by farms and trees. Sampled at bar with water plants. Nearby ditch input.** | | | | | |

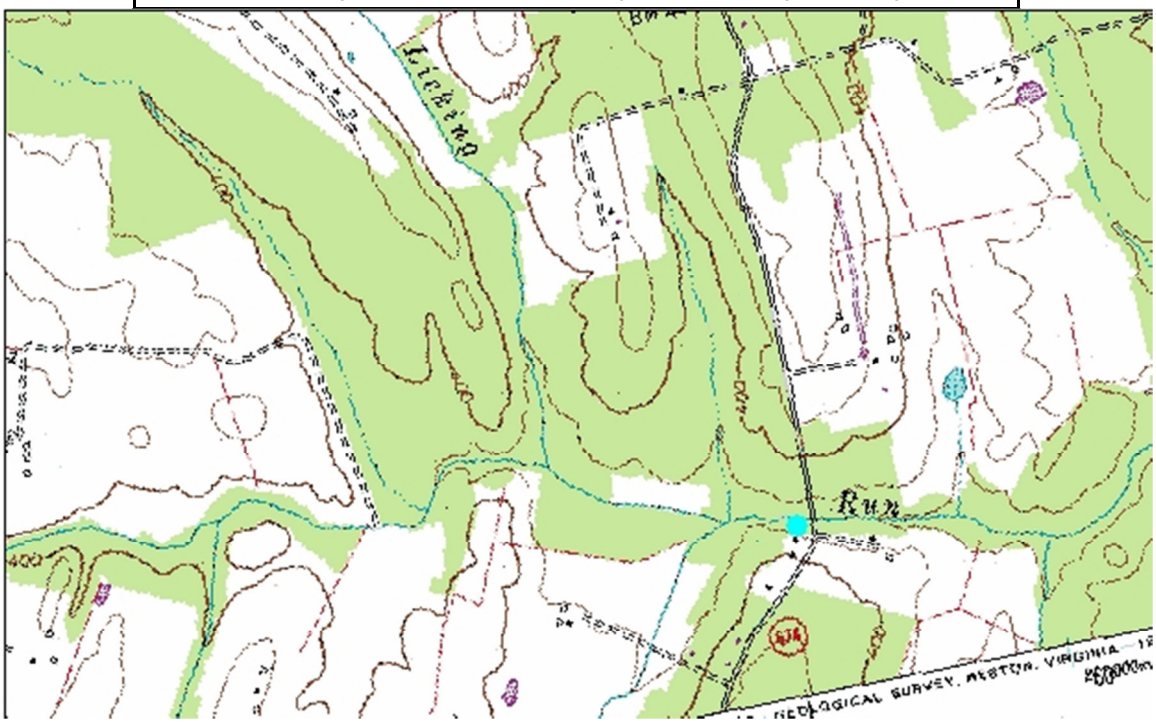

| Sample Site | **POT-31** | Sampler **Charles Trodick** | | Stream Name | **Slate Run** |
|---|---|---|---|---|---|
| Elevation | | Latitude | **38.668758** | Longitude | **-77.537427** |
| Description | | | | | |
| **Downstream from Fleetwood Bridge. Surrounded by farmland. Mainly shale point bar in middle of stream.** | | | | | |

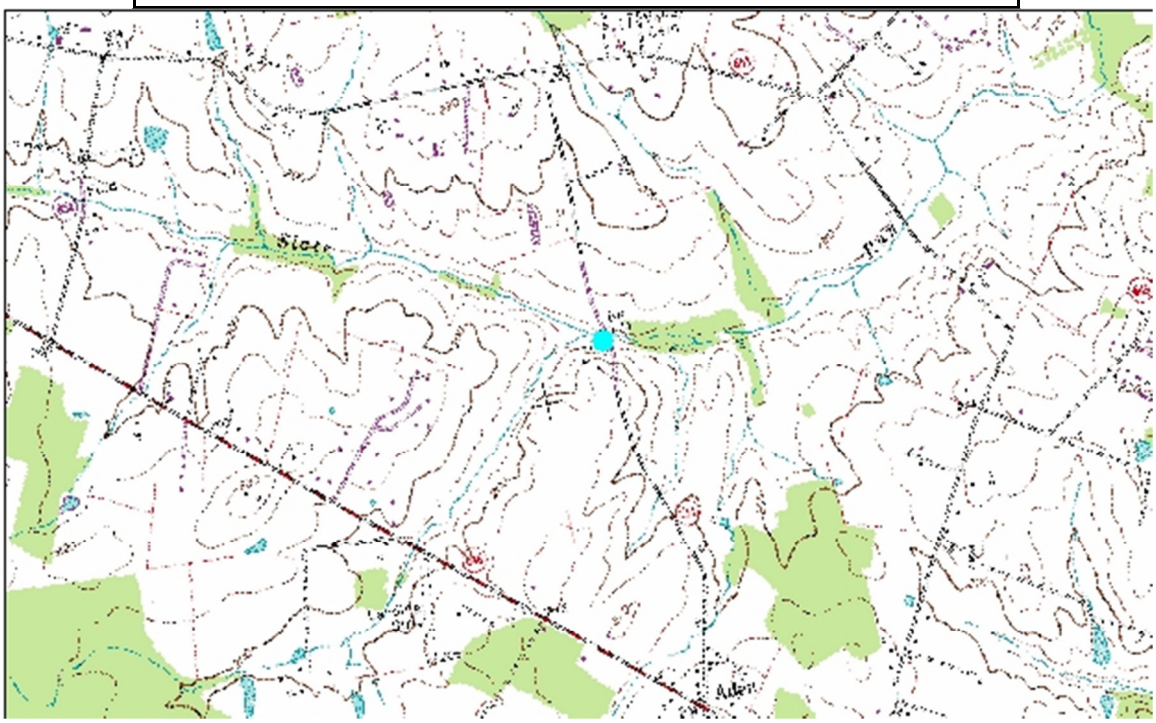

| Sample Site | **POT-32** | Sampler **Charles Trodick** | | Stream Name | **Powell's Creek** |
|---|---|---|---|---|---|
| Elevation | | Latitude | **38.61744** | Longitude | **-77.372117** |
| Description | | | | | |
| **Just downstream from Spriggs Road Bridge. Upstream from Mont Clare Lake. New construction everywhere. Samples from forested area. Parked in circle near stream. Walked 1/4 mile to stream.** | | | | | |

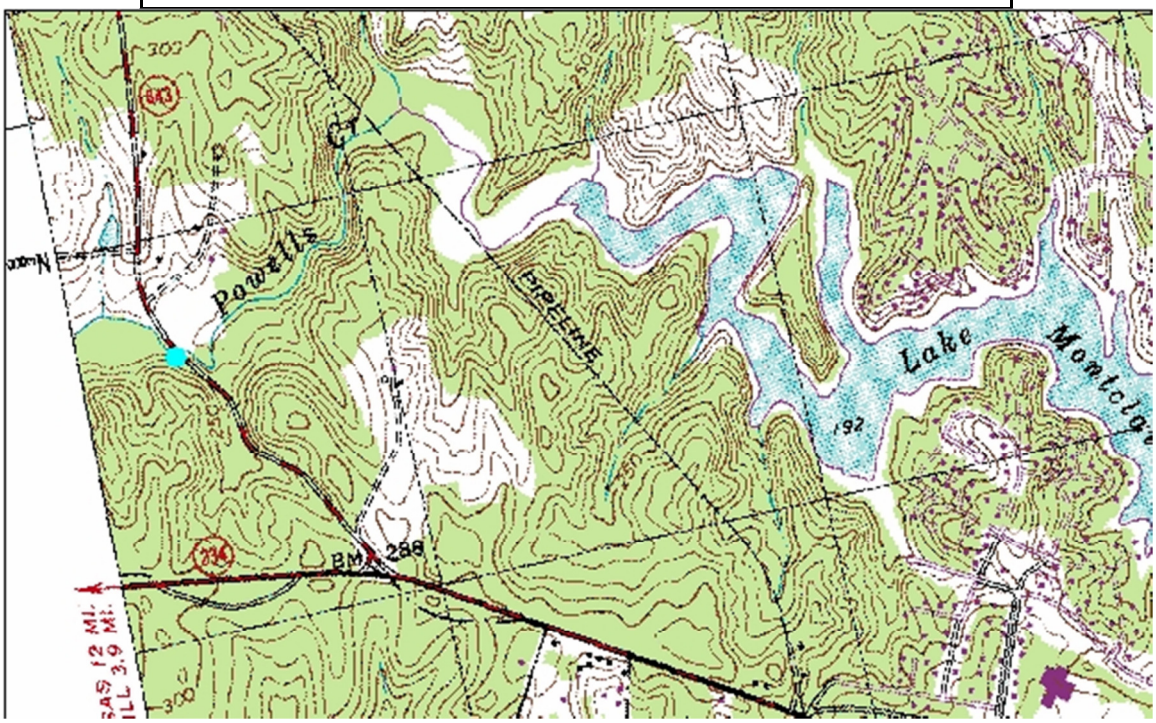

| Sample Site | **POT-33** | Sampler **Charles Trodick** | | Stream Name | **Popes Head Creek** |
|---|---|---|---|---|---|
| Elevation | | Latitude | **38.781789** | Longitude | **-77.387953** |
| Description | | | | | |
| **Just off a bridge on Newhaven Road. Upstream at small beach, kind of in a person's backyard. Path on bank. Forested residential area.** | | | | | |

| Sample Site | **POT-34** | Sampler **Charles Trodick** | | Stream Name | **Head Creek East Fork** |
|---|---|---|---|---|---|
| Elevation | | Latitude | **38.797979** | Longitude | **-77.351861** |
| Description | | | | | |
| **Off Fairfax Station Road. Upstream from bridge. Forested residential area. Just down a small terrace.** | | | | | |

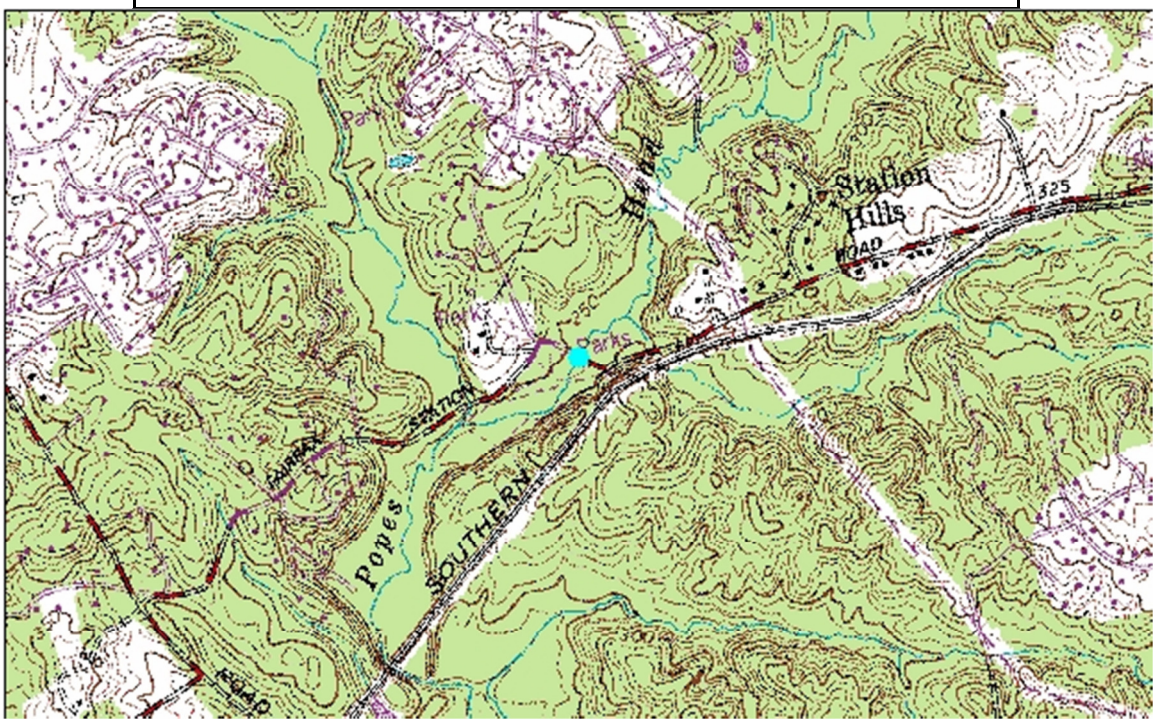

| Sample Site | **POT-35** | Sampler **Charles Trodick** | | Stream Name | **Lenah Run** |
|---|---|---|---|---|---|
| Elevation | | Latitude | **38.959309** | Longitude | **-77.538328** |
| Description | | | | | |
| **Upstream from bridge on Belmont Ridge Road. Shale stream. Sampled from underwater bar on south side of stream, upstream from small confluence.** | | | | | |

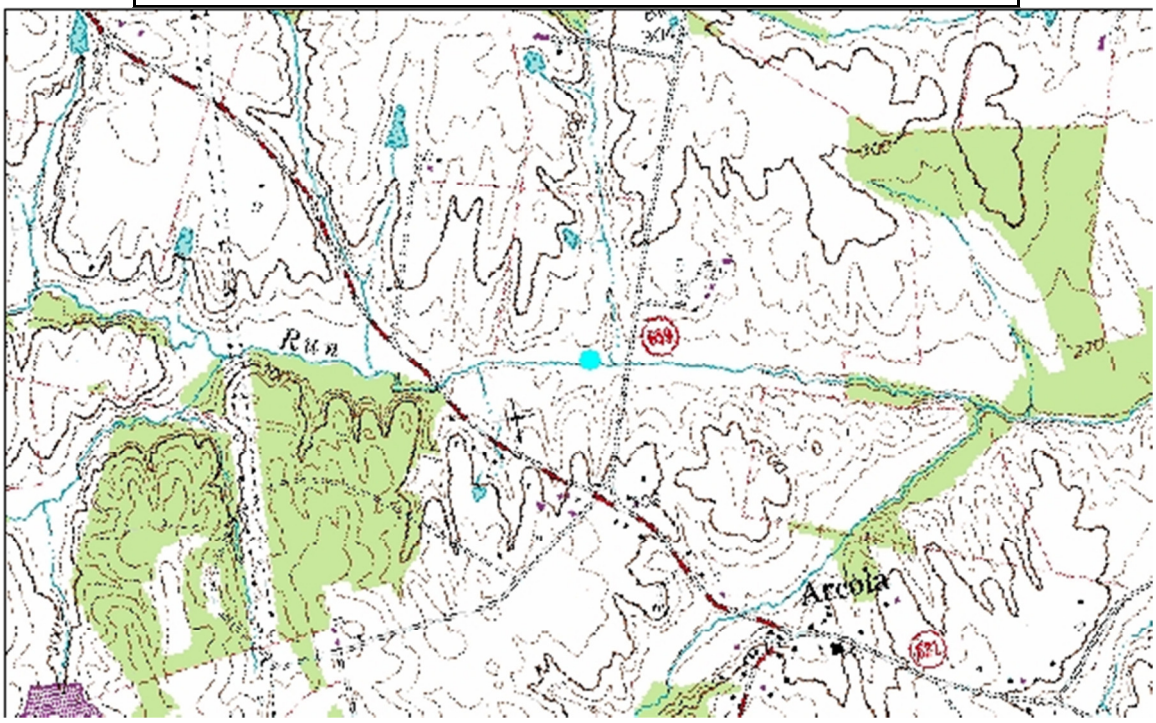

| Sample Site | **POT-36** | Sampler **Charles Trodick** | | Stream Name | **Little Creek** |
|---|---|---|---|---|---|
| Elevation | | Latitude | **38.950832** | Longitude | **-77.71956** |
| Description | | | | | |
| **Just upstream from Landmark School Road. Sample taken from sand bar across stream from old mill. Forested area near vineyards and small town, Middleburg.** | | | | | |

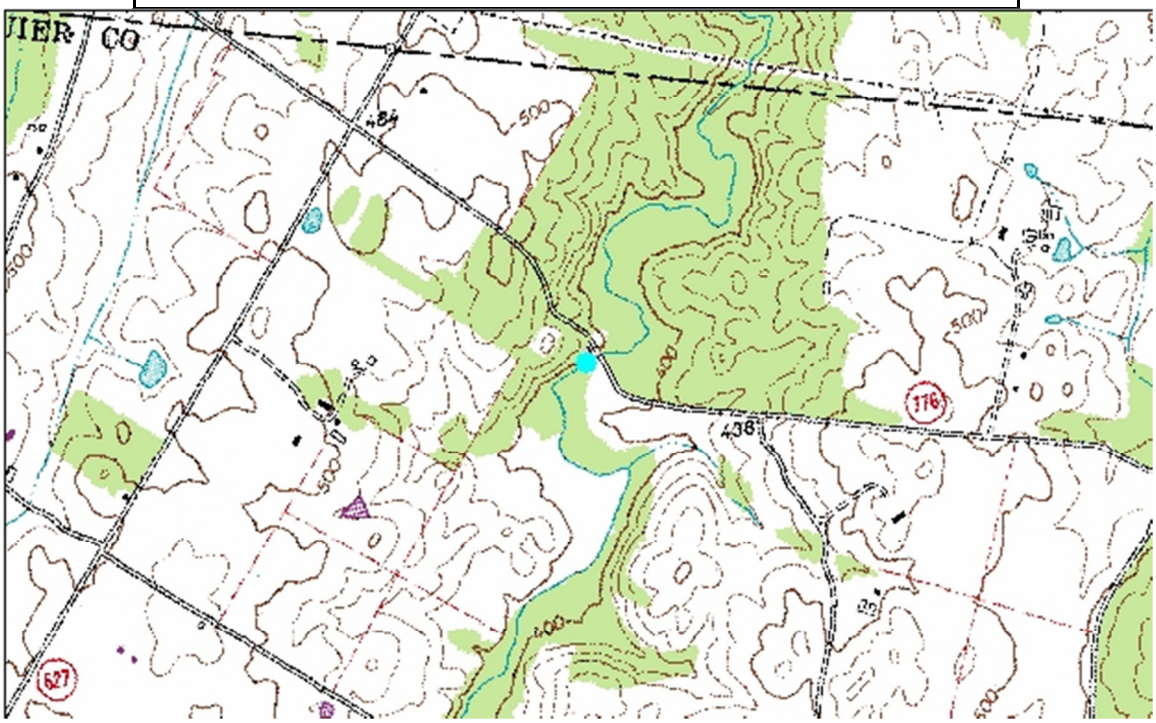

| Sample Site | **POT-37** | Sampler **Charles Trodick** | | Stream Name | **North Fork Beaver Dam Creek** |
|---|---|---|---|---|---|
| Elevation | | Latitude | **39.061616** | Longitude | **-77.754321** |
| Description | | | | | |
| **Just upstream from St. Louis Road Bridge. Stream is all coarse to fine sand. Surrounded by farms and a few trees.** | | | | | |

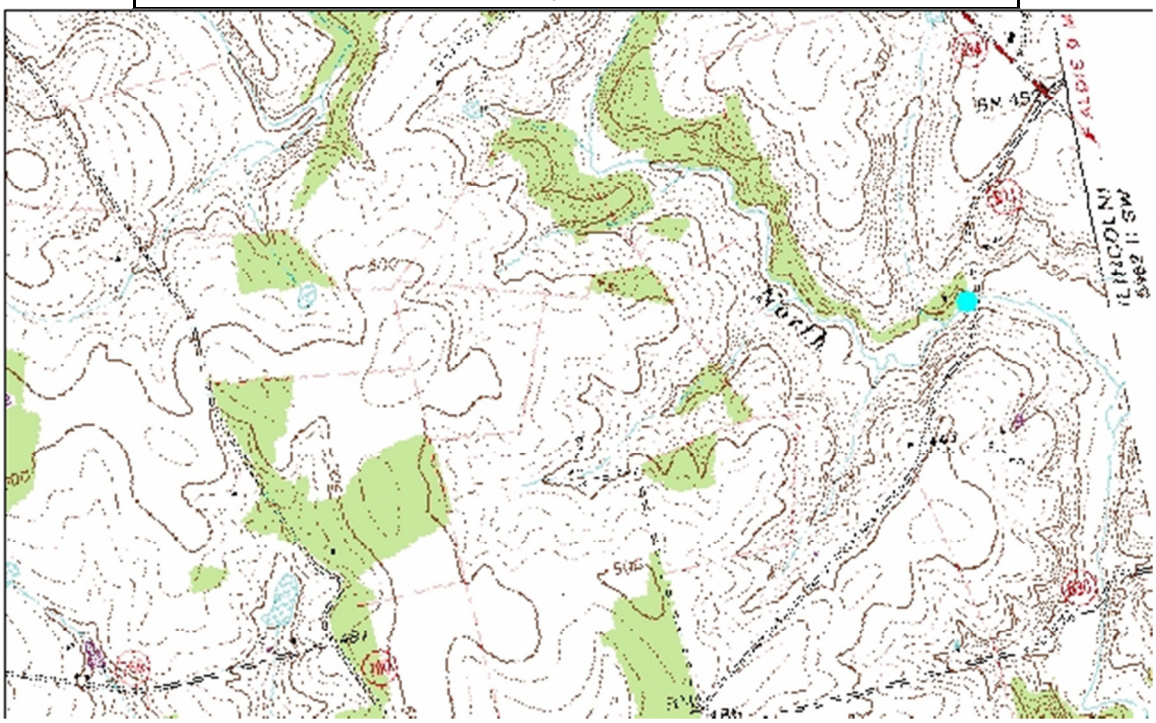

| Sample Site | **POT-38** | Sampler **Charles Trodick** | | Stream Name | **Opequon Creek** |
|---|---|---|---|---|---|
| Elevation | | Latitude | **39.082839** | Longitude | **-78.126397** |
| Description | | | | | |
| **Where Armel Road turns to Crismere Road. Upstream from bridge. Sample from point bar nearly under bridge. Border between Frederick and Clarke County. Hard sampling. Coarse bedded shale.** | | | | | |

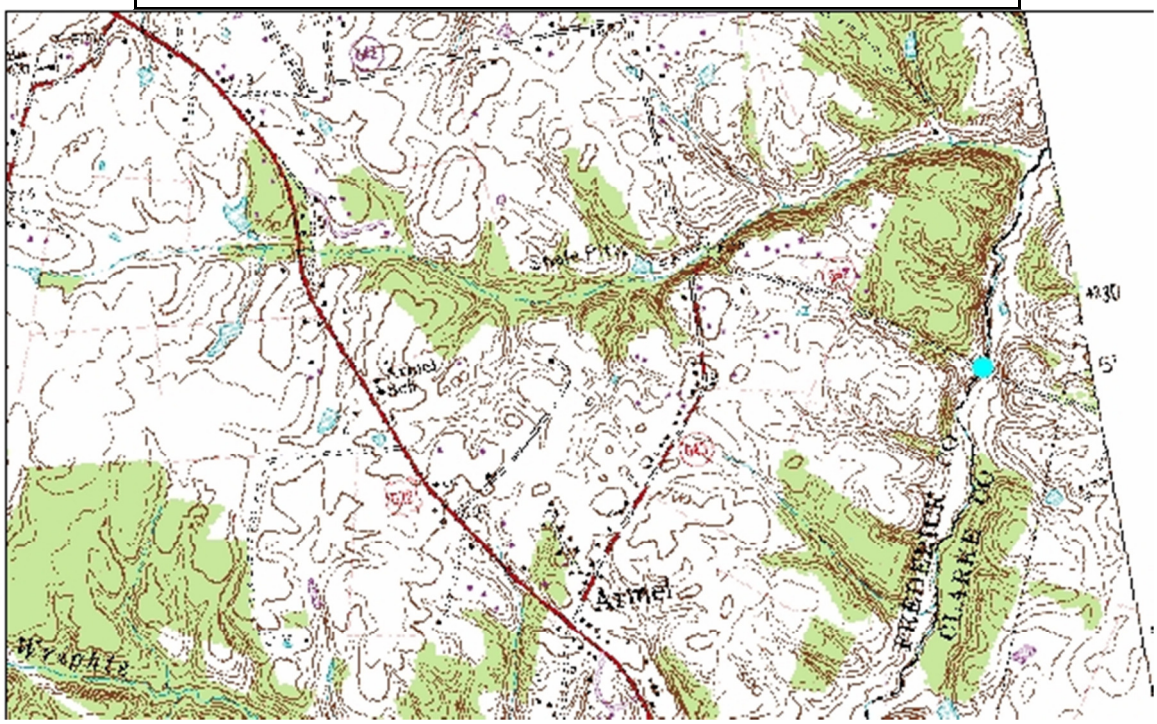

| Sample Site | **POT-39** | Sampler **Charles Trodick** | | Stream Name | **Howellsville Branch** |
|---|---|---|---|---|---|
| Elevation | | Latitude | **38.973523** | Longitude | **-78.082023** |
| Description | | | | | |
| **Bridge on Howellsville road. Downstream from bridge. Mainly coarse gravel and sand. Plenty of quartz. 40 feet from bridge. Surrounded by trees, nearby farm.** | | | | | |

| Sample Site | **POT-40** | Sampler **Charles Trodick** | | Stream Name | |
|---|---|---|---|---|---|
| Elevation | | Latitude | **38.735808** | Longitude | **-78.530574** |
| Description | | | | | |
| **Sampled where Moreland gap road bridge crosses stream. Sampled upstream and under bridge. Wooded area with some residential. Easy sample.** | | | | | |

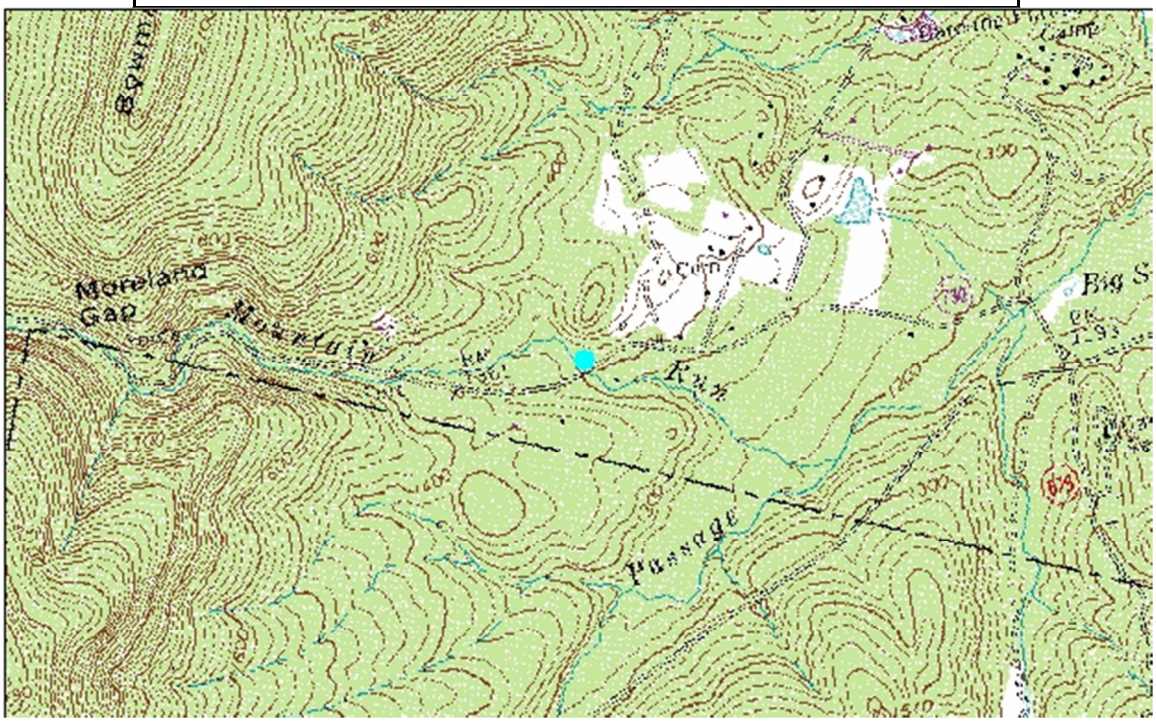

| Sample Site | **POT-41** | Sampler **Charles Trodick** | | Stream Name | **Hawksbill Creek** |
|---|---|---|---|---|---|
| Elevation | | Latitude | **38.347143** | Longitude | **-78.612027** |
| Description | | | | | |
| **Sample taken from under Beldor Road Bridge in a pocket of coarse sand. Stream is mainly bedrock. Surrounded by farmland. Bridge is one lane.** | | | | | |

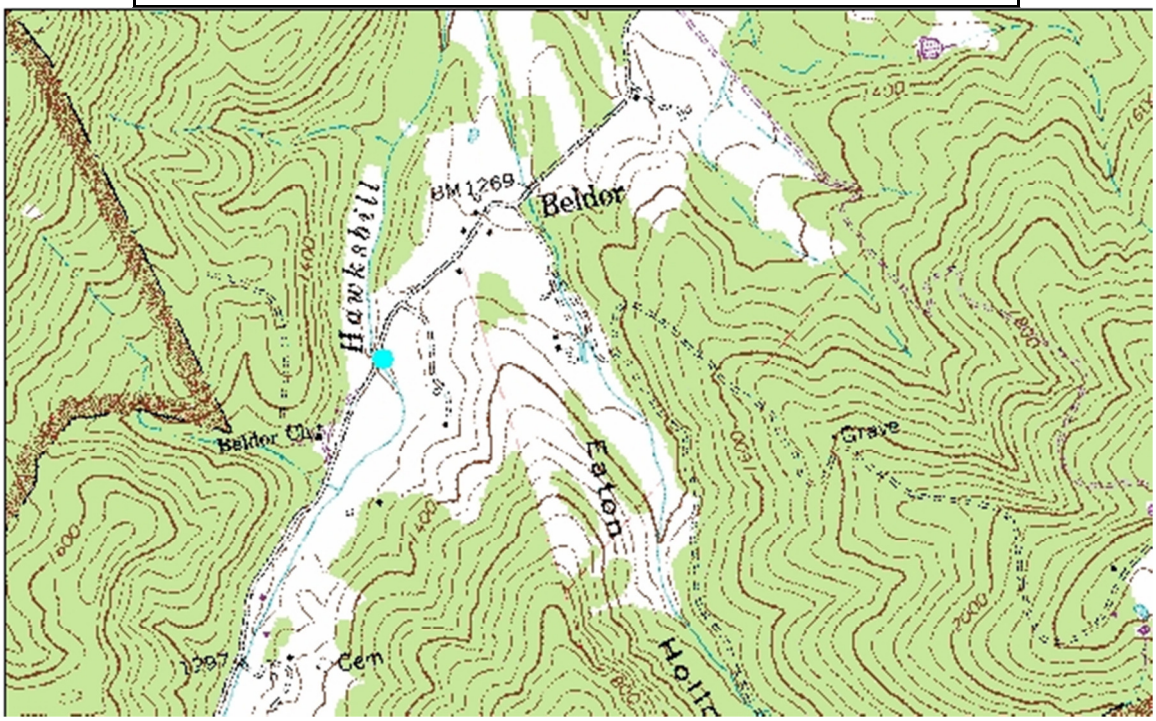

| Sample Site | **POT-42** | Sampler **Charles Trodick** | | Stream Name | |
|---|---|---|---|---|---|
| Elevation | | Latitude | **38.250988** | Longitude | **-78.892007** |
| Description | | | | | |
| **Sample taken under bridge for 900 VA near Shenandoah Airport. Stream coarse sand and gravel with mud matrix. Hard to sample. Airport and farm near stream.** | | | | | |

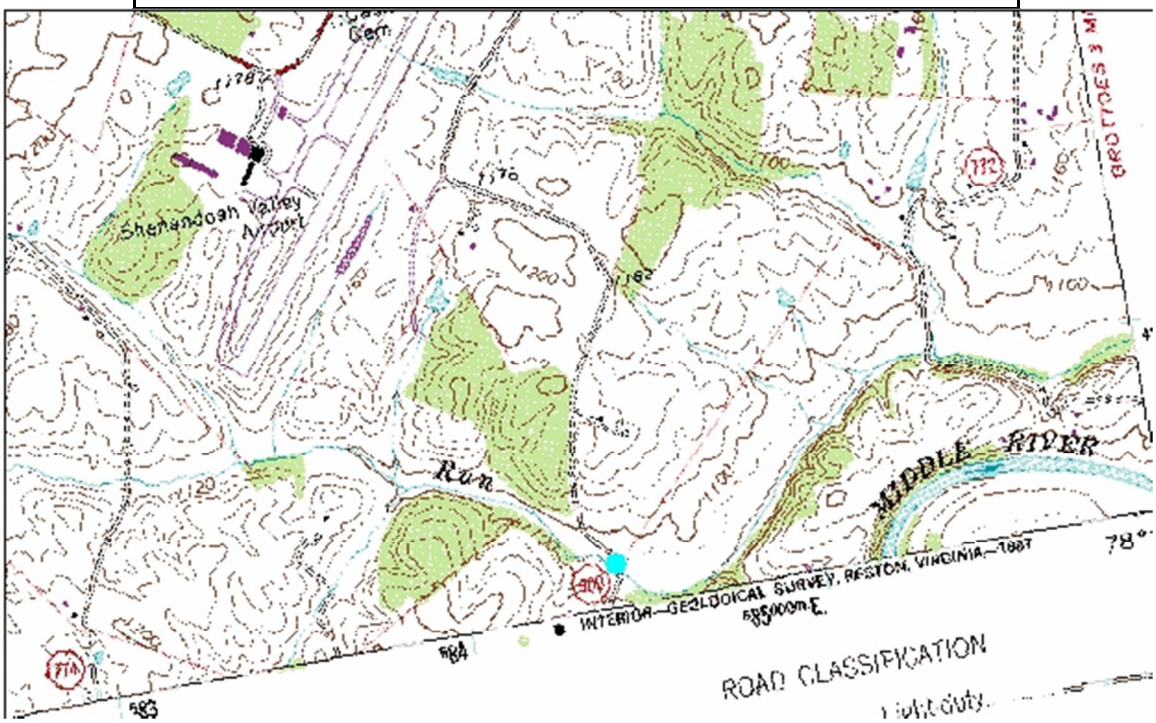

| Sample Site | **POT-43** | Sampler **Charles Trodick** | | Stream Name | **Sawmill Run** |
|---|---|---|---|---|---|
| Elevation | | Latitude | **38.101435** | Longitude | **-78.860335** |
| Description | | | | | |
| **Sampled near 340 parked on Al Gore Road at East Side Speedway. Stream is bedrock and sandstone. Sampled from a pocket of sand on far side.** | | | | | |

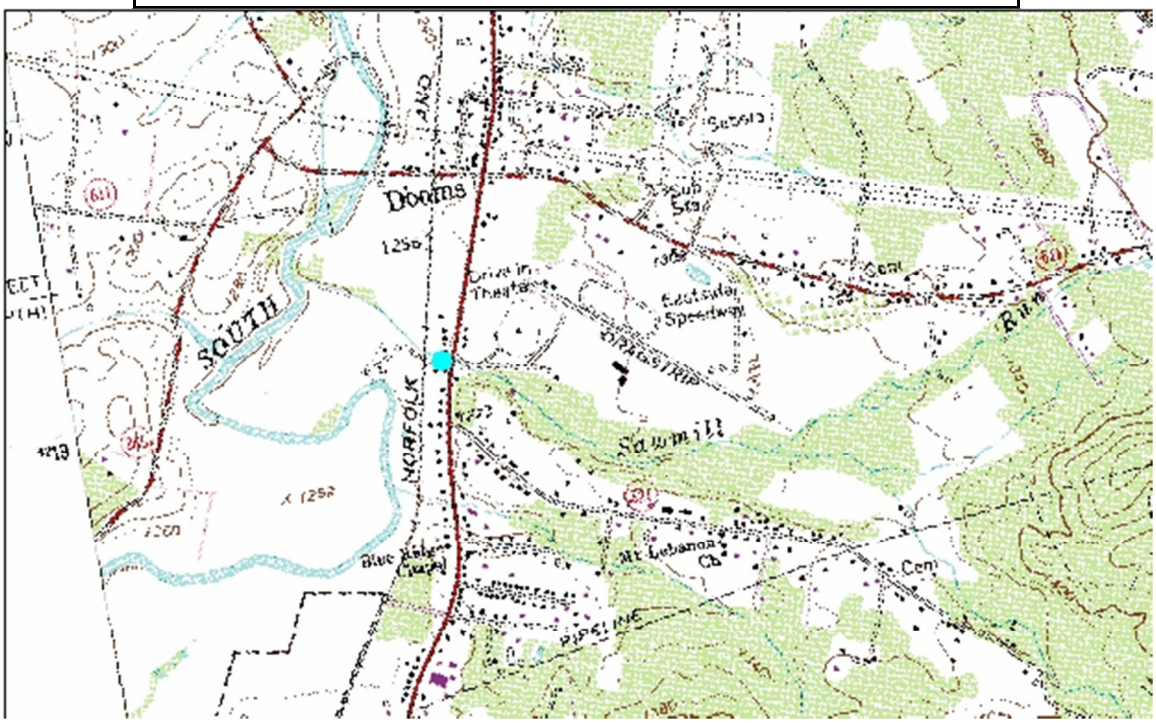

| Sample Site | **POT-44** | Sampler **Charles Trodick** | | Stream Name | **Back Creek** |
|---|---|---|---|---|---|
| Elevation | | Latitude | **37.940339** | Longitude | **-78.968182** |
| Description | | | | | |
| **Just upstream from VA 664 bridge. Sample taken from pockets of fine sand all around stream. Surrounded by farms and a few trees. Steam mainly coarse gravel.** | | | | | |

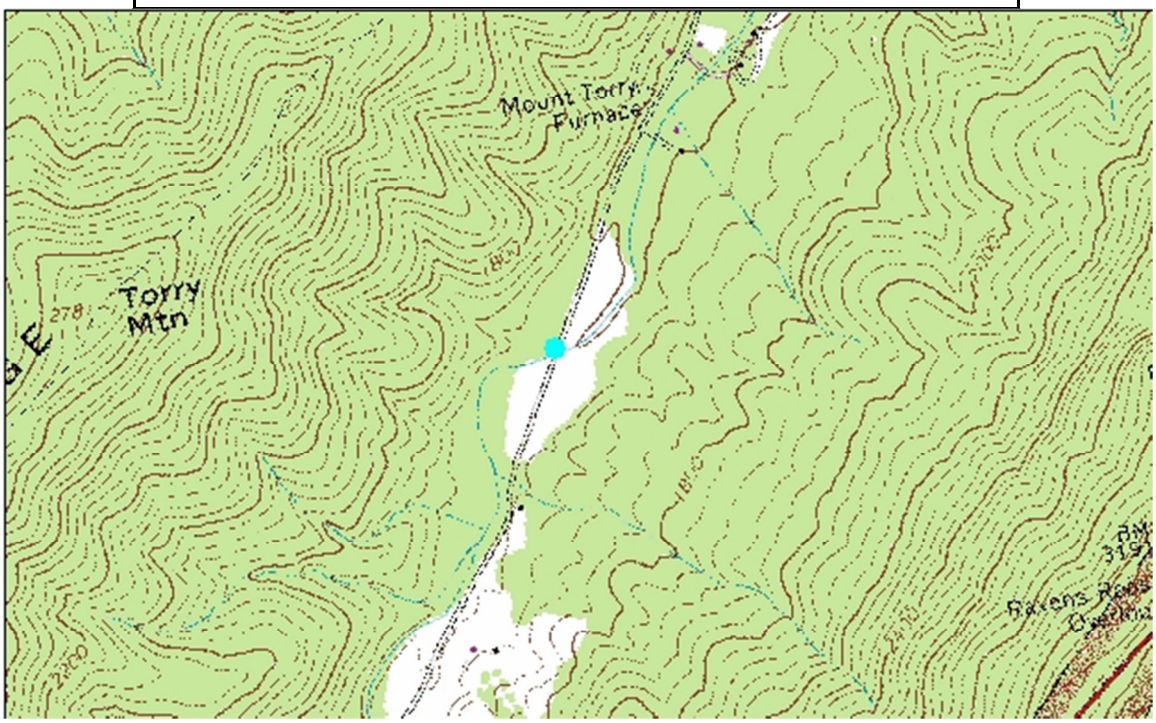

| Sample Site | **POT-45** | Sampler **Charles Trodick** | | Stream Name | **Skidmore Fork** |
|---|---|---|---|---|---|
| Elevation | | Latitude | **38.558167** | Longitude | **-79.152031** |
| Description | | | | | |
| **Sample taken from pockets on each downstream side of ford for FR227. Just upstream from reservoir. Valley, forested area. Gravel, boulder stream.** | | | | | |

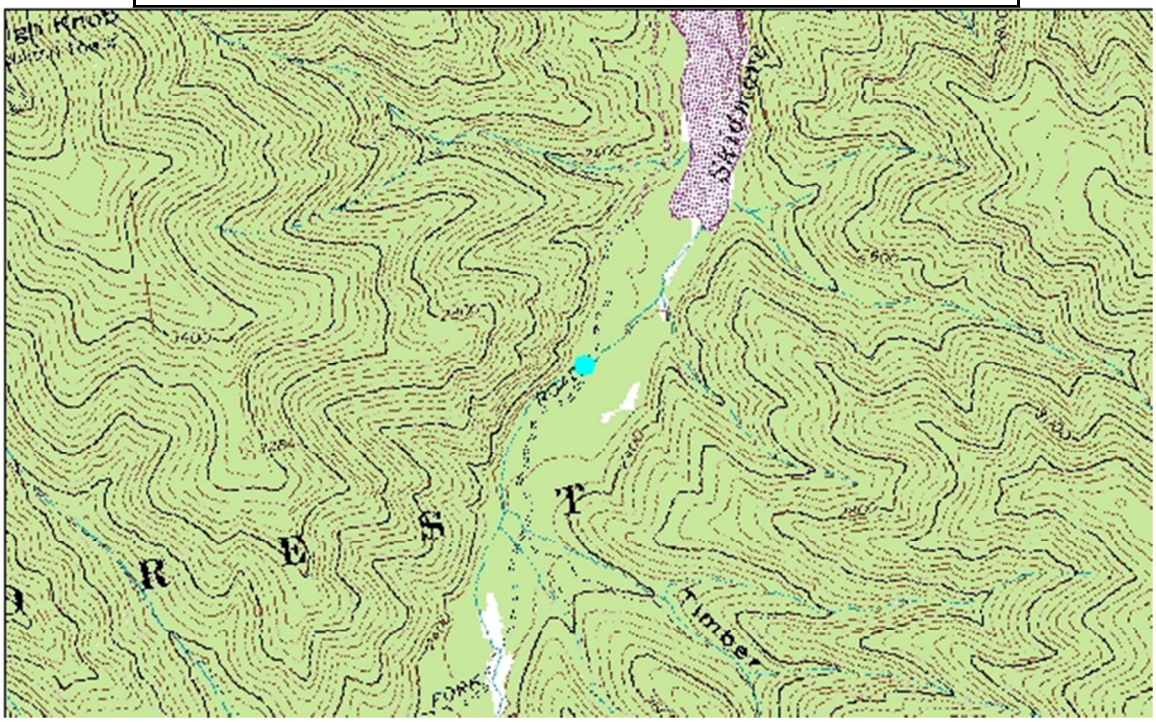

| Sample Site | **POT-46** | Sampler **Charles Trodick** | | Stream Name | **Laurel Fork** |
|---|---|---|---|---|---|
| Elevation | | Latitude | **38.492563** | Longitude | **-79.665341** |
| Description | | | | | |
| **Sample taken downstream from bridge and confluence. Turned on to FR54. Sample at 1' by 1' island. Boulder stream. Good Sand. Use GPS.** | | | | | |

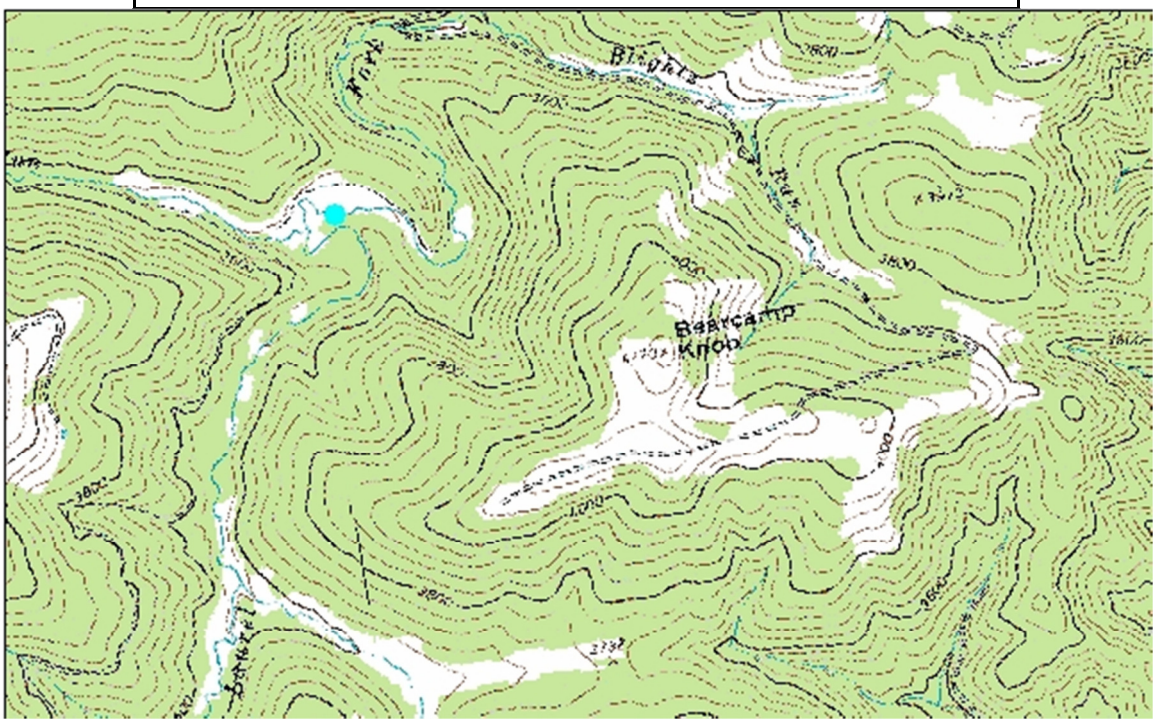

| Sample Site | **POT-47** | Sampler **Charles Trodick** | | Stream Name | **Crab Run** |
|---|---|---|---|---|---|
| Elevation | | Latitude | **38.809617** | Longitude | **-78.945694** |
| Description | | | | | |
| **Sampled under bridge on East Side of Crab Run Road. Mainly coarse sand and gravel. Talked to local who has lived on creek for 34 years. He said stream 22 years ago was deep enough to swim in. Now mostly ankle deep. Change occurred when chicken coops moved in. Also, the river floods more, about once a year, causing a large amount of erosion, much more than has occurred in the past.** | | | | | |

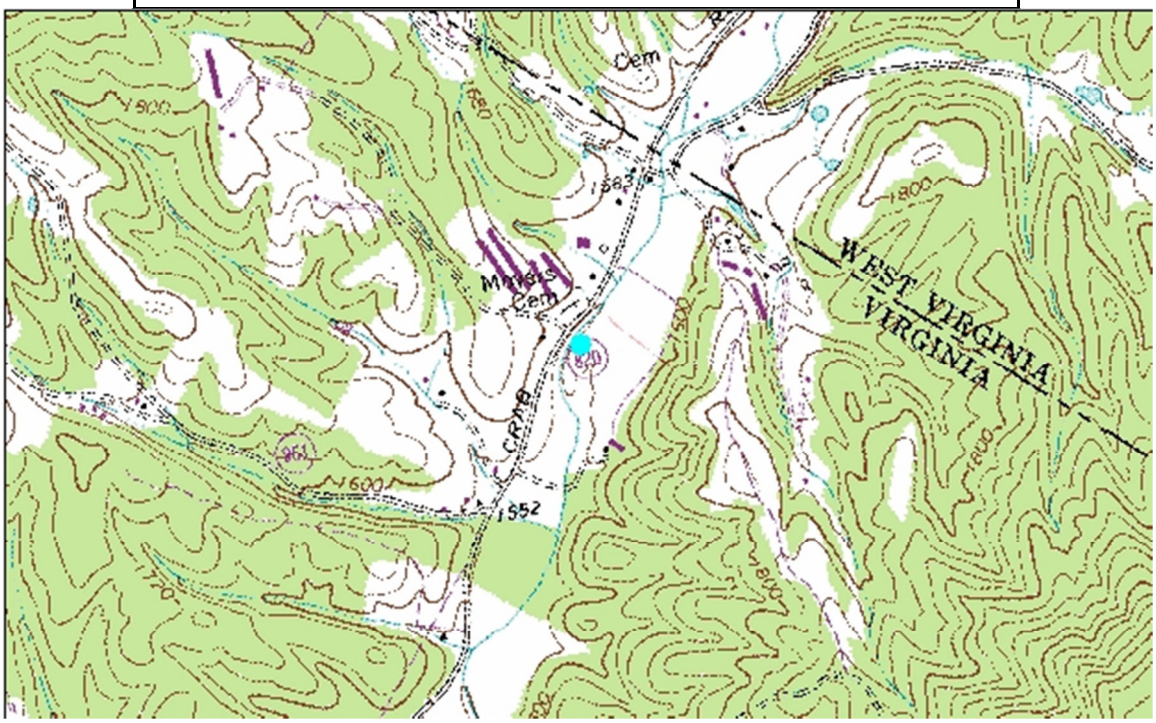

| Sample Site | **POT-48** | Sampler **Charles Trodick** | | Stream Name | **Dumpling Run** |
|---|---|---|---|---|---|
| Elevation | | Latitude | **39.070046** | Longitude | **-78.957539** |
| Description | | | | | |
| **Sampled just downstream from 55 bridge. Stream mainly gravel and coarse sand. Sampled from sand bar on east side of stream. Sampled in a small town.** | | | | | |

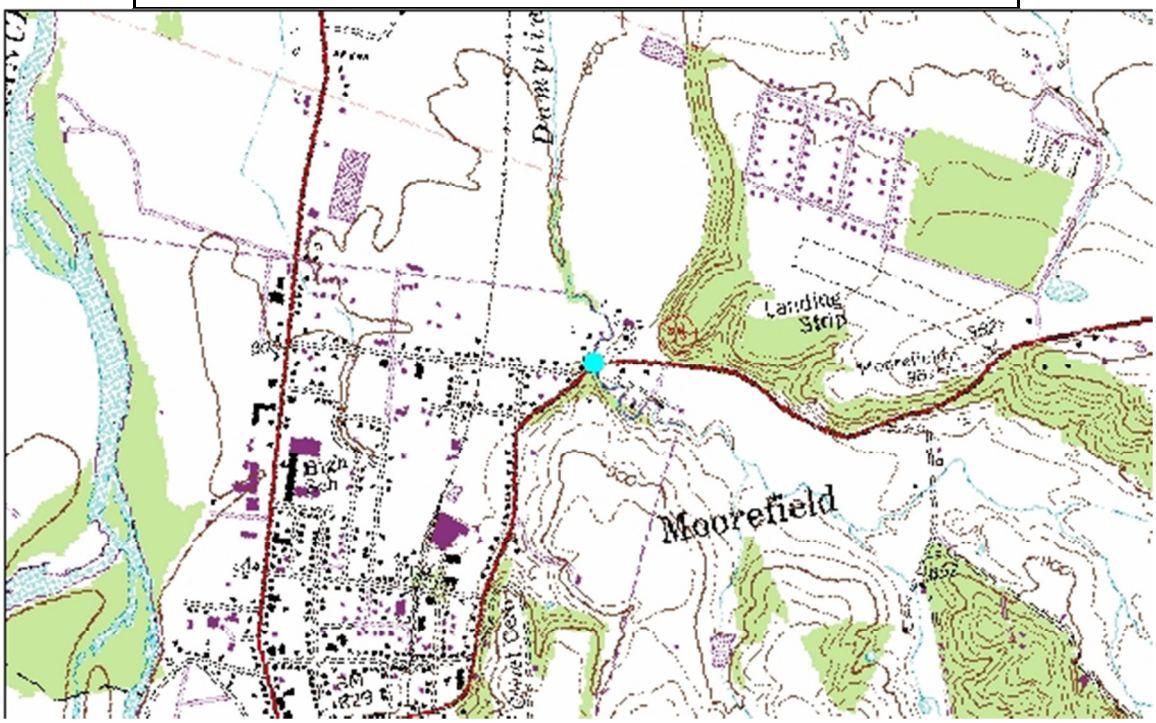

| Sample Site | **POT-49** | Sampler **Charles Trodick** | | Stream Name | **North River** |
|---|---|---|---|---|---|
| Elevation | | Latitude | **39.13735** | Longitude | **-78.771715** |
| Description | | | | | |
| **Sample taken downstream from bridge on North River Road. Stream in mainly forest with light residential. Stream mainly sandstone gravel and boulders, some bedrock. Sample taken from fine sand pocket north bank of stream.** | | | | | |

| Sample Site | **POT-50** | Sampler **Charles Trodick** | | Stream Name | **Roaring Creek** |
|---|---|---|---|---|---|
| Elevation | | Latitude | **38.889463** | Longitude | **-79.403086** |
| Description | | | | | |
| **Sampled at Y in Roaring Creek Road, just downstream of ford. Creek is mainly bedrock and boulders. Samples came from coarse sand pockets on east side of stream.** | | | | | |

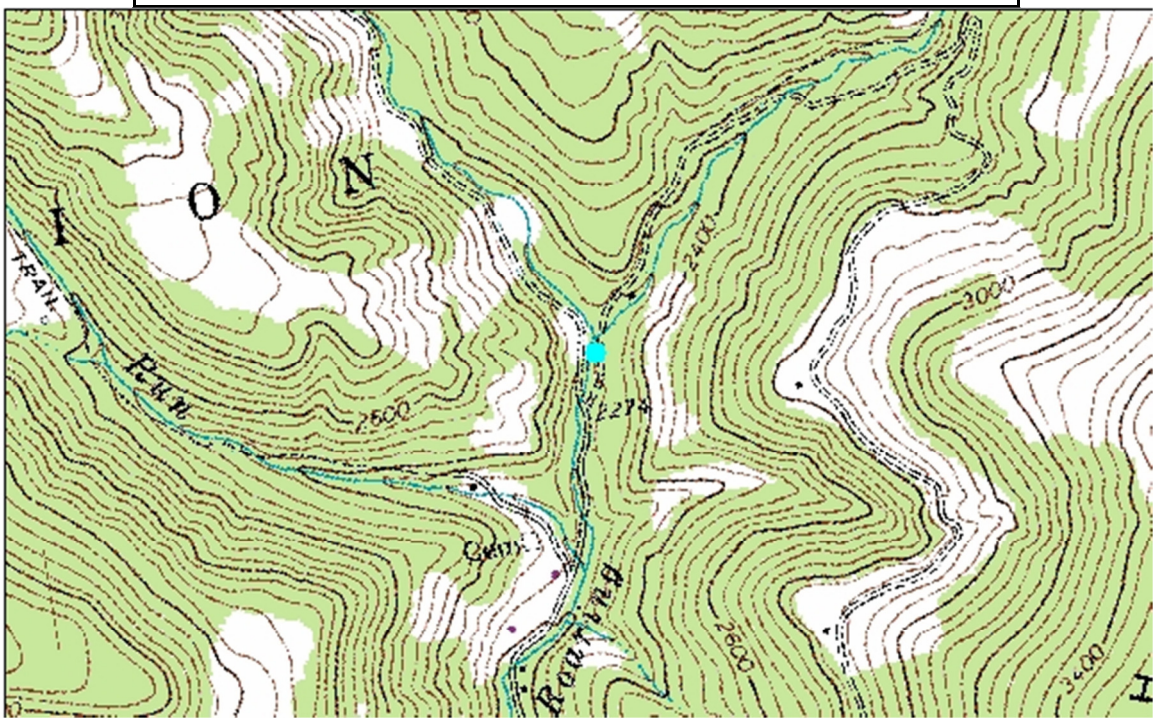

| Sample Site | **POT-51** | Sampler **Charles Trodick** | | Stream Name | **Laural Run** |
|---|---|---|---|---|---|
| Elevation | | Latitude | **39.237272** | Longitude | **-79.449005** |
| Description | | | | | |
| **Sampled just upstream from Kempton Road Bridge at little sand and gravel bar on south side of stream. Land was mainly forested with some agriculture. Logging was occurring in the area. Stream was a light tan color possibly indicating logging effects.** | | | | | |

| Sample Site | **POT-52** | Sampler **Charles Trodick** | | Stream Name | **Laural Run** |
|---|---|---|---|---|---|
| Elevation | | Latitude | **39.348403** | Longitude | **-79.285069** |
| Description | | | | | |
| **Sample taken at edge of Potomac State Forest, sample taken upstream of Audley Riley Bridge. North side sand and gravel bar. All forested area.** | | | | | |

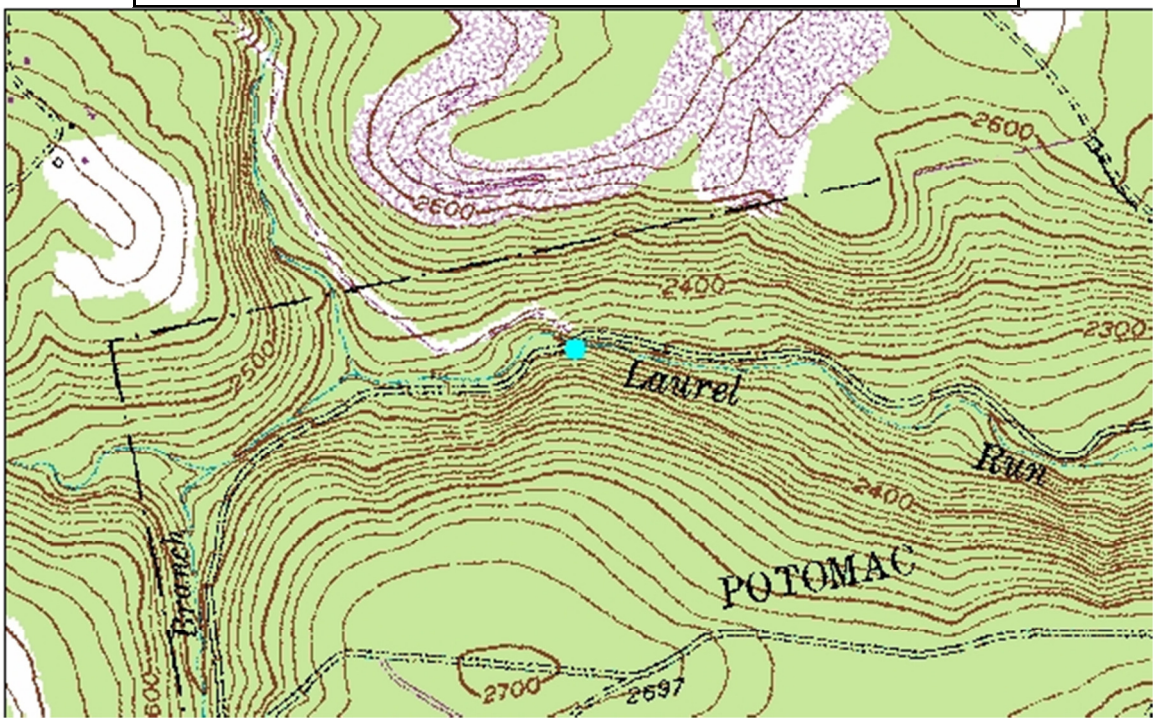

| Sample Site | **POT-53** | Sampler **Charles Trodick** | | Stream Name | **Deep Run Cranberry Run** |
|---|---|---|---|---|---|
| Elevation | | Latitude | **39.398563** | Longitude | **-79.133406** |
| Description | | | | | |
| **Sampled just off WV 46, downstream of bridge for small road. Sampled sand/gravel bar on north side. Mostly forest with light residential.** | | | | | |

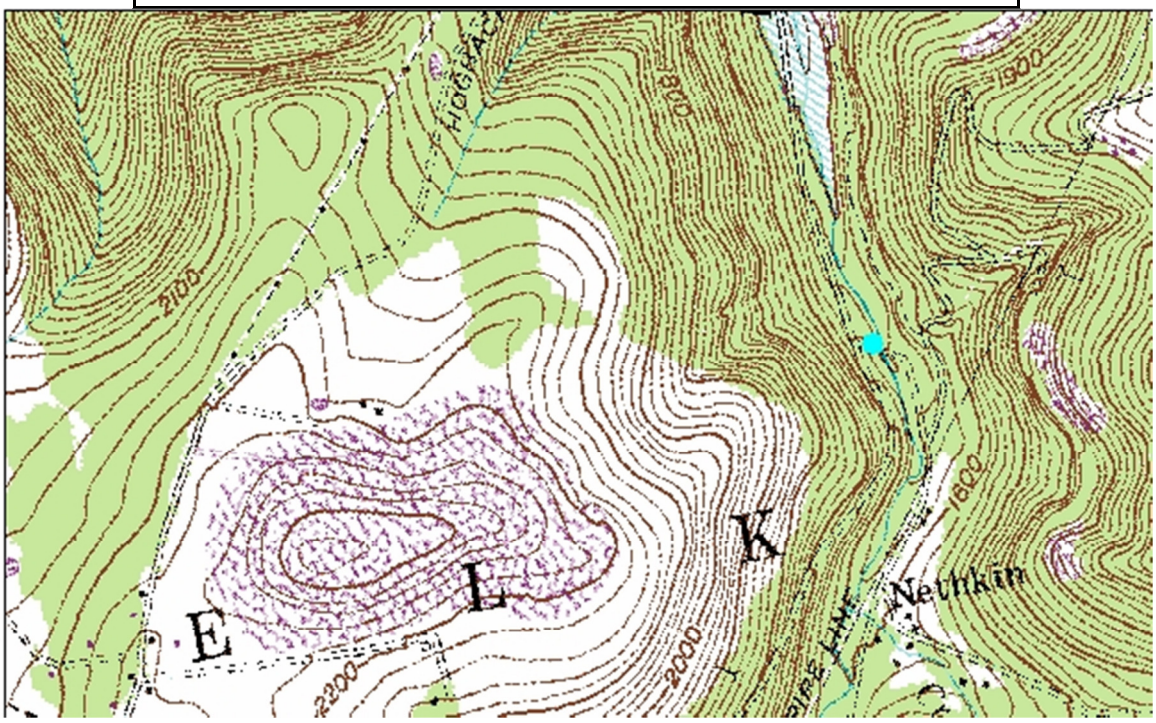

| Sample Site | **POT-54** | Sampler **Charles Trodick** | | Stream Name | **Reinhardt Run** |
|---|---|---|---|---|---|
| Elevation | | Latitude | **39.455182** | Longitude | **-78.804073** |
| Description | | | | | |
| **Sampled under bridge for CR 46-114 in pocket of sand. Most of stream was gravel shale. Agriculture with forest up stream. Fossils in shale.** | | | | | |

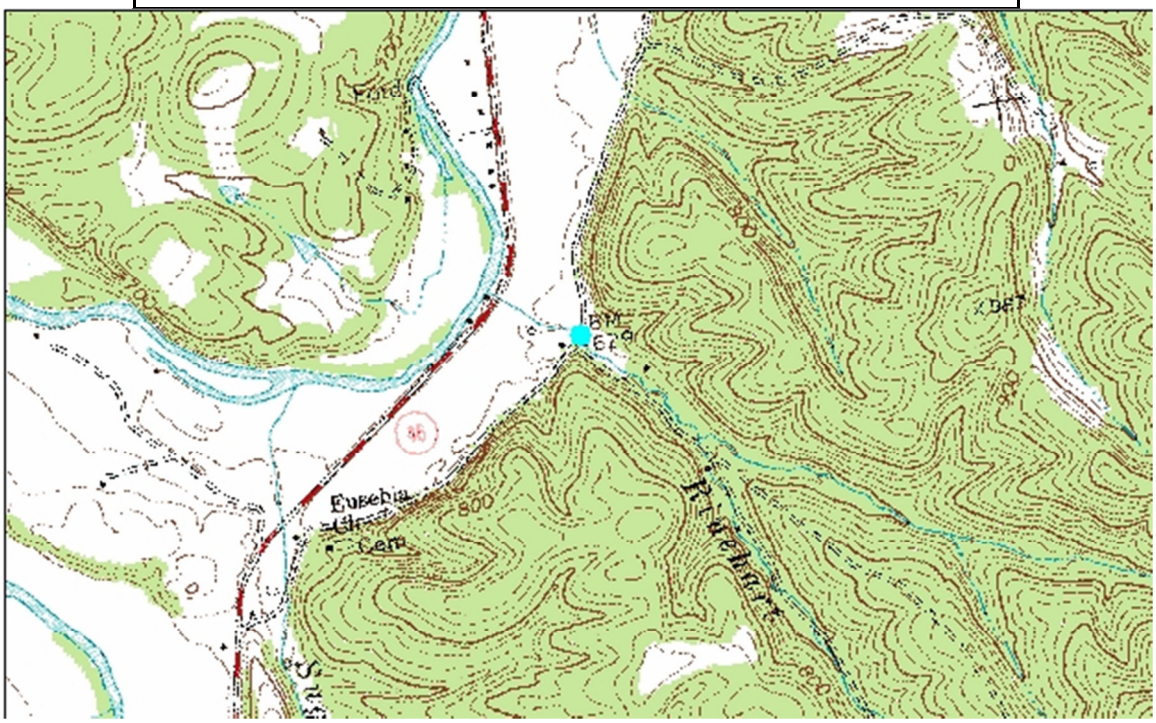

| Sample Site | **POT-55** | Sampler **Charles Trodick** | | Stream Name | **Crabtree Creek** |
|---|---|---|---|---|---|
| Elevation | | Latitude | **39.457833** | Longitude | **-79.228077** |
| Description | | | | | |
| **Sampled under Swanton Road Bridge. Large sand deposit. In very small town (kid). Mainly shale gravel.** | | | | | |

| Sample Site | **POT-56** | Sampler **Charles Trodick** | | Stream Name | **Middle Fork** |
|---|---|---|---|---|---|
| Elevation | | Latitude | **39.513378** | Longitude | **-79.154863** |
| Description | | | | | |
| **Sampled upstream from Savage River Road Bridge and Savage River Reservoir. Bedrock stream with boulders. Sampled sand pocket behind a large rock on east side of stream.** | | | | | |

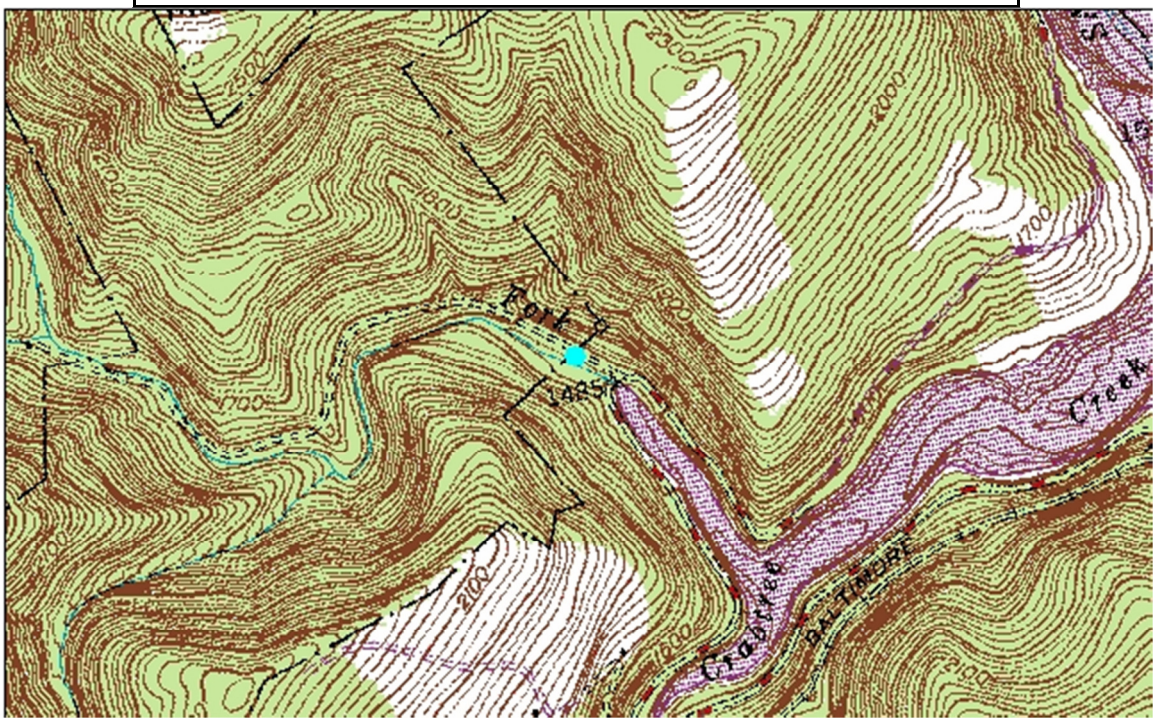

| Sample Site | **POT-57** | Sampler **Charles Trodick** | | Stream Name | **Blacklick Run** |
|---|---|---|---|---|---|
| Elevation | | Latitude | **39.603374** | Longitude | **-79.079118** |
| Description | | | | | |
| **Sampled just upstream from Westernport Road off of a small gravel road in front of a house. Stream is mainly gravel and boulders. Sampled from a pocket of sand on west side. Area mainly agriculture with some forest.** | | | | | |

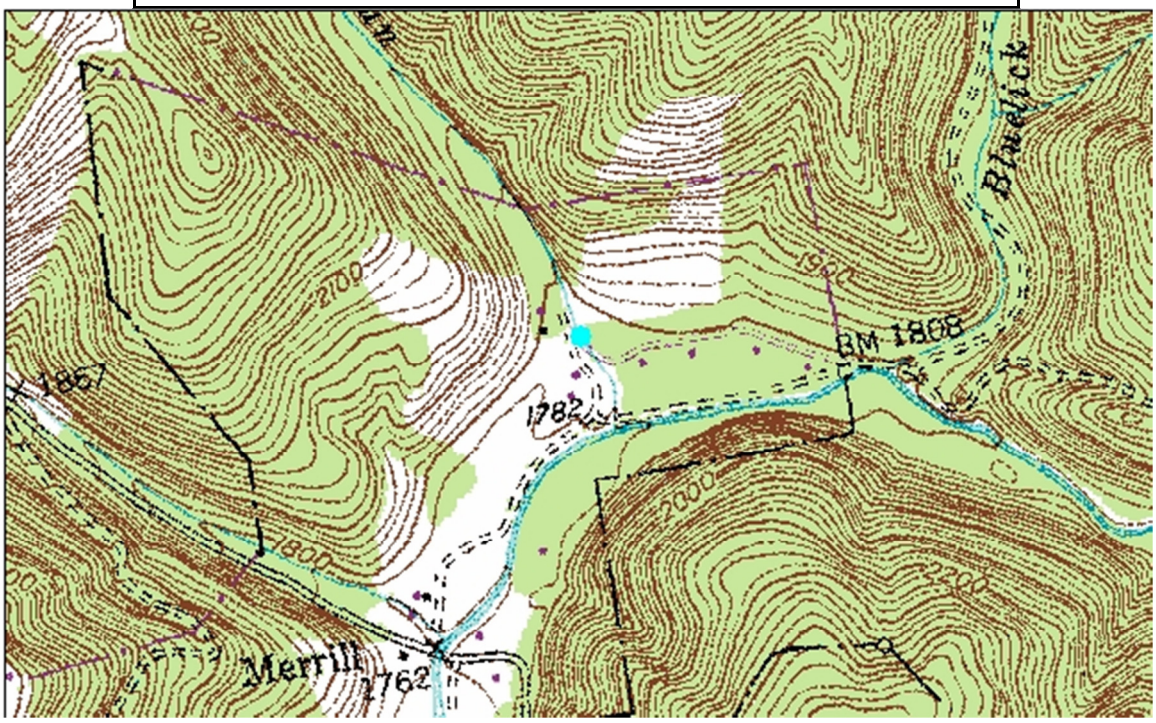

| Sample Site | **POT-58** | Sampler **Charles Trodick** | | Stream Name | **George's Creek** |
|---|---|---|---|---|---|
| Elevation | | Latitude | **39.565669** | Longitude | **-78.97994** |
| Description | | | | | |
| **Sampled stream just east of MD 36. Mainly gravel and boulder stream sampled under bridge. Lot of organics in stream. Sampled in small town Lonaconing.** | | | | | |

| Sample Site | **POT-59** | Sampler **Charles Trodick** | | Stream Name | **Willis Creek** |
|---|---|---|---|---|---|
| Elevation | | Latitude | **39.819052** | Longitude | **-78.937583** |
| Description | | | | | |
| **Sample under Gameland Road Bridge just off Witt Road. Stream is mostly gravel. Sample taken at fine sand and mud bank. Taken in forested light residential area.** | | | | | |

| Sample Site | **POT-60** | Sampler **Charles Trodick** | | Stream Name | |
|---|---|---|---|---|---|
| Elevation | | Latitude | **39.905885** | Longitude | **-78.835487** |
| Description | | | | | |
| **Sampled under bridge for SR2017 at sand bar under bridge. Stream is mainly gravel surrounded by farms.** | | | | | |

| Sample Site | **POT-61** | Sampler **Charles Trodick** | | Stream Name | **Sand Spring Run** |
|---|---|---|---|---|---|
| Elevation | | Latitude | **39.893341** | Longitude | **-78.601899** |
| Description | | | | | |
| **Sample taken just downstream from 220 bridge. Light residential area. Gravel stream. Found quartz sand bars on north side of stream.** | | | | | |

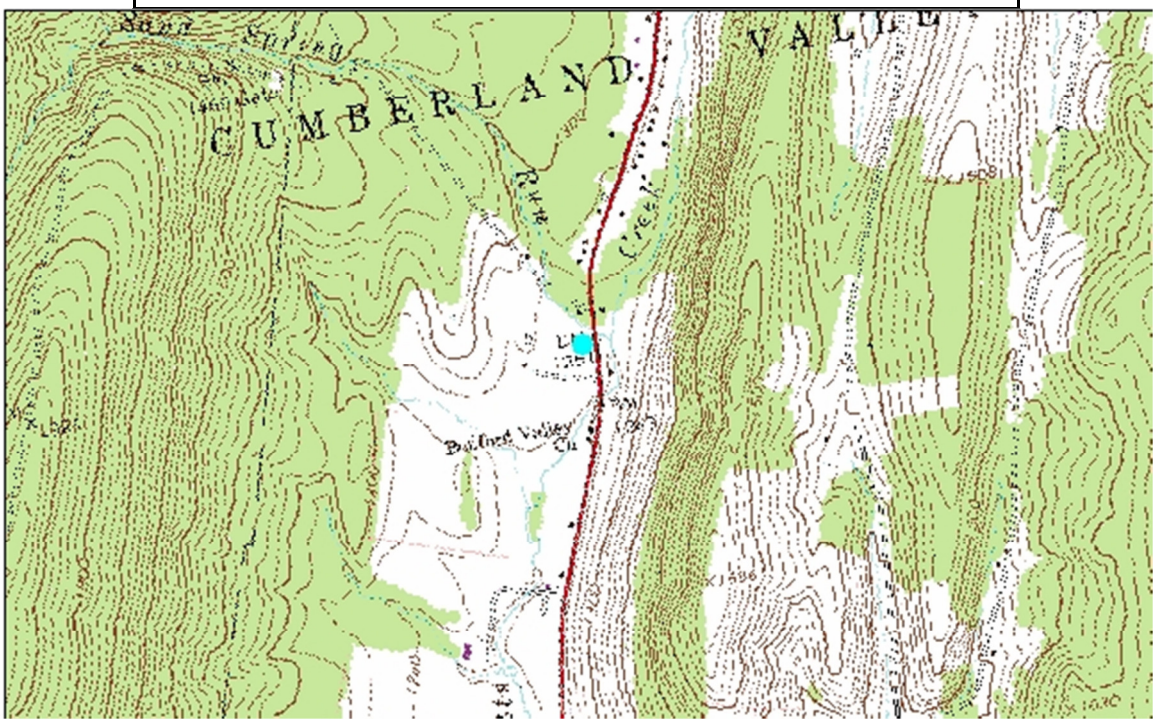

| Sample Site | **POT-62** | Sampler **Charles Trodick** | | Stream Name | |
|---|---|---|---|---|---|
| Elevation | | Latitude | **39.687011** | Longitude | **-78.585806** |
| Description | | | | | |
| **Sample taken up stream from Murley Branch Road Bridge and confluence with Murley Branch Stream. Stream mainly shale gravel and boulders. Sample taken from tire. Surrounded by farms.** | | | | | |

| Sample Site | **POT-63** | Sampler **Charles Trodick** | | Stream Name | **Critton Run** |
|---|---|---|---|---|---|
| Elevation | | Latitude | **39.471218** | Longitude | **-78.437963** |
| Description | | | | | |
| **Sampled downstream from 29 bridge. Large boulder stream. Sampled a gravel bar. Shale dominated stream. Mainly forested.** | | | | | |

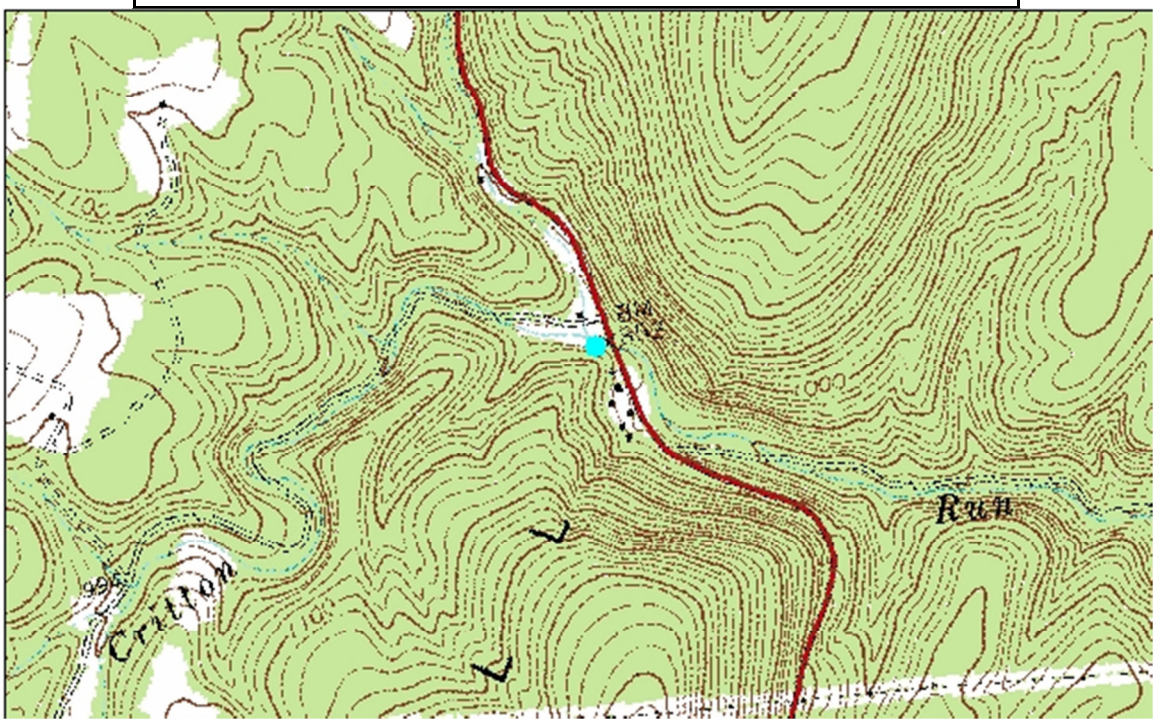

| Sample Site | **POT-64** | Sampler **Charles Trodick** | | Stream Name | **McKee's Run** |
|---|---|---|---|---|---|
| Elevation | | Latitude | **39.795513** | Longitude | **-78.254671** |
| Description | | | | | |
| **Just downstream from T330 bridge and confluence with Slate Run. Shale dominate stream. Forested area.** | | | | | |

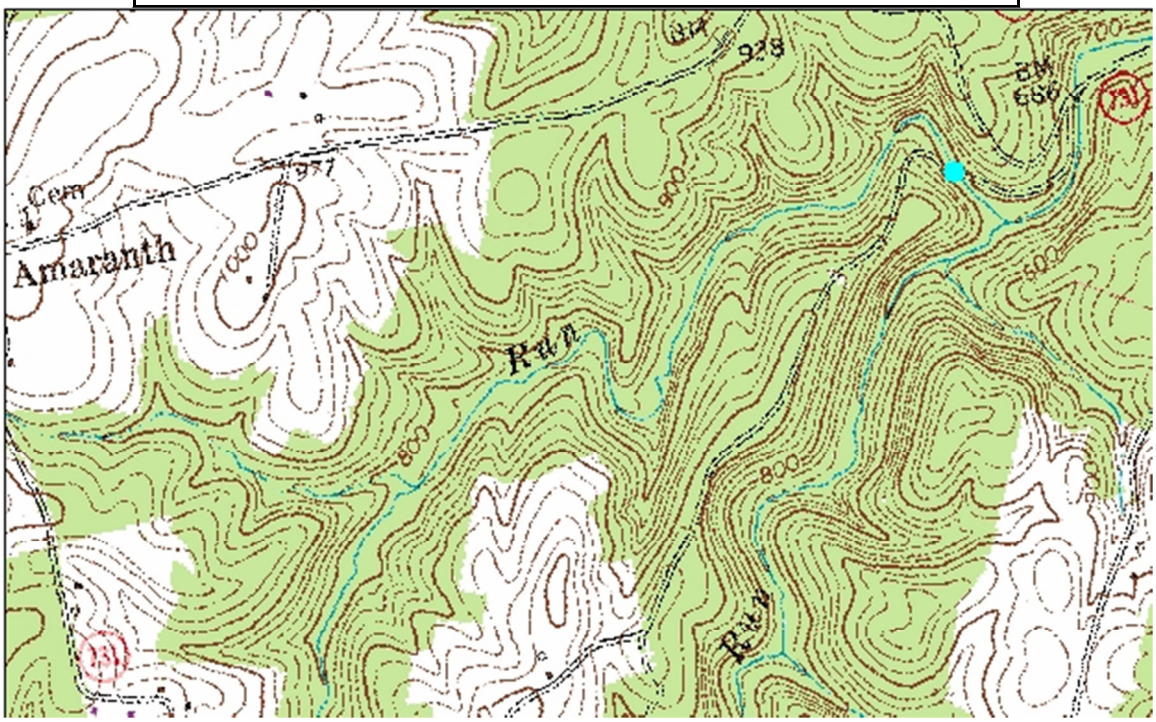

| Sample Site | **POT-65** | Sampler **Charles Trodick** | | Stream Name | **Branch of East Branch** |
|---|---|---|---|---|---|
| Elevation | | Latitude | **39.861461** | Longitude | **-78.301706** |
| Description | | | | | |
| **Sample taken downstream of 355PA bridge. Complete bedrock stream. Sampled over bank deposit. Mix of agriculture and forest. Mainly shale.** | | | | | |

| Sample Site | **POT-66** | Sampler **Charles Trodick** | | Stream Name | **Liching Fortune Teller Creek** |
|---|---|---|---|---|---|
| Elevation | | Latitude | **40.017985** | Longitude | **-78.040094** |
| Description | | | | | |
| **Sampled downstream from T417 bridge. Stream is mainly bedrock with some gravel. Sampled from some gravel on east side of stream. Shale. Almost all agriculture.** | | | | | |

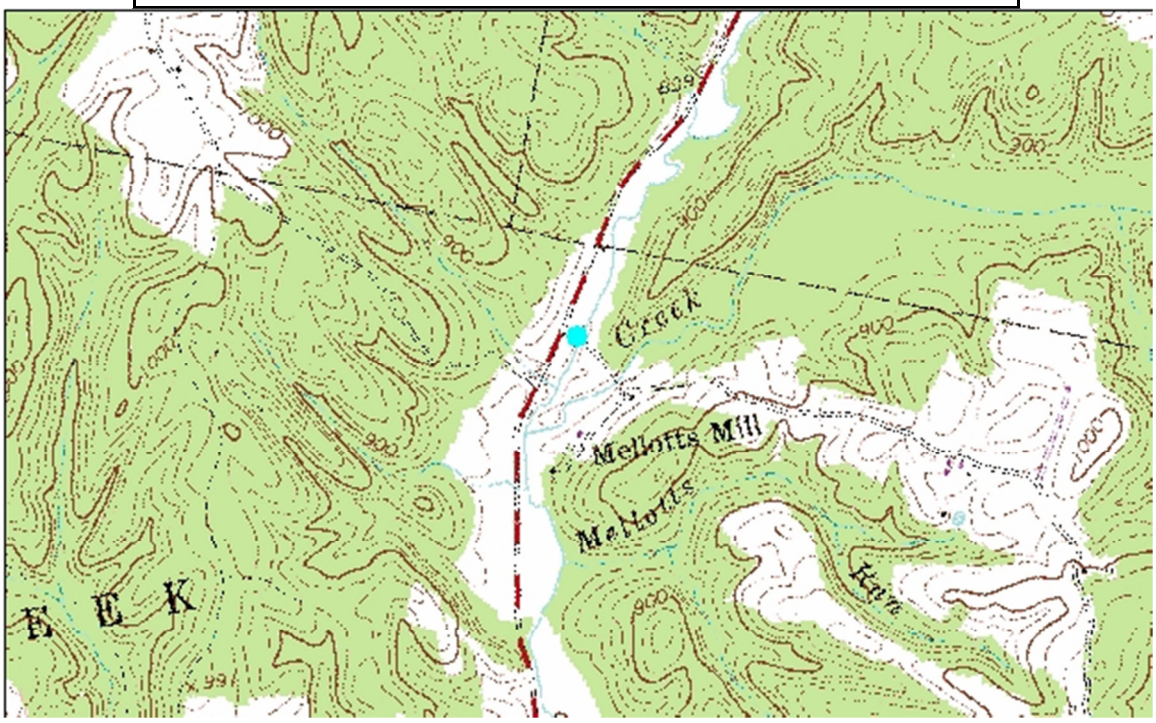

| Sample Site | **POT-67** | Sampler **Charles Trodick** | | Stream Name | |
|---|---|---|---|---|---|
| Elevation | | Latitude | **40.177332** | Longitude | **-77.66304** |
| Description | | | | | |
| **Sampled downstream from bridge for T591. Edge of private land. Large gravel and small boulder stream. Sampled pockets in middle of stream behind rock. Agriculture and lightly forested.** | | | | | |

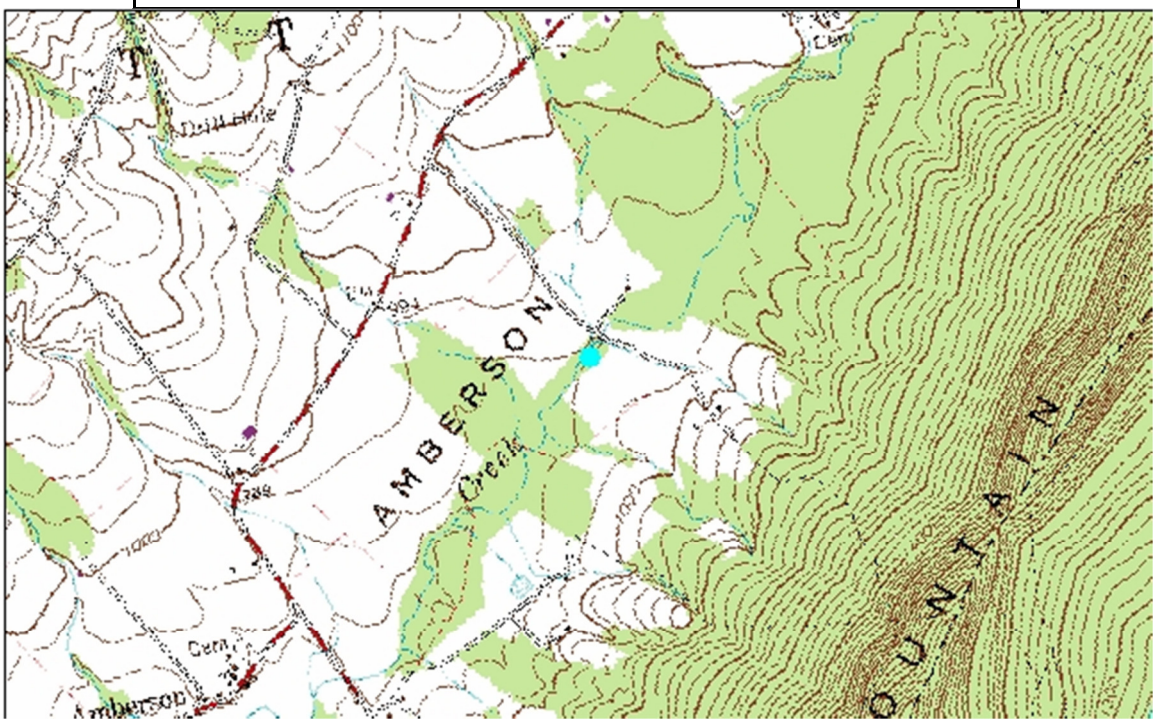

| Sample Site | **POT-68** | Sampler **Charles Trodick** | | Stream Name | **Branch of Rock Creek** |
|---|---|---|---|---|---|
| Elevation | | Latitude | **39.867126** | Longitude | **-77.222729** |
| Description | | | | | |
| **Sampled upstream from Table Rock Road Bridge. Stream is mainly shale bedrock. Almost no sand. Sample taken from mix of stuff near plants on side. Residential agriculture.** | | | | | |

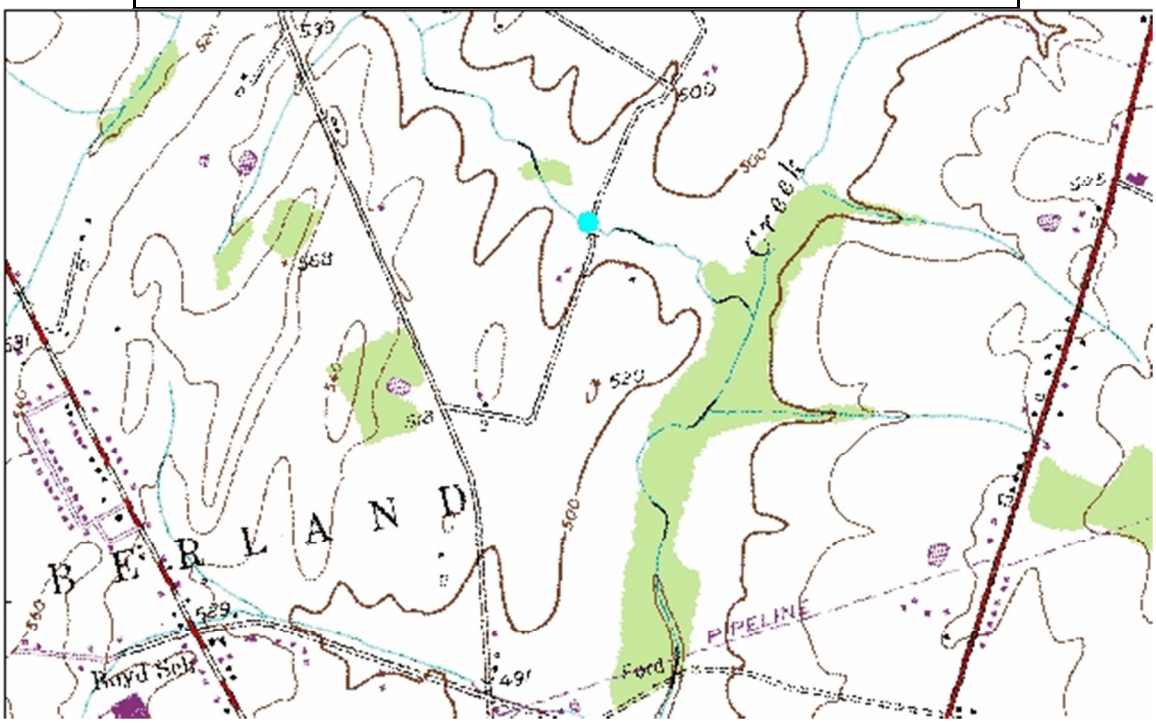

| Sample Site | **POT-69** | Sampler **Charles Trodick** | | Stream Name | **Mummasburg Run** |
|---|---|---|---|---|---|
| Elevation | | Latitude | **39.879445** | Longitude | **-77.293582** |
| Description | | | | | |
| **Sampled upstream from bridge on small gravel road off Mummasburg Road. Agriculture area. Bedrock and sand. Sampled sand bar on east side of stream. Plenty of quartz.** | | | | | |

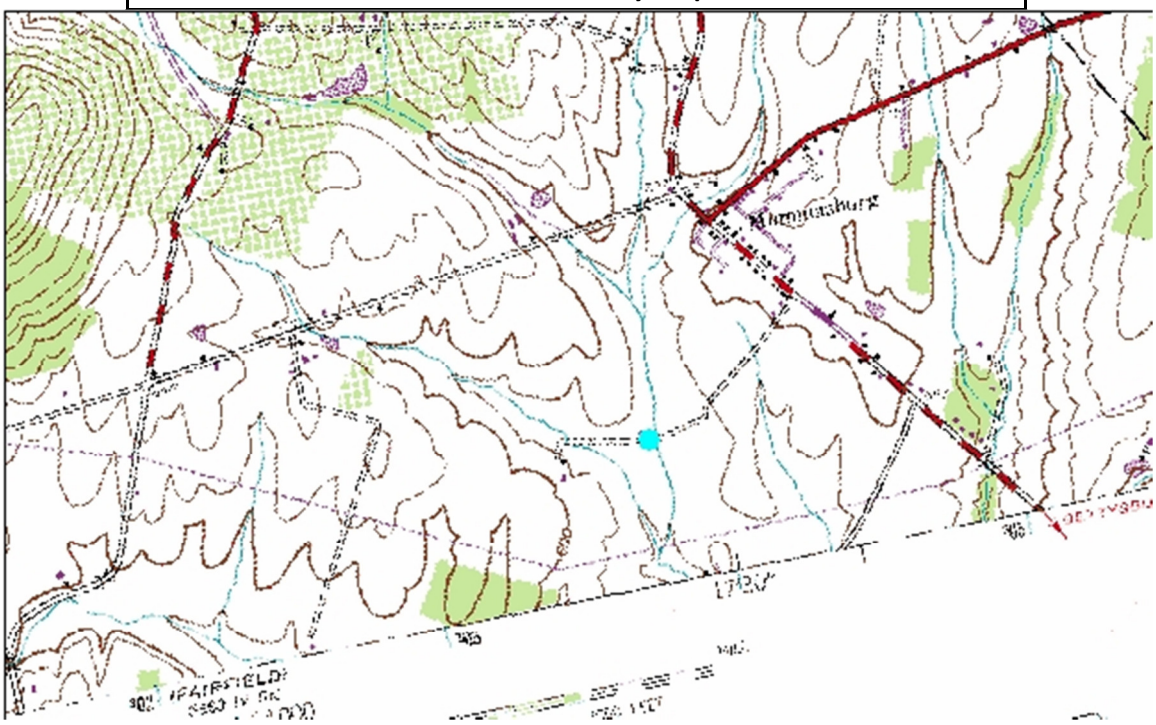

| Sample Site | **POT-70** | Sampler **Charles Trodick** | | Stream Name | **Branch of Back Creek** |
|---|---|---|---|---|---|
| Elevation | | Latitude | **39.916254** | Longitude | **-77.748227** |
| Description | | | | | |
| **Sampled sand and gravel bar just upstream from T458 bridge. Agriculture area. Stream is mainly bedrock and gravel. Shale is dominate rock.** | | | | | |

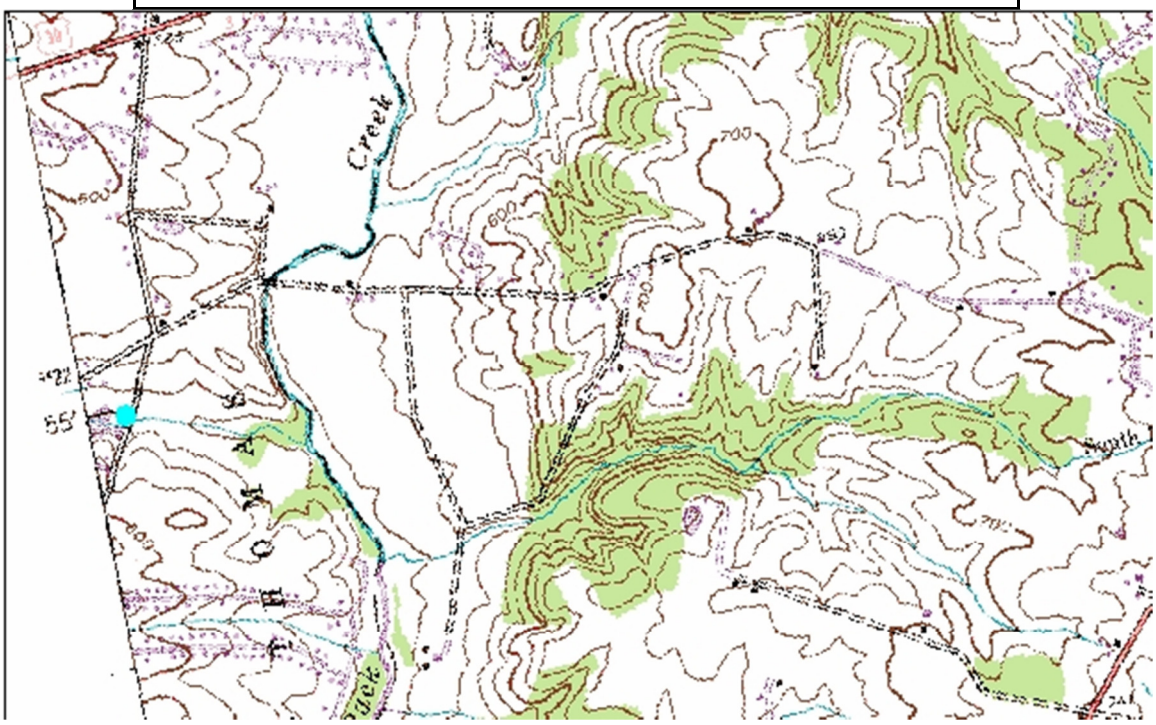

| Sample Site | **POT-71** | Sampler **Charles Trodick** | | Stream Name | **Birch Run** |
|---|---|---|---|---|---|
| Elevation | | Latitude | **39.950477** | Longitude | **-77.444472** |
| Description | | | | | |
| **Sampled in pool just down from Birch Run Road Bridge and upstream from reservoir. Pure quartz sand. Forested area.** | | | | | |

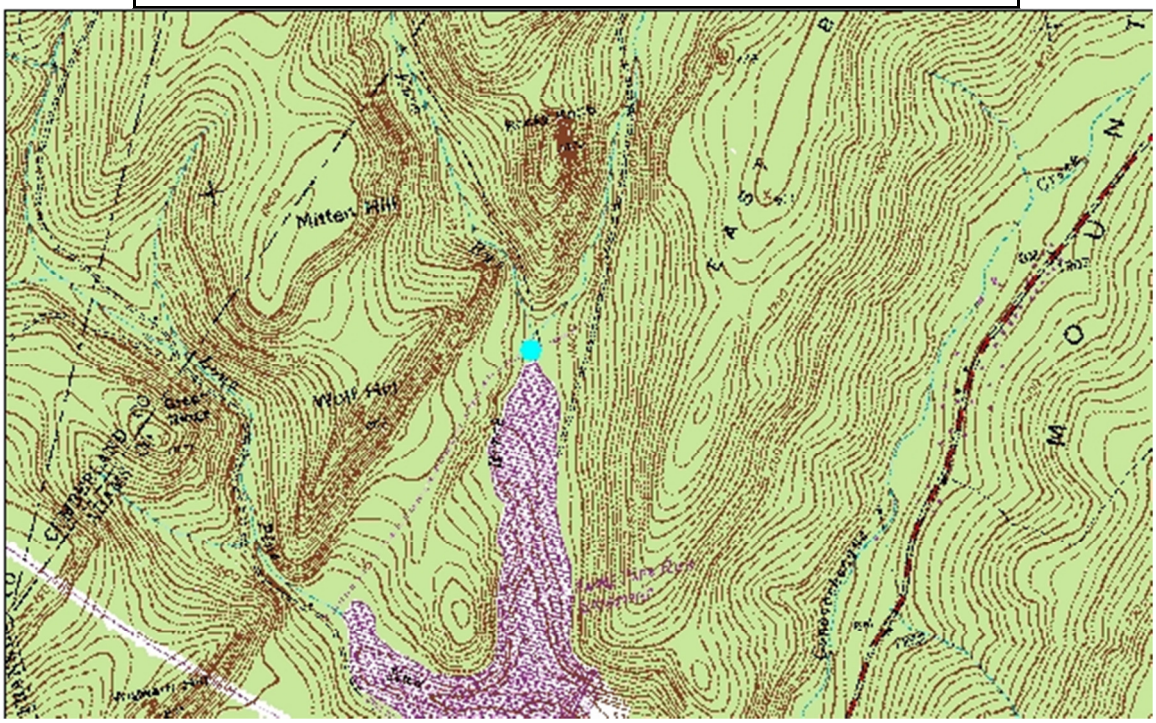

| Sample Site | **POT-72** | Sampler **Charles Trodick** | | Stream Name | **Turkeyfoot Run** |
|---|---|---|---|---|---|
| Elevation | | Latitude | **39.567456** | Longitude | **-77.059822** |
| Description | | | | | |
| **Under bridge where Roops Mill Road and Rockland Road meet. Agriculture area. Stream mainly coarse sand, gravel with a little bedrock. Sampled sand bar under bridge.** | | | | | |

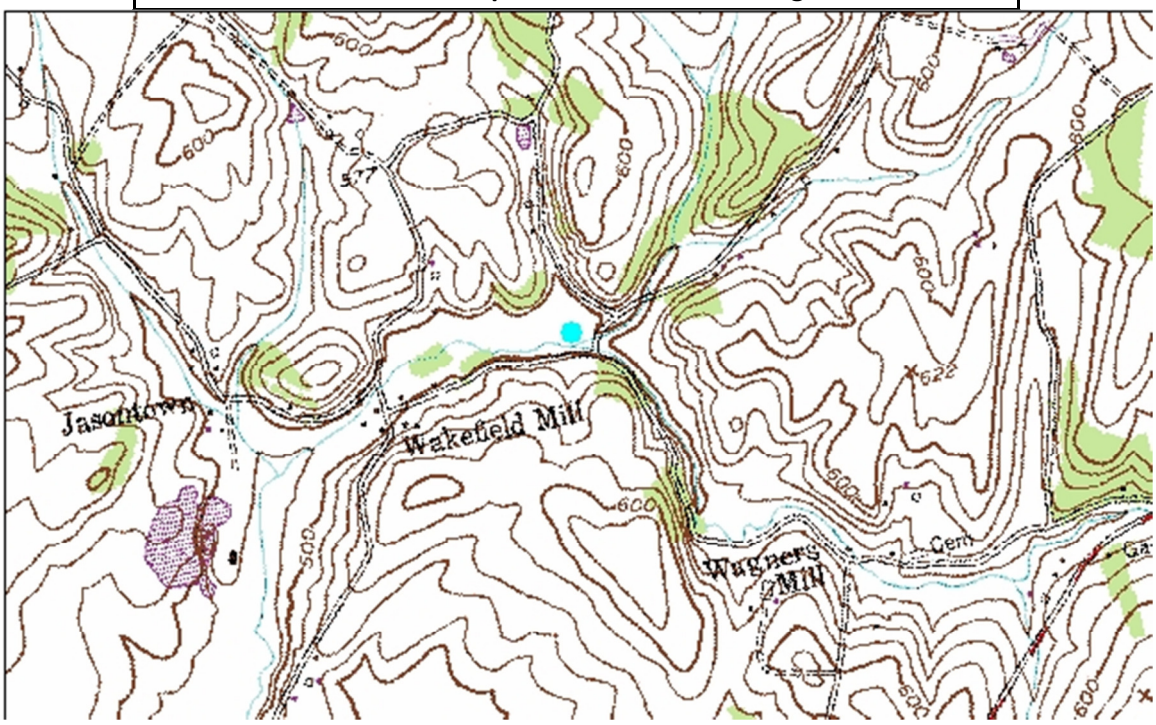

| Sample Site | **POT-73** | Sampler **Charles Trodick** | | Stream Name | **Big Pipe Creek** |
|---|---|---|---|---|---|
| Elevation | | Latitude | **39.66097** | Longitude | **-76.948189** |
| Description | | | | | |
| **Sampled under New Bachman Valley Road Bridge. Stream is mainly coarse sand and gravel. Agriculture region.** | | | | | |